

University of Kentucky

UKnowledge

---

Theses and Dissertations--Pharmacy

College of Pharmacy

---

2011

**STUDIES OF SOLUBILIZATION OF POORLY WATER-SOLUBLE  
DRUGS DURING *IN VITRO* LIPOLYSIS OF A MODEL LIPID-BASED  
DRUG DELIVERY SYSTEM AND IN MIXED MICELLES**

Lin Song

*University of Kentucky*, [lsong4@email.uky.edu](mailto:lsong4@email.uky.edu)

[Right click to open a feedback form in a new tab to let us know how this document benefits you.](#)

**Recommended Citation**

Song, Lin, "STUDIES OF SOLUBILIZATION OF POORLY WATER-SOLUBLE DRUGS DURING *IN VITRO* LIPOLYSIS OF A MODEL LIPID-BASED DRUG DELIVERY SYSTEM AND IN MIXED MICELLES" (2011). *Theses and Dissertations--Pharmacy*. 1. [https://uknowledge.uky.edu/pharmacy\\_etds/1](https://uknowledge.uky.edu/pharmacy_etds/1)

This Doctoral Dissertation is brought to you for free and open access by the College of Pharmacy at UKnowledge. It has been accepted for inclusion in Theses and Dissertations--Pharmacy by an authorized administrator of UKnowledge. For more information, please contact [UKnowledge@lsv.uky.edu](mailto:UKnowledge@lsv.uky.edu).

## **STUDENT AGREEMENT:**

I represent that my thesis or dissertation and abstract are my original work. Proper attribution has been given to all outside sources. I understand that I am solely responsible for obtaining any needed copyright permissions. I have obtained and attached hereto needed written permission statements(s) from the owner(s) of each third-party copyrighted matter to be included in my work, allowing electronic distribution (if such use is not permitted by the fair use doctrine).

I hereby grant to The University of Kentucky and its agents the non-exclusive license to archive and make accessible my work in whole or in part in all forms of media, now or hereafter known. I agree that the document mentioned above may be made available immediately for worldwide access unless a preapproved embargo applies.

I retain all other ownership rights to the copyright of my work. I also retain the right to use in future works (such as articles or books) all or part of my work. I understand that I am free to register the copyright to my work.

## **REVIEW, APPROVAL AND ACCEPTANCE**

The document mentioned above has been reviewed and accepted by the student's advisor, on behalf of the advisory committee, and by the Director of Graduate Studies (DGS), on behalf of the program; we verify that this is the final, approved version of the student's dissertation including all changes required by the advisory committee. The undersigned agree to abide by the statements above.

Lin Song, Student

Dr. Paul M. Bummer, Major Professor

Dr. Jim Pauly, Director of Graduate Studies

ABSTRACT OF DISSERTATION

Lin Song

The Graduate School  
University of Kentucky

2011

STUDIES OF SOLUBILIZATION OF POORLY WATER-SOLUBLE DRUGS  
DURING *IN VITRO* LIPOLYSIS OF A MODEL LIPID-BASED DRUG DELIVERY  
SYSTEM AND IN MIXED MICELLES

---

ABSTRACT OF DISSERTATION

---

A dissertation submitted in partial fulfillment of the  
requirements for the degree of Doctor of Philosophy in the  
College of Pharmacy  
at the University of Kentucky

By

Lin Song

Lexington, Kentucky

Director: Dr. Paul M. Bummer, Associate Professor of Pharmaceutical Sciences

Lexington, Kentucky

2011

Copyright © Lin Song 2011

## Abstract of Dissertation

### Studies of Solubilization of Poorly Water-soluble Drugs During *in vitro* Lipolysis of a Model Lipid-based Drug Delivery System and in Mixed Micelles

Lipid-based drug delivery systems (LBDDSs) are becoming an increasingly popular approach to improve the oral absorption of poorly-water soluble drugs. Several possible mechanisms have been proposed to explain the means by which LBDDSs act *in vivo* to enhance absorption. The goal of the current dissertation is to provide a better understanding of one proposed mechanism; the capability of lipoidal components in LBDDS formulations to create and maintain a drug in a supersaturated state under simulated GI conditions. Moreover, molecular details of equilibrium solubilization of a drug in a series of model lipid assemblies were examined. The results of these studies will aid formulators in choosing the optimal LBDDS to improve oral absorption of poorly water-soluble drugs.

Time-dependent solubilization behavior of progesterone,  $17\beta$ -estradiol and nifedipine in a simple model LBDDS composed of Polysorbate 80 was assessed employing the *in vitro* dynamic lipolysis model. The results illustrated the extent to which the supersaturated state was dependent on the extent of lipolysis of Polysorbate 80 and the initial drug concentration. Area-under-the curve-supersaturation was proposed as a means of quantifying the time-dependent extent of supersaturation in LBDDSs in simulated intestinal conditions.

Concurrently, a series of model mixed micellar solutions, composed of Polysorbate 80 and oleic acid, were prepared to represent the lipid assemblies produced during the lipolysis experiments. The ability of these aggregates to solubilize progesterone,  $17\beta$ -estradiol and nifedipine were evaluated and the aggregate/water partition coefficients were determined. The Treinor model was found to successfully fit the partition coefficients of the drugs in a range of mixed micelles. The equilibrium solubility of drugs in the mixed micelles was calculated and compared to that found under lipolytic conditions. The best agreement between calculated and experimental conditions was observed for nifedipine.

These studies have established a foundation for the evaluation of time-dependent extent of supersaturation with more complex LBDDS formulations exposed to lipolytic conditions.

Key Words: Lipolysis, Lipid-based Drug Delivery System (LBDDS), Solubilization, Supersaturation

Lin Song

November 2011

STUDIES OF SOLUBILIZATION OF POORLY WATER-SOLUBLE DRUGS  
DURING *IN VITRO* LIPOLYSIS OF A MODEL LIPID-BASED DRUG DELIVERY  
SYSTEM AND IN MIXED MICELLES

By  
Lin Song

Paul M. Bummer, Ph.D.

*Director of Dissertation*

Jim Pauly, Ph.D.

*Director of Graduate Studies*

November 10th, 2011

## RULES FOR THE USE OF DISSERTATIONS

Unpublished dissertations submitted for the Doctor's degree and deposited in the University of Kentucky Library are as a rule open for inspection, but are to be used only with due regard to the rights of the authors. Bibliographical references may be noted, but quotations or summaries of parts may be published only with the permission of the author, and with the usual scholarly acknowledgements.

Extensive copying or publication of the dissertation in whole or in part also requires the consent of the Dean of the Graduate School of the University of Kentucky.

A library that borrows this dissertation for use by its patrons is expected to secure the signature of each user.

Name

Date

---

---

---

---

---

---

---

---

---

---



DISSERTATION

Lin Song

The Graduate School  
University of Kentucky  
2011

STUDIES OF SOLUBILIZATION OF POORLY WATER-SOLUBLE DRUGS  
DURING *IN VITRO* LIPOLYSIS OF A MODEL LIPID-BASED DRUG DELIVERY  
SYSTEM AND IN MIXED MICELLES

---

DISSERTATION

---

A dissertation submitted in partial fulfillment of the  
requirements for the degree of Doctor of Philosophy in the  
College of Pharmacy  
at the University of Kentucky

By

Lin Song

Lexington, Kentucky

Director: Dr. Paul M. Bummer, Associate Professor of Pharmaceutical Sciences

Lexington, Kentucky

2011

Copyright © Lin Song 2011

## ACKNOWLEDGEMENTS

I would like to give my sincere gratitude and appreciation to my adviser, Dr. Paul M. Bummer, for his excellent guidance, patience, caring and persevering with me throughout the time it took me to complete this research and write the dissertation.

I would also like to thank the members of my dissertation committee, Dr. Bradley Anderson, Dr. Barbara Knutson and Dr. Tonglei Li, for generously giving their time and expertise to improve my work. I appreciate their contribution and their good-natured support.

I would like to acknowledge as well the many friends, colleagues, students and teachers who supported, assisted, and advised my research over the years. Especially, many thanks are given to John Layton for helping me on the NMR techniques. My research would not have been completed without his wise advice.

Finally, I am grateful too to my husband, Dr. Guangrong Zheng, for encouragement and emotional support over the years. He is always there sharing my happiness and unhappiness.

## TABLE OF CONTENTS

ACKNOWLEDGEMENTS .....	III
LIST OF TABLES .....	VIII
LIST OF FIGURES .....	X
LIST OF SCHEMES.....	XVIII
Chapter 1 Statement of Problems and Aims .....	1
Chapter 2 Background and Literature Review.....	3
2.1. Summary .....	3
2.2. Oral lipid-based drug delivery systems (LBDDSs).....	3
2.2.1. Poorly water-soluble drugs .....	3
2.2.2. Oral lipid-based dosage forms .....	5
2.2.3. Classification of LBDDS formulations.....	7
2.3. Proposed mechanisms of enhanced absorption by LBDDSs .....	11
2.3.1. Biological and biochemical mechanisms.....	12
2.3.2. Physicochemical mechanisms.....	13
2.4. Enzymatic hydrolysis of lipids.....	16
2.4.1 Digestion of lipids.....	16
2.4.2. Evaluation of effect of lipolysis on LBDDS and drug solubilization.....	23
2.5. Unanswered questions.....	25
2.6. Summary.....	26
Chapter 3 Characterization and Validation of Dynamic <i>In Vitro</i> Lipolysis Model .....	27
3.1. Summary.....	27
3.2. Introduction .....	28
3.3. Material and methods .....	31
3.3.1. Materials .....	31
3.3.2. Preparation of tris maleate buffer solution.....	32
3.3.3. Preparation of simulated digestion buffer.....	32
3.3.4. Preparation of enzyme solution .....	32
3.3.5. Preparation of formulations .....	33
3.3.6. Determination of calcium content.....	33
3.3.7. Qualitative determination of phosphatidylcholine during the lipolysis of SIFs .....	34
3.3.8. Setup of pH-stat titration system.....	34
3.3.9. <i>In vitro</i> lipolysis .....	35

3.4. Results and discussion.....	36
3.4.1. Enzyme preparation: effect of volume and storage conditions.....	36
3.4.2. Sensitivity of the model .....	38
3.4.3. The effect of digestion media components on the extent of lipolysis.....	44
3.5. Conclusion.....	54
Chapter 4 Solubilization of Poorly-water Soluble Drugs in Simple LBDDSs Containing Surfactant PS80 Only Under Simulated Intestinal Conditions.....	55
4.1. Summary.....	55
4.2. Introduction .....	56
4.3. Materials and methods.....	59
4.3.1. Materials .....	59
4.3.2. Equilibrium solubility of model drugs in neat PS80.....	60
4.3.3. Preparation of the model drug loaded PS80 formulations .....	61
4.3.4. Dispersion of drug-containing PS80 formulations .....	62
4.3.5. <i>In vitro</i> lipolysis of drug-containing PS80 formulations .....	63
4.3.6. Determination of equilibrium solubility in digested blank formulation .....	63
4.3.7. Determination of octanol/water partitioning coefficient of model drugs .....	64
4.3.8. HPLC methods.....	64
4.3.9. Characterization of solid formed during the <i>in vitro</i> dispersion of drug-containing PS80 formulations.....	67
4.4. Results and discussion.....	67
4.4.1. Extent of lipolysis as measured by production of fatty acid.....	67
4.4.2. Solubilization of model drugs in PS80 solutions.....	72
4.4.4. Solubilization of model drugs formulated in PS80 during <i>in vitro</i> lipolysis ....	90
4.4.5. Extent of supersaturation during <i>in vitro</i> lipolysis.....	104
4.5. Conclusion.....	111
Chapter 5 Solubilization of Poorly-water Soluble Drugs in Model Mixed Micellar Systems Composed of Selected Lipolytic Products of Polysorbate 80.....	112
5.1. Summary.....	112
5.2. Introduction .....	112
5.3. Materials and methods.....	114
5.3.1. Materials .....	114
5.3.2. Calculation of the molar ratio of PS80 to oleic acid.....	114
5.3.3. Preparation of model mixed micellar systems.....	115
5.3.4. Determination of molar solubilization capacity of mixed micellar systems...	116

5.3.5. Determination of micelle-water partition coefficient ( $K_{m/w}$ ) in mixed micellar system .....	117
5.3.6. Determination of molar solubilization capacity and micelle-water partition coefficient in sodium oleate .....	118
5.3.7. Calculation of total drug solubility in model micellar system.....	119
5.4. Results and discussion.....	120
5.4.1. Solubilization capacity ( $\kappa$ ) as a function of molar fraction of PS80 in mixed micellar systems.....	120
5.4.2. Micelle-water partition coefficient ( $K_{m/w}$ ) as a function of molar fraction of PS80 in the model systems .....	146
5.4.3. Predicted total drug solubility in SIF solution as function a time.....	151
5.5. Conclusion.....	155
Chapter 6 Characterization of Model Mixed Micellar Systems and Studies on Inter-molecular Interactions Between Micelles and Drugs.....	156
6.1. Summary.....	156
6.2. Introduction .....	157
6.3. Materials and methods.....	157
6.3.1. Materials .....	157
6.3.2. Determination of apparent pKa of micellar oleic acid.....	158
6.3.3. NMR sample preparation.....	161
6.3.4. Pulsed -gradient spin -echo nuclear magnetic resonance (PGSE-NMR).....	161
6.3.5. Spin-lattice relaxation time (T1) measurement.....	166
6.3.6. Measurement of chemical shifts of PS80 in the presence of model drugs ....	167
6.3.7. Dynamic light scattering (DLS).....	167
6.3.8. Fourier transform infrared (FTIR) .....	169
6.4. Results and discussion.....	170
6.4.1. Characteristics of model systems critical for drug solubilization.....	170
6.4.2 Inter-molecular interactions between model drugs and mixed micelles.....	186
6.4.3. Summary of solubilization of model drugs in the micelles and proposed location.....	194
6.5. Conclusions .....	197
Chapter 7 Conclusions and Future Studies	
APPENDIX.....	202
Appendix 1. The stability of nifedipine.....	202
A1.1. Solid characterization of nifedipine collected in determination of equilibrium solubility .....	202

A1.2. Stability assay for nifedipine .....	202
A1.3. Results and discussion .....	203
Appendix 2. Surfactant composition during the lipolysis of formulations .....	208
Appendix 3. Calculation of aggregation number, total micelle surface area and total micelle core volume .....	213
Reference.....	215
Vita.....	232

## LIST OF TABLES

Table 2.1 The lipid formulations classification system (LFCS) (Pouton, 2000; Pouton, 2006) .....	8
Table 2.2 Solubilizing excipients used in commercially available LBDDSs (Haus, 2007) .....	10
Table 3.1 Amount of weighed selected surfactants, molecular weight and theoretical fatty acid released from selected surfactants .....	42
Table 4.1 Drug properties and dose number .....	60
Table 4.2 Drug concentration in each formulation .....	61
Table 4.3 HPLC conditions and protocols for analysis of progesterone, 17 $\beta$ -estradiol and nifedipine .....	65
Table 4.4 Equilibrium solubility of progesterone, 17 $\beta$ -estradiol and nifedipine in neat PS80 at 25 $\pm$ 0.5 $^{\circ}$ C and in 1% of PS80 solution in SIFs buffer at 37 $\pm$ 0.5 $^{\circ}$ C (n=3).....	80
Table 4.5 The concentration area under the curve ( $\mu\text{g}\cdot\text{min}\cdot\text{mL}^{-1}\pm\text{SD}$ ) in the <i>in vitro</i> dispersion of formulations in the absence of enzyme preparation and the presence of inactivated enzyme preparation .....	94
Table 4.6 The concentration area under the curve ( $\mu\text{g}\cdot\text{min}\cdot\text{mL}^{-1}\pm\text{SD}$ ) in the <i>in vitro</i> dispersion of formulations in the presence of active enzyme preparation and the presence of inactivated enzyme preparation .....	97
Table 4.7 The summary of maximum supersaturation ratio ( $\text{SS}_{\text{max}}$ ), time at $\text{SS}_{\text{max}}$ ( $t_{\text{max}}$ ), area under the supersaturation curve and maximum concentration ( $\text{C}_{\text{max}}$ ), time at $\text{C}_{\text{max}}$ and area under the concentration curve .....	110
Table 5.1 The molar fraction of PS80 and molar ratio of PS80 to OA in the mixture of PS80 and OA prepared in tris maleate buffer (T-series) and SIFs buffer (5 mM NaC/1.25 mM PC) (S-series) .....	116
Table 5.2 The fitted molar solubilization capacity ( $\kappa$ , mole of drug/mole of micellar surfactant) of mixed micellar systems for progesterone prepared in tris maleate buffer and SIF buffer .....	121
Table 5.3 The fitted molar solubilization capacities ( $\kappa$ , mole of drug /mole of micellar surfactant) of mixed micellar systems for 17 $\beta$ -estradiol prepared in tris maleate buffer and SIFs buffer .....	127
Table 5.4 The fitted molar solubilization capacity ( $\kappa$ , mole of drug / mole of micellar surfactant) of mixed micellar systems for nifedipine prepared in tris maleate buffer and SIF buffer .....	130
Table 5.5 The normalized molar solubilization capacity ( $\kappa^*$ ) in SIF buffer for progesterone, 17 $\beta$ -estradiol and nifedipine in model micellar systems composed of PS80/OA at 37 $^{\circ}$ C .....	136
Table 5.7 The micelle-water partition coefficients of progesterone, 17 $\beta$ -estradiol and nifedipine in the model mixed micellar systems ( $\pm$ 95% CI) .....	146
Table 5.8 Fitting parameters for progesterone, 17 $\beta$ -estradiol and nifedipine.....	151



Table 6.1 Response time of pH electrode and $\Delta E$ at infinite time in pure water and aqueous solution of PS80 at different concentrations at 37°C.....	160
Table 6.2 The drift of glass electrode in 5 min at 37°C.....	160
Table 6.3 The fitted $K_a$ , fitting parameters and calculated apparent pKa of oleic acid in the mixed micelle solutions composed of PS80 and oleic acid at molar ratio of 9/1 and 1/1 (n=3).....	173
Table 6.4 Interaction parameter ( $\beta$ ) of mixing ionic surfactant and nonionic surfactant in the literature .....	178
Table 6.5 Diffusion coefficients and hydrodynamic radii of lipid aggregates in the PS80 solution and mixture of PS80 and oleic acid at different molar ratios.....	182
Table 6.6 Hydrodynamic radii of PS80 micelle in tris maleate buffer and polydispersity index at 37°C (Average $\pm$ SD, n=3).....	183
Table 6.7 Hydrodynamic radii of PS80 micelle in SIFs buffer and polydispersity index at 37°C as measured by DLS (Average $\pm$ SD, n=3) .....	184
Table 6.8 Hydrodynamic radii of mixed micelle of PS80 with oleic acid at molar ratio of 9/1 in SIFs buffer and polydispersity index at 37°C as measured by DLS(Average $\pm$ SD, n=3) .....	185
Table 6.9 Hydrodynamic radii of mixed micelle of PS80 with oleic acid at molar ratio of 1/1 in SIFs buffer and polydispersity index at 37°C as measured by DLS (Average $\pm$ SD, n=3).....	185
Table 6.10 Absorption of C-O on polyoxyethylene (POE) group in absence and presence of progesterone and nifedipine.....	193
Table 6.11 The physical properties and molar solubilization capacity of PS80 and PS80/oleic acid (1/1) for progesterone, 17 $\beta$ -estradiol and nifedipine .....	195
Table A1.1 The stability of nifedipine in the presence or absence of pancreatic enzyme .....	206
Table A2.1 Fatty acid (FA) released from PS80 and molar ratio of PS80 to fatty acid released from PS80 during the lipolysis of blank formulation. ....	209
Table A2.2 Fatty acid (FA) released from PS80 and molar ratios of PS80 to fatty acid released from PS80 during the lipolysis of progesterone-loaded formulations .....	210
Table A2.3 Fatty acid (FA) released from PS80 and molar ratios of PS80 to fatty acid released from PS80 during the lipolysis of 17 $\beta$ -estradiol-loaded formulations .....	211
Table A2.4 Fatty acid (FA) released from PS80 (PS80) and molar ratio of PS80 to fatty acid released from PS80 during the lipolysis of nifedipine-loaded formulations .....	212

## LIST OF FIGURES

Figure 2.1 Biopharmaceutical Classification System .....	4
Figure 2.2 Structure of a triglyceride and its components. ....	11
Figure 2.3 General process of lipid digestion in the GI tract (Yamagata, Kusu- hara et al., 2007) .....	18
Figure 2.4 The mechanism of hydrolysis of triglyceride by a catalytic triad including serine, histine and an acidic amino acid.....	21
Figure 3.1 Structures of selected substrates .....	31
Figure 3.2 pH-stat titration system.....	35
Figure 3.3 Amount of fatty acid released in the lipolysis of CrRH40 by adding 0.5 mL (diamond), 1 mL (triangle) and 2 mL (star) of enzyme preparation. Enzyme solution was stored on ice until use after preparation. Condition: NaC solution (5 mM, 25 mL), CrRH40 (0.48 g, 0.18 mmol) at 37 °C. ....	37
Figure 3.4 Amount of fatty acid released in the lipolysis of CrRH40 hydrolyzed by enzyme solution stored at room temperature (square), on the ice (triangle), and incubated at 37°C before addition to the solution (cross). Condition: NaC solution (5 mM, 25 mL), CrRH40 (~0.48 g, 0.18 mmol) and enzyme preparation (1 mL) at 37°C. ....	38
Figure 3.5 The structure of 1,2-diacyl-sn-glycero-3-phosphocholine. ....	39
Figure 3.6a Total amount of NaOH consumed during the lipolysis of 25 mL of SIFs, with and without PC at 37°C. Profiles were recorded from three batches of enzyme prepared on three separate days (square, cross and circle). Triangle represents the amount of NaOH titrated in the tris maleate buffer containing 5 mM of NaC (no PC) after addition of enzyme preparation (pH 7.8 at 0°C) at 37°C. .40	
Figure 3.6.b Amount of fatty acid released in the lipolysis of 25 mL of simulated fasted digestion buffer composed of 5 mM of NaC /1.25 mM of PC at 37°C. Profiles were recorded from three batches of enzyme preparation prepared in day 1 (square), day 2 (cross) and day 3 (circle). (Enlarged for the first 10 min. from Figure 3.6a) .....	39
Figure 3.7 Amount of fatty acid released in the lipolysis of CrRH40, CrEL, TPGS and PS80 solution in SIFs buffer. Condition: SIFs buffer (25 mL, 5 mM of NaC/1.25 mM of PC) and enzyme preparation (1 mL) at 37°C .....	42
Figure 3.8 Amount of fatty acid released during the lipolysis of 0.48 g (0.18mmol) CrRH40, 0.8 g F1 composed of 55% of CrRH40, 37.5% of soybean oil and 7.5% of ethanol in SIFs buffer and 25 mL SIFs buffer as control at 37°C.....	43
Figure 3.9 Amount of fatty acid released in the lipolysis of 0.48 g CrRH40 only in simulated fed-state digestion buffer, 0.8 g F1 composed of 55% of CrRH40, 37.5% of soybean oil and 7.5% of ethanol in simulated fed-state digestion buffer and 25 mL simulated fed-state digestion buffer as control at 37°C.....	44
Figure 3. 10 The structure of bile salts used. ....	46
Figure 3.11 Amount of fatty acid released in the lipolysis of 25 mL of SIFs composed of NaTC/PC (molar ratio 4:1) at 37°C. Each profile was recorded from a freshly- prepared enzyme solution. ....	46

Figure 3.12 Representative total amount of fatty acid released in the lipolysis of PS80 in the SIFs buffer composed of NaC/PC (cross) and composed of NaTC/PC (triangle) at 37°C. ....	47
Figure 3.13 Amount of fatty acid released in the lipolysis of 0.48 g CrRH40 and 0.8 g F1 composed of 55% of CrRH40, 37.5% of soybean oil and 7.5% of ethanol in 5 mM of NaC solution in the presence and absence of 1.25 mM of PC at 37°C. ....	49
Figure 3.14 Amount of fatty acid released in the lipolysis of 0.48 g CrRH40 and 0.8 g F1 composed of 55% of CrRH40, 37.5% of soybean oil and 7.5% of ethanol in 20 mM of NaC solution in the presence and absence of 5 mM of PC at 37°C. ....	49
Figure 3.15 Amount of fatty acid released in the lipolysis of SIFs composed of 5 mM NaC/1.25 mM PC in the presence (square) and absence (cross) of 5 mM of CaCl <sub>2</sub> at 37°C. Theoretical amount of fatty acid from 1.25 mM PC is 31 μmol/25 mL .....	51
Figure 3.16 Amount of fatty acid released in the lipolysis of SIFs buffer composed of NaTC in the presence (square) and absence (cross) of 5 mM of CaCl <sub>2</sub> at 37°C. Theoretical amount of fatty acid from 1.25 mM PC is 31 μmol/25 mL.....	51
Figure 3.17 Amount of fatty acid released in the lipolysis of PS80 in tris maleate buffer (pH 7.5 at 37°C) in the presence and absence of 5 mM of CaCl <sub>2</sub> . ....	52
Figure 3.18 Amount of fatty acid released in the lipolysis of PS80 in SIFs buffer (pH 7.5 at 37°C) in the presence and absence of 5 mM of CaCl <sub>2</sub> . ....	52
Figure 3.19 Calcium concentration change during in vitro lipolysis of PS80 in the SIFs buffer at 37°C.....	53
Figure 3.20 Thermogram of precipitate collected from the lipolysis of PS80 in the presence of calcium.....	54
Figure 4.1 The structures of model poorly-water soluble drug .....	60
Figure 4.2 HPLC chromatogram of progesterone.....	66
Figure 4.3 HPLC chromatogram of 17β-estradiol.....	66
Figure 4.4 HPLC chromatogram of nifedipine .....	67
Figure 4.5a Representative of amount of fatty acid released in the lipolysis of blank PS80 and PS80 in the presence of progesterone from formulations P-12, P-20 and P-31. Shown are raw data before subtraction of blank.....	68
Figure 4.5b Representative amount of fatty acid released in the lipolysis of blank PS80 and PS80 in the presence of 17β-estradiol from formulations E-5, E-7 and E-14. Shown are raw data before subtraction of blank.....	68
Figure 4.5c Representative Amount of fatty acid released in the lipolysis of blank PS80 and PS80 in the presence of nifedipine from formulations N-11, N-20 and N-35. Shown are raw data before subtraction of blank.....	68
Figure 4.6a The Percentage of titratable fatty acid from PS80 in the presence of progesterone during the <i>in vitro</i> lipolysis of formulations P-12, P-20 and P-31. (n=3) Shown are transformed data after subtraction of blank .....	71
Figure 4.6b The Percentage of titratable fatty acid from PS80 in the presence of 17β-estradiol during the <i>in vitro</i> lipolysis of formulations E-5, E-7 and E-14. (n=3) Shown are transformed data after subtraction of blank .....	70

Figure 4.6c The percentage of titratable fatty acid from PS80 in the presence of nifedipine during the <i>in vitro</i> lipolysis of formulations N-11, N-20 and N-35. (n=3) Shown are transformed data after subtraction of blank .....	71
Figure 4.7a The progesterone concentration from the dispersion of stock solution in DMSO in the SIFs buffer containing PS80 at 0% (triangle), 0.01% (diamond), 0.02% (cross), 0.2% (star) and 1% (square) at 37±0.5°C. Dashed line is the equilibrium solubility in 1% P PS80 solution at the same condition.....	74
Figure 4.7b The 17β-estradiol concentration from the dispersion of stock solution in DMSO in the SIFs buffer containing PS80 at 0% (triangle), 0.01% (diamond), 0.02% (cross), 0.2% (star) and 1% (square) at 37±0.5°C. Dashed line is the equilibrium solubility in 1% PS80 solution at the same condition .....	73
Figure 4.7c The nifedipine concentration from the dispersion of stock solution in DMSO in the SIFs buffer containing PS80 at 0% (triangle), 0.01% (diamond), 0.02% (cross), 0.2% (star) and 1% (square) at 37±0.5°C. Dashed line is the equilibrium solubility of nifedipine in 1% of PS80 at the same condition.....	74
Figure 4.8a The supersaturation ratio of progesterone from the dispersion of stock solution in DMSO in the SIFs buffer containing PS80 at 0% (diamond), 0.01% (triangle), 0.02% (cross), 0.2% (star) and 1% (square) at 37±0.5°C. ....	77
Figure 4.8b The supersaturation ratio of 17β-estradiol from the dispersion of stock solution in DMSO in the SIFs buffer containing PS80 at 0% (triangle), 0.01% (star), 0.02% (cross), 0.2% (diamond) and 1% (square) at 37±0.5°C.....	76
Figure 4.8c The supersaturation ratio of nifedipine from the dispersion of stock solution in DMSO in the SIFs buffer containing PS80 at 0% (diamond), 0.01% (cross), 0.02% (triangle), 0.2% (star) and 1% (square) at 37±0.5°C.....	77
Figure 4.9 Solubility-temperature diagram (Adapted from Mullin, J. W.) (Mullin, 1961). ....	79
Figure 4.10 The drug concentration as a function of PS80 above the CMC. ....	79
Figure 4.11 The progesterone concentration during the <i>in vitro</i> dispersion of P-12 (triangle), P-20 (diamond) and P-31 (square) in the absence of enzyme preparation at 37°C. Dashed line is the equilibrium solubility in the equivalent PS80 solution. Inserted figure is the concentration during 24 h. ....	81
Figure 4.12 The 17β-estradiol concentration during the <i>in vitro</i> dispersion of E-7 (square) and E-14(diamond) in the absence of enzyme preparation at 37°C. Dashed line is the equilibrium solubility in the equivalent PS80 solution. ....	84
Figure 4.13 The nifedipine concentration in the dispersion of N-20 (diamond) and N-35 (square) in the absence of enzyme preparation at 37°C. Dashed line is the equilibrium solubility in the equivalent PS80 solution. ....	85
Figure 4.14 The supersaturation ratios during the <i>in vitro</i> dispersion of progesterone formulation (P-31, diamond), 17β-estradiol formulation (E-14, square) and nifedipine formulation (N-35, triangle). Dashed line is the baseline where the supersaturation ratio equals 1.....	86

Figure 4.15 The birefringence of precipitation of progesterone (upper), 17 $\beta$ -estradiol (middle) and nifedipine (bottom) during <i>in vitro</i> dispersion of drug-containing formulations at 37°C.....	87
Figure 4.16 The equilibrium solubility of progesterone (star), 17 $\beta$ -estradiol (diamond) and nifedipine (triangle) in the blank PS80 after digestion by lipase enzyme at 37°C. The enzyme was inhibited by 4-BPB during the equilibrium solubility experiment.....	89
Figure 4.17 The percentage of progesterone (star), 17 $\beta$ -estradiol (diamond) and nifedipine (triangle) in the solutions of digested blank PS80 at 37°C relative to the equilibrium solubility at time zero. The dashed line is the percentage of PS80 remaining.....	90
Figure 4.18 Progesterone concentration during the <i>in vitro</i> dispersion of P-20 in the absence of enzyme (diamond) and presence of inactivated enzyme (square). Dashed line represents the equilibrium solubility in PS80 solution at the same concentration at 37°C.....	92
Figure 4.19 Progesterone concentration during <i>in vitro</i> dispersion of P-31 in the absence of enzyme (diamond) and the presence of inactivated enzyme (triangle). Dashed line represents the equilibrium solubility in PS80 solution at the same concentration at 37°C.....	92
Figure 4.20 Nifedipine concentration during the <i>in vitro</i> dispersion of N-35 in the absence of enzyme (square) and presence of inactivated enzyme (triangle). Dashed line represents the equilibrium solubility in PS80 solution at the same concentration at 37°C.....	93
Figure 4.21 The progesterone concentration change in the <i>in vitro</i> lipolysis of P-12 (triangle), P-20 (diamond), and P-31(square). Five millimolar Ca <sup>2+</sup> was not included in the SIFs buffer. The cross represents the equilibrium solubility in the digested blank formulation.....	98
Figure 4.22 The progesterone concentration change in the <i>in vitro</i> lipolysis of P-12 (triangle), P-20 (diamond), and P-31(square). Ca <sup>2+</sup> was included in the SIFs buffer. The cross represents the equilibrium solubility of progesterone in the digested blank formulation. ....	99
Figure 4.23 The 17 $\beta$ -estradiol concentration change in the <i>in vitro</i> lipolysis of E-5 (triangle), E-7 (square), and E-14 (diamond). The cross represents the equilibrium solubility of estradiol in the digested blank formulation. The circle with dash line is the drug concentration during the <i>in vitro</i> dispersion of E-14.....	100
Figure 4.24 The nifedipine concentration change in the <i>in vitro</i> lipolysis of N-11 (triangle), N-20 (diamond), and N-35 (square) formulations. The cross represents the equilibrium solubility of nifedipine in the digested blank formulation.....	102
Figure 4.25a The supersaturation ratio during the <i>in vitro</i> lipolysis of progesterone formulation P-12 (triangle), P-20 (cross) and P-31 (diamond). Dashed line is where the supersaturation ratio equals 1.....	106

Figure 4. 26b The supersaturation ratio during the <i>in vitro</i> lipolysis of 17 $\beta$ -estradiol formulations E-5 (triangle), E-7 (cross) and E-14 (diamond). Dashed line is where the supersaturation ratio equals 1 .....	106
Figure 4. 26c The supersaturation ratio during the <i>in vitro</i> lipolysis of nifedipine formulations N-11 (triangle), N-20 (cross) and N-35 (diamond). Dashed line is where the supersaturation ratio equals 1 .....	107
Figure 4. 26 The approximate stability index of progesterone, 17 $\beta$ -estradiol and nifedipine in supersaturated state during the lipolysis of formulations. $W_{EST}$ , $W_{NIF}$ and $W_{Prog}$ are ranges of stability index for 17 $\beta$ -estradiol, nifedipine and progesterone, respectively.....	108
Figure 4. 27 The linear relationship of AUC-SS and AUC-C. ....	110
Figure 5.1 The solubilization of progesterone in PS80/OAmixed micelle with molar fraction of PS80 at 1 (diamond), 0.9 (triangle), 0.8 (cross), 0.6 (circle) and 0.5 (star) at 37 $\pm$ 0.5 $^{\circ}$ C. Micellar solutions were prepared in tris maleate buffer (T-series). ....	121
Figure 5.2 The solubilization of progesterone in PS80/OA mixed micelle with molar fraction of PS80 at 1(triangle), 0.9 (diamond), 0.7 (cross), and 0.5 (square) at 37 $\pm$ 0.5 $^{\circ}$ C. Micellar solutions were prepared in SIFs buffer (S-series).....	122
Figure 5.3 The solubilization of progesterone in mixture of NaC and phospholipids (fixed ratio at 4:1) at 37 $^{\circ}$ C (Error bar is within the symbol). Dashed line is the linear-regression fitting of all data from 3 replicates (slope= $(1.44\pm 0.06) \times 10^{-2}$ , $R^2=0.98$ ). Solid lines are linear-regression of data before and after 5 mM (slope1 = $(0.84\pm 0.05) \times 10^{-2}$ , $R^2=0.99$ ; slope2 = $(1.67\pm 0.02) \times 10^{-2}$ , $R^2=0.97$ ). Slopes of the two segments were significantly different as indicted by the F-test ( $P<0.001$ ).....	124
Figure 5.4 The solubilization of 17 $\beta$ -estradiol in PS80/OA mixed micelle with molar fraction of PS80 at 1(diamond), 0.9 (square) and 0.5 (triangle) at 37 $\pm$ 0.5 $^{\circ}$ C. Micellar solutions were prepared in tris maleate buffer (T-series).....	126
Figure 5.5 The solubilization of 17 $\beta$ -estradiol in PS80/OAmixed micelle with molar fraction of PS80 at 1(diamond), 0.9 (square), 0.8 (triangle), 0.7 (cross) and 0.5 (star) at 37 $\pm$ 0.5 $^{\circ}$ C. Micellar solutions were prepared in SIFs buffer (S-series).....	126
Figure 5.6 The solubility of 17 $\beta$ -estradiol in mixture of NaC and phospholipids (fixed ratio at 4:1) at 37 $^{\circ}$ C (Error bar is within the symbol). Dashed line is the linear-regression fitting of all data from 3 replicates (slope = $(4.11\pm 0.15) \times 10^{-3}$ , $R^2=0.98$ ). Solid lines are linear-regression of data before and after 2.5 mM (slope1= $(4.71\pm 0.15) \times 10^{-3}$ , $R^2=0.99$ ; slope2 = $(3.23\pm 0.33) \times 10^{-3}$ , $R^2=0.93$ ). Slopes of the two lines were significantly different as indicted by the F-test ( $P<0.02$ ) .....	128
Figure 5.7 The solubilization of nifedipine in PS80/OA mixed micelle with molar fraction of PS80 at 1(cross), 0.9 (diamond), and 0.5 (triangle) at 37 $\pm$ 0.5 $^{\circ}$ C. Micellar solutions were prepared in tris maleate buffer (T-series).....	129
Figure 5.8 The solubilization of nifedipine in PS80/OA mixed micelle with molar fraction of PS80 at 1(cross), 0.9 (diamond), 0.8 (circle), 0.7 (star) and 0.5 (triangle) at 37 $\pm$ 0.5 $^{\circ}$ C. Micellar solutions were prepared in SIFs buffer (S-series). ....	130

Figure 5.9 The solubilization of nifedipine in mixture of NaC and phospholipids (fixed ratio at 4:1) at 37°C (Error bar is within the symbol). Dashed line is the linear-regression fitting of all data from 3 replicates (slope = $(8.41 \pm 0.20) \times 10^{-3}$ , $R^2 = 0.99$ ). Solid lines are linear-regression of data with a presumed breakpoint at 5 mM (For data at less than 5 mM slope = $(8.86 \pm 0.39) \times 10^{-3}$ , $R^2 = 0.99$ ; for data greater than 5 mM slope = $(8.37 \pm 0.40) \times 10^{-3}$ , $R^2 = 0.98$ ). Slopes of the two segments were not significantly different as indicated by the results of the F-test (P=0.43). .....	131
Figure 5.10 The correlation of molar fraction of PS80 with ratio of $\kappa$ for progesterone (diamond, $R^2 = -0.0068$ ), 17 $\beta$ -estradiol (cross, $R^2 = 0.8805$ ) and nifedipine (triangle, $R^2 = 0.9735$ ). .....	137
Figure 5.11a Solubilization of progesterone in the sodium oleate at 25 $\pm$ 2°C at pH 10.5 $\pm$ 0.1. ....	140
Figure 5.11b Total Solubilization of unionized and ionized 17 $\beta$ -estradiol (triangle) and solubilization of unionized 17 $\beta$ -estradiol (cross) in the sodium oleate at 25 $\pm$ 2°C at pH 10.5 $\pm$ 0.1 .....	140
Figure 5.11c Solubilization of nifedipine in the sodium oleate at 25 $\pm$ 2°C at pH 10.5 $\pm$ 0.1.....	141
Figure 5.12a Comparison of experimental with ideal molar solubilization capacity for progesterone in model systems. ....	143
Figure 5.12b Comparison of experimental with ideal molar solubilization capacity for 17 $\beta$ -estradiol in model systems .....	143
Figure 5.12c Comparison of experimental with ideal molar solubilization capacity for nifedipine in model systems.....	144
Figure 5.13 The deviation ratios between the $\kappa_{\text{exp}}$ and the $\kappa_{\text{ideal}}$ for solubilization of progesterone (cross), 17 $\beta$ -estradiol (square) and nifedipine (triangle) in model systems as a function of molar fraction of PS80.....	144
Figure 5.14 The correlation between micelle –water partition coefficient of progesterone (cross, $R^2 = 0.0016$ ), 17 $\beta$ -estradiol (square, $R^2 = 0.9098$ ) and nifedipine (triangle, $R^2 = 0.9757$ ) and molar fraction of PS80 in the model systems at 37°C. ....	147
Figure 5.15 The correlation of $\log K_{o/w}$ and $\log K_{m/w}$ at molar fraction of PS80 of 1 (diamond), 0.9 (square), 0.7 (triangle) and 0.5 (cross). ....	148
Figure 5.16a Micelle-water partition coefficient ( $K_{m/w}$ ) for progesterone in mixed micelle of PS80 and oleic acid in SIFs buffer. The solid line represents the calculated $K_{m/w}$ values fitted by using Eq. 5.16.....	150
Figure 5.16b Micelle-water partition coefficient ( $K_{m/w}$ ) for 17 $\beta$ -estradiol in mixed micelle of PS80 and oleic acid in SIFs buffer. The solid line represents the calculated $K_{m/w}$ values fitted by using Eq. 5.16.....	150
Figure 5.16c Micelle-water partition coefficient ( $K_{m/w}$ ) for nifedipine in mixed micelle of PS80 and oleic acid in SIFs buffer. The solid line represents the calculated $K_{m/w}$ values fitted by using Eq. 5.16.....	151
Figure 5.17a Comparison of the experimental equilibrium progesterone concentration in digested blank formulation (solid line), calculated progesterone concentration in model systems composed of selective lipolytic products of PS80 and OA in	

SIFs at different molar ratio at B= -2.08 (short dashed line) and calculated progesterone concentration in model systems composed of selective lipolytic products of PS80 and OA in trisma buffer at different molar ratio at B=-2.68 (long dashed line).....	153
Figure 5.17b Comparison of the experimental equilibrium 17 $\beta$ -estradiol concentration in digested blank formulation (solid line), calculated 17 $\beta$ -estradiol concentration in model system composed of selective lipolytic products PS80 and OA in SIFs at different molar ratio at B= -1.76 (short dashed line) and calculated 17 $\beta$ -estradiol concentration in model systems composed of selective lipolytic products of PS80 and OA in trisma buffer at different molar ratio at B=-1.76 (long dashed line).....	154
Figure 5.17c Comparison of the experimental equilibrium nifedipine concentration in digested blank formulation (solid line), calculated nifedipine concentration in model system composed of selective lipolytic products PS80 and OA at different molar ratio at B= -1.35 (short dashed line) and calculated nifedipine concentration in model systems composed of selective lipolytic products of PS80 and OA in trisma buffer at different molar ratio at B=-1.30 (long dashed line).....	155
Figure 6.1 Response curve of electrode in pure water (open circle, E= 425.18+60.19logC, R=0.996), 0.15M NaCl solution(open square, E= 421.29+60.29logC, R=0.996 ), 1 mM PS80 (open triangle, E= 426.15+61.03logC, R=0.996), 10 mM PS80 (cross, E= 440.67+64.78logC, R=0.996) and 30 mM PS80 (star, E= 466.15+77.16logC, R=0.996) in 0.15M NaCl solution at 37°C. ....	159
Figure 6.2 <sup>1</sup> HNMR spectrum of PS80 in D <sub>2</sub> O buffer solution. ....	164
Figure 6.3 <sup>1</sup> HNMR spectrum of PS80/oleic acid (1/1) in D <sub>2</sub> O buffer solution.....	165
Figure 6. 4 The Stejskal-Tanner exponential plot. (Insert is attenuated signals from polyoxyethylene protons).....	166
Figure 6.5 Titration curves of ionized form of oleic acid in mixed micelle of PS80/oleic acid (9/1) at 37°C (n=3). Symbols are experimental data and solid lines are the calculated values by fitting the data to Eq. 6.1. ....	172
Figure 6.6 Titration curves of ionized form of oleic acid in mixed micelle of PS80/oleic acid (1/1) at 37°C (n=3). Symbols are experimental data and solid lines are the calculated values by fitting the data to Eq. 6.1. ....	173
Figure 6.7 The apparent diffusion coefficient of micelle of PS80 (diamond) and mixed micelle of PS80 with oleic acid (OA) at molar ratio 8/2 (cross), 6/4 (triangle) and progesterone saturated micelle of PS80 (circle) at 37±0.1°C. ....	177
Figure 6.8 D <sub>obs</sub> *[Surf] <sub>total</sub> change as total surfactant concentration in the aqueous solution of PS80 in the absence of bile salt/phospholipids.....	181
Figure 6.9 D <sub>obs</sub> *[Surf] <sub>total</sub> change as total surfactant concentration in the aqueous solution of PS80/oleic acid (8/2) in the absence of bile salt/phospholipids. ....	181
Figure 6.10 D <sub>obs</sub> *[Surf] <sub>total</sub> change as total surfactant concentration in the aqueous solution of PS80/oleic acid (6/4) in the absence of bile salt/phospholipids. .	182
Figure 6.11 The hydrodynamic radii of micelles measured by DLS method (triangle) and PGSE-NMR method (diamond) at different molar fraction of PS80 in the absence of bile salt/phospholipids. ....	183
Figure 6.12 <sup>1</sup> H chemical shifts on PS80 in the presence of progesterone. ....	189



Figure 6.13 $^1\text{H}$ chemical shifts on PS80 in the presence of $17\beta$ -estradiol.....	190
Figure 6.14 $^1\text{H}$ chemical shifts on PS80 in the presence of nifedipine.....	191
Figure 6.15 FTIR spectrum of neat PS80. ....	192
Figure 6.16 Relative change of absorption of C-O on POE chain and C=O on PS80 in PS80 solution prepared in the $\text{D}_2\text{O}$ saturated with nifedipine at 3 h, 24 h, 48 h and 72 h.....	194
Figure A1.1 HPLC chromatograms of nifedipine exposed to natural light at 2 h and 19 h at ambient temperature.....	204
Figure A1.2 The stability of nifedipine at ambient temperature (diamond) and $37\pm 0.5^\circ\text{C}$ (square) protected from exposing in nature light and the stability in the exposure to nature light at ambient temperature (triangle). ....	205
Figure A1.3a DSC plot of commercial nifedipine. ....	207
Figure A1.3b DSC plot of collected solid material from the determination of aqueous solubility of nifedipine in tris maleate buffer at $37^\circ\text{C}$ (pH7.5).....	211
Figure A3.1 The schematic presentation of radius of hydrophobic core ( $r_{\text{core}}$ ) and radius of micelle ( $r_{\text{micelle}}$ ). ....	213

## LIST OF SCHEMES

Scheme 2.1 The schematic presentation of advantage of LBDDSs for Class II drugs.....	7
Scheme 2.2 The summary of the possible mechanisms for enhanced adsorption in lipid-based drug delivery system in the GI tract (O'Driscoll, 2002). .....	12
Scheme 2.3 The lipolytic products of triglycerides. ....	20
Scheme 2.4 Lipid aggregates formed during digestion of lipids in the GI tract. ....	22
Scheme 2.5 Schematic presentation of drug released from LBDDS. ....	24
Scheme 4.1 The hydrolysis of PS80 by pancreatic lipase. ....	68
Scheme 4.2 Schematic present of the hydrophobic continuum pathway in the digestion of lipids.....	104
Scheme 4.3 Partitioning of drug between supersaturated micelle and aqueous solution.	104
Scheme 5.1 The schematic presentation of equilibrium between the mixed micelles of bile salt/ phospholipies and bile salt monomer, simple micelles of bile salt and vesicles.....	125
Scheme 5.2 Possible aggregates in the mixture of PS80 and oleic acid in the presence of NaC/PC. A, two populations of mixed micelles, PS80/OA and NaC/PC; B, one population of mixed micelle, PS80/OA/NaC/PC.....	135
Scheme 5.3 The equilibrium between ionized and unionized 17 $\beta$ -estradiol in aqueous phase and micelle phase.....	138
Scheme 6.1 Pulse sequence for pulsed-gradient stimulated spin-echo NMR.....	162
Scheme 6.2 Pulse sequence of inversion recovery for measurement of T1.....	167
Scheme 6.3 Possible arrangements of oleic acid in mixtures of PS80 and oleic acid. A and C, PS80/oleic acid (9/1); B and D, PS80/oleic acid (1/1) .....	174
Scheme 6.4 Possible loci of major amount of poorly-water soluble drugs in the micelles of PS80 and mixed micelles of PS80 with oleic acid. ....	187
Scheme 6.5 Secondary magnetic field induced by $\pi$ -electrons on the benzene ring. ....	188
Scheme 6.6a Possible loci of drugs in the PS80 micelles.....	197
Scheme 6.6b Possible loci of drugs in the PS80/oleic acid (1/1) mixed micelles.....	200

## Chapter 1

### Statement of Problems and Aims

Lipid-based drug delivery systems (LBDDSs) are one of several popular approaches to improving the oral absorption of poorly-water soluble drugs with high lipophilicity. Some proposed mechanisms of enhancing bioavailability include increasing the dissolution rate or maintaining the drug in solution through the GI tract. However, little is known about the creation and maintenance of poorly-water soluble drugs in their supersaturated state when the LBDDSs are subject to digestion in the GI tract. As a result, considerable challenges remain in selecting the formulation that will optimize oral absorption.

The goal of the current dissertation is to provide a better understanding of the capability of lipoidal components in LBDDS formulations to create and maintain drugs in a supersaturated state in simulated GI conditions. Moreover, molecular details of solubilization in terms of drug-aggregate interactions and lipid-lipid interactions in aggregates are explored. From a solubilization standpoint, evaluating the ability of each component of LBDDSs to induce and maintain the supersaturation of poorly-water soluble drugs will provide useful information for fully understanding the mechanism by which digestible surfactants and lipids modulate the oral absorption of poorly-water soluble drugs in the GI tract.

Two hypotheses are to be tested. The first hypothesis is that lipolysis of Polysorbate 80 in the model LBDDS results in a supersaturated state for model poorly-water soluble compounds and the extent of the supersaturation is dependent on the extent of hydrolysis of surfactant as well as on the initial concentration of the drug. The second hypothesis is that it is possible to relate the equilibrium solubilization of model drugs formulated in Polysorbate 80-oleic acid mixed micelles to the solubilization behavior of lipid aggregates generated during lipolysis of the surfactant formulation.

The specific aims are:

- 1) Demonstrate that the dynamic *in vitro* lipolysis model is a reliable and sensitive method to monitor the extent of lipolysis of ester-containing lipoidal excipients.
- 2) Demonstrate that lipolysis of Polysorbate 80 in formulations of the model drugs progesterone, estradiol and nifedipine will result in a supersaturated state for each and that the extent of supersaturation will be dependent upon the extent of hydrolysis of Polysorbate 80 as well as upon the initial drug concentration.
- 3) Determine drug solubilization in model mixed micellar systems and then fit micelle-water partition coefficients to the Treinor model. The solubilization values will be compared to those obtained during the *in vitro* lipolysis of Polysorbate 80.
- 4) Characterize the properties of model mixed micellar systems with respect to size, population and ionization state of the micellar oleic acid.
- 5) Probe the interaction of drugs with mixed micelles formed during lipolysis.

## Chapter 2

### Background and Literature Review

#### **2.1. Summary**

In this chapter, the background and literature review will focus on the following aspects: 1) methods used to enhance the solubility of poorly water-soluble drugs; 2) types of lipid-based drug delivery systems (LBDDSs) and the classification system of LBDDSs; 3) proposed mechanisms of enhanced oral absorption by LBDDSs; 4) excipients employed in LBDDSs and the effect of digestion of LBDDSs on the absorption of poorly water-soluble drugs; and 5) *in vitro* evaluation of the effect of lipolysis on LBDDSs and drug solubilization. Finally, several unanswered questions concerning the mechanism of solubilization of drugs by LBDDSs in the GI tract will be identified.

#### **2.2. Oral lipid-based drug delivery systems (LBDDSs)**

##### **2.2.1. Poorly water-soluble drugs**

Patient convenience, compliance, and low cost of production make the oral route the preferred means for the administration of most drugs. A prerequisite for oral absorption is the presentation of the drug in solution followed by subsequent passage across the gastrointestinal membrane. It is believed that the efficiency of drug absorption via the GI tract is strongly influenced by solubility and permeability (Amidon, Lennernäs et al., 1995) and as a result, the Biopharmaceutics Classification System (BCS) has been suggested as guidance for predicting intestinal absorption (Figure 2.1). Drugs in Class I with high solubility and high permeability can be absorbed readily. Drugs in Class II are highly permeable, but absorption is limited by poor solubility in the GI tract. In Class III, the absorption is limited by the permeation rate because the drug is highly soluble. Poor and highly variable absorption is expected for Class IV drugs that are both poorly soluble and poorly permeable. Combinatorial chemistry and high-throughput screening have increased the number of drug candidates in Class II with more than 40% of new active compounds exhibiting poor-water solubility (Lipinski, Lombardo et al., 2001). Moreover,

a high percentage of drug failures has resulted from the poor biopharmaceutical properties (Prentis, 1988).

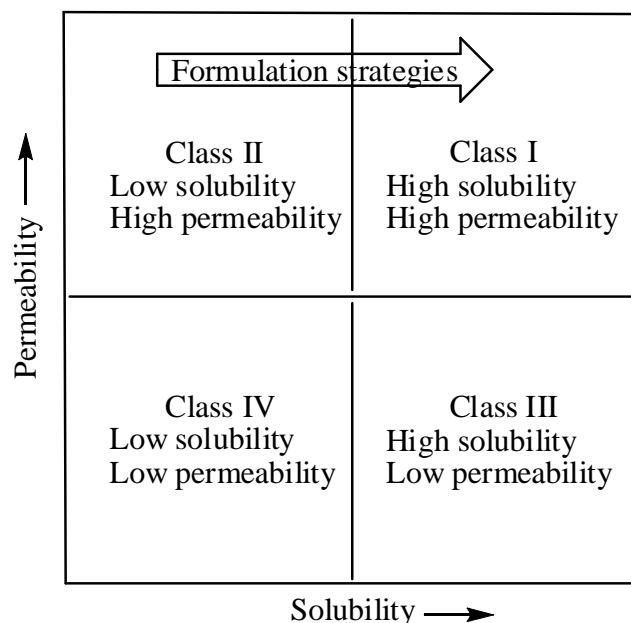


Figure 2.1 Biopharmaceutical Classification System

As indicated above, the rate-limiting step in the absorption of Class II drugs is solubilization. Increasing the dissolution rate or presenting and maintaining the drug in solution throughout the GI tract will potentially enhance absorption. Many methods can be used to enhance the solubility of Class II drugs in the GI tract and achieve a biopharmaceutical profile similar to Class I drugs. These approaches would include amorphous formulations, pH adjustment, salt formation, cosolvent-based formulations and lipid-based formulations (Gomez-Orellana, 2005). As expected, each method has advantages and disadvantages. Compared to the crystalline solid, an amorphous solid is in a higher free energy state, resulting in a higher solubility and dissolution rate. On the other hand, the physical stability is problematic, resulting in phase changes and possible precipitation. Adjustment of pH and salt formation are only suitable for molecules with ionizable groups. The chemical stability of drugs and biocompatibility at pH extremes are major concerns for these formulations. Large quantities of organic solvent used in cosolvent formulations may result in the loss of solvent capacity of the formulation upon dilution in aqueous media *in vivo*. Biocompatibility of surfactant excipients in lipid-based formulations is a major concern. Moreover, the effects of digestion of lipid excipients by

digestive enzymes in the GI tract on the solubilization of poorly water-soluble drugs are not clearly understood.

### **2.2.2. Oral lipid-based dosage forms**

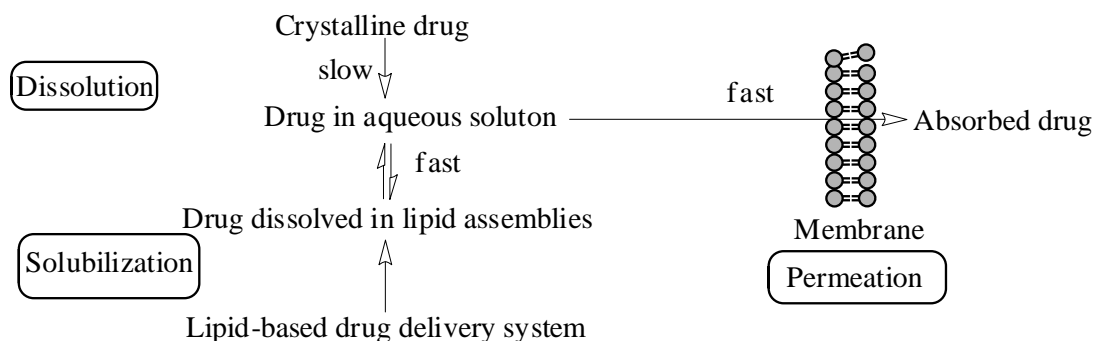
Despite the disadvantages listed, LBDDSs are gaining in popularity for oral applications. Typically, LBDDSs employ surfactants and oil to dissolve the drug in a concentrate suitable for administration. In some cases, cosolvents and some water may also be included. Upon dilution in aqueous media *in vivo*, the mixture of surfactant and oil may undergo morphological changes giving rise to assemblies such as micelles, bilayer vesicles, emulsions, microemulsions and solid particles. It is these assemblies that are responsible for dissolving poorly-water soluble molecules.

In the absence of an oil component, aggregates of surfactant molecules (micelles) are formed when the concentration of surfactant is above the critical micellar concentration. Depending on the type of phospholipids, different sizes and types of bilayer vesicles can be formed, such as small unilamellar vesicles (SUV, size~50 nm), large unilamellar vesicles (LUVs, size 100~1000 nm), multilamellar vesicles (MLVs) and multivesicular liposomes (MVLs) types. Emulsions include self-emulsifying drug delivery systems (SEDDSs) and self micro-emulsifying drug delivery systems (SMEDDSs). SEDDSs are systems composed of an easily dispersible mixture of oil, surfactants and drug, such that when diluted in the GI tract, they will form a fine oil-in-water emulsion with little or no energy input. SMEDDSs are somewhat similar in that they too form micro-emulsions spontaneously when diluted in the stomach. When diluted, SMEDDSs form small droplets such that the dispersion is clear, isotropic and thermodynamically stable. Solid particle LBDDSs are comprised of a solid or semi-solid lipid matrix in which the drug is in a crystalline, amorphous or solubilized state. A portion of the drug in the solid LBDDS dissolves rapidly upon dilution *in vivo*. Neoral<sup>®</sup> (cyclosporin A) and Kaletra<sup>®</sup> (lopinavir and ritonavir) are just two examples of highly successful LBDDS products.

As demonstrated in numerous studies, the oral bioavailability of drugs in Class II can be improved by LBDDSs (Chakrabarti, 1978; Tokumura, Tsushima et al., 1987; Pouton, 1997; Hauss, Fogal et al., 1998; Neslihan Gursoy and Benita, 2004; Pouton, 2006; Atef and Belmonte, 2008; Porter, Pouton et al., 2008; Balakrishnan, Lee et al., 2009; Kohli,

Chopra et al., 2010; Khamkar, 2011). The advantages of LBDDSs for enhancing drug absorption are demonstrated in Scheme 2.1. LBDDSs are thought to influence the process of dissolution and solubilization of poorly water-soluble drug in the GI tract. The primary mechanism of action leading to improved absorption is presenting the drug in the solubilized state, avoiding the slow dissolution rate associated with most poorly-water soluble drugs from solid dosage forms. Additionally, lipid aggregates may prevent the precipitation of drug during transit through the GI tract. Excipients such as triglycerides and surfactants in LBDDSs, and the associated lipid digestion products may act as absorption enhancers by altering the barrier properties of the membrane by increasing lipid membrane fluidity and/or interacting with hydrophilic domains of the membrane (Aungst, 2000). In addition to passive diffusion, drugs can also be absorbed by active and facilitated transport (Hunter, Hirst et al., 1993; Kim, Fromm et al., 1998; Suzuki and Sugiyama, 2000; Borst and Elferink, 2002). Enhancement of influx transporters or inhibition of efflux transporters will increase the intracellular drug concentrations (Chiu, Higaki et al., 2003). Several excipients commonly used in LBDDSs, such as Cremophor, d-alpha tocopheryl polyethylene glycol 1000 succinate (TPGS) and Polysorbate 80, are believed to inhibit P-gp mediated efflux resulting in enhanced oral drug absorption (Chiu, Higaki et al., 2003; Cornaire, Woodley et al., 2004; Constantinides and Wasan, 2007). Studies have suggested that high fat meals could inhibit P-gp mediated efflux due to stimulated secretion of endogenous bile salts and phospholipids (Frijters, Ottenhoff et al., 1997). In the remainder of this chapter, the focus will be on drug solubilization by LBDDSs with emphasis on the effect of lipid digestion of these formulations.





Scheme 2.1 Advantage of LBDDSs for enhancing absorption of Class II drugs

### 2.2.3. Classification of LBDDS formulations

Pouton (Pouton, 2000) introduced the Lipid Formulation Classification System (LFCS) to categorize LBDDSs into four different types based on their excipient composition and the morphology of lipid aggregates formed upon dilution in aqueous media (Table 2.1). The LFCS enables *in vivo* studies to be interpreted more readily and facilitates the identification of the most appropriate formulations for a particular drug. As shown in Table 2.1, the Type I formulations are composed of oils without surfactants. Depakene® (valproic acid formulation in corn oil), Marinol® (dronabinol in sesame oil) and Prometrium® (progesterone in peanut oil) are a few examples of commercial Type I formulations. Type I formulations are not readily dispersed upon dilution. Digestion of the lipid excipients in the GI tract is generally required for the drug to be released from the formulation. Non-digestible lipids such as mineral oil tend to retain poorly water-soluble drugs within the oil phase resulting in limited drug release and poor absorption (Charman, Porter et al., 1997; Dahan, 2006). Type I formulations may not always provide sufficient solubilization capacity to dissolve the required dose in a reasonable quantity of oil. The most frequently employed LBDDS formulations on the market are Type II and Type III. The introduction of surfactants and cosolvents to the oils improves the solubilization capacity and dispersibility of formulation upon dilution in aqueous media such as gastric fluid. Type II and Type III formulations rapidly and spontaneously form fine oil-in-water emulsions (particle size > 200 nm, opaque) or microemulsions (particle size < 200 nm, optical clear or slightly opalescent). The drug is present in fine droplets of oil/surfactant mixture with a large oil/water interfacial area (Charman, Charman et al., 1992; Mueller, Kovarik et al., 1994; Shah, Carvajal et al.,

1994). As a result of the large interfacial area both the rate of drug release and formation of mixed micelles of lipolytic products to solubilize the poorly water-soluble drug are enhanced. How the large oil/water interfacial area facilitates the hydrolysis of lipids will be discussed in Section 2.4.1.

Oil is not included in Type IV formulations. Upon dilution in aqueous media, a micellar solution is formed leading to rapid drug release and enhanced drug absorption. However, surfactants alone are rarely used as formulations and require cosolvents to aid in dispersion. The major question with this type formulation is whether it is capable of preventing the drug from precipitating as the formulation is diluted during transit through the GI tract. Moreover, the sensitivity of the GI tract to high concentrations of surfactants impedes the application of Type IV systems, and few Type IV formulations are on the market. Examples of Type IV formulations are Agenerse® (amprenavir formulation in TPGS, PEG400 and PEG) and Targretin® (bexarotene formulation in Polysorbate 20, PEG400, povidone and BHA).

Table 2.1 The Lipid Formulation Classification System (Pouton, 2000; Pouton, 2006)

Formulation type	Excipients in formulation	Characteristics
Type I	Oils (tri-, di- and monoglycerides) without surfactants	Non-dispersing, requires digestion
Type II	Oils and water-insoluble surfactants (HLB<12)	SEDDS formed without water-soluble components
Type III	Oils, surfactants and cosolvents	SEDDS/SMEDDS formed with water – soluble components
Type IV	Water-soluble surfactants (HLB>12) and cosolvent, but no oils.	Formation of micellar solution

Table 2.2 is a list of lipid excipients used in marketed LBDDSs. The list reveals that most commonly used pharmaceutically-relevant lipid excipients include fatty acids,

natural oils and fats, semi-synthetic mono-, di- and triglycerides, semi-synthetic polyethylene glycol (PEG) derivatives of glycerides and fatty acids, polyglycerol esters of fatty acid, cholesterol and phospholipids. In general, these lipid excipients are fatty acids and fatty acid esters. Natural oils and fats are mixtures of fatty acid tri-esters of glycerol (triglycerides) (Figure 2.2). Based on the fatty acids, triglycerides can be categorized as having short (<5), medium (6-12) or long (>12) hydrocarbon chains. Compared to the oils and fats from natural sources, semi-synthetic lipid excipients provide more uniform compositions (Bhat, Dar et al., 2008). Even in the semi-synthetic excipients variability exists in the relative positions on the glycerol backbone to which the individual fatty acids are esterified.

Fatty acids and their ester derivatives are prone to oxidation and hydrolysis. The oxidation can be catalyzed by impurities such as peroxides, metal ions and photochemical sensitizers (Hauss, 2007). Hydrolysis could be either chemical or enzymatic. For example, the rate of hydrolysis of phosphatidylglycerol has been shown to be pseudo-first order and to depend strongly on the pH and temperature (Crommelin, Talsma et al., 1993; Crommelin and Schreier, 1994). Also, it has been shown in the dissertation and by others that phospholipids are susceptible to hydrolysis upon exposure to pancreatic lipase preparations (Kossena, Boyd et al., 2003).

Table 2.2 Solubilizing excipients used in commercially available LBDDSs (Haus, 2007)

Water insoluble excipients	Triglycerides	Surfactants
Beeswax	Corn oil	Glycerol monooleate
Oleic acid	Olive oil	Polyoxyl 35 castor oil (Cremophor EL)
Soy fatty acids	Peanut oil	Polyoxyl 40 hydrogenated castor oil (Cremophor RH40)
d- $\alpha$ -tocopherol (Vitamin E)	Rapeseed oil	Polyoxyl 60 hydrogenated castor oil (Cremophor RH60)
Corn oil mono, diglycerides	Sesame oil	Polysorbate 20 (Tween 20)
Medium-chain mono, diglycerides	Soybean oil	Polysorbate 80 (Tween 80)
Propylene glycol esters of fatty acids	Hydrogenated soybean oil	d- $\alpha$ -tocopherol polyethylene glycol 1000 succinate (TPGS)
	Hydrogenated vegetable oil	Sorbitan monolaurate (Span 20)
		PEG 300 oleic glycerides (Labrafil <sup>®</sup> M-1944CS)
		PEG 300 linoleic glycerides (Labrafil <sup>®</sup> M-2125CS)
		PEG 400 caprylic/capric glycerides (Labrasol <sup>®</sup> )
		PEG 1500 lauric glycerides (Gelucire <sup>®</sup> 44/14)

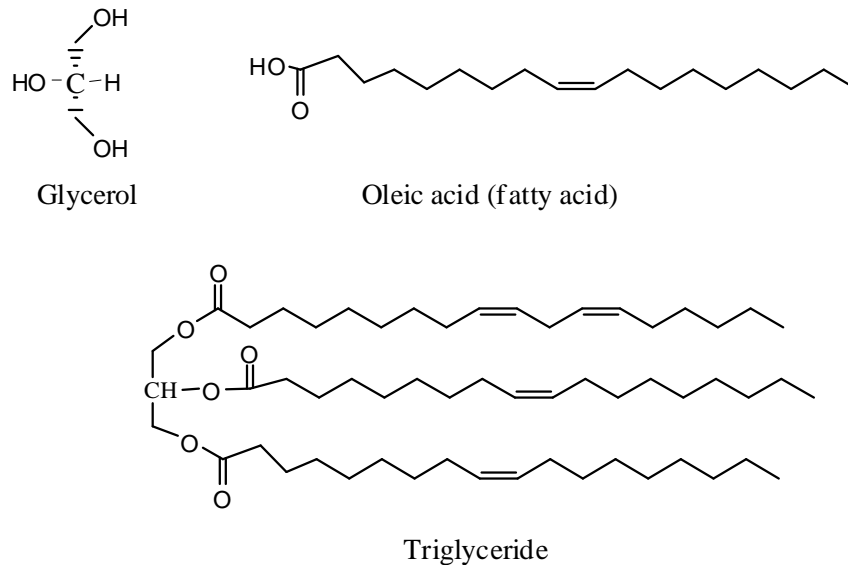
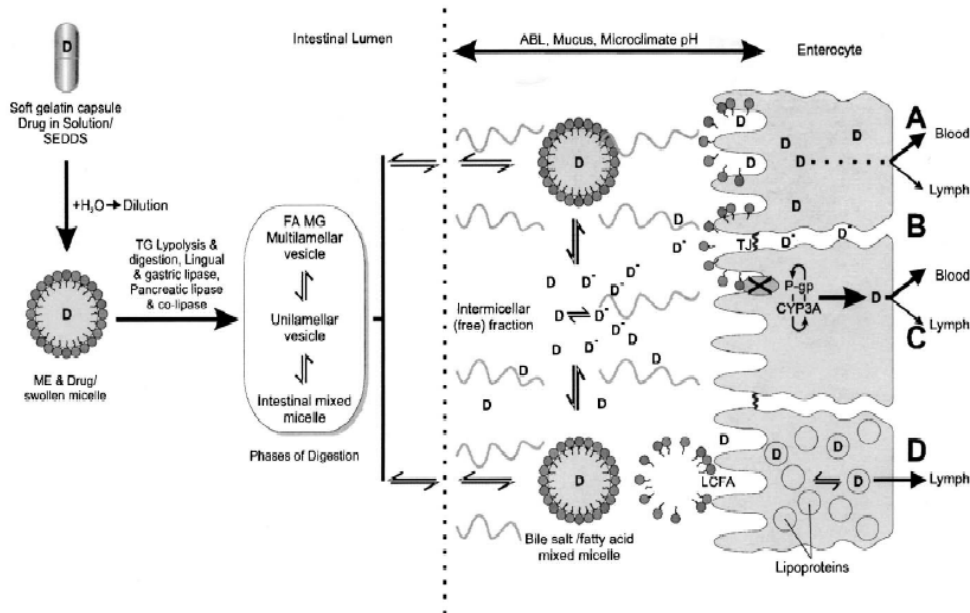


Figure 2.2 Structure of a triglyceride and its components

### 2.3. Proposed mechanisms of absorption enhancement by LBDDSs

Drug absorption across the intestinal membrane is a complex multi-pathway process. Scheme 2.2 summarizes the possible routes of absorption in the GI tract of a poorly water-soluble drug formulated in an LBDDS. With the aid of various lipid aggregates, the poorly water-soluble drug is present in a solubilized state and may experience facilitated diffusion through the unstirred water layer. Upon reaching the gut wall, molecules can be absorbed passively through transcellular and paracellular routes. Passage of drug across a biological membrane can also be facilitated by an active or facilitated transporter. For highly lipophilic molecules ( $\log P > 5$ , solubility in long chain triglycerides  $> 50$  mg/mL), lymphatic transport is a significant route of absorption (Hauss, Fogal et al., 1998; Gershkovich and Hoffman, 2007; Gershkovich, Qadri et al., 2007). Multiple routes of transport make it difficult to apply a single model to accurately predict drug absorption in the GI tract. Based on these routes, the mechanisms by which LBDDSs enhance oral absorption can be divided into two categories – physicochemical mechanisms and biological/biochemical mechanisms. Biological and biochemical mechanisms will be covered in Section 2.3.1. The physicochemical mechanisms will be covered in Section 2.3.2.



Scheme 2.2 The summary of the possible mechanisms for enhanced drug absorption from a lipid-based drug delivery system in the GI tract (O'Driscoll, 2002)

### 2.3.1. Biological and biochemical mechanisms

There are several possible biological and biochemical mechanisms to enhance the absorption of drugs formulated in LBDDSs. Ingested lipids, especially triglycerides and long chain fatty acids, effectively inhibit gastric motility resulting in prolonged residence times of co-administered drugs in the small intestine (Raybould, Meyer et al., 1998; Fleisher, Li et al., 1999; Van Citters and Lin 1999; Mu and Porsgaard, 2005). Consequently, the drugs have more time to dissolve and spend a longer time at the absorptive site, thereby improving absorption.

A variety of lipids have been shown to alter the barrier properties of GI membranes by increasing membrane fluidity, opening tight junctions, or interacting with hydrophilic membrane domains (Constantinides and Wasan, 2007). As mentioned previously, inhibition of efflux transporters in the GI tract has been shown to be an effective mechanism to increase the fraction of drug absorbed (Nerurkar, Burton et al., 1996; Dintaman and Silverman, 1999). Moreover, this mechanism may reduce intra-enterocyte metabolism due to the interplay between P-gp and CYP3A4. Many surfactants used in LBDDSs, such as TPGS, Labrasol and Polysorbates, can inhibit efflux transporters

resulting in enhanced oral absorption (Cornaire, Woodley et al., 2004; Varma and Panchagnula 2005; Yamagata, Kusuhara et al., 2007).

The majority of digested products and poorly-water soluble drugs gain access to the systemic circulation via the portal vein. However, highly lipophilic molecules ( $\log P > 5$ , solubility in long chain triglycerides  $> 50$  mg/mL) or large macromolecules can enter the systemic circulation via the lymphatic system (Li, Fleisher et al., 2001; Martinez, Amidon et al., 2002). This alternative absorption pathway has been shown to contribute significantly to the overall bioavailability of poorly-water soluble drugs formulated in LBDDSs (Kuksis 1987; Hauss, Fogal et al., 1998; Khoo, Edwards et al., 2001; Holm, Porter, et al., 2003; Karpf, Holm et al., 2004; Grove, Nielsen et al., 2006; Dahan, Mendelman et al., 2007). The intracellular association of the drug with the lipidic core of chylomicrons is considered to be the primary mechanism of intestinal lymphatic drug absorption.

### **2. 3.2. Physicochemical mechanisms**

The primary mechanism of enhanced absorption by LBDDSs is the solubilization of poorly water-soluble drugs in the GI tract. A number of studies have correlated the solubilization behavior of poorly-water soluble drugs with oral bioavailability (Christensen, Schultz et al., 2004; Porter, Kaukonen et al., 2004; Grove, Pedersen et al., 2005; Goddeeris, Coacci et al., 2007). All these studies were conducted in an attempt to determine the factors influencing the solubilization of drugs and improving the design of LBDDSs to increase the oral absorption of poorly water-soluble drugs. Namely, these factors are the physicochemical properties of the drug, the rate and extent of digestion of LBDDSs, the digestion products formed, the properties of lipid aggregates generated during the digestion of LBDDSs and the rate of drug transfer between the various lipid assemblies and the aqueous phase. Saquinavir is an example of a drug that exhibited improved bioavailability from an LBDDS formulation. The bioavailability of its mesylate salt was highly variable and as low as 4%. In an attempt to improve absorption, the free base was formulated in an LBDDS composed of medium chain mono- and diglycerides. The bioavailability of Saquinavir in humans given the LBDDS formulation improved 3-times over that of the salt (Perry and Noble, 1998). Subsequent studies in rats showed that the enhanced solubilization and permeability of the free base in the lipid-rich

intestinal environment led to the increased bioavailability (Griffin and O'Driscoll, 2006). The solubilization mechanisms for the enhanced oral absorption were further demonstrated by *in vivo* evaluation of dexamethasone and griseofulvin in LBDDSs composed of long, medium or short chain triglycerides (Dahan and Hoffman, 2007). Equivalence of bioavailability was observed in dexamethasone from the different LBDDSs. Conversely, the oral bioavailability of griseofulvin was dependent upon the nature of lipid excipients with the highest oral bioavailability in medium chain triglyceride LBDDSs. The solubilization and distribution pattern across the different phases formed from the *in vitro* lipolysis of all three LBDDSs revealed that a high fraction of dexamethasone was solubilized in the aqueous phase. On the other hand, griseofulvin had the highest solubility in medium chain triglycerides whereas a lower amount of drug was solubilized in long chain triglycerides. The poorest solubility was observed during lipolysis of the formulations containing short chain triglycerides.

For a BCS Class II molecule in solution, ignoring biological factors, diffusion across the unstirred water layer is the rate-limiting step for absorption. Incorporation into lipid aggregates facilitates lipid and drug absorption by overcoming the resistance of the unstirred water layer. In 1982, Amidon et al. provided a physical model which described the simultaneous diffusion of free drug and micelle-solubilized drug across the aqueous boundary layer associated with a silastic membrane (Amidon, Higuchi et al., 1982). According to Fick's First Law, the rate of drug transport is proportional to its diffusivity and concentration gradient. Enhanced mass transport of drug resulting from solubilization and facilitated diffusion by a variety of lipid aggregates has been demonstrated (Land, Li et al., 2006).

Transit of oral LBDDSs through the GI tract is a dynamic process in which some excipients are susceptible to digestion. Consequently, the solubilization and distribution pattern of the drug may change as a function of time *in vivo*. A study of danazol LBDDS formulations in fasted beagle dogs demonstrated that the solubilization of drug in the intestinal fluid is critical for drug bioavailability (Kossena, Boyd et al., 2003). Danazol was formulated in a simple long chain triglyceride solution, in a SEDDS composed of long chain lipids and in a SEDDS containing medium chain lipids. Relative to the SEDDS with medium chain lipids, a significant increase in oral bioavailability was



observed in the long chain triglycerides solution and SEDDS containing long chain lipids. An *in vitro* assay revealed that over 70% of the drug precipitated during the lipolysis of SEDDS containing medium chain lipid excipients. On the other hand, the SEDDS containing long chain lipids resulted in over 90% danazol solubilized despite the lipolysis of lipid. For the same drug, Cuiné et al. showed that, in beagle dogs, the loss of solubilization capacity of the aggregates formed in the digestion process could result in a decrease in oral bioavailability (Cuiné, McEvoy et al., 2008). However, in all these studies, apparent solubilization of poorly water-soluble drugs was investigated only in the lipid aggregates present at the end of the experimental period. The time-dependent effect of alteration of the solution composition during lipolysis on the solubilization was not addressed.

As has been stated previously, absorption requires the partitioning of drug from the aqueous phase to the enterocyte. Thus poor solubility of a drug in the aqueous phase limits absorption. For Class II molecules where the total amount of drug solubilized in lipid aggregates is great, the fraction of drug free in solutions remains quite small (Poelma, R. et al., 1991; Chiu, Higaki et al., 2003). Higuchi was among the first to recognized the potential impact of supersaturation in the aqueous phase on the transport of drugs through biological membranes (Higuchi, 1960). Supersaturation creates an intraluminal free drug concentration in excess of the drug's equilibrium solubility. The increased thermodynamic activity of drug results in a pronounced enhancement of the uptake flux. It has been suggested that the enhanced absorption observed in studies of LBDDSs may result from supersaturation upon dilution in aqueous media in the GI tract. A successful example of utilizing the supersaturation strategy is the development of SEDDSs of paclitaxel. The marketed paclitaxel formulation for I.V. administration (Taxol<sup>®</sup>) contains drug solubilized in ethanol and a high concentration of the surfactant Cremophor EL. However, the same dosage form did not provide therapeutic drug plasma concentrations in rats when administrated orally. Gao et al., developed a new dosage form containing a reduced amount of surfactant and included the polymer HPMC as a precipitation inhibitor (Gao, Rush et al., 2003). The drug was maintained in a supersaturated state when the HPMC-containing formulation was diluted in biorelevant media. Furthermore, it was found that the rate of drug precipitation from the

supersaturated state was significantly slowed. Oral administration of HPMC-containing formulations in rats resulted in five-fold higher AUCs compared to orally-administered Taxol<sup>®</sup>. Enhanced bioavailability was also observed in the supersaturable SEDDSs of AMG517 and PNU-91325 (Gao, Guyton et al., 2004; Gao, Akrami et al., 2009). These results suggested that the increased free drug concentration exceeding the saturation solubility was a major mechanism of enhancement of the oral bioavailability of poorly water-soluble drugs. However, the mechanism of creating and maintaining drugs in a supersaturated state induced by LBDDSs *in vitro* and *in vivo* is not clear, especially when the critical excipients of LBDDSs are subject to digestion. The capability of lipid aggregates to create and maintain drugs in a supersaturated state has not been adequately addressed in the literature.

#### **2.4. Enzymatic hydrolysis of lipids**

Many excipients employed in LBDDSs contain one or more ester bonds (see Section 2.2.2) that may be sensitive to hydrolysis by gastric or pancreatic lipase enzymes. Of critical importance to this dissertation is the extent to which lipolysis influences the structure of lipid assemblies and the accompanying solubilization enhancement *in vivo*. Covered in Section 2.4.1 will be details of the enzymatic hydrolysis of various lipids and the morphology of the digests. In Section 2.4.2, the digestion of LBDDS formulation excipients will be reviewed. The goal will be to examine the means by which lipolysis of LBDDSs is studied *in vitro*, and the linkage of lipolysis to the solubilization of poorly water-soluble drugs.

##### **2.4.1 Digestion of lipids**

Since Crouse first reported the food-dependent bioavailability enhancement of griseofulvin, food effects on bioavailability of drugs has drawn much attention (Crouse 1961; Winstanley and Orme 1989; Amidon, Lennernäs et al., 1995; Charman, Porter et al., 1997; Dressman, Amidon et al., 1998; Hörter and Dressman, 2001). Studies of the mechanisms of food effects revealed that the ability of dietary lipids to be digested in the GI tract plays an important role in determining the rate and extent of drug absorption (Hunt and Knox 1968; Ladas, Isaacs et al., 1984; Cunningham, Baker et al., 1991; Feinle, Rades et al., 2001). The enzymatic hydrolysis of lipids will result in changes in the

composition and morphology of aggregates. Potentially, the solubilization capability of these assemblies will be altered.

Fats and oils are the most significant dietary lipids. Typically, there are four distinct steps in lipid digestion in the GI tract: emulsification, hydrolysis at the emulsified oil droplets surface, micellization, and uptake through enterocytes (Figure 2.3). It is believed that emulsification facilitates the access of substrates to the oil/water (o/w) interface where the digestive enzymes gastric lipase and pancreatic lipase/colipase are bound preferably (Aloulou, Rodriguez et al., 2006). The most common emulsifying agents in the acidic environment of the stomach include dietary phospholipids, peptic digests of dietary proteins and complex polysaccharides, all of which adsorb strongly at the oil/water interface. In addition to these emulsifying agents, digestion products such as monoglycerides and fatty acids may also help to stabilize the crude emulsion. About 15% of triglycerides are hydrolyzed by gastric lipase to release fatty acids. Released fatty acids play two roles in the stomach (Mazer and Carey, 1983). Firstly, they inhibit further hydrolysis in the stomach by blocking the accessibility of enzyme to the o/w surface resulting in partial hydrolysis. Secondly, they promote the emulsification of oil upon dilution in intestinal fluid. Compared to short or medium chain fatty acids which are soluble in the aqueous phase in either ionized or unionized forms, protonated long chain fatty acids are unable to dissociate from the oil droplets and stay at the o/w interface under the acidic conditions of the stomach.

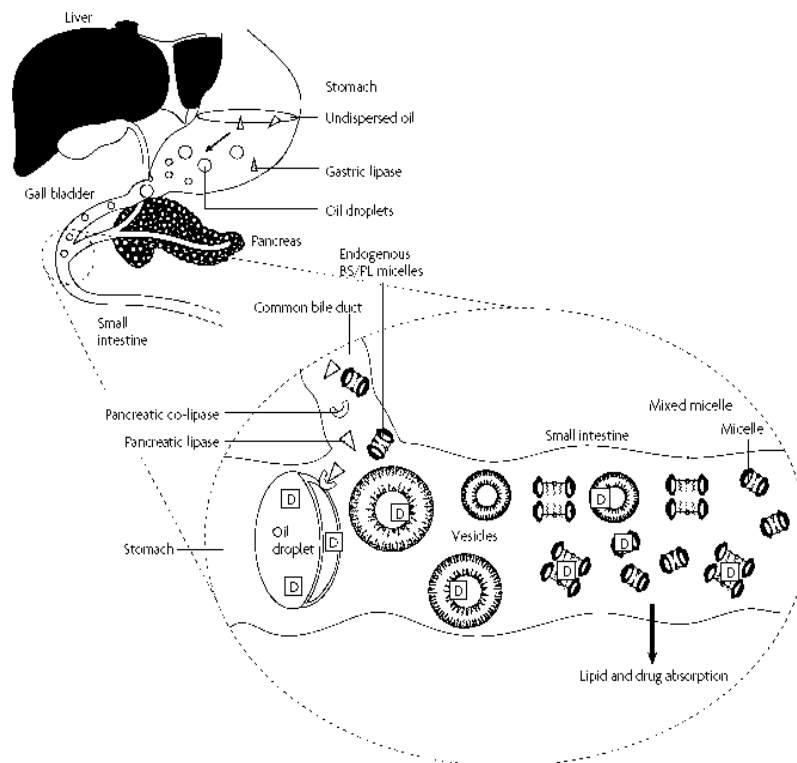
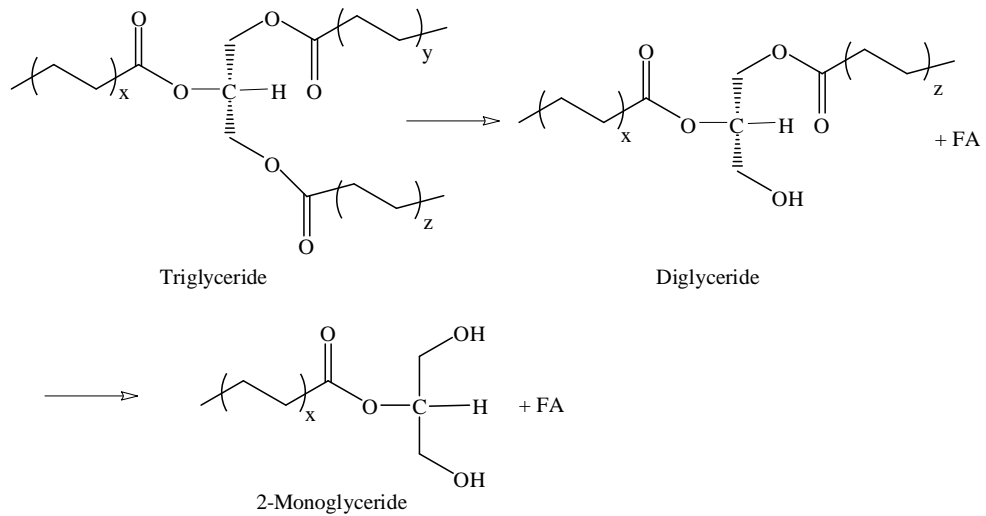


Figure 2.3 General process of lipid digestion in the GI tract (Yamagata, Kusuhara et al., 2007)

The majority of lipid digestion is carried out in the small intestine by pancreatic lipase/colipase. Other enzymes, such as carboxylic-ester hydrolase, may also be involved in the hydrolysis of lipids (Fernandez, Jannin et al., 2007; Fernandez, Rodier et al., 2008). The presence of lipids in the duodenum stimulates secretion of bile salts, biliary lipids and pancreatic lipase/colipase. Enzymatic hydrolysis of lipids occurs at the surface of the emulsified oil droplets followed by formation of mixed micelles with bile salt and biliary lipids (Khosravi, Kao et al., 2002; Seeballuck, Ashford et al., 2003). Normally, the 1, 3-ester bonds on the glycerol backbone are hydrolyzed in two steps to release free fatty acids and monoglycerides (Scheme 2.3) (Mattson and Beck, 1955). The catalytic mechanism of pancreatic lipase is similar to that of serine proteases in which the active site is comprised of a serine, histidine and an acidic amino acid as a catalytic triad (Figure 2.4) (Garrigues, Segura-Bono et al., 1994). In the presence of an o/w interface, the enzyme is activated by interfacial binding, resulting in its full catalytic activity. Crystal structure studies suggest that interfacial binding triggers a conformation change and

movement of a lid domain and some surface loops allowing the substrate access to the active site (Winkler, D'Arcy et al., 1990). The conformation change of the lid domain and the  $\beta$ -5 loop changes the environment of the catalytic triad dramatically. In the open, conformation serine is more accessible to solvent and orients to the bottom of a hydrophobic pocket where it binds the lipid substrate. In addition to the active site, a second binding site is required for the lipase to bind on the o/w interface. However, the pancreatic lipase is easily replaced by bile salts either by solubilization by bile salt micelles, or by competition for the interface (Patton, Albertsson et al., 1978). A cofactor, colipase, is needed to facilitate the binding of lipase on the surface. For colipase, an interfacial recognition site and a pancreatic lipase binding site are required for activity. It has been shown that the binding of colipase to lipase is independent on ionic strength and inhibited by bile salt at concentrations in excess of the CMC (Patton, Albertsson et al., 1978). The neutron crystal structure suggests that micelles help to stabilize the open conformation of the lipase-colipase complex prior to binding to the o/w interface (Hermoso, Pignol et al., 1997). Micelles with radii of gyration between 13 and 36 Å are able to bind to the lipase-colipase whereas smaller micelles or monomer cannot stabilize the complex for activation of the enzyme. Recently, Freie et al. suggested that bile salt micelles impact the binding of lipase-colipase by interaction with the  $\beta$ -5 loop (Freie, Ferrato et al., 2006).



Scheme 2.3 The lipolytic products of triglycerides

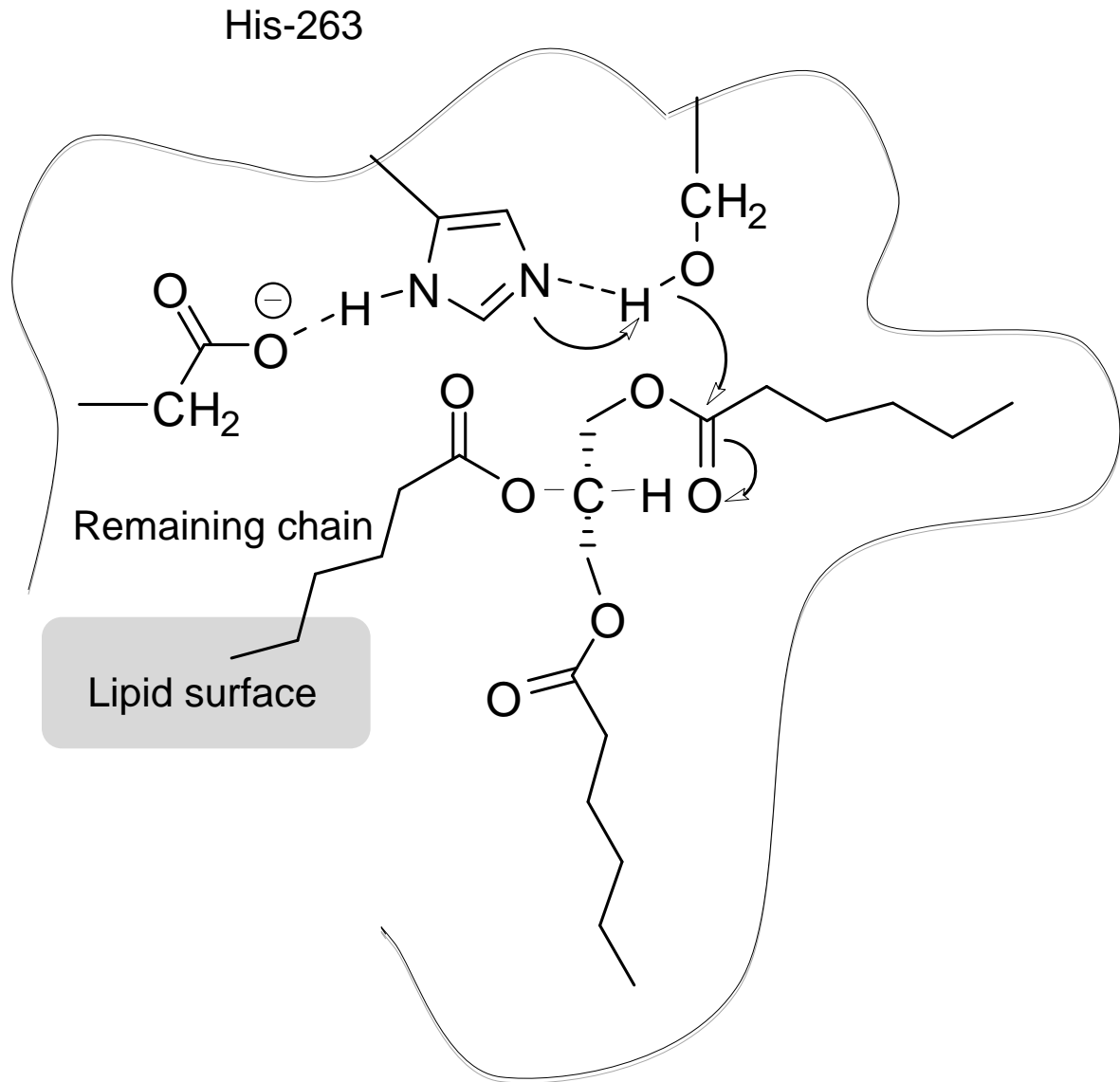
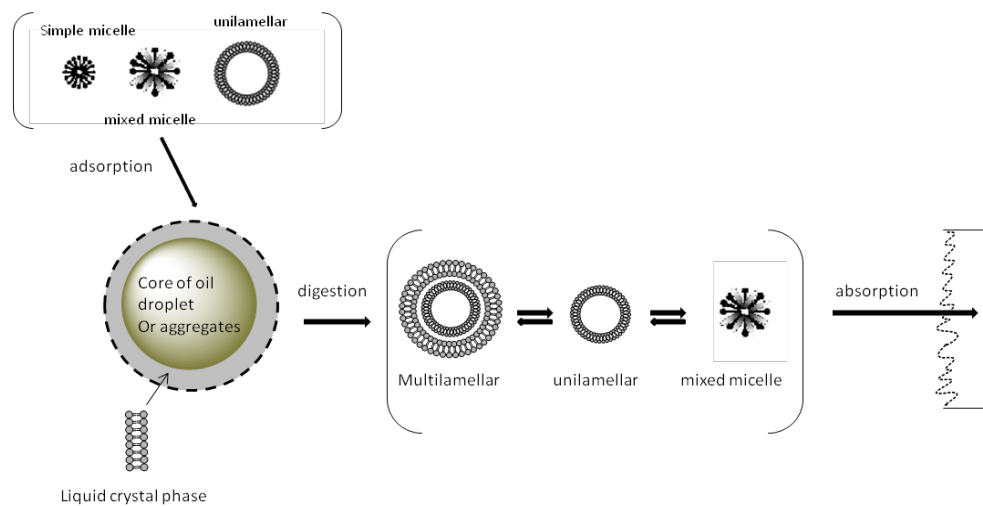


Figure 2.4 The mechanism of hydrolysis of triglyceride by a catalytic triad including serine, histine and an acidic amino acid

In the 1960s, Hofmann and Borgstrom concluded that there are two phases present during lipid digestion. One phase, rich in triglyceride and diglyceride, is called the oily phase. The other phase, called the aqueous micellar phase, contains bile salt and lipolytic products such as monoglycerides and fatty acids (Hofmann and Borgström, 1962; Hofmann and Borgström, 1964). However, their model could not explain the turbid appearance of the aqueous phase since the micelle solution should be optically clear and free of light-scattering particles. Using light microscopy, Patton and Carey identified a

viscous, gel-like, birefringent phase layered between the oily and aqueous micellar phases (Patton, Vetter et al., 1985). This liquid crystalline phase can be solubilized in the presence of unsaturated bile salt micelles. Lipolytic products, such as monoglycerides and fatty acid, localize at the oil surface forming a local liquid crystalline phase. Spontaneously, the liquid crystalline phase erodes into the aqueous phase to form multilamellar vesicles, unilamellar vesicles and mixed micelles containing bile salts and phospholipids (Scheme 2.4). Formation of bile salt mixed micelles facilitates the uptake of lipolytic products, such as fatty acid, in the GI tract (Westergaard and Dietschy, 1976). The rate of uptake of fatty acid is dependent upon the physicochemical properties of the fatty acid and the concentration of bile salts. At a constant concentration of bile salts, the rate of fatty acid uptake is a linear function of the concentration of fatty acid in the bulk phase (Westergaard and Dietschy, 1976). Increasing the concentration of bile salts increases the rate of uptake of fatty acids (Clark, Lanz et al., 1969).



Scheme 2.4 Lipid aggregates formed during digestion of lipids in the GI tract

Cryogenic transmission electron microscopy and small angle x-ray scattering measurements have revealed the entire sequence of the phase transitions during *in vitro* lipolysis of LBDDSs (Fatouros, Deen et al., 2007; Fatouros, Bergenstahl et al., 2007). The results were consistent with a previously proposed model in which micelles co-exist with multilamellar and unilamellar vesicles (Rigler, Honkanen et al., 1986). Typically, the *ex vivo* mean hydrodynamic radii of micelles are less than 40 Å whereas the unilamellar vesicles are in the range of 20-60 nm, as determined by quasielastic light

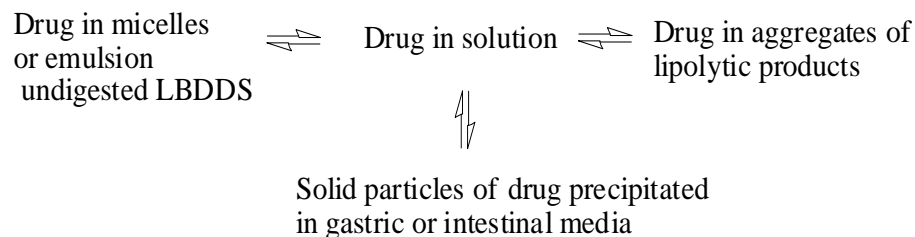


scattering (Staggers, Hernell et al., 1990). About 10 nm micelles were also observed during lipolysis. Transformation of oil droplets to spherical or elongated unilamellar vesicles was visualized by the combined use of cryo-TEM, small angle x-ray and *in vitro* dynamic lipolysis (Fatouros, Bergenstahl et al., 2007).

#### **2.4.2. Evaluation of effect of lipolysis on LBDDSs and drug solubilization**

The availability of a drug in the solubilized state during transit in the GI tract depends upon the rate and extent of the drug released from the formulation and upon the solubility of the drug in the GI fluids. Evaluation of the performance of LBDDSs must take into account formulation dispersibility and digestibility, as well as the kinetics of drug transfer between the digested formulation and the aqueous solution. The LBDDSs often must be emulsified by endogenous emulsifiers in the stomach and small intestine to form fine oil droplets to expedite the drug release. In addition to the triglycerides, ester-bond containing surfactants, such as Polysorbate 80, Cremophor RH40, Cremophor EL, Labrasol and Gelucire 44/14, can be hydrolyzed by gastric lipase in the stomach and pancreatic lipase in the small intestine (Fernandez, Jannin et al., 2007; Cuiné, McEvoy et al., 2008; Fernandez, Rodier et al., 2008; Fernandez, Chevrier et al., 2009). In principle, hydrolysis of these excipients can result in altered - either increased or decreased - solubilization power. Studies on solubilizing power of mixed micelles formed from hydrolysis products of LBDDS excipients have not been reported.

When formulated in the liquid LBDDS, the drug will be released to the aqueous media by a partitioning process (Scheme 2.5). The availability of free drug in aqueous solution for oral absorption may be limited by the rate of drug release from micelles and emulsions of undigested LBDDSs as well as lipid aggregates of lipolytic products. When the drug is formulated as a solid LBDDS, dissolution of drug from solid particles may also serve as a rate-limiting step for releasing the drug into the aqueous solution.



Scheme 2.5 Schematic presentation of drug released from LBDDS

In order to help formulators assess and predict the *in vivo* performance of oral LBDDSs, several *in vitro* tests have been developed. The dispersion/precipitation test is designed to assess the dispersibility of formulation, size distribution of formed lipid aggregates upon dilution of an LBDDS, and the solubilization of drug. The method has been accepted as important test for oral formulation screening and development (Vinod, 2005). For oral LBDDS formulation, the dispersion/precipitation of LBDDSs can be carried out in the USP dissolution methods with a basket (USP I) or a paddle (USP II). The dispersibility can be evaluated visually. The size and distribution of lipid aggregates can be evaluated by laser light diffraction or photon correlation microscopy. The effect of dilution upon size distribution and solubilization capacity of formed lipid aggregates has been investigated employing this test (Ilardia-Arana, Kristensen et al., 2006; Cuiné, McEvoy et al., 2008). The rate and extent of drug precipitation can be determined by measuring total amount of the drug remaining in solution as a function of time. By measuring the drug concentration in the solution during dispersion for different LBDDS formulations, Mohsin et al. suggested that the use of hydrophilic formulations for delivery of lipophilic drugs may result in a greater extent of drug precipitation in the stomach (Mohsin, Long et al., 2009). A correlation between drug *in vivo* precipitation and oral bioavailability has been observed (Dai, Dong et al., 2007; Dai, 2010).

Drug release test is designed to determine the rate of drug release from formulation in the simulated physiological environment of the GI tract. In drug release test, only the free drug concentration in the aqueous solution is determined. When poorly water-soluble drug is formulated in the LBDDS, the test is complicated by the fact that the free drug must be separated from that associated with lipid aggregates prior to the determination of free drug concentration. A variety of methods are used to measure the *in vitro* drug

release from lipid aggregates, such as membrane diffusion techniques, *in situ* methods, and continual flow methods (Washington, 1990; Abdel-Mottaleb and Lamprecht, 2011).

The *in vitro* lipolysis test is designed to probe the extent of drug precipitation under intestinal conditions. The test simulates the intestinal conditions by adding pancreatic lipase into biorelevant media. The *in vitro* digestion test takes into consideration the hydrolysis of lipid excipients and formation of lipolytic products in the GI tract. Either total drug concentration or free drug concentration in solution is determined as a function of time. As stated previously, lipolysis results in the loss of some lipoidal excipients in LBDDSs and, simultaneously, the generation of new lipid aggregates. The effect of lipolysis on the nature of lipid aggregates in solution is time-dependent. Consequently, the ability to solubilize poorly water-soluble drug can be expected to be time-dependent as well. The close similarity to physiologic conditions in the GI tract makes the *in vitro* lipolysis test more suitable for the *in vitro-in vivo* correlation (Reymond and Sucker, 1988; MacGregor, Embleton et al., 1997; Christensen, Schultz et al., 2004; Porter, Kaukonen et al., 2004; Dahan and Hoffman, 2006; Dahan and Hoffman, 2008).

## **2.5. Unanswered questions**

Among proposed physicochemical means by which LBDDSs enhance absorption, the primary mechanism is the solubilization of a poorly water-soluble drug in the GI tract. When the free drug concentration is limited due to the low aqueous solubility, a supersaturated solution created and maintained by the LBDDS is proposed to increase absorption. However, little is known about capability of lipoidal compositions in LBDDS formulations to create and maintain drug in a supersaturated state in simulated GI conditions. From a solubilization standpoint, evaluating the ability of a LBDDS, along with each component, to maintain a poorly water-soluble drug in a supersaturated state will provide useful information for understanding the mechanism by which digestible surfactants and lipids modulate the oral absorption of poorly water-soluble drugs in the GI tract.

Lastly, studies in the literature were limited to apparent solubilization in the formed lipid aggregates, but little information is available on the molecular details of solubilization in terms of drug-aggregate interactions and lipid-lipid interactions in

aggregates. From a dynamic perspective, the effect of alteration of composition in solution on drug solubilization during lipolysis is not fully understood.

## **2.6. Summary**

LBDDSs are an effective approach to enhance oral bioavailability of poorly-water soluble drugs. There is a clear need for a mechanistic understanding of the absorption potential of poorly-water soluble drugs by LBDDSs. A systematic approach to understanding the time-dependency of drug solubilization on lipolysis would be a first step in developing a mechanistic approach to formulation of poorly water-soluble drugs. By probing the physicochemical mechanism of LBDDS-associated solubilization of poorly-water soluble drugs in the GI tract a better understanding of interactions between poorly-water soluble drugs and digestible excipients under conditions in the GI tract will emerge. The results of these studies will aid formulators in choosing the optimal LBDDSs to improve oral absorption of poorly water-soluble drugs.

## Chapter 3

### Characterization and Validation of a Dynamic In Vitro Lipolysis Model

#### 3.1. Summary

The dynamic *in vitro* lipolysis model mimics *in vivo* physiology by adding digestive enzyme (pancreatic lipase) to a simulated digestion buffer. The model is widely applied to evaluate lipid-based drug delivery system (LBDDS) performance *in vitro*. However, a standard protocol for the use of this model system has not yet been established. Different specifications have been defined by different research groups. The objectives of this chapter are to characterize this model with respect to enzyme preparation, sensitivity of potential substrates to lipolysis and the effect of solution conditions. The results from different batches of enzyme stored under a variety of conditions before addition to simulated digestion buffer showed that enzyme stored on ice until use preserved the highest activity while enzyme incubated at 37°C for 15 min showed the least activity. By using the enzyme preparation stored on ice, the extent of lipolysis was assessed for different substrates including Cremophor RH40 (CrRH40), Cremophor EL (CrEL), vitamin E d- $\alpha$ -tocopheryl polyethylene glycol 1000 succinate (TPGS), Polysorbate 80 (PS80) and a complex LBDDS (F1) composed of 37.5% soybean oil, 55% CrRH40 and 7.5% ethanol. All substrates contain ester bonds which can be potentially hydrolyzed by pancreatic lipase. Except for TPGS, surfactants CrRH40, CrEL and PS80 could be hydrolyzed by the crude porcine pancreatic lipase in the presence and absence of bile salt/PC. In the absence of PC in buffer, the extent of F1 lipolysis was similar to that in the buffer containing only sodium cholate (NaC). Lipolysis of F1 was inhibited in the presence of PC at low concentration. Different extents of lipolysis were observed in buffers in the presence and the absence of bile salt, phospholipids and calcium. Generally, in the presence of calcium, the initial rate of lipolysis of either PC or surfactant excipients was faster compared to that observed in the absence of calcium. The rate of lipolysis tended to decrease with time as did the calcium concentration in solution. Differential

scanning calorimetry (DSC) and elemental analysis showed that calcium precipitated as a fatty acid salt.

### **3.2. Introduction**

Combinatorial chemistry and high-throughput screening have increased the number of poorly-water soluble drug candidates such that more than 40% of new active compounds are lipophilic and poorly-water soluble resulting in poor bioavailability (Prentis, 1988; Lipinski, Lombardo et al., 2001). As a result, a great challenge to formulations is to enhance the oral bioavailability of poorly-water soluble drugs. There are a number of formulation strategies that could be used to improve the bioavailability of poorly-water soluble drugs with high lipophilicity, such as increasing the dissolution rate, presenting the drug in solution or by maintaining the drug in solution through the GI tract. The use of a LBDDS is one popular approach to enhance oral bioavailability (Haus, Fogal et al., 1998; Porter, Trevaskis et al., 2007; Porter, Pouton et al., 2008).

The lipid excipients in LBDDSs are susceptible to hydrolysis by digestive enzymes in the stomach and small intestine (Porter, Trevaskis et al., 2007). Enzymatic hydrolysis of lipid occurs at the surface of the emulsified oil droplets in the small intestine. The emulsified oil droplets are coated by phospholipid, bile salts, and lipolytic products including di- and monoglycerides and fatty acids. The state and composition of the surface would affect the characteristics of the oil droplet, thereby modulating the lipase activity (Hwang, Tamm et al., 1995; Peters, Toxvaerd et al., 1995; Lipp, Lee et al., 1996). The effects of formulation surfactants in LBDDSs on the activity of an enzyme may be either inhibitory or accelerative depending on the binding location. Activation of enzyme could be triggered by the binding of surfactant analogues of endogenous substrates (Egloff, Marguet et al., 1995; Hermoso, Pignol et al., 1996). If exogenous surfactant binds to the active site, lipolysis will be inhibited. On the contrary, lipolysis will be enhanced if the active site is still available. The mechanism of fatty acid effects on lipolysis is not clear. However, the common findings are that fatty acids, especially dodecanoic (C12:0), oleic (C18:1) and linoleic (C18:2) acids, can stimulate the activity of lipase-colipase (Borgstrom, Erlanson-Albertsson et al., 1979). Some evidence suggests that the enhancement of activity by fatty acids may originate from promotion of lipase adsorption onto colipase, which is influenced by the molar ratio of colipase to fatty acid. The hypothesis is that the fatty acid

is concentrated laterally around colipase facilitating the adsorption of lipase in the lid opened conformation (Dahim and Brockman, 1998). The effects are also related to fatty acid chain unsaturation. Moreover, the inhibition induced by phosphatidylcholine can be reversed by fatty acids.

Due to all of the above factors, the state of oral LBDDSs in the GI tract is a dynamic process in which digestible excipients are susceptible to digestion and the phases are changing as a function of time. Consequently, drug solubilization and distribution may also change as a function of time *in vivo*. As a result of these factors, there is a need in the formulation design for a method to predict and correlate the *in vitro* data to the performance of LBDDSs *in vivo*. Toward this goal various *in vitro* approaches, such as dissolution, particle sizing and lipolysis of formulations in relevant media, have been proposed (Dressman and Reppas, 2000; Porter, Kaukonen et al., 2004; Kalantzi, Goumas et al., 2006). A dynamic *in vitro* lipolysis model has been developed over the past few years. Biorelevant dissolution tests were proven to be suitable models for poorly-water soluble drug release from LBDDSs by using digestion buffers to simulate the fasted and fed states in the GI tract (Pedersen, Brøndsted et al., 2000). In principal, the dynamic *in vitro* lipolysis model mimics the *in vivo* physiology by including digestive enzymes in the buffer and titrating the released fatty acid from ester-containing lipoidal components.

Zangenberg et al. characterized and evaluated the dynamic *in vitro* lipolysis model by analyzing the composition of the aqueous phase, including the concentration of model drug (Zangenberg, Müllertz et al., 2001). The analysis showed that the concentration of lipolytic products was dependent upon the concentration of bile salt. Drug concentrations in the aqueous phase were dependent upon lipophilicity. The authors also evaluated a model in which  $\text{Ca}^{2+}$  was added continuously at a controlled rate while two other parameters - bile salt concentration and lipase activity – were varied. Their studies indicated that all three parameters influenced the initial rate of lipolysis. However, only the  $\text{Ca}^{2+}$  concentration and lipase activity had effects on the subsequent stages. Moreover, it was shown that the rate of lipolysis can be controlled by the rate of addition of  $\text{Ca}^{2+}$ . By using the dynamic *in vitro* lipolysis model, Sek et al. showed that the rate and extent of lipolysis of medium chain triglycerides were greater than long chain triglycerides (Sek, Porter et al., 2002). The kinetics of lipolysis was independent of the bile salt

concentration. Furthermore, it was found that the presence of the drug reduced the initial rate of lipolysis (Christensen, Schultz et al., 2004; Ljusberg-Wahren, Seier Nielsen et al., 2005). Dahan et al. highlighted the usefulness of the dynamic *in vitro* lipolysis model in the optimizing of oral LBDDSs in the case of presystemic metabolism in the GI tract (Dahan and Hoffman, 2006). This model has also been applied successfully in a number of studies correlating oral bioavailability with solubilization behavior of drug in the lipid assemblies formed during lipolysis in the GI tract (Christensen, Schultz et al., 2004; Grove, Pedersen et al., 2005; Goddeeris, Coacci et al., 2007).

Despite the wide acceptance of the lipolysis model, a standard experimental protocol is not yet established. To accommodate the study purposes, different specifications are defined by different research groups. The first aim of this chapter was to characterize and evaluate the dynamic *in vitro* model in terms of enzyme activity, sensitivity of formulation components to hydrolysis and solution factors influencing the extent of lipolysis by measuring the production released fatty acids. The second aim of this chapter was to establish a reproducible model for the hydrolysis of surfactant to support later studies on dynamic solubilization of poor-water soluble drugs during the lipolysis of a model LBDDS. A relatively simple ester-containing surfactant-only LBDDS and a complex LBDDS containing oil and surfactant were chosen as substrates. Selected ester-containing surfactant excipients included Cremophor RH40 (CrRH40), Cremophor EL (CrEL), Vitamin E d- $\alpha$ -tocopheryl polyethylene glycol 1000 succinate (TPGS) and PS80 (PS80). In addition, a complex LBDDS (F1) composed of 37.5% soybean oil, 55% CrRH40 and 7.5% ethanol was employed. The chemical structures of selected substrates are shown in Figure 3.1. The extent of lipolysis for each substrate under various conditions was monitored by the production of fatty acids.



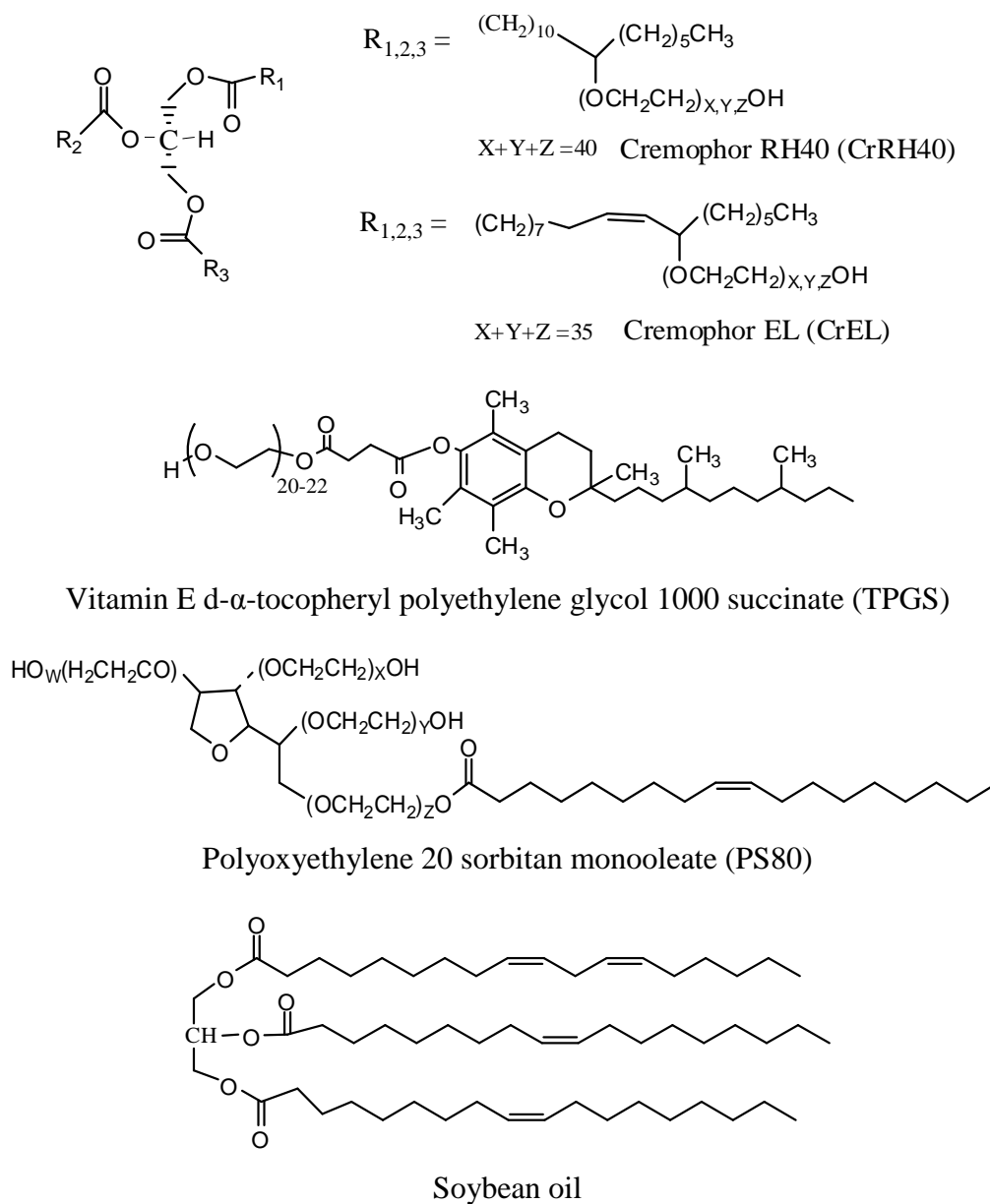


Figure 3.1 Structures of selected substrates

### 3.3. Material and methods

#### 3.3.1. Materials

Polysorbate 80 (Tween80<sup>®</sup>, PS80) was a generous gift from Croda Inc. (Edison, NJ, USA). Cremophor RH40 (CrRH40) and Cremophor ELP (CrEL) were purchased from BASF (Germany). Vitamin E d- $\alpha$ -tocopheryl polyethylene glycol 1000 succinate (TPGS) was purchased from Eastman Chemical Company (Kingsport, TN, USA). Soybean oil, 1,2-diacyl-sn-glycero-3-phosphocholine (type XVI-E) from egg yolk (PC),

4-bromophenylboric acid, Trisma® maleate, calcium chloride hydrate (purity  $\geq 99\%$ ), sodium cholate hydrate (NaC) (purity  $\geq 99\%$ ), sodium taurocholate hydrate (NaTC) (purity  $\geq 95\%$ ) and lipase (Type II, crude from porcine pancreas) were purchased from Sigma-Aldrich (St. Louis, MO, USA). NaOH (0.1 M) was purchased from Fisher Scientific (Pittsburgh, PA, USA). All chemicals were used as received. Water for buffer solution was from a Milli-Q water purification system. Hydrophilic PTFE filters (13 mm, 0.2  $\mu\text{m}$  pore size) were purchased from Advantec MFS, Inc. (Japan).

### **3.3.2. Preparation of tris maleate buffer solution**

To make 1 L of 50 mM buffer solution with an ionic strength of 0.15 M, 11.86 g of tris maleate and 8.766 g of NaCl were dissolved in 900 mL Milli-Q water. The pH was adjusted to 7.8 by 1 M NaOH at room temperature ( $\sim 25^\circ\text{C}$ ) and then the volume was increased to 1 L by the addition of Milli-Q water. The pH of this buffer will be 7.5 at  $37^\circ\text{C}$  (pH is checked at  $37^\circ\text{C}$ ). In selected conditions,  $\text{CaCl}_2$  (5 mM) was included when the effect of  $\text{Ca}^{2+}$  was evaluated.

### **3.3.3. Preparation of simulated digestion buffer**

Simulated digestion buffer contained bile salt (BS) and PC at a fixed molar ratio of 4:1 in tris maleate buffer (pH 7.5 at  $37^\circ\text{C}$ ). The BS/PC (5 mM/1.25 mM) represented the fasted-state condition and 20 mM BS/5 mM PC mimicked the fed-state condition in the GI tract (Schersten, 1973). PC was dissolved in chloroform/methanol (2:1) followed by solvent evaporation by nitrogen with rotation to form a thin film of PC on the wall of the flask. The thin film was dried for two days under vacuum at room temperature. To prepare the simulated fasted-state digestion buffer (SIFs buffer), a known volume of 5 mM BS solution in tris maleate buffer was added to the above flask and the suspension was stirred overnight at room temperature until clear. To prepare simulated fed-state digestion buffer, a known volume of 20 mM BS solution in tris maleate buffer was added and the suspension was stirred overnight at room temperature until clear. The pH was checked and adjusted as necessary.

### **3.3.4. Preparation of enzyme solution**

The enzyme solution was prepared on the day of use. Unless stated otherwise, the enzyme solution was prepared by adding 1 g of crude porcine pancreatic lipase to 5 mL

of tris maleate buffer (pH 7.5). The suspension was stirred for 15 min and subsequently centrifuged by Jouan CR412 centrifuge (Jouan, Inc., Winchester, Virginia, USA) for 20 min at 5000 rpm at room temperature. Supernatant was stored on ice until used. The process was followed strictly in order to reduce the variation of enzyme activity.

### **3.3.5. Preparation of formulations**

Two types of LBDDS were employed. Simple LBDDS were composed of only ester-containing surfactant excipient. A more complex LBDDS composed of 55% w/w of Cremphore RH40, 37.5% w/w of soybean oil and 7.5% w/w of ethanol was also examined. The exact amount of each of component was weighed to a 20 mL glass scintillation vial and the mixture was rotated for three days at room temperature. Formulations were stored at room temperature.

### **3.3.6. Determination of calcium content**

#### **3.3.6.1. Concentration of $\text{Ca}^{2+}$ in the solution during the *in vitro* lipolysis**

Quantitative analysis of calcium concentration in samples obtained during *in vitro* lipolysis of PS80 was conducted by inductively coupled plasma emission spectroscopy (ICP) (Varian, Vista-pro CCD simultaneous ICP-OES). *In vitro* lipolysis experiment was performed as described in Section 3.3.8. Aliquots taken during *in vitro* lipolysis were filtered through 0.2  $\mu\text{m}$  PTFE membranes, and 0.8 mL of filtrate was added to the same volume of nitric acid. All samples were heated at 80°C to make sure components were digested completely. Fully digested samples were diluted with Milli-Q water to make a total volume of 5 mL. A standard curve was constructed by using eight standard calcium solutions in the concentration range 0.05 ppm to 250 ppm. Calcium emission wavelengths of 318.127 nm and 422.673 nm were employed.

#### **3.3.6.2. Composition of calcium precipitation**

Precipitate formed during the *in vitro* lipolysis of PS80 was collected by filtration and dried under vacuum. Solid material was characterized by differential scanning calorimetry (DSC) (TA instruments 2920 modulated DSC, USA) and elemental analysis. A vacuum-dried sample weighing 1.876 mg was sealed in aluminum DSC pans. Initially, the sample was cooled to -15°C at 20°C/min then heated to 350°C at 5°C/min. The sample was then cooled to room temperature. The same batch of the sample for DSC was

also analyzed by elemental analysis by Atlantic Microlab, Inc., giving average C (68.74%), H (10.90%), and O (11.49%) from two replicates. Theoretical values of C, H, and O in  $\text{Ca}^{2+}$  salt are 68.88%, 10.73%, and 11.21%, respectively.

### **3.3.7. Qualitative determination of phosphatidylcholine during the lipolysis of SIFs**

The phosphatidylcholine in the SIFs during the lipolysis was determined qualitatively by thin layer chromatography (TLC). *In vitro* lipolysis experiment was performed as described in the Section 3.3.8. Aliquots (2 mL) were taken at 5, 15, 30 and 60 min during *in vitro* lipolysis of SIFs. Extraction of lipids was carried out by addition of equal volume of chloroform/methanol (v/v 2/1) to 2 mL aliquots taken at each time. Extraction was repeated three times for each lipolysis sample and organic phases were combined. After evaporation of the organic phase, the residue was dissolved in a minimum volume of chloroform/methanol (v/v 2/1). The solution of extract was applied on a silica gel 60 thin layer chromatography plates and developed in chloroform/methanol/acetic acid/water (50/60/6/0.6 v/v). The spots were identified by staining with iodine vapor (Andersson, Sternby et al., 1994). The appearance of phosphatidylcholine was monitored as a function of time.

### **3.3.8. Setup of pH-stat titration system**

The components of pH-stat titration system are shown in Figure 3.2. The system includes an autoburette, a pH electrode and a temperature control electrode. Autoburette was connected to a pH electrode and continuously titrated the released fatty acid and maintained pH at 7.5 with sodium hydroxide. Since the stoichiometric reaction ratio between the released fatty acid and sodium hydroxide is 1:1, the extent of lipolysis can be followed by the profile of concentration of sodium hydroxide versus time.

The pH-stat was controlled by a Model 842 Titrand system (Merohem Ltd, Switzerland) with control program version 4.1 which included a model 807 dosing unit with a burette volume of 10 mL and a pH electrode. The temperature for all experiments was  $37 \pm 0.5^\circ\text{C}$ . The reaction glass bottle was immersed in a water bath, the temperature of which was controlled by Fisher scientific isotemp refrigerated circulator model 910 (Fisher Scientific, USA). Agitation was provided by 5 mm magnetic stir bar at 500 rpm on a direct drive motor/magnetic system.

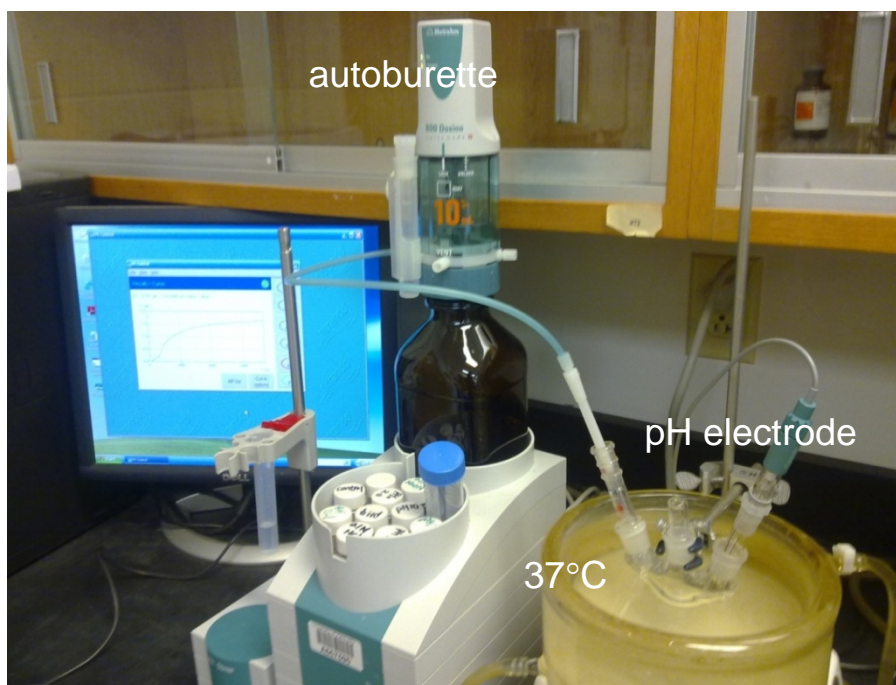


Figure 3.2 pH-stat titration system

### 3.3.9. *In vitro* lipolysis

The *in vitro* lipolysis was carried out in the simulated digestion buffers as prepared in Section 3.3.3. The pH of the reaction medium was fixed at 7.5. Experiments were performed by adding excess amount of substrate in relation to the enzyme activity so as to produce a maximum rate of lipolysis. Interfacial area of substrates and the amount and specific activity of lipase enzyme determines the lipolysis rate. As lipolysis proceeds, the rate of reaction is also influenced by the lipolytic products. To validate the instrument accuracy and precision, measurements were carried out on different days and/or with different enzyme batches. Due to possible differences in enzyme activities, the extent of lipolysis may vary even though all other parameters remain constant.

The pH-stat was set to maintain pH constant at 7.5 and was started ~1 min before the lipase solution was added (0.5-2 mL) to the buffer solution containing the well dispersed LBDDS. The lipolysis was monitored for 30-120 min period depending on the substrate and extent of lipolysis. The extent of lipolysis was expressed as  $\mu\text{mol}$  of titrated fatty acid in 25 mL of buffer solution unless stated otherwise. The amount of fatty acid was

calculated based on 1:1 stoichiometric reaction ratio between the released fatty acid and 0.1 M sodium hydroxide.

### **3.4. Results and discussion**

#### **3.4.1. Enzyme preparation: effect of volume and storage conditions**

Assuming there is no inhibition by products or intermediates and no cooperativity, the enzymatic reaction follows Michaelis-Menten kinetics which relates the initial reaction rate and substrate concentration by Eq. 3.1

$$v_0 = \frac{v_{\max} [S]}{K_m + [S]} \quad (3.1)$$

where  $v_0$  and  $v_{\max}$  are the initial and maximum reaction rates;  $[S]$  is the concentration of substrate;  $K_m$  is Michaelis constant. When the substrate concentration is much higher than  $K_m$ , the reaction rate is independent of the substrate concentration. All experiments were designed such that the amount of lipase enzyme and its specific activity determined the lipolysis rate.

To verify that the substrates were in excess, known volumes of enzyme preparation were added to tris maleate buffer solution composed of 5 mM of NaC and the 0.48 grams of CrRH40. Figure 3.3 shows the amount of titratable fatty acid formed as a function of time over 30 min. One half milliliter of enzyme preparation resulted in the least release of fatty acid while 2 mL of enzyme preparation showed the highest extent of lipolysis. The initial rate was calculated from the initial slope of curve (within 5 min) in Figure 3.3. The initial rate of lipolysis increased with increasing amount of lipase enzyme, indicating that the amount of lipase enzyme and its specific activity were rate limiting under all conditions. However, the reaction rate after 5 min may not reflect solely the amount and activity of lipase enzyme because the accumulation of lipolytic products on the enzyme may retard the reaction. The theoretical amount of fatty acid is 355  $\mu\text{mol}$  from 0.48 g CrRH40. According to the amount of titratable fatty acid in Figure 3.3, 0.48 g of CrRH40 was not hydrolyzed completely in 30 min. Moreover, the rate of lipolysis slowed down and approached a plateau in 30 min of the addition of enzyme preparation. We also tested lower amount of enzyme (0.25 ml) but were unable to obtain a stable signal.

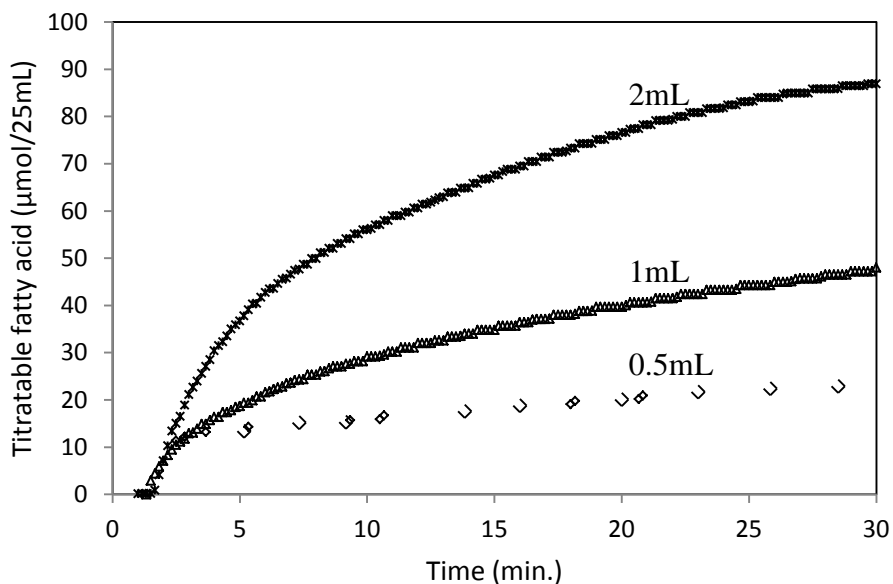


Figure 3.3 Amount of fatty acid released in the lipolysis of CrRH40 by adding 0.5 mL (diamond), 1 mL (triangle) and 2 mL (star) of enzyme preparation. Enzyme solution was stored on ice until use. Condition: NaC solution (5 mM, 25 mL), CrRH40 (0.48 g, 0.18 mmol) at 37 °C.

Standard preparation and storage conditions for lipase enzyme have not been addressed in the literature. The supplier of the crude lipase from porcine pancreas (Type II) indicated that the product exhibits both the amylase and the protease activity. It is possible that the protease would have an impact on the lipase enzyme activity. Experiments were carried out to evaluate the effect of temperature on the activity of the enzyme preparation. Once prepared, the enzyme preparation was stored on ice (0°C), at room temperature (~25°C) or at 37°C for 15 min. Following storage, the extent of lipolysis of 0.48 g CrRH40 was determined as described in Section 3.3.8. The results showed that enzyme activity was unchanged when the enzyme preparations were stored at 0°C and room temperature (Figure 3.4). However, incubation at 37°C reduced the enzyme activity resulting in significantly less titratable fatty acid generated during the *in vitro* lipolysis. Probably, incubation at 37°C provided an optimal condition for protease activity as well. Thus, the storage condition chosen was 0°C.

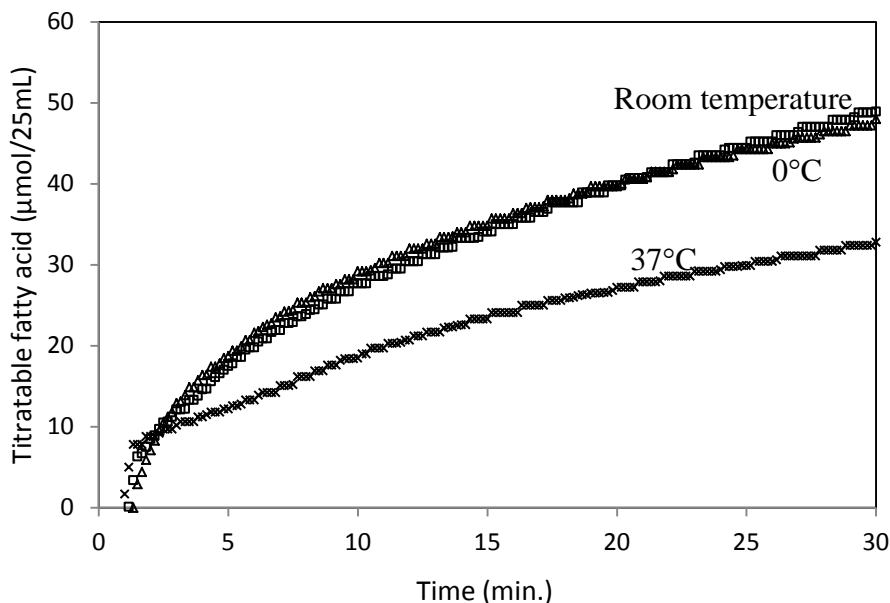


Figure 3.4. Amount of fatty acid released in the lipolysis of CrRH40 hydrolyzed by enzyme solution stored at room temperature (square), on the ice (triangle), and incubated at 37°C before addition to the solution (cross). Condition: NaC solution (5 mM, 25 mL), CrRH40 (~0.48 g, 0.18 mmol) and enzyme preparation (1 mL) at 37°C.

### 3.4.2. Sensitivity of the model

#### 3.4.2.1. Lipolysis of components in simulated fasted state intestinal fluid

The dynamic *in vitro* model mimics the *in vivo* physiology by adding the enzyme to simulated digestion buffer (SIF). Simulated digestion buffer consists of bile salt (BS) and phospholipid (PC) at fixed molar ratio of 4 to 1; 5 mM of BS/1.25 mM of PC representing the fasted state and 20 mM of BS/5 mM of PC representing the fed state. Type XVI-E 1,2-diacyl-sn-glycero-3-phosphocholine from egg yolk was chosen to represent the phospholipids in the GI tract. As seen in Figure 3.5, phosphatidylcholine contains a glycerol backbone and two ester fatty acid chain linkages suggesting that it may be subject to hydrolysis by lipase enzyme. Boucrot et al. had shown that phosphatidylcholines in bile are not hydrolyzed in the intestinal lumen while dairy phospholipids can be hydrolyzed by phospholipase (Boucrot, 1972). The lipolysis of phosphatidylcholine by crude pancreatic lipase has been observed by others (Kossena, Boyd et al., 2003).



The lipolysis of SIF was carried out with a freshly prepared batch of enzyme on three different days. Lipolysis profiles are shown in Figure 3.6a. A control solution, containing only 5 mM BS (no PC), was also subject to the lipolysis assay. The results, shown in Figure 3.6a, indicated that only a small amount of NaOH titrant was added to the 5 mM BS solution (5.7  $\mu\text{mol}/25\text{ mL}$  total at 30 min) and only in the first 5 min. There is no functional group susceptible to pancreatic lipase on NaC and so the small change of pH resulted from the addition of enzyme preparation, probably due to temperature dependence of ionization of maleate and protein.

Theoretically, 1.25 mM of PC in 25 mL solution would be able to generate 31.25  $\mu\text{mol}$  of fatty acid upon hydrolysis of one ester bond. Considering the amount of NaOH consumed by the addition of enzyme preparation stored at 0°C and the amount of PC present in SIF, the total amount of NaOH consumed would be expected to be about 37  $\mu\text{mol}$ . The data presented in Figure 3.6a indicate that about 35-38 mmols of NaOH was consumed, suggesting that only one of the fatty acid chains was cleaved from PC under the conditions employed. Samples of the reaction mixture were taken at 5, 15, and 30 min and subjected to TLC analysis. The TLC results show that no PC was found in the reaction mixture by 30 minutes, supporting the conclusions of the lipolysis experiment. The TLC analysis was not capable of detecting fatty acid or lysoPC, the two putative degradation products of PC. The variation on the amount of titratable fatty acid in three replicates was less than 10% which was judged to be acceptable. The enlarged figure showing the initial 10 min (Figure 3.6b) of reaction indicated a good reproducibility of lipolysis measured by the dynamic *in vitro* lipolysis model.

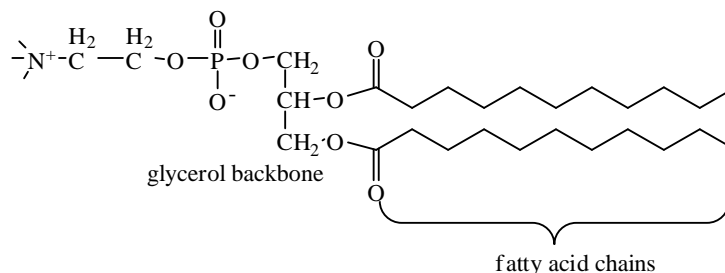


Figure 3.5 The structure of 1,2-diacyl-sn-glycero-3-phosphocholine

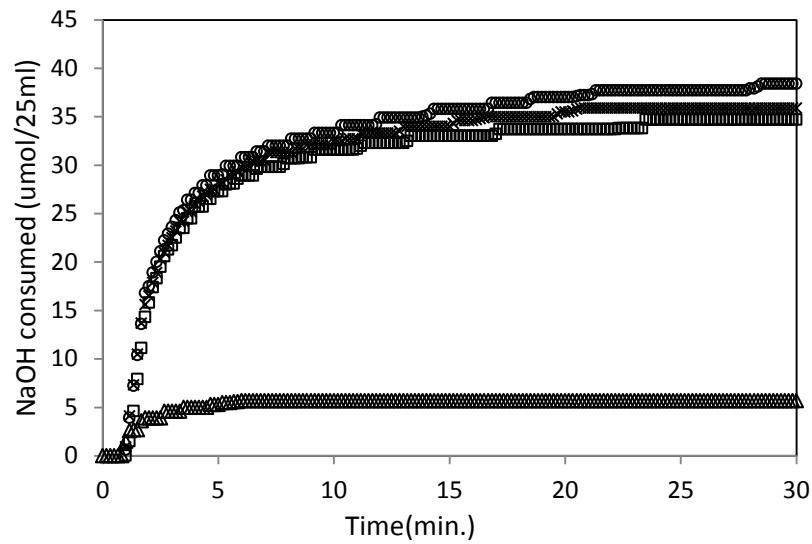


Figure 3.6a. Total amount of NaOH consumed during the lipolysis of 25 mL of SIF, with and without PC at 37°C. Profiles were recorded from three batches of enzyme prepared on separate three days (square, cross and circle). Triangle represents the amount of NaOH titrated in the tris maleate buffer containing 5 mM of NaC (no PC) after addition of the enzyme preparation (pH 7.8 at 0°C) at 37°C.

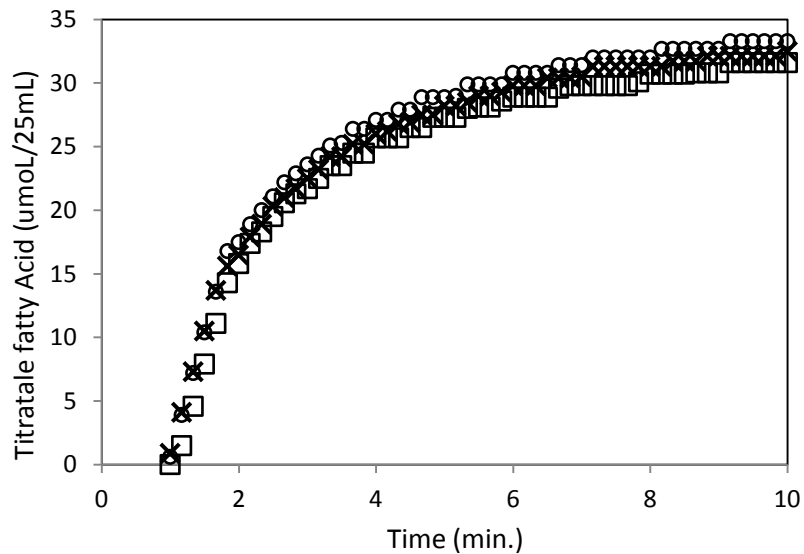


Figure 3.6b Amount of fatty acid released in the lipolysis of 25 mL of simulated fasted digestion buffer composed of 5 mM of NaC /1.25 mM of PC at 37°C. Profiles were recorded from three batches of enzyme preparation prepared on day 1 (square), day 2 (cross) and day 3 (circle) (enlarged for the first 10 min from Figure 3.6a).

### 3.4.2.2. Lipolysis of selected ester-containing surfactants

In this section, the ability of lipase enzyme to hydrolyze selected ester-containing surfactants was examined in SIF buffer. In all experiments, the extent of lipolysis was expressed relative to the total amount of fatty acid available from all sources - surfactant, oil and PC.

The extents of lipolysis of CrRH40, CrEL, and PS80 were recorded up to 120 min. The lipolysis of TPGS was monitored for 30 min, after which time the reaction reached a plateau indicating the lipolysis was stopped. The theoretical yield of fatty acid was calculated from the average molecular weight of surfactant and indicated weight of surfactant. By subtraction of amount of titrated NaOH from control (no surfactant), the maximum released fatty acid from surfactant can be obtained at 2 h. As shown in Table 3.1, in all the cases, the lipolysis did not result in 100% of the theoretical value. TPGS showed the least extent of lipolysis; the reaction reached maximum at about 30 min. PS80 hydrolysis reached a plateau at 120 min. Hydrolysis of CrEL was more extensive than that of RH40 (Figure 3.7). Given the same amount of enzyme preparation, observed different extent lipolysis of surfactants may reflect either the accessibility of enzyme to the ester bond of surfactants or the inhibition of surfactant or lipolytic products on the activity of lipase enzyme. The rank order of extent of lipolysis of surfactants agreed with that reported in the literature (Cuiné, McEvoy et al., 2008). These results indicated that the dynamic *in vitro* lipolysis model, under the conditions employed, is sensitive to the selected surfactants.

Table 3.1 Amount of weighed selected surfactants, molecular weight and theoretical fatty acid released from selected surfactants

	Cr EL	CrRH40	TPGS	PS 80
Weight(g)	0.172	0.166	0.252	0.249
M.W(D)	2473	2699	1513	1310
Theoretical FA( $\mu\text{mol}$ )	139	123	167	190
Maximum release from surfactant observed( $\mu\text{mol}$ ) at 2 h	126	27	12.5	100

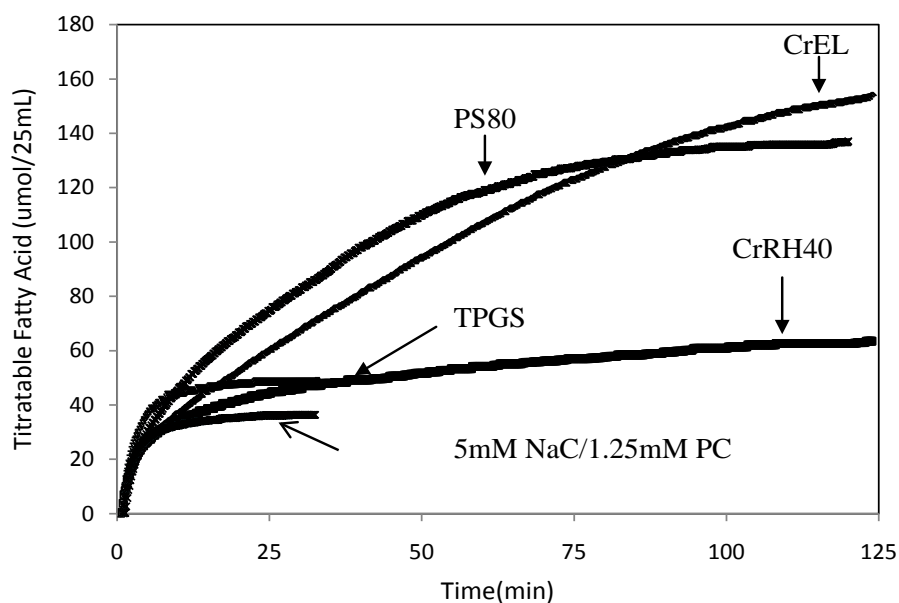


Figure 3.7 Amount of fatty acid released in the lipolysis of CrRH40, CrEL, TPGS and PS80 solution in SIF buffer. Condition: SIF buffer (25 mL, 5 mM of NaC/1.25 mM of PC) and enzyme preparation (1 mL) at 37°C.

### 3.4.2.3. Lipolysis of a complex LBDDS containing oil and surfactant

To further test the sensitivity of the dynamic model to a complex system, an LBDDS containing soybean oil and CrRH40 (F1) was examined. The extents of lipolysis of SIF

buffer as well as CrRH40 and F1 in SIF buffer were followed for less than 60 min (Figure 3.8). In the first 5 min, the initial rates of lipolysis of PC in SIF buffer and CrRH40 in the absence of oil were identical. However, lipolysis of F1 showed a significant slower initial rate than CrRH40. Furthermore, the extent of lipolysis of F1 was less than CrRH40 even though the theoretical amount of fatty acid from F1 is greater than CrRH40 alone. The results suggested that the presence of soybean oil inhibited or slowed down the lipolysis. With respect of morphology, dispersion of CrRH40 resulted in a micellar solution while dispersion of F1 formed an emulsion. One possible explanation for the slower rate and lesser extent of hydrolysis of F1 compared to CrRH40 may be related to binding and accessibility of the enzyme to the emulsion versus micelle surfaces. As an alternative, the total accessible surface of CrRH40 micelles might be much greater than F1 emulsion droplets.

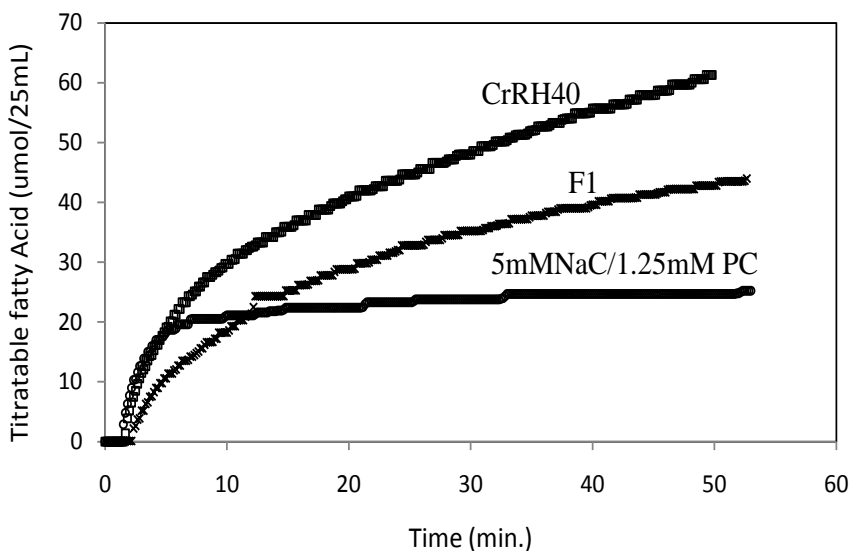


Figure 3.8 Amount of fatty acid released during the lipolysis of 0.48 g (0.18 mmol) CrRH40, 0.8 g F1 composed of 55% of CrRH40, 37.5% of soybean oil and 7.5% of ethanol in SIFs buffer and 25 mL SIFs buffer as control at 37°C.

Lipolysis of CrRH40 and F1 were also examined in simulated fed-state digestion media, containing 20 mM NaC/5 mM PC in trisma maleate buffer. The extents of lipolysis of surfactant and formulation were significantly greater than those in simulated fasted-state buffer (Figure 3.9). Although the titration assay is not able to identify the source of fatty

acid, the results in Figure 3.9 do indicate that the total amount fatty acid produced during the lipolysis of CrRH40 was not simply the sum of amounts fatty acid from PC and CrRH40. On the contrary, within the first 15 min, the amount of fatty acid released from PC was more than that released from CrRH40 in simulated fed-state digestion buffer. Nonetheless, the initial rate and extent of lipolysis of F1 were less than those of lipolysis of CrRH40. This is possibly due to the same reasons proposed in simulated fasted-state digestion buffer. The results do indicate that the dynamic *in vitro* lipolysis model is sensitive in both simulated fasted-state and fed-state conditions.

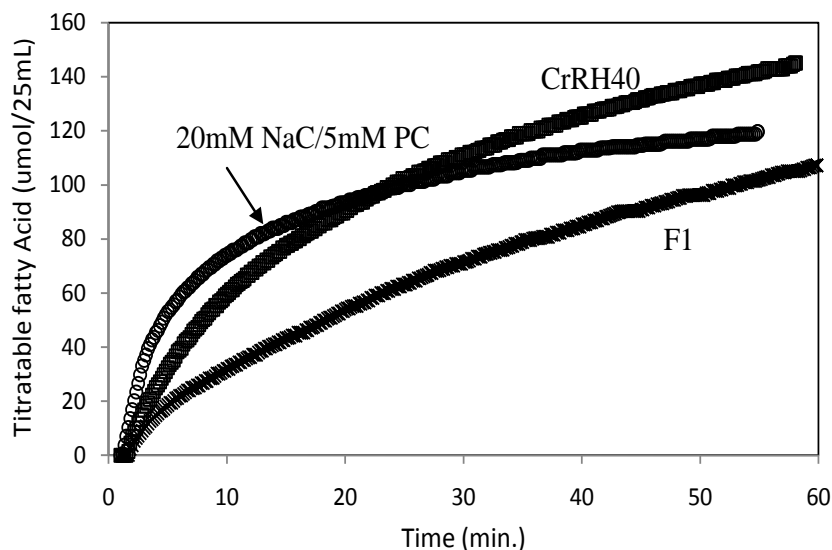


Figure 3.9 Amount of fatty acid released in the lipolysis of 0.48 g CrRH40 only in simulated fed-state digestion buffer, 0.8 g F1 composed of 55% of CrRH40, 37.5% of soybean oil and 7.5% of ethanol in simulated fed-state digestion buffer and 25 mL simulated fed-state digestion buffer as control at 37°C.

### 3.4.3. The effect of digestion media components on the extent of lipolysis

The presence of lipids in the duodenum stimulates secretion of bile salts, biliary lipids and pancreatic lipase/colipase. Pancreatic lipase is an interfacial enzyme which preferentially acts at the surface of oil droplets or interface. The hydrolysis takes place at the surface of emulsified droplets or small aggregates in small intestine. It has been recognized that bile salts, phospholipids, fatty acid and  $\text{Ca}^{2+}$  can influence the lipolysis of triglycerides either by affecting the activity of enzyme or by affecting the adsorption of

enzyme on surface (Larsson and Erlanson-Albertsson, 1986; Alvarez and Stella, 1989; Wickham, Garrod et al., 1998; Wickham, Wilde et al., 2002). In this section, the effects of selected factors on the pH-titration method outlined in Section 3.3.7 will be examined.

#### **3.4.3.1. Bile salts**

Bile salts play a very important role in the GI tract to facilitate the digestion and absorption of lipids. The formation of mixed micelles of bile salts and phospholipids facilitates the solubilization of lipolytic products and removes the lipolytic products from the surface of aggregates and assures the accessibility of enzyme to the surface of aggregates. It is believed that incorporation into the mixed micelle facilitates lipid and poorly-water soluble drug absorption by overcoming the resistance of unstirred water layer. There are a variety of bile salts secreted in the GI tract. For this study, sodium taurocholate and sodium cholate were chosen as representatives. The structures of two bile salts are shown in Figure 3.10.

Taurocholic acid has a pKa of 2; it is totally ionized at pH 7.5 (O'Máille and Richards, 1977). The pKa of monomer cholic acid is ~4-5. Ionized bile acid can form micelles. Upon the formation of micelles, the apparent pKa of cholic acid appears to rise to 6 (Small, Cabral et al., 1984). The initial rate and extent of lipolysis of SIFs buffer containing either NaC or NaTC are comparable (Figure 3.6a and Figure 3.11). In 15 min, the lipolysis reached a plateau value and, by calculation, the PC was hydrolyzed completely. However, the type of bile salts had a significant influence on the lipolysis of PS80. In the presence of NaC, the lipolysis reached a plateau in 120 min. In comparison, the presence of NaTC in SIF buffer the extent of lipolysis continued to rise past 120 minutes (see Figure 3.12). Possibly more, or larger, mixed micelles of lipolytic products were formed in the presence of NaTC. Consequently, the lipolytic products would remove more efficiently from the surface of PS80 aggregates. Despite the differences in rate and extent of lipolysis of PS80, cholic acid was chosen as the bile salt components of both simulated fasted-state and simulated fed-state digestion media.

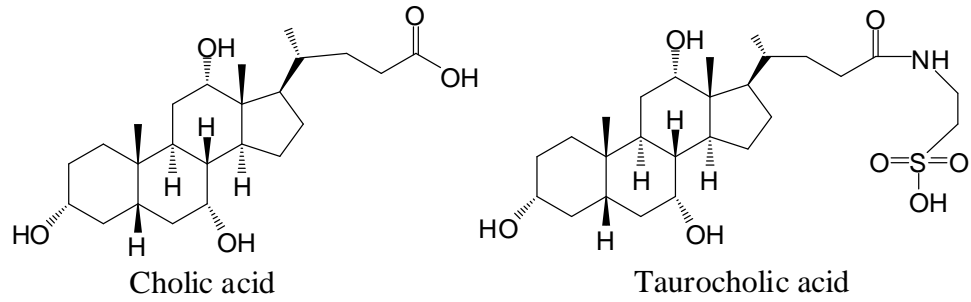


Figure 3.10 The structure of bile acids.

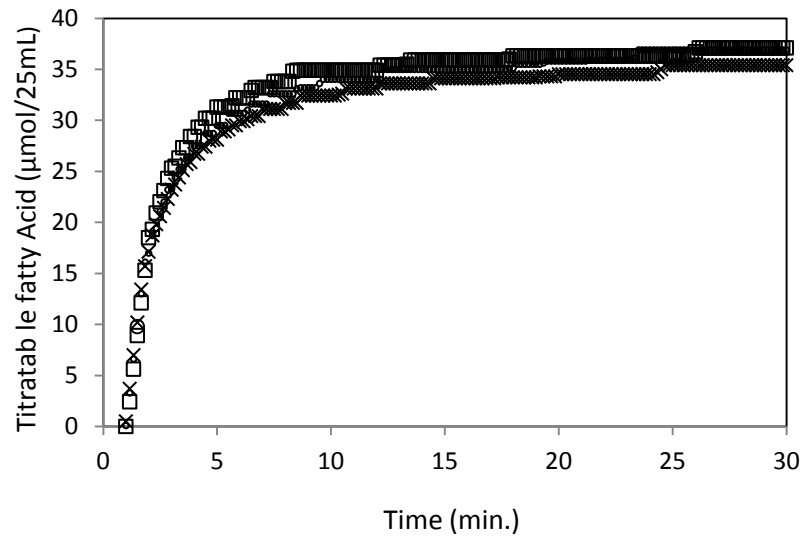


Figure 3.11 Amount of fatty acid released in the lipolysis of 25 mL of SIF composed of NaTC/PC (molar ratio 4:1) at 37°C. Each profile was recorded from a freshly-prepared enzyme solution.



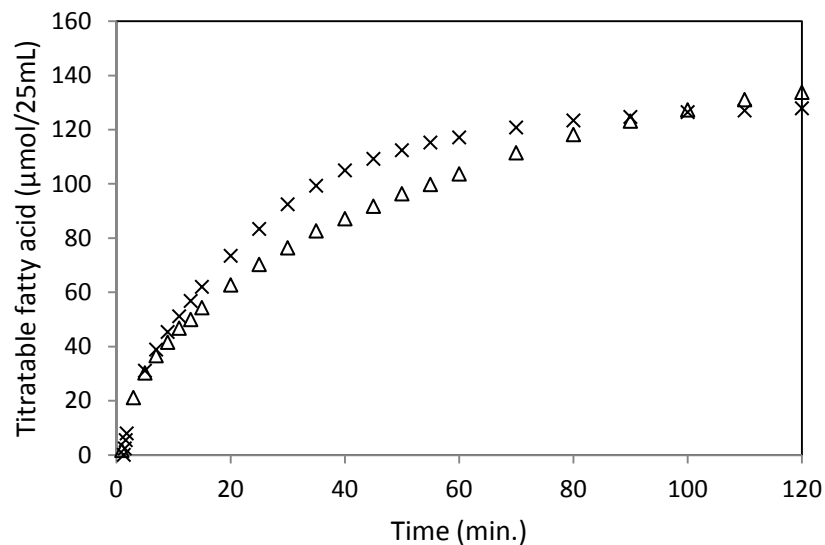


Figure 3.12 Representative total amount of fatty acid released in the lipolysis of PS80 in the SIF buffer composed of NaC/PC (cross) and composed of NaTC/PC (triangle) at 37°C

### 3.4.3.2. Simulated fasted-state and fed-state media digestion media

Typically, the simulated fasted-state digestion media contains 5 mM of bile salt and 1.25 mM of PC while 20 mM of bile salt and 4 mM of PC are included in the simulated fed-state digestion media. Thus, the effect of BS/PC concentration on the lipolysis of CrRH40 and F1 was examined by the dynamic *in vitro* lipolysis model. As shown in Figure 3.13 and Figure 3.14, generally, the high concentration of bile salt promoted lipolysis. The extent of the lipolysis of CrRH40 was greater in the presence of PC in both 5 mM NaC and 20 mM NaC solutions (CrRH40 w/PC and CrRH40 w/ PC in Figure 3.13 and Figure 3.14). The relative high production of fatty acid in the simulated fed-state digestion media may simply reflect the lipolysis of CrRH40 and PC simultaneously. The amount of CrRH40 in F1 is comparable to the amount of CrRH40 used. The calculated content of fatty acid in F1 is greater than that of CrRH40 due to the possible hydrolysis of soybean oil. However, inclusion of soybean oil in the F1 appeared to inhibit the lipolysis in both the simulated fasted-state (F1 w/PC in Figure 3.13) and fed-state digestion media (F1 w/PC in Figure 3.14). The slower rate and lesser extent of hydrolysis of F1 may result from the slower binding and accessibility of lipase enzyme to the surface of oil droplets than those to micellar interface.

In addition, at a low concentration of bile salt, the production of fatty acid from F1 was further inhibited by the presence of PC (F1 w/PC in Figure 3.13). On the other hand, such inhibition was not observed at high concentration of bile salt (Figure 3.14). It is believed that phospholipids may decrease the binding of enzyme to the substrate resulting in the displacement of protein into bulk aqueous solution. Some studies had indicated that the effect on lipolysis may also be mediated by colipase (Patton and Carey, 1981). It has been suggested that the colipase binds to the phospholipid-bile salts mixed micelle which is formed either on the surface of emulsified oil droplets or in the bulk aqueous solution. The activity would be increased if the complex is located at the o/w interface. On the other hand, the lipid digestion would be inhibited if the complex is in the bulk aqueous solution. As suggested by fluorescence microscopy, the phosphatidylcholine and colipase are miscible on the interface. The colipase may mediate the species distribution of substrate which may be exposed to the bound lipase (Momsen, Dahim et al., 1997). In the crude of pancreatic lipase we used here, there is no indication by the manufacturer of the presence of colipase. Therefore, the inhibition of lipolysis of F1 in simulated fasted-state digestion media could be due to altered accessibility/binding of enzyme to emulsified oil droplets. Any change the quality of the interface or enzyme inhibition may be reduced by the efficient removal of lipolytic products from emulsified oil droplets by mixed micelles of BS/PC.

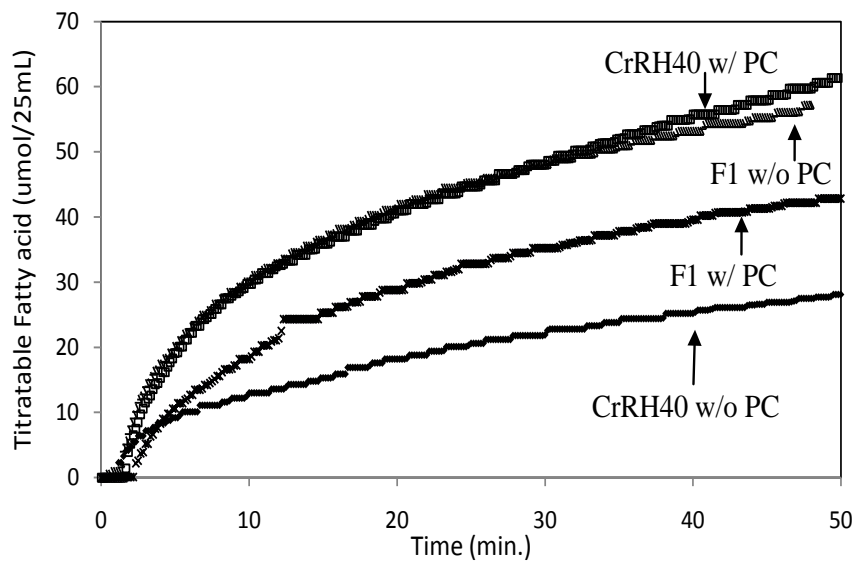


Figure 3.13 Amount of fatty acid released in the lipolysis of 0.48 g CrRH40 and 0.8 g F1 composed of 55% of CrRH40, 37.5% of soybean oil and 7.5% of ethanol in 5 mM of NaC solution in the presence and absence of 1.25 mM of PC at 37°C

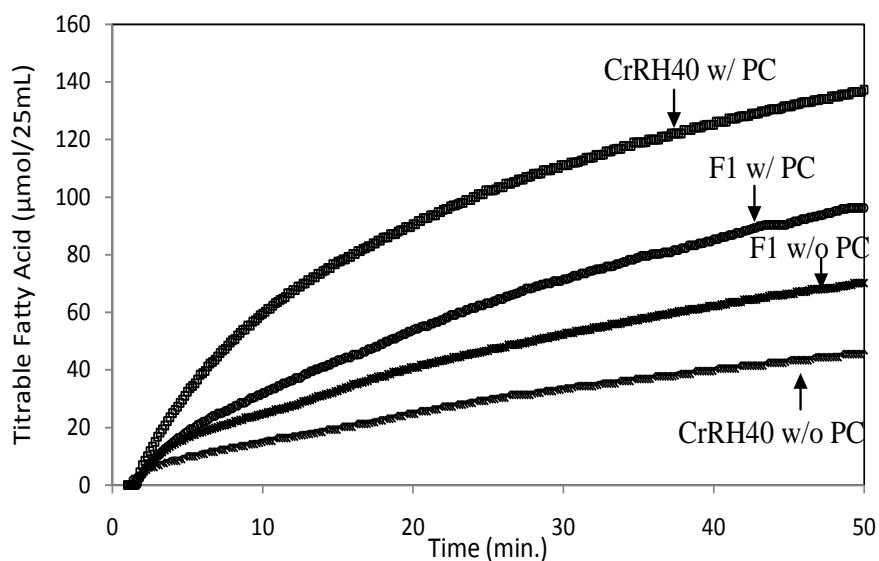


Figure 3.14 Amount of fatty acid released in the lipolysis of 0.48 g CrRH40 and 0.8 g F1 composed of 55% of CrRH40, 37.5% of soybean oil and 7.5% of ethanol in 20 mM of NaC solution in the presence and absence of 5 mM of PC at 37°C

### **3.4.3.3. Calcium**

Calcium is present in the bile. Its role in the lipolysis has been proposed in some studies. Alvarez et al. studied dependence of the zero-order rate of lipolysis on the concentration of  $\text{Ca}^{2+}$  (Alvarez and Stella, 1989). They showed rate increases as the concentration of  $\text{Ca}^{2+}$ . Further, they proposed that an active complex of colipase-lipase- $\text{Ca}^{2+}$  was formed. Later, Zangenberg et al. clearly demonstrated that the lipolysis was completed in the high concentration of  $\text{Ca}^{2+}$  and it was attributed to the formation of fatty acid or bile acid-calcium salt (Zangenberg, Müllertz et al., 2001).

#### **3.4.3.3.1. The effect of calcium on the extent of lipolysis**

As shown in Figures 3.15 and 3.16, the initial rates of production of fatty acid during the lipolysis of PC in simulated digestion buffer were different in the presence and absence of 5 mM  $\text{Ca}^{2+}$ . The presence of  $\text{Ca}^{2+}$  increased the initial lipolysis rate of fasted-state buffer containing either cholic acid or taurocholic acid. However, by 30 min, the PC was hydrolyzed completely no matter if  $\text{Ca}^{2+}$  was included or not. The different effect on initial rates was more obvious in the simulated digestion buffer composed of NaTC and PC (Figure 3.16). Without BS/PC, the  $\text{Ca}^{2+}$  also had a significant effect on the lipolysis of PS80. The extent of lipolysis of PS80 in tris maleate buffer is shown in Figure 3.17. A rapid production of fatty acid was observed in the presence of  $\text{Ca}^{2+}$  followed by a relatively slow production of fatty acid. The lipolysis of PS80 reached a plateau in 100 min indicating lipolysis had stopped. By calculation of theoretical production of fatty acid from the amount of added PS80, only half of PS80 had been hydrolyzed. In comparison, the lipolysis of PS80 was maintained at what appeared to be a steady state in the absence of  $\text{Ca}^{2+}$  after 10 min of addition of enzyme preparation. Interestingly, a reversed pattern of lipolysis was observed in the presence of BS/PC (Figure 3.18).  $\text{Ca}^{2+}$  promoted the production of fatty acid and maintained the rate of lipolysis at steady state.

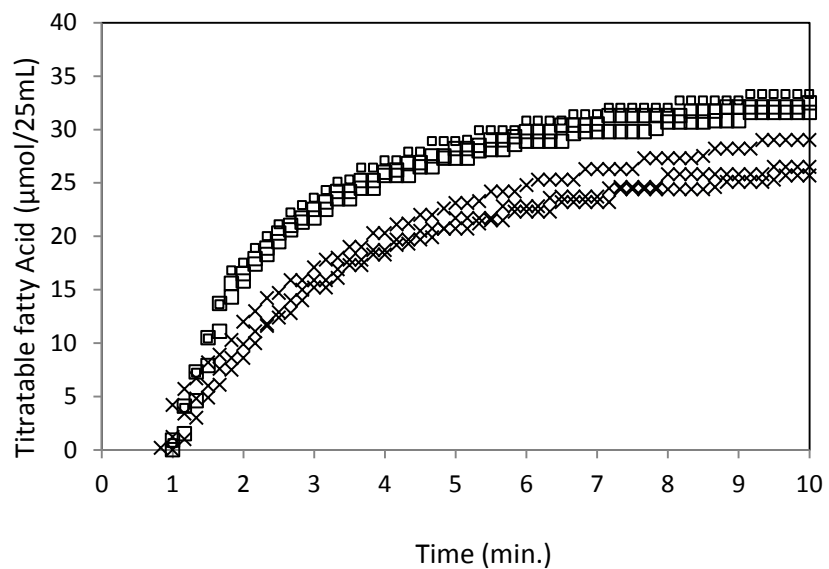


Figure 3.15 Amount of fatty acid released in the lipolysis of SIF composed of 5 mM NaC/1.25 mM MPC in the presence (square) and absence (cross) of 5 mM of CaCl<sub>2</sub> at 37°C. Theoretical amount of fatty acid from 1.25 mM PC is 31 µmol/25 mL.

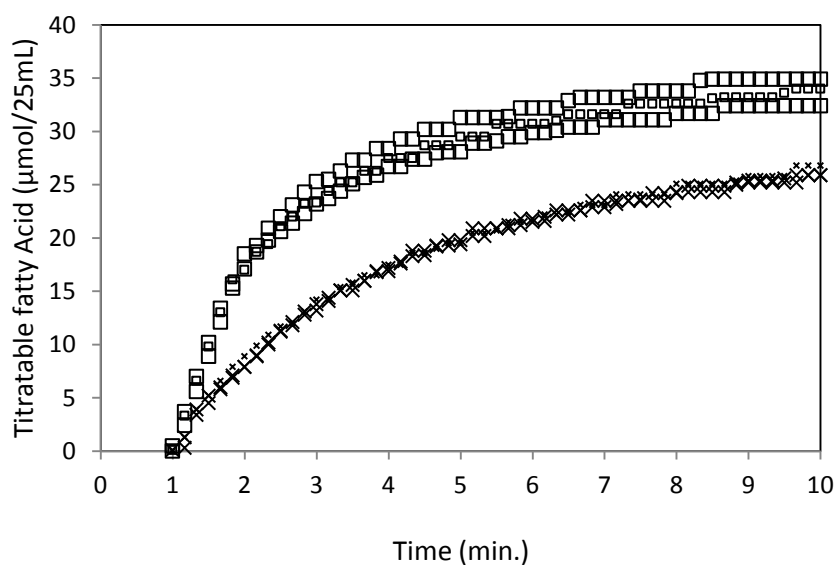


Figure 3.16 Amount of fatty acid released in the lipolysis of SIF buffer composed of NaTC in the presence (square) and absence (cross) of 5 mM of CaCl<sub>2</sub> at 37°C. Theoretical amount of fatty acid from 1.25 mM PC is 31 µmol/25 mL.

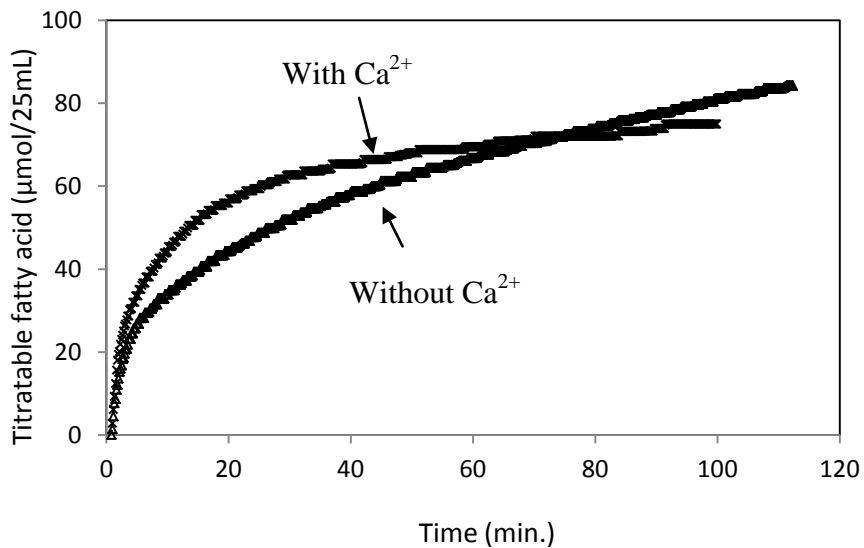


Figure 3.17 Amount of fatty acid released in the lipolysis of PS80 in tris maleate buffer (pH 7.5 at 37°C) in the presence and absence of 5 mM of CaCl<sub>2</sub>.

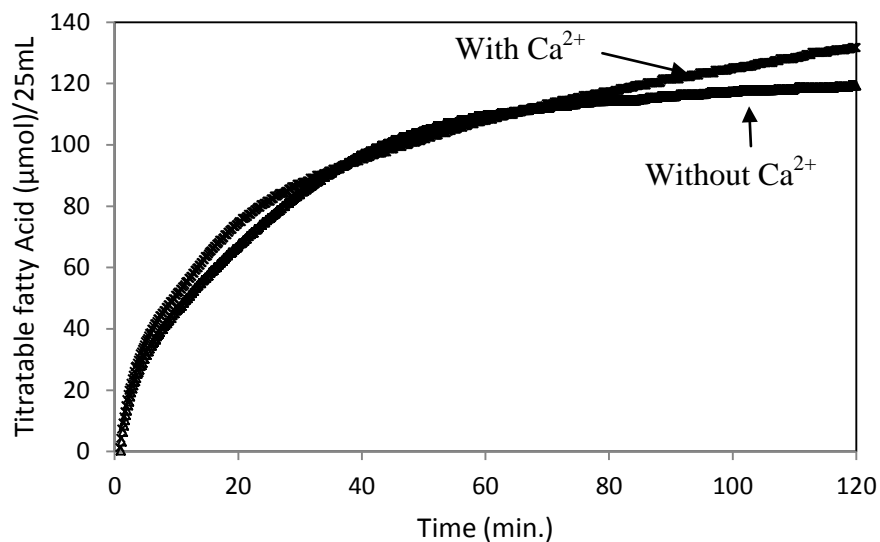


Figure 3.18 Amount of fatty acid released in the lipolysis of PS80 in SIF buffer (pH 7.5 at 37°C) in the presence and absence of 5 mM of CaCl<sub>2</sub>

#### 3.4.3.3.2. Change of calcium concentration in solution during the lipolysis and composition of calcium salt

To further elucidate the influence of calcium on the lipolysis, the calcium concentration in solution as a function of time was measured by inductively coupled plasma spectroscopy. When the sample is introduced into the instrument, a characteristic

emission wavelength of calcium will be detected. Even very low concentrations of calcium can be quantitatively determined by this technique. Figure 3.19 shows the percentage of calcium in the solution during *in vitro* lipolysis of PS80 in SIF buffer. The calcium concentration dropped to 56% by the end of the experiment. A precipitate was observed during the lipolysis and was collected. The solid material was characterized by DSC and elemental analysis. In DSC analysis of desiccated samples, there was no obvious water peak detected. An endothermic peak was observed at 77°C which is close to the literature report value of calcium oleic acid salt (Figure 3.20). Elemental analysis gave the formula of  $\text{Ca}(\text{oleic acid})_2 \cdot 0.4\text{H}_2\text{O}$  for two independent batches of solid material with less than 0.3% of the difference between the theoretical value and observed value of each element. From these results, it can be concluded that the fatty acid released from the lipolysis precipitated as a calcium salt. Precipitation as  $\text{Ca}^{2+}$  salt could potentially reduce the availability of fatty acid to form the mixed micelles with BS/PC.

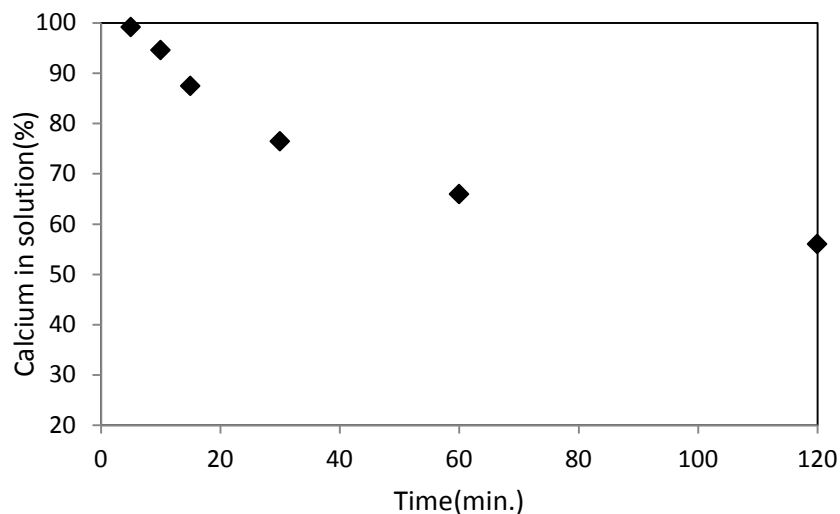


Figure 3.19 Calcium concentration change during *in vitro* lipolysis of PS80 in the SIF buffer at 37°C

Sample: precipitation of Ca  
Size: 1.8620 mg  
Method: Ca salt

DSC

File: C:\Lin\Lin.004  
Operator: Lin  
Run Date: 1-Dec-08 17:24

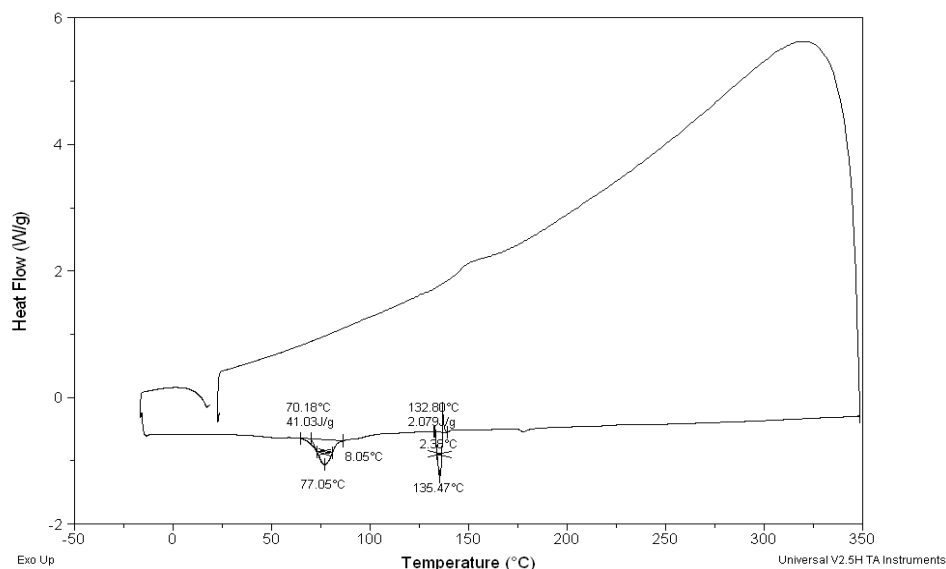


Figure 3.20 Thermogram of precipitate collected from the lipolysis of PS80 in the presence of calcium

### 3.5. Conclusion

The dynamic *in vitro* lipolysis model was sensitive to different ester-containing substrates under the optimal conditions. A  $\pm 10\%$  variation of fatty acid released at 120 min was considered acceptable. Bile salts, phospholipid and calcium all showed significant effects on the lipolysis of PS80. The precipitate from the lipolysis of PS80 in the presence of  $\text{Ca}^{2+}$  was identified as fatty acid salt. A reproducible dynamic *in vitro* lipolysis model was established.



## Chapter 4

### Solubilization of Poorly-water Soluble Drugs in Polysorbate 80 Under Simulated Intestinal Conditions

#### 4.1. Summary

In this chapter, the solubilization of progesterone, 17 $\beta$ -estradiol, and nifedipine during the *in vitro* dispersion and lipolysis of a simple model LBDDS composed of PS80 were assessed under simulated intestinal conditions. Initial supersaturation ratios, 2, 1, and less than 1, were created by the dispersion of known amounts of formulations containing drug in simulated intestinal fasted-state buffer (SIF buffer) at 37°C. To be clear, these experiments did not include the use of lipase enzyme. The concentrations of drug in solution were monitored as function of time. The supersaturation ratio area under the curve (AUC-SS) was used to quantify the time-dependent supersaturation during the *in vitro* dispersion and lipolysis of PS80. Maintenance of the supersaturated state was found to be drug-dependent. At supersaturation ratio of 2, AUC<sub>0-120</sub>-SS of progesterone was 26 $\pm$ 4 min while AUC<sub>0-120</sub>-SS 17 $\beta$ -estradiol and nifedipine were 92 $\pm$ 7 min and 113 $\pm$ 7 min, respectively, indicating that 17 $\beta$ -estradiol and nifedipine remained in supersaturated state to a greater extent. When supersaturation ratio was close to 1, precipitation of all drugs was prevented by PS80. Results in digested blank PS80 showed that equilibrium solubilities of 17 $\beta$ -estradiol and nifedipine were decreased indicating that the driving force for precipitation - the degree of supersaturation - increased. Equilibrium solubility of progesterone increased slightly and then remained constant.

Upon exposure of formulations to the lipase enzyme, supersaturated solutions were created and maintained to various extents. The values of concentration area under the curve (AUC-C) in the presence of inactivate enzyme and active enzyme indicated that the lipolysis of PS80 had no effect on the solubilization of progesterone. On the other hand, 17 $\beta$ -estradiol remained in supersaturated state up to 120 min, with a maximum supersaturation ratio of 4.1. Nifedipine was in the supersaturated state at 120 min for

formulations starting at the initial supersaturation ratio of 1 and 0.6. The duration for the supersaturated state was only 30 min from the formulation (N-35) with an initial supersaturation ratio of 2. AUC-SS demonstrated that 17 $\beta$ -estradiol exhibited the greatest extent of supersaturation and progesterone the least.

#### **4.2. Introduction**

Aqueous solubility and gastrointestinal permeability are believed to be among the important factors that govern the absorption of drug in the GI tract (Amidon, Lennernäs et al., 1995). There are a number of formulation strategies that have been used to improve the oral absorption of poorly-water soluble drugs, either by increasing the dissolution rate or by presenting the drug in solution and maintaining the drug in solution through the GI tract. Some examples include solid dispersions, eutectic mixtures, cosolvent formulations, and lipid-based formulations. Lipid-based drug delivery systems (LBDDSs) such as oil solution, emulsion and self-emulsifying systems are popular approaches to improve the oral bioavailability (Hauss, Fogal et al., 1998; Porter, Trevaskis et al., 2007; Porter, Pouton et al., 2008). Products such as Neoral®, Lopinavir and Ritonavir are just a few examples of successful LBDDSs. Typical excipients for LBDDSs include triglyceride oils, mixed glycerides, lipophilic surfactants, hydrophilic surfactants and water-soluble cosolvents. Of particular interest to LBDDSs is the observation that some lipidic excipients may be hydrolyzed enzymatically, the products of which may form mixed micelles with endogenous surfactants such as bile salt and biliary lipids.

As stated by Fick's First Law, the rate of drug diffusing through the intestinal biological membrane at steady state is proportional to the drug concentration in the GI tract, assuming a sink condition. In general, absorption of a poorly-water soluble drug will be limited due to poor solubilization upon dilution and dispersion of a dosage form *in vivo*. Upon oral administration, an LBDDS undergoes dilution and dispersion in the GI tract, forming a variety of lipid aggregates such as emulsion droplets and micelles. Presumably, the drug remains in the solubilized state primarily within these lipid aggregates. It has been suggested that the solubilization capacity of the lipid aggregates is insufficient to account for the amount of drug remaining in the solubilized state *in vivo* (Gao, Rush et al., 2003; Gao and Morozowich, 2006). This has led to the hypothesis that once dispersed in

the GI tract, LBDDSs may also enhance absorption by inducing and maintaining the drug in a supersaturated state.

The possible role of supersaturation in enhancing the oral absorption has drawn much attention (Gao and Morozowich, 2006; Vaughn, McConville et al., 2006; Guzmán, Tawa et al., 2007; Brewster, Vandecruys et al., 2008; Mellaerts, Mols et al., 2008; Overhoff, McConville et al., 2008). In the laboratory, supersaturation can be created by various methods which modulate either the solute concentration or the equilibrium solubility. The solute concentration can be regulated by methods like solvent evaporation and dissolution of metastable solid. The change of temperature, pH, and addition of anti-solvent can alter the equilibrium solubility.

By definition, the supersaturated state is thermodynamically unstable and thus such a state will spontaneously precipitate. To be useful as a technique for enhancing drug delivery, some methods must be employed to kinetically stabilize the supersaturated state. It has been observed that the rate of precipitation may be slowed by additives such as polymers (e.g., hydroxymethylcellulose, polyvinylpyrrolidone). Gao et al. employed supersaturable self-emulsifying drug delivery systems (S-SEDDSs) to create supersaturated solutions of paclitaxel, PNU-91325 and AMG 517 (Gao, Rush et al., 2003; Gao, Guyton et al., 2004; Gao, Akrami et al., 2009). Nonionic surfactants like Cremophor RH40, Polysorbates and TPGS were observed to enhance the extent of supersaturation during the dilution of formulation (Vandecruys, Peeters et al., 2007).

Of importance to this work, the lipolysis of LBDDSs could possibly modulate both the apparent solubility and the equilibrium solubility. The driving force for precipitation - the degree of supersaturation - could be altered by changes in equilibrium solubility. The change of lipid composition due to lipolysis may alter both the structure of lipid assemblies and their capability of solubilizing drug (Borné, Nylander et al., 2002; Kossena, Charman et al., 2004). With respect to kinetics of precipitation of drug, components in LBDDSs and any lipolytic products could potentially influence the critical nucleation and crystal growth steps. In most situations, it would be expected that these two factors are active simultaneously during the lipolysis of LBDDSs. Because of the

complex action of lipolysis of LBDDSs and the effects on thermodynamic and kinetic aspects of precipitation, it is very difficult to establish reliable *in vivo-in vitro* correlation.

A number of studies have correlated the solubilization behavior of poorly-water soluble drugs evaluated by *in vitro* lipolysis models with oral bioavailability (Christensen, Schultz et al., 2004; Porter, Kaukonen et al., 2004; Grove, Pedersen et al., 2005; Goddeeris, Coacci et al., 2007). More recently, studies also have demonstrated that the lipoidal surfactants can be hydrolyzed by digestive enzymes and that the overall composition of the solution may impact the solubilization of a poorly-water soluble drug. Sek et al. examined the *in vitro* solubilization and oral bioavailability of atovaquone formulated in LBDDSs composed of long chain glycerides, Cremphor EL, and a range of pluronic surfactants (Sek, Boyd et al., 2006). Subsequently, the same group observed that the oral bioavailability of self-emulsifying lipid-based formulation of danazol in beagle dogs was reduced by increasing the content of Cremophor EL relative to lipid (Cuiné, Charman et al., 2007). After a systemic evaluation of the bioavailability of danazol following oral administration of lipidic self-emulsifying formulation to dogs, Cuine' et al. suggested that surfactant lipolysis resulted in a reduction in the solubilization capacity. The decrease in oral bioavailability of surfactant-only formulations was attributed to the generally poor dispersibility of surfactants. Fernandez et al. tried to correlate the solubilization of poorly-water soluble drugs, piroxicam and cinnarine, as a function of the *in vitro* lipolysis of Labrasol and Gelucire 44/14. The lipolysis of these two excipients resulted in variety of products including C<sub>8</sub>-C<sub>10</sub> and C<sub>8</sub>-C<sub>10</sub> diglycerides and triglycerides as well as PEG diesters (Fernandez, Chevrier et al., 2009). The lipolytic products responsible for the solubilization drugs during the lipolysis of two surfactants were suggested and the importance of the lipolysis of surfactants on drug solubilization was demonstrated.

Little is known about the mechanism by which LBDDS formulations create and maintain drugs in a supersaturated state in simulated GI conditions. Evaluating the ability of each component to induce and maintain a supersaturated state of poorly-water soluble drug will provide useful information. Surfactants are included widely in LBDDSs and not only aid the dispersibility of formulations but also provide a means of solubilization of a

poorly-water soluble drug by forming the micelles. However, it has been proposed that precipitation of a poorly-water soluble drug solubilized in LBDDS may be attributed either to the lower solubilization capacity upon dispersion or to hydrolysis of lipoidal components by pancreatic enzyme (Cuiné, Charman et al., 2007; Mohsin, Long et al., 2009). To our knowledge, few studies have been conducted to probe the capability of surfactant to creation and maintain drug in a supersaturated state under the simulated GI conditions.

So as to be able to quantitatively examine the effect of lipolysis, we propose a model LBDDS composed of only one component that is sensitive to pancreatic lipase enzyme. In this chapter, time-dependent solubilization behaviors of progesterone, 17 $\beta$ -estradiol and nifedipine during the *in vitro* dispersion and lipolysis of polysorbate 80 (PS80) under simulated intestinal conditions are assessed. PS80 is widely used in LBDDSs and has been shown to be sensitive to the lipase enzyme in Chapter 3 and in the literature. We hypothesize that lipolysis of surfactant excipient in the model LBDDS results in a supersaturated state for model poorly-water soluble compounds progesterone, 17 $\beta$ -estradiol and nifedipine. Further, we hypothesize that the extent of the supersaturation is dependent on the extent of hydrolysis of surfactant and on the initial concentration of the drug. The extent of time-dependent supersaturation will be quantified by the supersaturation ratio area under the curve (AUC-SS).

### **4.3. Materials and methods**

#### **4.3.1. Materials**

Polysorbate 80 was a generous gift from Croda Inc. (Edison, NJ, USA). Progesterone (Prog, purity  $\geq 99\%$ ), Nifedipine (NIF, purity  $\geq 98\%$ ), 17 $\beta$ -estradiol (EST, purity  $\geq 98\%$ ), 1,2-diacyl-sn-glycero-3-phosphocholine (type XVI-E) from egg yolk (PC), 4-bromophenylboric acid, trisma® maleate, calcium chloride hydrate (purity  $\geq 99\%$ ), sodium cholate hydrate (NaC, purity  $\geq 99\%$ ) and lipase (type II, crude from porcine pancreas) were purchased from Sigma-Aldrich (St. Louis, MO, USA). NaOH (0.1 M) were purchased from Fisher Scientific (Pittsburgh, PA, USA). All chemicals were used as received. Water for buffer solution was from a Milli-Q water purification system. Hydrophilic PTFE filters (13 mm diameter and 0.2  $\mu\text{m}$  pore size) were purchased from

Advantec MFS Inc. (Japan). Drug structures are shown in Figure 4.1 and properties and dose number are shown in Table 4.1.

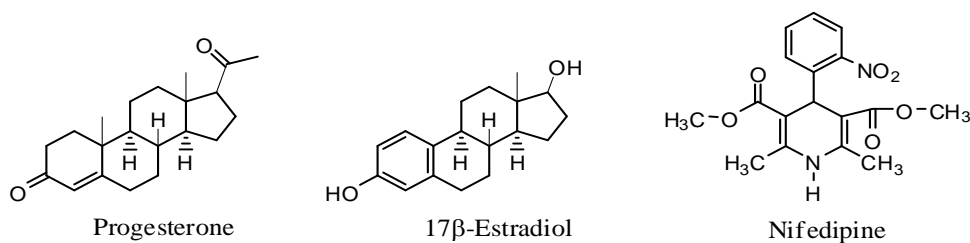


Figure 4.1 The structures of model poorly-water soluble drug

Table 4.1 Drug properties and dose number

Drug	Aqueous solubility (M) at 37°C	T <sub>m</sub> (°C)	LogP(exp.)	Dose number (mL)
Progesterone	$(3.3 \pm 0.1) \times 10^{-5}$	126	4.14 ± 0.003	1953
17β-estradiol	$(6.7 \pm 0.3) \times 10^{-6}$	178	4.20 ± 0.02	273
Nifedipine	$(2.5 \pm 0.1) \times 10^{-5}$	173	3.63 ± 0.01	1134

#### 4.3.2. Equilibrium solubility of model drugs in neat PS80

To prepare the formulations containing a known amount of the model drug, the solubility of each model drug in neat PS80 was determined at 25 ± 0.5°C. An excess amount of model drug was added to PS80 and the vial rotated for a week. The viscous PS80 sample was filtered through hydrophilic PTFE filter with 0.2 μm pore size. An accurate amount of filtrate was weighed and dissolved in 10 mL of isopropanol/water (1/1). All experiments related to nifedipine were conducted under protection from light due to the photosensitivity of the drug (see Appendix 1). The solutions obtained above were analyzed with a corresponding HPLC method. The drug concentration in neat PS80 was expressed as mg of drug/g of PS80 calculated by Eq. (4.1)

drug concentration (mg/g) =

$$\frac{\text{Drug concentration determined in solution (mg/L)} \times 0.01\text{L}}{\text{Weight of drug-loaded polysorbate 80 (g)}} \quad (4.1)$$

#### 4.3.3. Preparation of the model drug loaded PS80 formulations

According to the solubility of model drugs in neat PS80 determined in 4.3.2, three formulations of each drug were prepared. The concentrations of each drug in each formulation are listed in Table 4.2.

Table 4.2 Drug concentrations in formulations

Drug concentration (mg/g)		
Progesterone	17 $\beta$ -Estradiol	Nifedipine
11.91 $\pm$ 0.25 (P-12)	5.07 $\pm$ 0.17 (E-5)	11.29 $\pm$ 0.37 (N-11)
19.90 $\pm$ 0.73 (P-20)	7.14 $\pm$ 0.30 (E-7)	20.02 $\pm$ 0.80 (N-20)
31.60 $\pm$ 0.46 (P-31)	14.26 $\pm$ 0.66 (E-14)	35.06 $\pm$ 0.88 (N-35)

##### 4.3.3.1. Formulations containing progesterone

As seen in Table 4.2, three progesterone-loaded PS80 formulations were prepared, P-12 (12mg/g), P-20 (20mg/g) and P-31(31mg/g). P-20 contained progesterone at near saturated solubility in neat PS80. P-31 formulation contained progesterone at 50% greater than saturated solubility. P-11 was prepared at 50% less than saturated solubility of progesterone. Exact amounts of progesterone and PS80 were weighed into a 4 mL glass vial with a PTFE-lined cap. P-12 and P20 formulations were rotated at 25 $\pm$ 0.5 $^{\circ}$ C until progesterone was dissolved totally. The complete absence of a drug crystal was verified by polarized microscopy. P-31 was rotated at 37 $^{\circ}$ C for two days and then 45 $^{\circ}$ C overnight before use. Except for formulation P-31, all formulations were kept at room temperature until use.

#### **4.3.3.2. Formulations containing 17 $\beta$ -estradiol**

17 $\beta$ -estradiol-loaded PS80 formulations were prepared at 5 mg/g (E-5), 7 mg/g (E-7) and 14 mg/g (E-14). E-5 was prepared at 15% of saturated solubility of 17 $\beta$ -estradiol in neat PS80. E-7 contained 17 $\beta$ -estradiol at 21% of saturated solubility. E-14 formulation contained drug at 42% of saturated solubility. Known amounts of 17 $\beta$ -estradiol and PS80 were weighed into a 4 mL glass vials with PTFE-lined cap. All formulations were rotated at 25 $\pm$ 0.5 $^{\circ}$ C for a week which resulted in complete dissolution of 17 $\beta$ -estradiol in PS80. All formulations were kept at room temperature until use.

#### **4.3.3.3. Formulations containing nifedipine**

Three nifedipine-loaded PS80 formulations were prepared, N-11 (11 mg/g), N-20 (20 mg/g) and N-35 (35 mg/g). N-11 contained nifedipine at 25% of saturated solubility in neat PS80. N-20 contained nifedipine at about 50% of saturated solubility. N-35 was prepared at near saturated solubility of nifedipine in PS80. Nifedipine was weighed into a 4 mL glass vial and PS80 was added giving formulations at designated concentrations. All formulations were rotated at 25 $\pm$ 0.5 $^{\circ}$ C in an incubator for a week and kept at room temperature until use. All vials were wrapped with aluminum foil to protect the drug from light.

#### **4.3.4. Dispersion of drug-containing PS80 formulations**

Dispersion experiments were carried out in a simulated intestinal fasted-state digestion buffer (SIF buffer) containing 5 mM sodium cholate (NaC)/1.25 mM phosphocholine (PC) in tris maleate buffer (pH 7.5) composed of 50 mM tris-maleate, 150 mM NaCl at 37 $^{\circ}$ C. CaCl<sub>2</sub> (5 mM) was included in selective studies. The final PS80 concentration upon dispersion was 1% and was achieved by adding a known amount of the drug-loaded formulation to SIF buffer in a stirred and thermostatted glass flask at 37 $\pm$ 0.5  $^{\circ}$ C. Agitation was provided by a 5 mm magnetic stir bar at 500 rpm on a direct drive motor/magnetic system. Prior to collection of sample, formulation was dispersed for 15 min to ensure the formation of a homogenous solution. Aliquots were taken at predetermined times and filtered through a 0.2  $\mu$ m PTFE syringe filter. The filtrates were diluted accordingly by isopropanol/water(1:1) for HPLC analysis.



The effects of particles in the enzyme preparation on the concentration were assessed by addition of inactivated enzyme to the dispersion of formulations in SIF buffer. The enzyme preparation, prepared as the standard procedure described in Chapter 3 (Section 3.3.4), was incubated at 110°C for 3 h. The pH was adjusted to 7.5 at room temperature before addition. There was only 70  $\mu$ L of 0.1M NaOH titrated into reaction solution during the experiment, indicating enzyme was totally inactivated by heating.

#### **4.3.5. *In vitro* lipolysis of drug-containing PS80 formulations**

*In vitro* lipolysis experiments were monitored with the characterized dynamic *in vitro* lipolysis model. Experiments were conducted in triplicate. In order to achieve PS80 concentration at 1%, a known amount of drug-loaded formulation was introduced into the SIF buffer in a stirred and thermostated glass flask at 37 °C (see Figure 3.2 in Chapter 3). The formulation was dispersed 15 min prior to the addition of enzyme preparation. Lipolysis was initiated by adding enzyme preparation (1 mL enzyme solution/25 mL of SIF buffer) to a well dispersed formulation. One milliliter of well-dispersed solution was withdrawn and to the solution was added 1 mL of enzyme preparation to maintain the total final volume of 25 mL. Enzyme solution was prepared by standard protocol described in Section 3.3.4. In brief, 1 g of crude porcine pancreatic lipase was added to 5 mL of trismaleate buffer. The suspension was stirred for 15 mins and subsequently centrifuged for 20 min at 5000 rpm at room temperature. The supernatant was stored on ice until use. The enzyme solution was prepared fresh daily. Released fatty acid was titrated with 0.1 M NaOH to maintain pH at 7.5 by the pH-stat titration unit. Each aliquot was taken at predetermined time and filtered through 0.2  $\mu$ m PTFE membranes immediately. The filtrate was added to an equal volume of isopropanol immediately to inhibit the enzyme activity. Concentration of drug was determined by the corresponding HPLC method.

#### **4.3.6. Determination of equilibrium solubility in digested blank formulation**

The equilibrium solubility of each model drug in blank digests of PS80 was determined. Blank formulations of PS80, that is surfactant but no drug, were subjected to *in vitro* lipolysis as described in Section 4.3.5. Aliquots were taken at predetermined times and enzyme inhibitor, 4-bromophenylboric acid (1 M in methanol), was added immediately to prevent further lipolysis. The pH was adjusted to 7.5 and checked before and after

incubation. To each sample of digest, an excess amount of drug was added. Samples were rotated at  $37\pm 0.5^{\circ}\text{C}$  for the days. Aqueous phases were filtered through  $0.2\ \mu\text{m}$  PTFE membranes and diluted by isopropanol/water (1/1) to appropriate concentration. All samples were analyzed by HPLC. Successive concentrations within  $\pm 5\%$  indicated equilibrium solubility was achieved.

#### **4.3.7. Determination of octanol/water partitioning coefficient of model drugs**

A known amount of drug was added into 1:1 (v/v) mixture of octanol and water. The mixture was rotated for three days at room temperature. After filtration, the concentration of drug in the organic phase and the aqueous phase were determined by HPLC. The concentration of drug in aqueous phase was assayed by injection of filtrate directly. It was necessary to dilute the organic phase by mobile phase prior to HPLC analysis.

The partition coefficient (direct) is calculated as the ratio of the concentration in octanol to the concentration in water.

#### **4.3.8. HPLC methods**

The HPLC conditions and protocols for progesterone,  $17\beta$ -estradiol and nifedipine are listed in Table 4.3. All mobile phases were pre-mixed and degassed online. With respect to the precision and linearity, HPLC methods were validated by standard protocols and all samples were diluted to the concentrations within the linear range of calibration including four to six working standards prepared from three independent stock solutions. The lack of interference with other components such as sodium cholate/phosphalipid was validated by spiking  $100\ \mu\text{L}$  or  $500\ \mu\text{L}$  of  $5\ \text{mM}$  NaC/PC to  $900\ \mu\text{L}$  or  $500\ \mu\text{L}$  of one working standard. The HPLC chromatograms for three model drugs are shown in Figures 4.2-4.4. A peak asymmetry factor less than 1.2 indicated an acceptable peak shape.

Table 4.3 HPLC conditions and protocols for analysis of progesterone, 17 $\beta$ -estradiol and nifedipine

	Progesterone	17 $\beta$ -Estradiol	Nifedipine
Pump	SpectraSYSTEM P4000		
Detector	SpectraSYSTEM UV1000		
Integrator	Peaksimple 321 chromatography data system		
Injector	SpectraSYSTEM AS3000		
Column	SUPELCOSIL™ ABZ+PLUS, 25 cm x 4.6 mm, 5 $\mu$ m		
Precolumn	Same type as column		
Mobile Phase (Acetonitrile%/ water% )	60/40	60/40	50/50
Flow Rate	1.5 mL/min	1.5 mL/min	1.0 mL/min
Wavelength	254 nm	282 nm	236 nm
Injection Size	20 $\mu$ L	50 $\mu$ L	20 $\mu$ L
Retention time	6.6 min	5.6 min	7.8 min

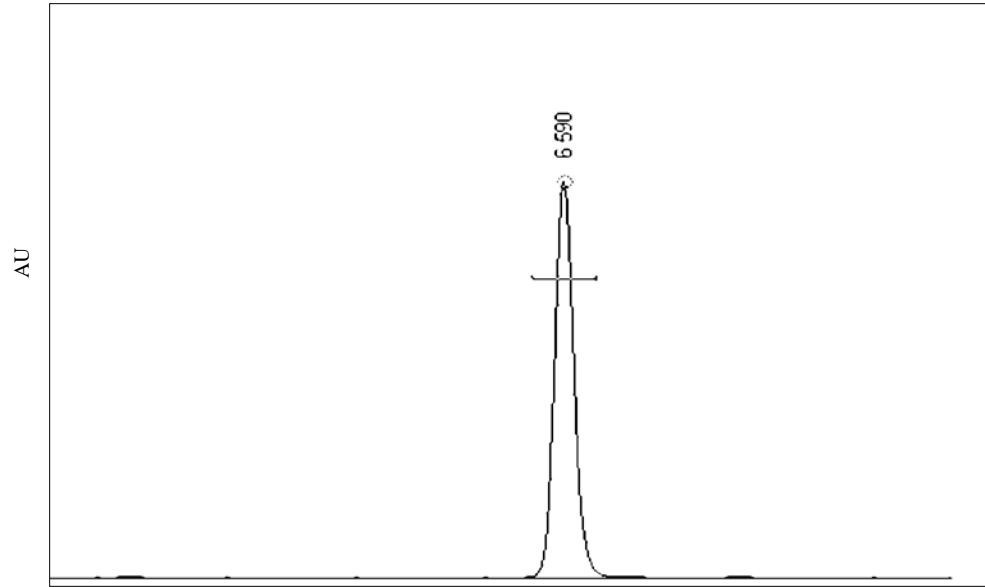


Figure 4.2 HPLC chromatogram of progesterone

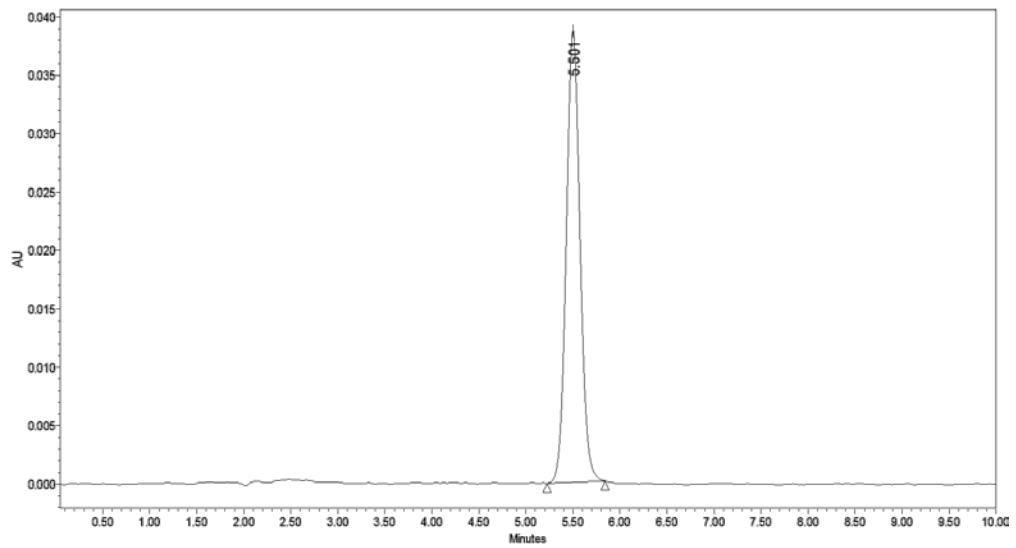


Figure 4.3 HPLC chromatogram of 17β-estradiol

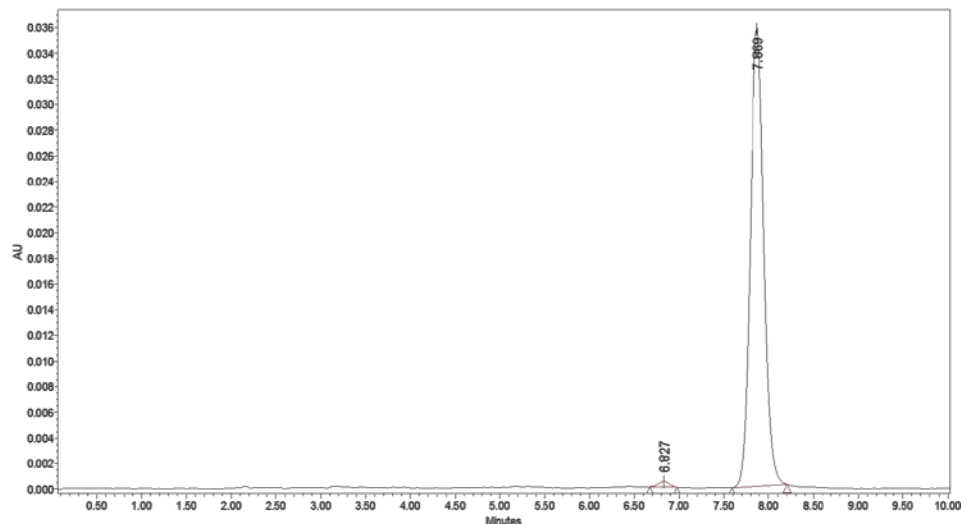


Figure 4.4 HPLC chromatogram of nifedipine

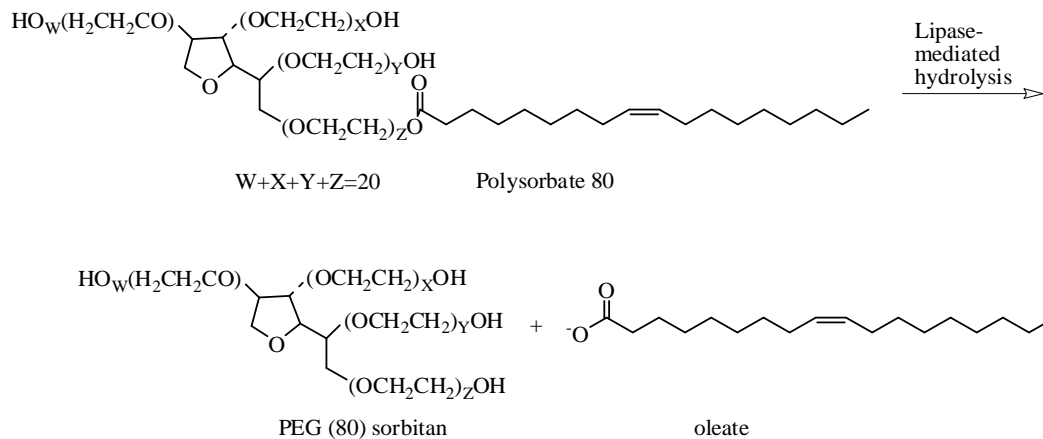
#### 4.3.9. Characterization of solid formed during the *in vitro* dispersion of drug-containing PS80 formulations

The dispersion experiments were conducted as described in Section 4.3.4. The precipitates formed during the *in vitro* dispersion of P-31, E-14 and N-35 formulations were characterized as a function of time by polarized microscopy (Olympus BX51 with Spot Advanced software). At predetermined time, a drop of the dispersed system was placed on the pre-warmed glass slide ( $\sim 37^\circ\text{C}$ ) and covered by glass cover to prevent water evaporation. The dispersion was observed immediately for evidence of birefringence. PS80 solution at concentration of 1% w/v in SIF buffer was used as control.

### 4.4. Results and discussion

#### 4.4.1. Extent of lipolysis as measured by production of fatty acid

The lipolytic products of PS80 during the *in vitro* lipolysis are PEG (80) sorbitan and oleic acid (Scheme 4.1). The production of fatty acid was monitored by titrating with 0.1 M NaOH. Amount of fatty acid was calculated based on 1:1 stoichiometric reaction ratio between the released fatty acid and 0.1 M NaOH. The extents of lipolysis of PS80 in the presence of progesterone (Figure 4.5a),  $17\beta$ -estradiol (Figure 4.5b) and nifedipine (Figure 4.5c) were compared over a 2 h period. Within 10% acceptable variation, total titratable fatty acid generated in the lipolysis of blank PS80 (that is, containing no drug) and drug-loaded PS80 were identical.



Scheme 4.1 The hydrolysis of PS80 by pancreatic lipase

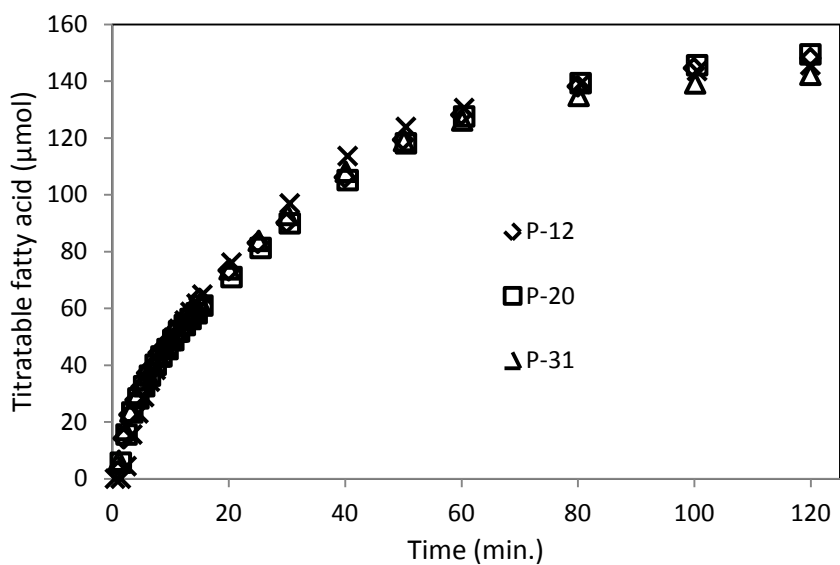


Figure 4.5a Representative of amount of fatty acid released in the lipolysis of blank PS80 and PS80 in the presence of progesterone from formulations P-12, P-20 and P-31. Shown are raw data before subtraction of the blank.

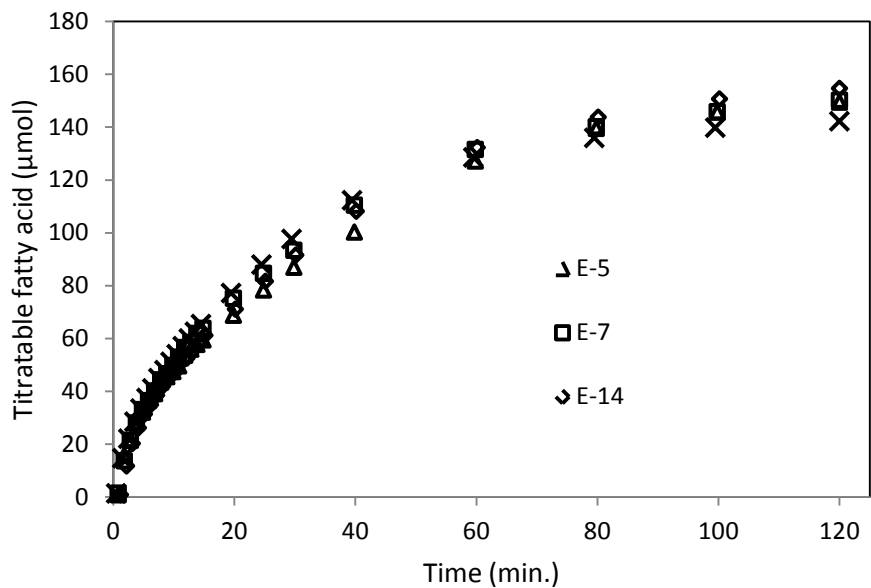


Figure 4.5b Representative Amount of fatty acid released in the lipolysis of blank PS80 and PS80 in the presence of  $17\beta$ -estradiol from formulations E-5, E-7 and E-14. Shown are raw data before subtraction of the blank.

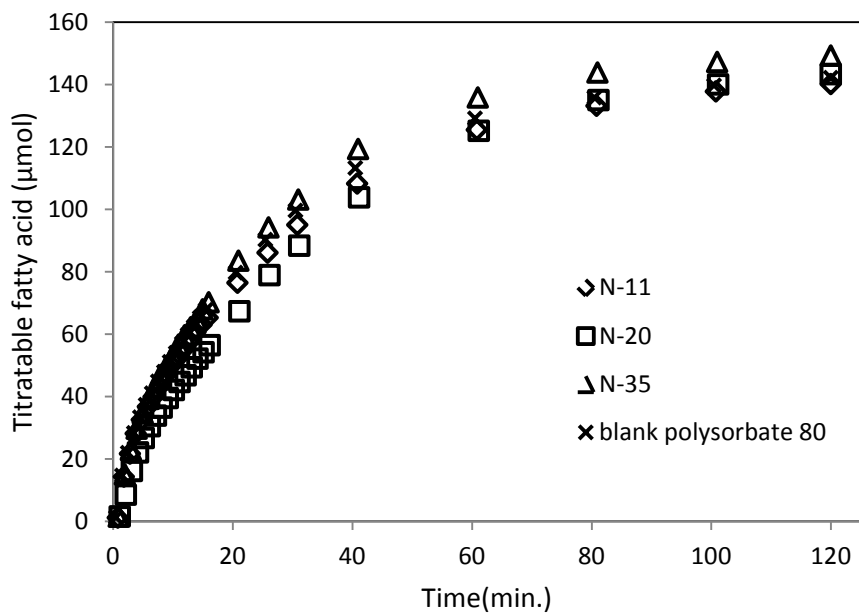


Figure 4.5c Representative amount of fatty acid released in the lipolysis of blank PS80 and PS80 in the presence of nifedipine from formulations N-11, N-20 and N-35. Shown are raw data before subtraction of the blank.

Assuming the extent of lipolysis of phosphatidylcholine (PC) in SIF buffer is not affected in the presence of PS80, the fatty acid from PS80 was calculated by subtraction of fatty acid produced from PC from the total amount of fatty acid generated (see Section 5.3.2). Figures 4.6a – 4.6c are the percentage of titratable fatty acid from PS80 during the *in vitro* lipolysis of drug-loaded formulations. About 6-7% PS80 was hydrolyzed within the first 5 min and 30% in 30 min. As lipolysis proceeded, the rate of production of fatty acid decreased. At 60 min, hydrolysis of PS80 approached a plateau giving 50% of substrate hydrolyzed. In 120 min, only 60% of PS80 was hydrolyzed, a value in agreement with literature reports (Cuiné, McEvoy et al., 2008).

The slow rate of production of fatty acid in the late stage may be attributed to the reduction of the enzyme activity. The enzyme is activated by interfacial binding to a lipid assembly. The crystal structure studies suggests that interfacial binding triggers a conformation change and movement of the lid domain and some surface loops, allowing the substrate access to the active site (Winkler, D'Arcy et al., 1990). The conformation change of the lid domain and  $\beta$ -5 loop changes the environment of catalytic triad dramatically. In the open conformation, serine is more accessible to solvent and orients to the bottom of the hydrophobic pocket where it binds to lipid substrate. Apparently, the hydrolysis at the interface could be affected by either the enzyme or the substrates. The state and composition of the lipid assembly influences lipase activity and extent of lipolysis. Further, pancreatic lipase is easily replaced by bile salts either by solubilization by bile salt micelles, or by competition for the interface (Svasti and Bowman, 1978) also resulting in reduced activity. In addition, some surfactants are able to bind to the active site of enzyme resulting in a reduction of lipase activity by competitive inhibition (Hermoso, Pignol et al., 1996). It has been reported that higher hydrophilic-lipophilic balance (12-17) surfactants could inhibit fatty acid liberation (MacGregor, Embleton et al., 1997). An acyl-enzyme intermediate is formed during the catalysis reaction. The build-up of products of lipolysis may inhibit or even prevent formation of such an intermediate resulting in a slow rate of production of fatty acid.



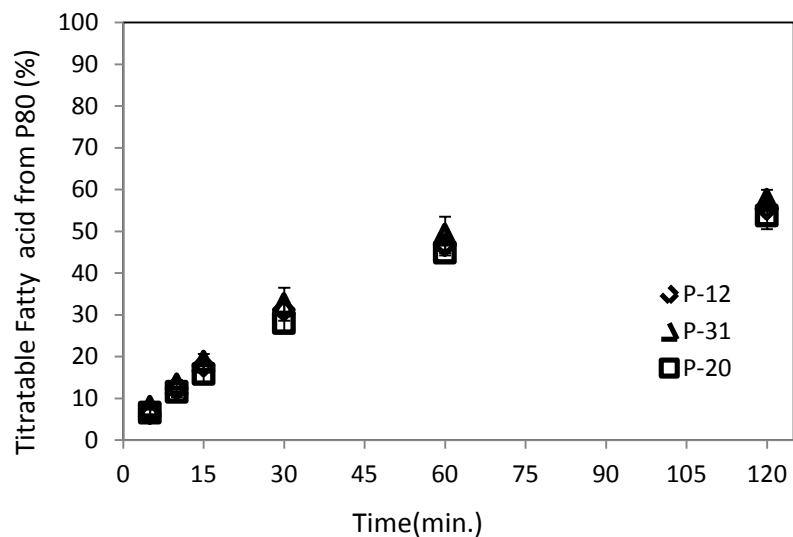


Figure 4.6a The Percentage of titratable fatty acid from PS80 in the presence of progesterone during the *in vitro* lipolysis of formulations P-12, P-20 and P-31 (n = 3). Shown are transformed data after subtraction of the blank.

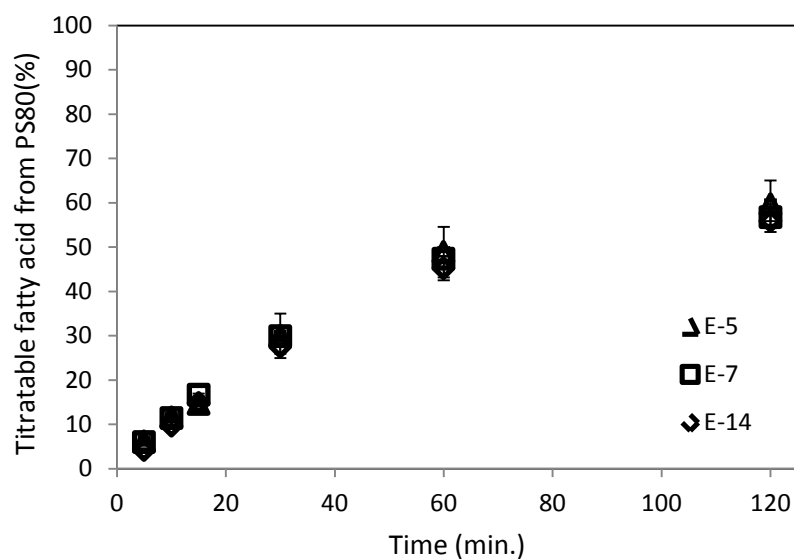


Figure 4.6b The percentage of titratable fatty acid from PS80 in the presence of 17β-estradiol during the *in vitro* lipolysis of formulations E-5, E-7 and E-14 (n = 3). Shown are transformed data after subtraction of the blank.

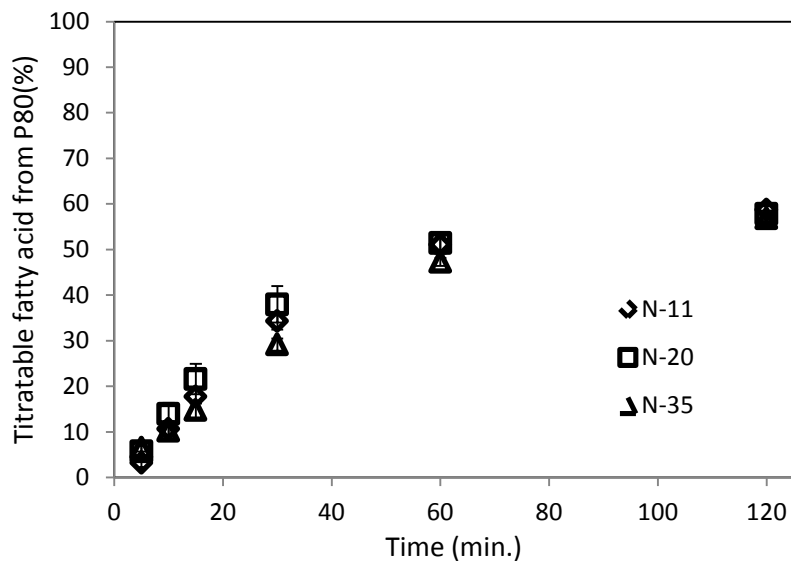


Figure 4.6c The Percentage of titratable fatty acid from PS80 in the presence of nifedipine during the *in vitro* lipolysis of formulations N-11, N-20 and N-35 (n = 3). Shown are transformed data after subtraction of the blank.

#### 4.4.2. Solubilization of model drugs in PS80 solutions

##### 4.4.2.1. Dispersibility of PS80

The dispersibility of PS80 in aqueous media was evaluated. The dispersibility was assessed by adding ~0.25 g of blank PS80 directly to 25 mL of SIF buffer containing 5 mM NaC/1.25 mM PC (pH7.5) at  $37 \pm 0.5^\circ\text{C}$  loaded in the pH-stat device. Initially, addition of PS80 to the digestion buffer resulted in a viscous gel. Complete dispersion was observed within 15 min, as judged visually.

##### 4.4.2.2. Ability of PS80 solutions to inhibit precipitation of model drug when formulated in DMSO and added to SIFs buffer

A set of experiments were carried out to determine the relationship between surfactant concentration and the ability to inhibit drug precipitation. Stock solutions of progesterone,  $17\beta$ -estradiol and nifedipine in DMSO were prepared at concentration of 53 mg/mL, 53 mg/mL and 24 mg/mL, respectively. Upon dispersion in the SIF buffer, the initial drug concentrations were  $190.8 \mu\text{g/mL}$  for progesterone and nifedipine and  $85.6 \mu\text{g/mL}$  for  $17\beta$ -estradiol. The final concentration of DMSO in 25 mL of the SIF buffer was 0.36% (v/v) and remained the same in all tested solutions. As a result of the low concentration,

the effect of DMSO on the solubilization of the drug in the SIF buffer was considered negligible. The rate of stirring and the rate of addition of DMSO to the solution were also strictly controlled in all the experiments. In brief, the DMSO stock solution was added using an automatic pipette and the addition to the tested solution was made over approximately 3 seconds. The results are given in Figures 4.7a – 4.7c. In the absence of PS80, obvious turbidity was observed as soon as the DMSO stock solution was added, indicating drug precipitated rapidly. These results indicate that all three model drugs are not resistant to precipitation in SIF buffer.

To further investigate whether surfactant monomer alone delays drug precipitation, a stock solution in DMSO was dispersed into a solution of PS80 at a concentration below reported CMC (0.01% w/v) (Yamagata, Kusuha et al., 2007), below the measured CMC (0.02% w/v), ten times above the measured CMC (0.2% w/v), and well above the measured CMC (1% w/v). Progesterone (Figure 4.7a) and nifedipine (Figure 4.7c) were observed to precipitate rapidly in the solutions of PS80 at concentrations up to ten times the measured CMC. It is worth noting that concentration of 17 $\beta$ -estradiol initially dropped rapidly and then remained constant up to 30 min in the solution of PS80 at a concentration of ten times the measured CMC (Figure 4.7b). These results suggest that neither the monomer nor micelles at low concentration can delay the precipitation efficiently. High concentration of PS80 (1% w/v), where a vast majority of surfactant is present in micelles, was highly effective in inhibiting precipitation of the model drugs. Note that the steady-state concentrations for dispersion in 1% PS80 are greater than the equilibrium solubilities. This indicates that the dispersions in 1% PS80 are in a supersaturated state. As shown in Figures 4.7a – 4.7c, drug concentrations decrease within the first 5 min and then remain constant up to 24 h. This initial decrease in drug concentration possibly resulted from the rapid injection of DMSO stock solution into the aqueous solution.

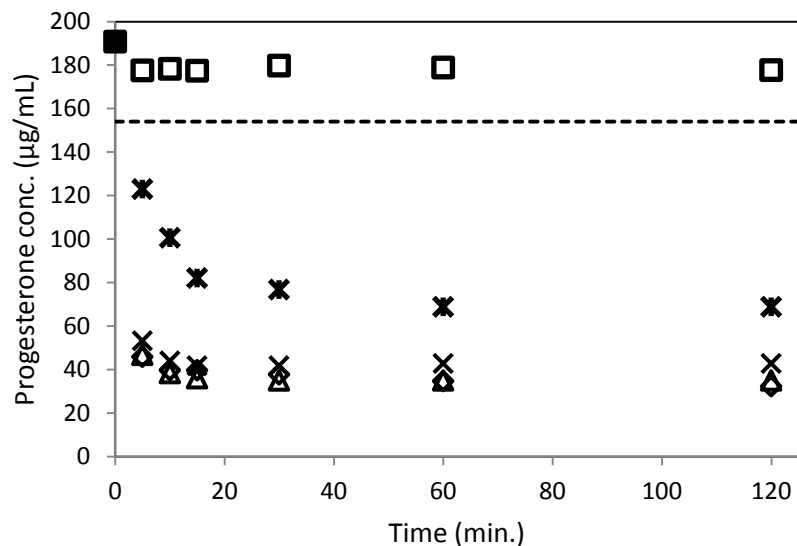


Figure 4.7a The progesterone concentration upon addition of stock solution in DMSO to the SIF buffer containing PS80 at 0% (triangle), 0.01% (diamond), 0.02% (cross), 0.2% (star) and 1% (square) at  $37\pm 0.5^\circ\text{C}$ . The dashed line is the equilibrium solubility in 1% PS80 solution at the same condition.

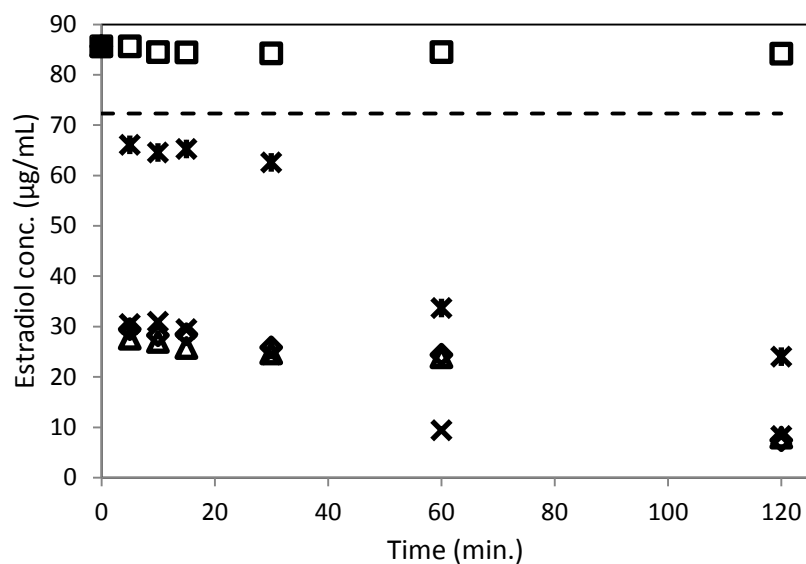


Figure 4.7b The  $17\beta$ -estradiol concentration upon addition of stock solution in DMSO to the SIF buffer containing PS80 at 0% (triangle), 0.01% (diamond), 0.02% (cross), 0.2% (star) and 1% (square) at  $37\pm 0.5^\circ\text{C}$ . The dashed line is the equilibrium solubility in 1% PS80 solution at the same condition.

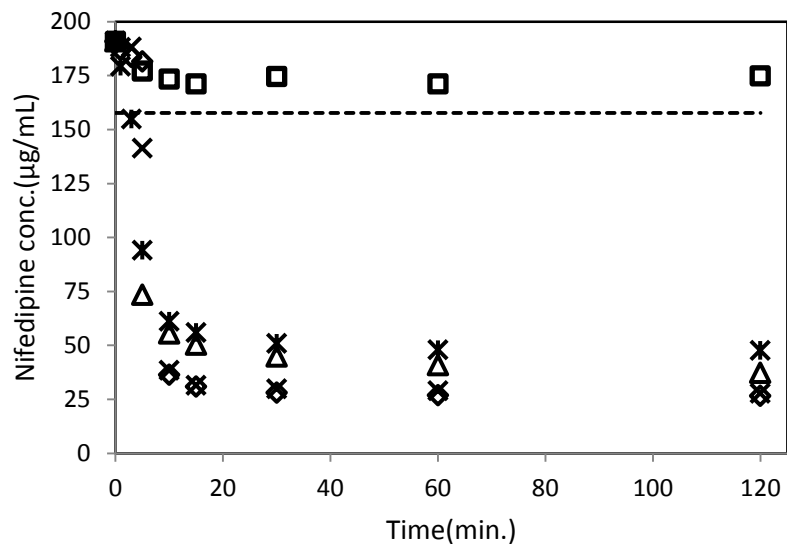


Figure 4.7c The nifedipine concentration concentration upon addition of stock solution in DMSO to the SIF buffer containing PS80 at 0% (triangle), 0.01% (diamond), 0.02% (cross), 0.2% (star) and 1% (square) at  $37\pm 0.5^\circ\text{C}$ . The dashed line is the equilibrium solubility of nifedipine in 1% of PS80 at the same condition.

Supersaturation is defined as drug concentration higher than the equilibrium solubility in the same concentration of PS80 solution. The supersaturation ratio (SS) is commonly used to express the degree of supersaturation (Eq. 4.2).

Supersaturation Ratio (SS) =

$$\frac{\text{Concentration determined at the time of sampling}}{\text{Equilibrium solubility in the same solution}} \quad (4.2)$$

The supersaturation ratios were calculated according to the corresponding equilibrium solubility of drugs in each tested solution. The results are shown in Figures 4.8a – 4.8c. The supersaturation ratios in progesterone and nifedipine decreased to values between 1.1 and 1.5 in 15 min and then remained at this level up to 24 h. When the supersaturation ratios were over 5, such as in the solutions of PS80 at concentration below 0.02% (w/v), progesterone and nifedipine precipitated rapidly and the observed concentrations approached the equilibrium solubility. The rapid precipitation suggested that the concentration of drug initially was above that of the metastable zone (Fig 4.9). Compared

to the case at high supersaturation ratio, the rates of precipitation (slope of the line, Fig 4.7a-c) were slower in the case of 0.2% (w/v) PS80 solution when initial supersaturation ratios were 3.5 (progesterone) and 4.1 (nifedipine). On the other hand, supersaturation ratios in 17 $\beta$ -estradiol appeared to exhibit three distinct zones. In the first 5 minutes supersaturation ratios decreased rapidly to around 4 from 14.8, 10.7 and 9.5 respectively for solutions at 0%, 0.01% and 0.02% PS80 concentration suggesting the drug concentration initially was above the metastable zone. In the time period of 5 to 60 minutes supersaturation ratios remained relatively constant between 3 and 4.8. At times longer than 60 minutes supersaturation ratios for 17 $\beta$ -estradiol decreased to around 1. Birefringence was observed at 2, 20, 50 and 100 minute time points, indicating the formation of a crystalline phase in each of these three zones.

Typically, precipitation is an unremitting process once started. The drug concentration will approach the equilibrium solubility continuously. A supersaturation profile as in the dispersion of 17 $\beta$ -estradiol stock solution in DMSO in the SIFs buffer containing PS80 at 0%, 0.01%, 0.02% suggested a typical solvent-mediated phase transformation (Davey, Cardew et al., 1986). The kinetic mechanisms of precipitation in these systems are not clear. In addition to the degree of supersaturation, a variety of factors could affect the drug precipitation kinetics such as mechanical agitation and the properties of the surface during nucleation and crystal growth (Mullin, 1961). The rate of stirring and the rate of addition of the DMSO solution to the SIF buffer were strictly controlled in all the experiments. However, it is difficult to control other factors in the current study.

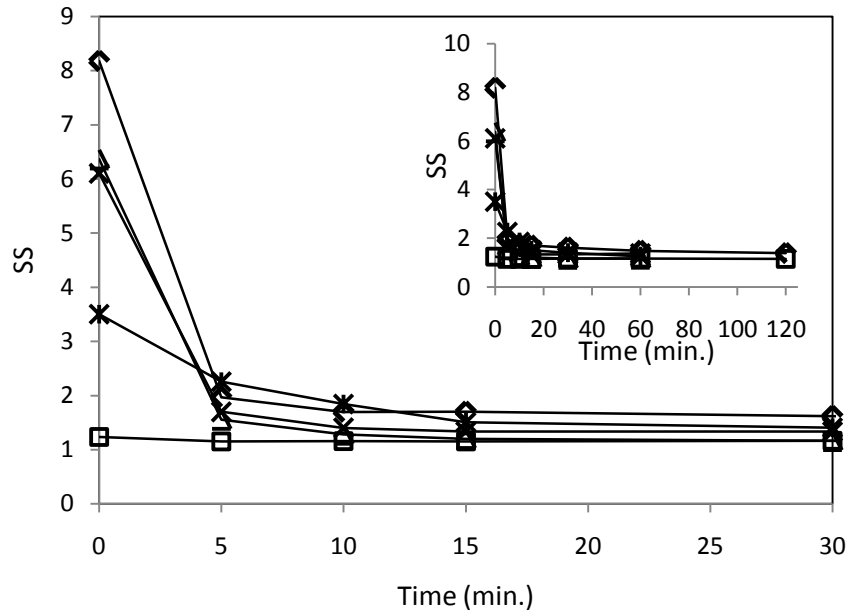


Figure 4.8a The supersaturation ratio of progesterone upon addition of stock solution in DMSO to the SIF buffer containing PS80 at 0% (diamond), 0.01% (triangle), 0.02% (cross), 0.2% (star) and 1% (square) at  $37\pm 0.5^\circ\text{C}$

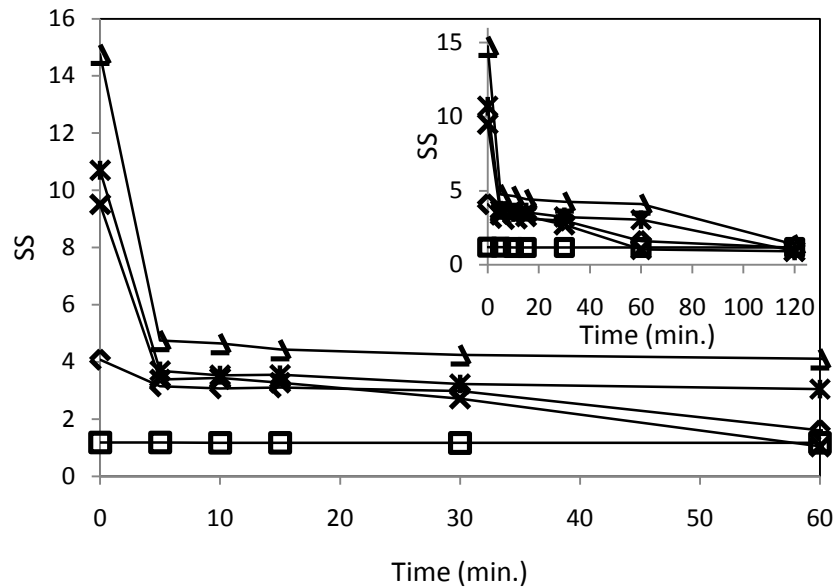


Figure 4.8b The supersaturation ratio of  $17\beta$ -estradiol upon addition of stock solution in DMSO to the SIF buffer containing PS80 at 0% (triangle), 0.01% (star), 0.02% (cross), 0.2% (diamond) and 1% (square) at  $37\pm 0.5^\circ\text{C}$

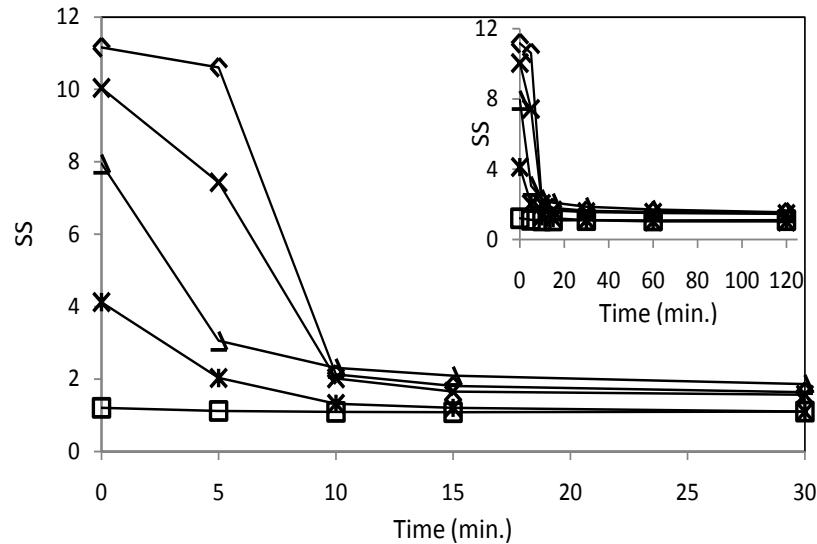


Figure 4.8c The supersaturation ratio of nifedipine upon addition of stock solution in DMSO to the SIF buffer containing PS80 at 0% (diamond), 0.01% (cross), 0.02% (triangle), 0.2% (star) and 1% (square) at  $37\pm 0.5^{\circ}\text{C}$

Studies of the relationship between the supersaturation and crystallization by Miers, et al. (Mullin, 1961). A typical solubility-temperature relationship is presented in Figure 4.9. The lower line is the equilibrium solubility of solute and the upper line is limit of solute remained in solution which is defined as metastable zone limit. In Zone 1, where the supersaturation ratio is below or equal to 1, drug will remain in solution and the system is at equilibrium. Zone 2, the metastable region, is located between the equilibrium solubility line and metastable zone limit. In this zone the supersaturation ratio is greater than 1, but the rate of crystallization is slow. Precipitation will eventually occur, but may not be observed within a given period of time. As the drug concentration enters Zone 3, precipitation occurs rapidly. A similar concept of three zones can be employed in the current study. As shown in Figure 4.10, the lower line is the equilibrium solubility of drug as function of PS80. Accordingly, the upper line represents a limit of rapid precipitation provided that all other kinetic factors are kept constant. At constant drug concentration, the driving force for precipitation would increase as the concentration of PS80 would decrease from Zone 1 to Zone 3. In the dispersion studies, the concentration of PS80 would not decrease as a function of time. Thus, any precipitation observed was



due to the initial concentration of drug starting out in Zone 2 or 3. In later studies, in the presence of lipase enzyme, the concentration of PS80 will decrease as a function of time.

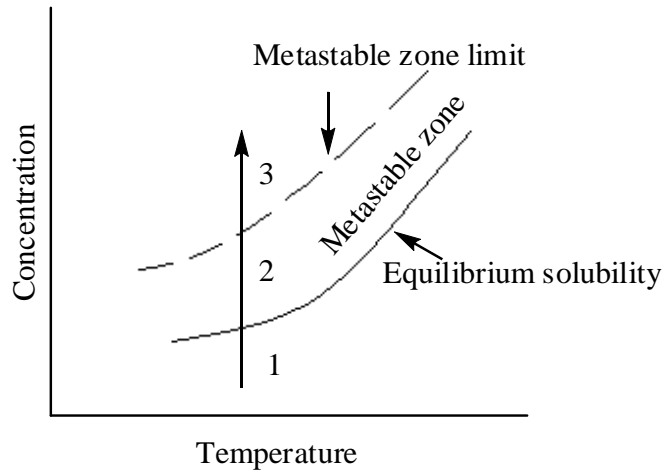


Figure 4.9 Solubility–temperature diagram.(Adapted from Mullin, J. W.) (Mullin, 1961)

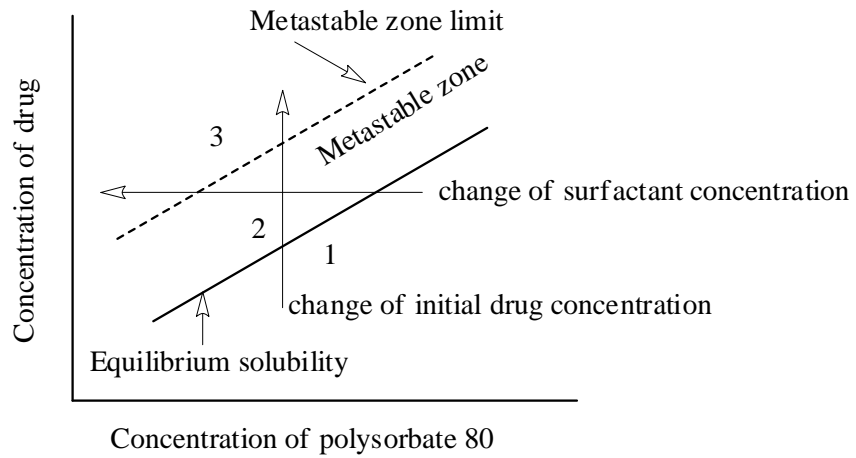


Figure 4.10. Solubility-PS80 concentration diagram. All PS80 concentrations are above the CMC.

#### 4.4.2.3. Solubilization of model drugs formulated with PS80 and dispersed in SIF buffer

In this section, a series of experiments were carried out to determine the extent to which model drugs remain in solution after dispersion of drug-loaded PS80 formulation into SIF buffer. These experiments are labeled as “dispersion” simply because SIF does not contain pancreatic enzyme.

The effect of drug concentration on the ability of PS80 formulation to maintain the drug in the solubilized state was examined. To carry out this study, it was first necessary to determine the solubility of the drug in neat PS80. The results are shown in Table 4.4. The rank order solubility is nifedipine > 17 $\beta$ -estradiol > progesterone. In addition, the equilibrium solubilities of the model drug in 1% PS80 in SIF buffer at 37°C are also listed in Table 4.4.

Table 4.4 Equilibrium solubilities of progesterone, 17 $\beta$ -estradiol and nifedipine in neat PS80 at 25 $\pm$ 0.5°C and in 1% of PS80 solution in SIF buffer at 37  $\pm$ 0.5°C (n=3)

Solubility	Progesterone	17 $\beta$ -estradiol	Nifedipne
neat PS80(mg/g)	21.0 $\pm$ 0.9	32.9 $\pm$ 0.6	39.8 $\pm$ 0.3
1% PS80 solution(mM)*	0.47	0.27	0.45

\*Calculated from the solubilization capacity

Dispersion experiments were carried out by adding drug-containing PS80 formulations to SIF buffers. The formulations were prepared such that the PS80 concentration upon dilution would be 1% w/v. Further, the formulations were designated such that, upon initial dilution, the supersaturation ratios (as defined by Eq. 4.2) would be  $\sim$ 2,  $\sim$ 1 and  $<$ 1. Higher degree of supersaturation will result in a very unstable system in which drug precipitates rapidly (Santos, Watkinson et al., 2011).

#### 4.4.2.3.1. Progesterone

The equilibrium solubility of progesterone in 1% PS80 in SIF buffer was found to be 154  $\mu\text{g/mL}$ . Upon dilution with SIF buffer, the initial concentrations of P-20 and P-31 were designed to be  $193 \pm 5 \mu\text{g/mL}$  and  $327 \pm 13 \mu\text{g/mL}$ , respectively. As shown in Figure 4.11, P-31, in which the initial supersaturation ratio is 2, showed rapid precipitation over 30 min. Over the same time period, there was no significant precipitation from P-12 and P-20. With SS close to 1, progesterone precipitation appeared able to be delayed in the dispersion of P-20 for up to 120 min. As expected, when examining P-12 no precipitation was observed (SS <1). In terms of percentage drug in solution within three replicates, the variability from dispersion of P-31 was also larger than those from dispersion of P-12 and P-20 probably due to the complex precipitation kinetics.

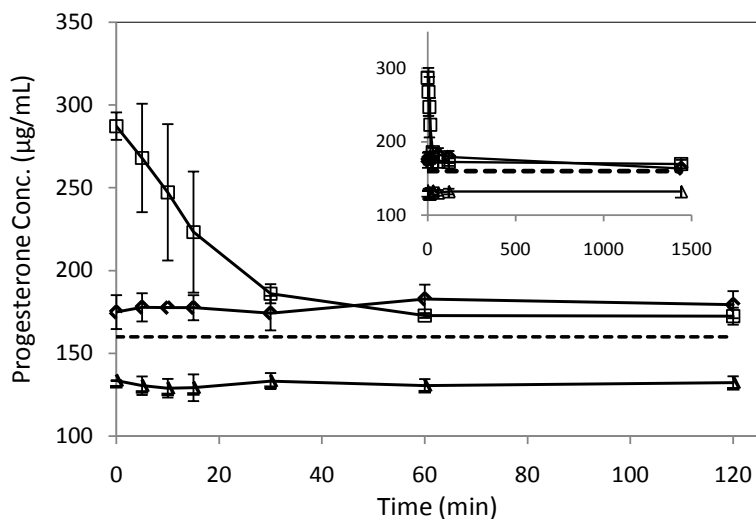


Figure 4.11 The progesterone concentration during the *in vitro* dispersion of P-12 (triangle), P-20 (diamond) and P-31 (square) at 37°C. The dashed line is the equilibrium solubility in 1% PS80 solution. The inserted figure is the concentration-time profile during 24 h.

The chemical potential of supersaturated solution is greater than that of the saturated solution and is thus thermodynamically unstable. As the degree of supersaturation increases, the stability of the system decreases. We can only speculate as to the possible factors influencing the kinetics of precipitation. In general, the rate of homogeneous

primary nucleation is determined by the temperature, degree of supersaturation and surface energy according to the Eq. 4.3 (Mullin, 1961).

$$J = A \exp \left[ - \frac{16\pi\sigma^3 v^2}{3k^3 T^3 (\ln S)^2} \right] \quad (4.3)$$

Where  $J$  is the nucleation rate;  $T$ ,  $\sigma$ , and  $S$  are temperature, surface energy and degree of supersaturation, respectively;  $k$  is Boltzmann constant;  $A$  is pre-exponential factor and  $v$  is molecular volume. Nucleation could occur at any value of supersaturation ratio greater than 1 if given sufficient time. The nucleation step is considered an activated process; once the degree of supersaturation exceeds a critical level, the rate of nucleation increases extremely rapidly. The initial concentration in the dispersion P-31 likely is located in Zone 3 of Figure 4.10. As a result, rapid precipitation in P-31 was as expected. The influence of foreign particles on the rate of precipitation of P-31 cannot be eliminated. Homogenous primary precipitation seldom occurs because foreign particles which act as nuclei usually are contained in solutions. The precipitation induced by foreign particles is known as heterogeneous primary nucleation. Due to the availability of solid surface of the foreign particle, the effective activation energy is lower for heterogeneous nucleation than that for homogeneous nucleation (Nielsen and Söhnel, 1971). Therefore, the precipitation is faster in the presence of foreign particles.

Rapid precipitation from the supersaturated state is not always observed. As an alternative to the nucleation step, the crystal growth may be the rate-limiting step. Two steps are included in the crystal growth in which molecules diffuse to the surface of nuclei from the bulk solution and then integrate into surface of nuclei. The rate of growth can be expressed by Eq. 4.4 (Lindfors, Forssén et al., 2008).

$$\frac{dr}{dt} = \frac{DvN_A}{r + D/k} (C - C_{eq}) \quad (4.4)$$

Where  $r$  is the crystal radius;  $D$  is the diffusion coefficient of the drug molecule;  $N_A$  is Avogadro constant;  $k$  is the surface integration factor; and  $C$  and  $C_{eq}$  are the equilibrium concentration in the bulk solution and on the surface of the cluster, respectively. When  $r$  is much greater than  $D/k$ , the growth is controlled by diffusion of the drug molecule to

the nuclei surface. On the other hand, the growth is controlled by the molecular integration on nuclei surface when  $D/k$  is much greater than  $r$ . Regardless of which process is the rate-controlling step, the rate of growth is proportional to the difference of concentration between that in the bulk solution and on the nuclei surface. Of course, the apparent degree of supersaturation determined in solution may not be the same as that defined in Eq. 4.4. The technique to determine the extent of supersaturation directly at the surface of the growing nuclei is still limited. However, the apparent degree of supersaturation in solution should correlate with the degree of supersaturation at the nuclei surface.

#### **4.4.2.3.2. 17 $\beta$ -Estradiol**

In spite of similar steroidal structure, the physicochemical properties of 17 $\beta$ -estradiol are quite different from those of progesterone. The equilibrium solubility of 17 $\beta$ -estradiol in neat PS80 is  $32.92 \pm 0.62$  mg/g at  $25 \pm 0.5^\circ\text{C}$  which is 1.6 times as much as that of progesterone ( $20.98 \pm 0.99$  mg/g) at  $25^\circ\text{C}$ . The equilibrium solubility of 17 $\beta$ -estradiol in 1% of PS80 micellar solution was determined to be  $72.3$   $\mu\text{g/mL}$  at  $37^\circ\text{C}$ .

Dispersion of E-7 and E-14 resulted in initial concentrations of  $78 \pm 2$   $\mu\text{g/mL}$  (SS=1) and  $153 \pm 7$   $\mu\text{g/mL}$  (SS=2), respectively. Upon dilution of E-14 formulation in SIF buffer, the drug concentration showed an apparent bi-phasic relationship. The rate of drug loss from solution was relatively rapid and approximately linear over the first 240 minutes, after which a slower rate was observed. Over the whole 24 hour study a supersaturated state was maintained. As expected, at low initial supersaturation ratio (SS=1.1), the concentration of 17 $\beta$ -estradiol did not change for up to 24 h following the dispersion of the E-7 formulation.

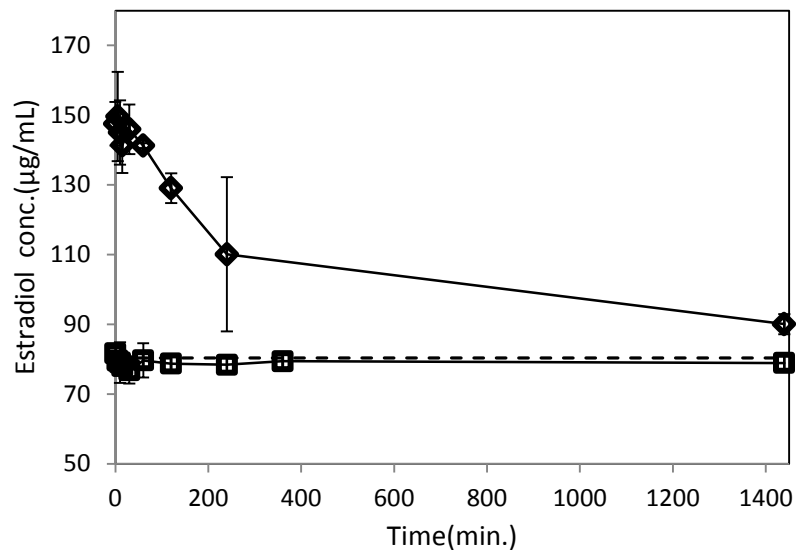


Figure 4.12 The  $17\beta$ -estradiol concentration during the *in vitro* dispersion of E-7 (square) and E-14 (diamond) in the absence of enzyme preparation at  $37^{\circ}\text{C}$ . The dashed line is the equilibrium solubility in 1% PS80 solution.

#### 4.4.2.3.3. Nifedipine

To examine the structures other than steroids, the solubilization behavior of nifedipine was investigated. N-11 gave an initial concentration of  $110\ \mu\text{g/mL}$  upon dispersion. The equilibrium solubility of nifedipine in 1% PS80 is  $156\ \mu\text{g/mL}$ . The creation and maintenance of the supersaturated state during the *in vitro* dispersion of N-20 and N-35 were also assessed (Figure 4.13). Calculated from the amount of added formulation and amount of drug in formulation, N-35 and N-20 gave the initial concentrations of  $377\pm 6\ \mu\text{g/mL}$  and  $195\pm 0.6\ \mu\text{g/mL}$ . Supersaturation ratios were 2.2 and 1.3 for N-35 and N-20, respectively. Significant nifedipine precipitation was not observed in the *in vitro* dispersion of N-20. Upon dispersion of N-35, nifedipine concentration dropped rapidly over a period of 200 minutes, followed by a gradual approach to the equilibrium value.

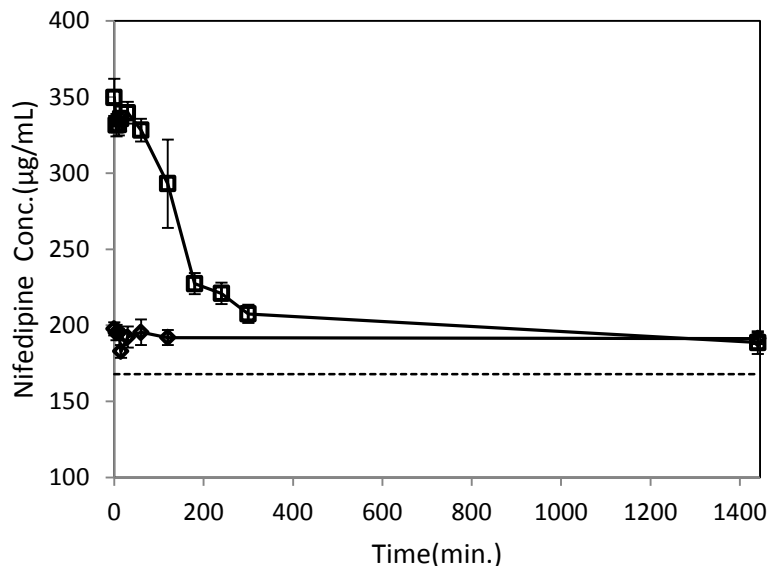


Figure 4.13 The nifedipine concentration in the dispersion of N-20 (diamond) and N-35 (square) in the absence of the enzyme preparation at 37°C. The dashed line is the equilibrium solubility in 1% PS80 solution.

According to the Fick's First Law, supersaturation would be expected to influence the rate of drug transport through the intestinal biological membrane. A good correlation between the degree of supersaturation and the drug transport through an artificial membrane has been reported (Davis and Hadgraft, 1991; Pellett, Davis et al., 1994; Pellett, Castellano et al., 1997; Schwarb, Imanidis et al., 1999; Iervolino, Raghavan et al., 2000; Raghavan, Trividic et al., 2000). In order to quantify the time-dependent supersaturation during the *in vitro* dispersion, the area under the supersaturation ratio-time curve (AUC-SS) was calculated. It is proposed that the AUC-SS may be a descriptor of the time-dependent extent to which a drug remains in the supersaturated state. The values of  $AUC_{0-120 \text{ min}}\text{-SS}$  of progesterone, 17 $\beta$ -estradiol and nifedipine are  $26\pm 4$ ,  $92\pm 7$  and  $113\pm 7$  min, respectively. Within the first 120 minutes, progesterone showed the least stability in supersaturated state while 17 $\beta$ -estradiol and nifedipine exhibited higher stability.

The maintenance of supersaturation during the *in vitro* dispersion may reflect the interaction of drug with PS80. Considering the structures of 17 $\beta$ -estradiol and nifedipine, both have a hydrogen-bonding capability with other molecules. It has reported that

formation of hydrogen-bonding between nifedipine and PVP was one of the factors that delayed drug crystallization (Marsac, Konno et al., 2006). Formation of a hydrogen-bond between the drug and the surfactant could potentially increase the activation energy for nucleation. Moreover, possible adsorption of surfactant/polymer on the crystal surface through hydrogen-bonds could slow down the precipitation (Raghavan, Trividic et al., 2000; Raghavan, Kiepfer et al., 2001; Vandecruys, Peeters et al., 2007; Overhoff, McConville et al., 2008). Of course, one would expect extremely slow precipitation at supersaturation degree close to 1 due to the low thermodynamic driving force. Possible interactions between drugs and PS80 will be examined in Chapter 6.

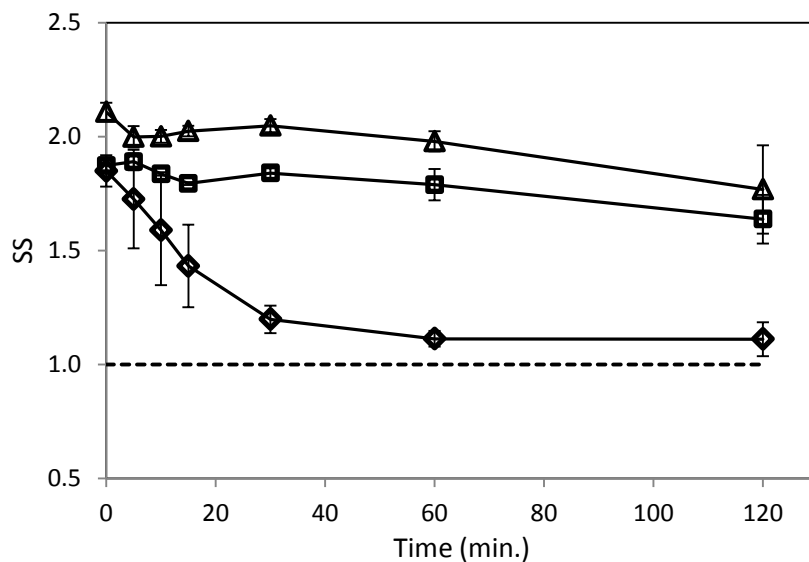


Figure 4.14 The supersaturation ratios during the *in vitro* dispersion of progesterone formulation (P-31, diamond), 17β-estradiol formulation (E-14, square) and nifedipine formulation (N-35, triangle). The dashed line is the baseline where the supersaturation ratio equals 1.

It should be noted that the formation of the original stable crystalline form during *in vitro* dispersion was assumed. In general, amorphous form has higher equilibrium solubility compared to the crystalline form due to high thermodynamic activity. Thus, it is critical to identify the polymorph of the solid generated during precipitation. Due to the material availability and time-dependent change of solid form during the precipitation, it was not



possible to identify the exact crystalline form generated at each time point in Figures 4.11-4.13. However, polarized microscopy may be applied to identify amorphous vs. crystalline forms at predetermined times during the *in vitro* dispersion of P-31, E-14 and N-35. As shown in Figure 4.15, birefringence was observed as function of time indicating the formation of a crystalline form of each drug. Birefringence was observed in 15 min in the dispersion of P-31 while it took at least 30 min to get a clear image in the dispersion of E-14 and N-35.

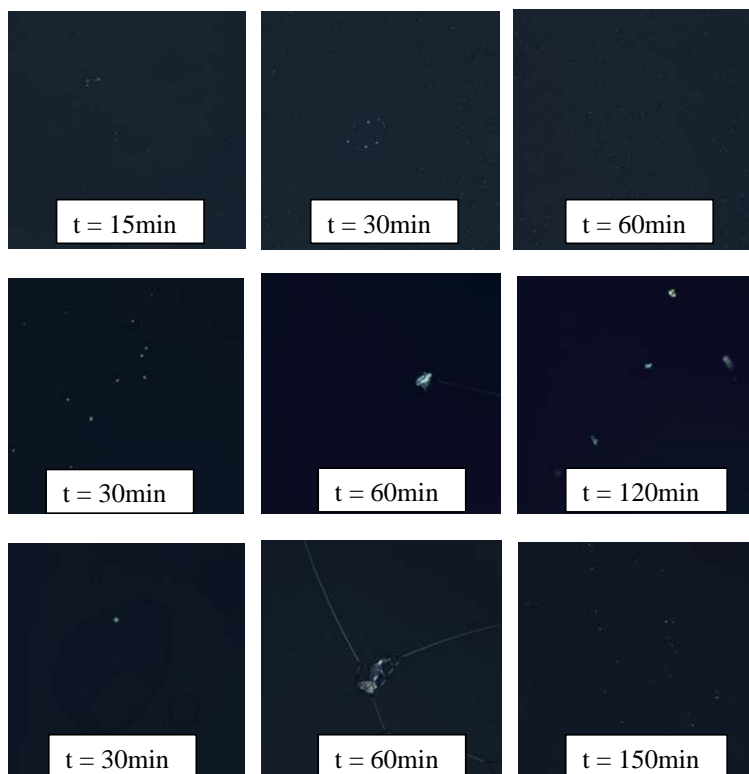


Figure 4.15 The birefringence of the precipitation of progesterone (top),  $17\beta$ -estradiol (middle) and nifedipine (bottom) during *in vitro* dispersion of drug-containing formulations at  $37^{\circ}\text{C}$

#### 4.4.3. Equilibrium solubility in the digested blank formulation

The thermodynamic driving force for drug precipitation is the difference between apparent solubility of a drug during the *in vitro* lipolysis and the equilibrium solubility of the drug in media containing the lipid aggregates of lipolytic products. One would expect that the lipolysis may result in an alteration of the ability of the formulation to solubilize the drug or to maintain the drug in solubilized state. This expectation is rooted in the observation that, on the one hand, lipolysis causes the loss of excipient surfactants, but on the other hand, it also results in the formation of fatty acids and new lipid assemblies. To examine the putative relationship between the thermodynamic driving force for drug precipitation and the extent of lipolysis, the equilibrium solubility of model drugs in digested blank formulations was assessed. The solubility values were determined by adding excess amount of a model drug to the blank PS80 samples taken at predetermined times of digestion.

Shown in Figure 4.16 is the equilibrium solubility of the three model drugs in products of lipolysis of PS80 formulation. To be clear, the x-axis represents the time of lipolysis of the blank formulation; the y-axis represents equilibrium solubility. As shown in Figure 4.16, the equilibrium solubility of progesterone in lipolytic products remained relatively constant. At the 95% confidence level, the equilibrium solubility of progesterone in PS80 was lower than in lipolytic products at each time point. In contrast, a decrease of equilibrium solubility in lipolytic products was evident in the cases of  $17\beta$ -estradiol and nifedipine. Equilibrium solubility decreased by about a factor of 2 for  $17\beta$ -estradiol and 3 for nifedipine in lipolytic products produced by 120 min. The results clearly show that the capability of lipolytic products to solubilize model compounds is drug-dependent.

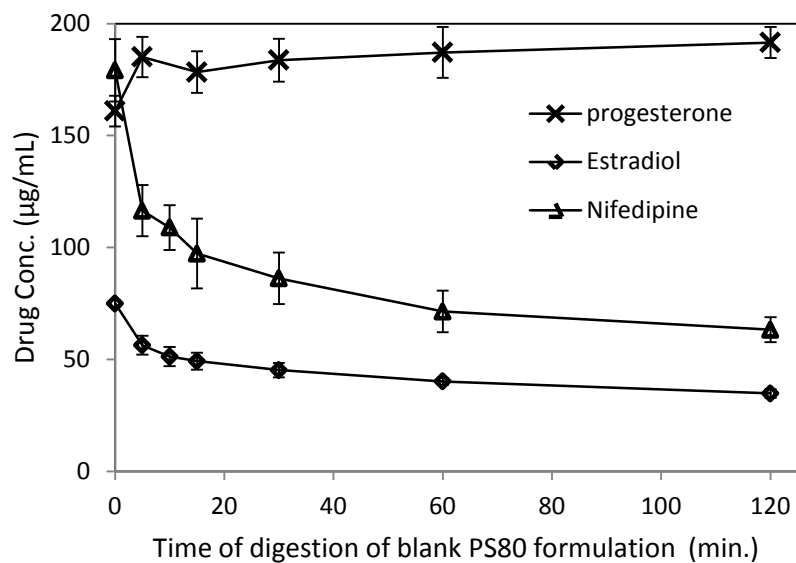


Figure 4.16 The equilibrium solubility of progesterone (star), 17 $\beta$ -estradiol (diamond) and nifedipine (triangle) in the blank PS80 after digestion by lipase enzyme at 37°C. The enzyme was inhibited by 4-BPB during the equilibrium solubility experiment.

In order to more clearly illustrate the relationship of equilibrium solubilities of model drugs and the content of PS80, the equilibrium solubility of a model drug in lipolytic products at predetermined times was normalized by dividing by the equilibrium solubility at time zero when PS80 is the only lipid in solution (Eq. 4.5). The results are shown in Figure 4.17. The equilibrium solubilities of 17 $\beta$ -estradiol and nifedipine in lipolytic products decreased over the first 10 min, resulting in 65% remaining for 17 $\beta$ -estradiol and 54% for nifedipine, respectively. The normalized equilibrium solubility of 17 $\beta$ -estradiol decreased to 54 % in 120 min where 58% of PS80 was hydrolyzed (dashed line in Figure 4.17). In contrast, the normalized equilibrium solubility of nifedipine decreased to 52% in lipolytic products present after 30 min and reached 35% in lipolytic products present at 120 min. The dependence of equilibrium solubility of drug upon the lipolysis time likely reflects the partitioning of the drug between the aqueous solution and the formed mixed micelles of lipolytic products. The detailed mechanisms of solubilization of the model drug in the lipolytic products will be studied in a series model of mixed micelles composed of PS80 and oleic acid (Chapter 5). The interactions of the drug with model mixed micelles will be examined in Chapter 6.

% drug remaining =

$$\frac{\text{Concentration determined at the time of sampling}}{\text{Concentration determined at time zero}} \times 100\% \quad (4.5)$$

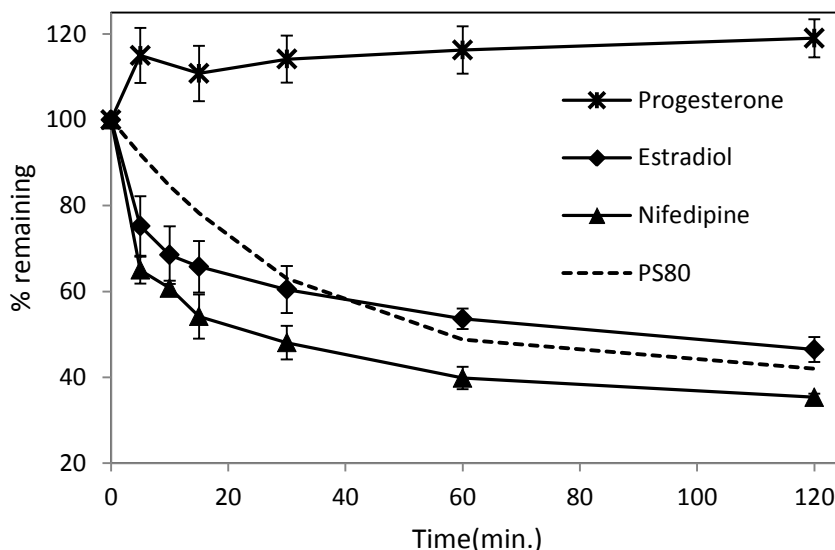


Figure 4.17 The percentage of progesterone (star), 17 $\beta$ -estradiol (diamond) and nifedipine (triangle) in the solutions of digested blank PS80 at 37°C relative to the equilibrium solubility at time zero. The dashed line is the percentage of PS80 remaining.

#### 4.4.4. Solubilization of model drugs formulated in PS80 during *in vitro* lipolysis

The purpose of these experiments was to determine the extent to which PS80 is able to create and maintain a supersaturated state during the exposure of the drug-loaded formulation to lipolysis under fasted-state conditions. It is evident that the lipolysis resulted in a dramatic reduction of PS80 concentration and a rise in production of fatty acid (Figures 4.5a – 4.5c in Section 4.4.1). The surfactant composition of the solution was altered by lipolysis and thus the structure of lipid aggregates, and their capability to solubilize a poorly-water soluble drug, may also be modified. In the following section the extent to which supersaturation of progesterone, 17 $\beta$ -estradiol and nifedipine is altered as a result of the lipolysis of surfactant PS80 will be determined

#### 4.4.4.1. Control experiments

There are several possible reasons for a decrease in drug concentration upon the addition of an enzyme to a drug-containing dispersion. So as to more clearly illustrate the effect of lipolysis on drug solubilization of drug-PS80 formulation, two control experiments were carried out. The first control experiment was designed to determine if particles in the enzyme preparation were able to act simply as nuclei and promote precipitation of the drug. As mentioned in Chapter 3, the enzyme preparation is not a clear solution, but is a suspension, probably including some undissolved protein from the isolation process. So as to eliminate the effect of lipolysis and focus solely on the putative nucleation properties of particles, dispersion studies were carried out in the presence of a denatured enzyme.

Shown in Figure 4.18 are results of dispersion studies of P-20 in the presence and absence of an inactivated enzyme. Clearly, there was little difference in the concentration of progesterone remaining in solution between the two treatments. This result is not surprising since dispersion of the P-20 formulation results in an initial supersaturation ratio close to one. Shown in Figure 4.19 are the results of dispersion studies of P-31 in the presence and in the absence of an inactivated enzyme. Within the first 30 min of dispersion, significantly more progesterone precipitated out of solution in the presence inactivated enzyme as compared to the absence of the enzyme. When initially dispersed, P-31 has a supersaturation ratio of about 2. The results in Figure 4.19 suggest that precipitation of progesterone from this thermodynamically unstable system may be accelerated by nucleation of solid particles in the enzyme preparation. Similar results were observed when N-35 formulation was dispersed in the presence and absence of inactivated enzyme (Figure 4.20). Here too, it may be concluded that N-35 formulation, with an initial supersaturation ratio of approximately 2 may be induced to precipitate in the presence of particles in the enzyme preparation.

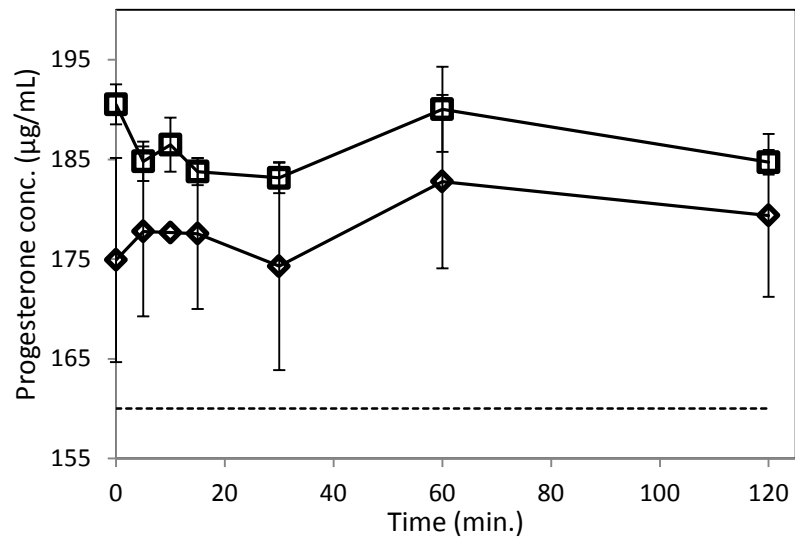


Figure 4.18 Progesterone concentration during the *in vitro* dispersion of P-20 in the absence of enzyme (diamond) and the presence of inactivated enzyme (square). The dashed line represents the equilibrium solubility in 1% PS80 solution at 37°C.

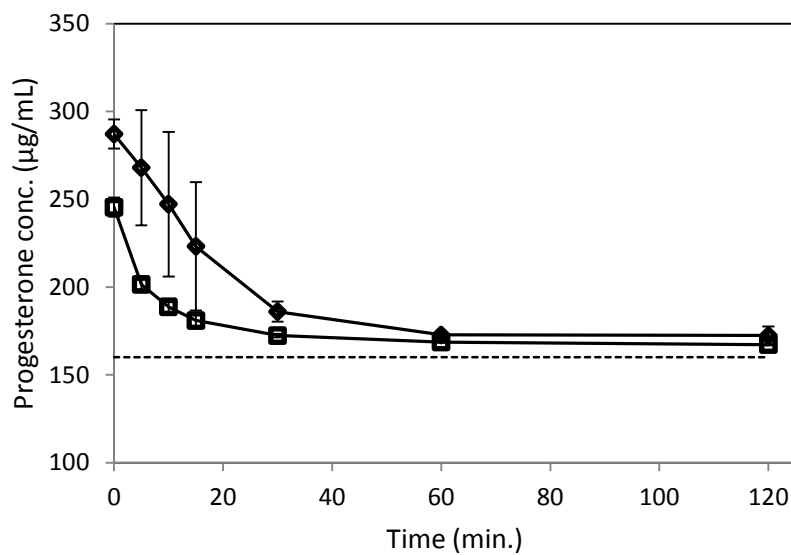


Figure 4.19 Progesterone concentration during *in vitro* dispersion of P-31 in the absence of enzyme (diamond) and the presence of inactivated enzyme (triangle). The dashed line represents the equilibrium solubility in 1% PS80 solution at 37°C.

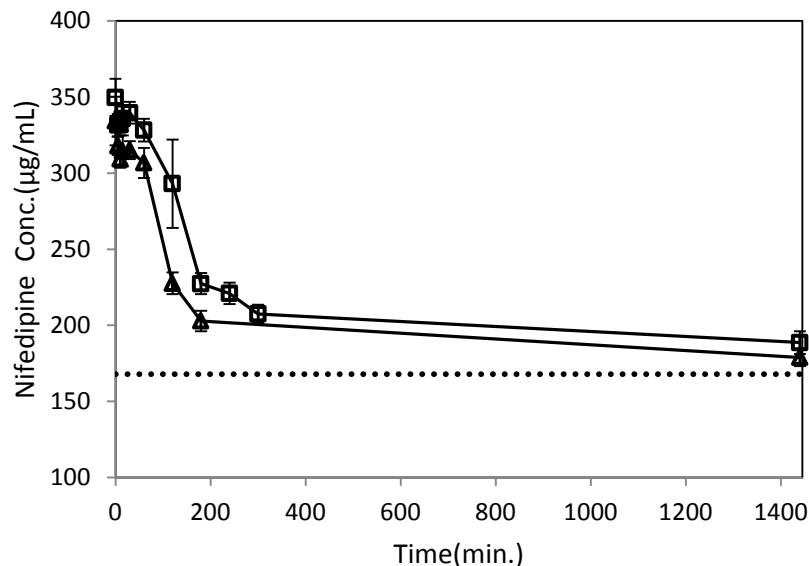


Figure 4.20 Nifedipine concentration during the *in vitro* dispersion of N-35 in the absence of enzyme (square) and in the presence of inactivated enzyme (triangle). The dashed line represents the equilibrium solubility in 1% PS80 solution at 37°C.

The effect of particles in the enzyme preparation on drug precipitation was further evaluated by the area under the curves in Figures 4.18-4.20. The results are listed in Table 4.5. Both values of  $AUC_{0-60 \text{ min}}$  and  $AUC_{0-24 \text{ h}}$  of P-20 were identical in the absence of the enzyme preparation and in the presence of an inactivated enzyme preparation. However, the value of  $AUC_{0-60 \text{ min}}$  of P-31 was about 20% higher in the absence of the enzyme preparation as compared to that with the inactivated enzyme. A significant difference on AUC was observed in the first 60 min. Similarly, the value of  $AUC_{0-180 \text{ min}}$  of N-35 was 17% higher in the absence of enzyme than in the inactivated enzyme preparation. In a 24-hour period, the values of  $AUC_{0-24 \text{ h}}$  of P-31 and N-35 were 10% and 7% higher in the absence of the enzyme than in the inactivated enzyme preparation, respectively. Thus, we concluded that particles in the enzyme preparation, probably acting as nuclei, accelerated the precipitation of the drug at a supersaturation ratio of 2. Therefore, any precipitation observed in the presence of active enzyme must be considered in the evaluation of the effect of lipolysis of highly supersaturated formulations.

Table 4.5 The concentration area under the concentration-time curve ( $\mu\text{g}\cdot\text{min}\cdot\text{mL}^{-1}\pm\text{SD}$ ) in the *in vitro* dispersion of formulations in the absence of enzyme preparation and in the presence of an inactivated enzyme preparation

Formulation	No enzyme preparation	Inactivated enzyme preparation	P*
P-20	$(1.09\pm 0.07)\times 10^4$ (0-60 min)	$(1.08\pm 0.02)\times 10^4$ (0-60 min)	>0.05
P-20	$(2.53\pm 0.09)\times 10^5$ (0-24 h)	$(2.50\pm 0.02)\times 10^5$ (0-24 h)	>0.05
P-31	$(1.23\pm 0.07)\times 10^4$ (0-60 min)	$(1.01\pm 0.06)\times 10^4$ (0-60 min)	<0.05
P-31	$(2.48\pm 0.07)\times 10^5$ (0-24 h)	$(2.24\pm 0.17)\times 10^5$ (0-24 h)	>0.05
N-35	$(5.44\pm 0.19)\times 10^4$ (0-180 min)	$(4.78\pm 0.09)\times 10^4$ (0-180 min)	<0.05
N-35	$(3.07\pm 0.09)\times 10^5$ (0-24 h)	$(2.88\pm 0.08)\times 10^5$ (0-24 h)	<0.05

\*p-value of student T-test

In any supersaturated solution nucleation can occur spontaneously or it may be induced by any particles present. Nucleation initiated by any insoluble matter, such as insoluble protein, is termed primary heterogeneous nucleation. Nucleation initiated by solute crystals is termed secondary nucleation. The primary heterogeneous nucleation is very difficult to avoid in reality. The presence of particles in the enzyme preparation could affect the rate of crystallization considerably since the particle surface can rapidly induce the crystallization. As evident in the dispersion of P-31 and N-35, the enzyme preparation



resulted in an earlier onset of precipitation compared to those same solutions in the absence of denatured enzyme. Acceleration of the rate of precipitation was only observed in the highly supersaturated solutions, but not in solutions of low supersaturation such as P-20. However, the mechanisms by which denatured enzyme may act as initiators of precipitation are not clear. The apparent rate of precipitation is a function of primary nucleation, including homogenous and heterogenous nucleations, secondary nucleation, and crystal growth. The influence of each step is highly dependent on the degree of supersaturation. In the case of active enzyme, lipolysis of excipients likely makes the situation even more complicated.

To this point, the loss of drug from solution has been ascribed solely to precipitation. A second, but much less likely, reason for a decrease in drug concentration in the presence of enzyme is protein-binding of the drug. To determine if model drugs were bound to the enzyme or other protein in the preparation, a known concentration of drug below the solubility limit was spiked into the solution containing inactivated enzyme. Drug recovered after the removal of the protein was determined by HPLC. The percentage of recovery for all drugs was over 98%. These results suggest that protein-binding of the drug has little influence on drug concentration.

#### **4.4.4.2. Progesterone in PS80 formulations exposed to lipolytic conditions**

With the control experiments completed and the behavior of the formulation upon dispersion in the absence of enzyme characterized, the effect of lipolysis on the drug-containing formulations was studied. The first set of experiments focused on progesterone. Progesterone concentration was determined as a function of time during the lipolysis of P-12, P-20 and P-31. As seen in Figure 4.21, in the absence of calcium, only a small change in drug concentration was observed from P-12 and P-20 in the first 5 min. After 5 min, progesterone concentration remained constant up to 24 hours. Compared to the equilibrium solubility in the lipolytic products of a blank formulation, the lipolysis of P-31 formulations resulted in a markedly reduced progesterone concentration. Lipolysis of P-12 and P-20 had no effect on progesterone concentration. The small percentage change of progesterone was seen in the experiments with the inactive enzyme in P-20 and P-31. For all three formulations, the concentrations at each time point collected under lipolysis conditions were compared to those collected with

inactive enzyme. Results of applying the Student t-test indicated that there was no significant difference between results from inactivated enzyme (Figure 4.18) and active enzyme (Figure 4.21) up to 24 hours. Areas under the curve in Figure 4.18 and Figure 4.21 were calculated for P-20 (Table 4.6). Both values of  $AUC_{0-60 \text{ min}}$  and  $AUC_{0-24 \text{ h}}$  are identical in the presence of inactivated enzyme and in the presence of active enzyme. The results strongly suggest that the lipolysis of the formulation had no effect on the solubilization of progesterone at a supersaturation ratio of 1. When the initial supersaturation ratio was 2 in P-31, approximately 50% of the progesterone precipitated within the first 10 min (Figure 4.21). If one compares the results from the inactivated enzyme, the decrease of progesterone concentration during *in vitro* lipolysis of P-31 is the result of the introduction of particles into the medium. This is supported by  $AUC_{0-60 \text{ min}}$  of P-31 in Figure 4.19 and Figure 4.21 (Table 4.6) where the values under the two treatments are not significantly different.

Quantitatively, the difference between the  $AUC_{\text{inactivated enzyme}}$  and  $AUC_{\text{active enzyme}}$  will give an estimation of magnitude of effect of the loss of PS80 alone on the precipitation during the *in vitro* lipolysis (Table 4.6). The results clearly demonstrated that the lipolysis of PS80 had no effect on progesterone solubilization where the difference between  $AUC_{\text{inactivated enzyme}}$  and  $AUC_{\text{active enzyme}}$  is not statistically significant. It can be concluded that the loss of progesterone upon exposing P-20 and P-31 to lipolysis is not due to hydrolysis of the surfactant, but rather is due to particles in the enzyme preparation acting as nuclei.

Table 4.6 The area under the concentration-time curves ( $\mu\text{g}\cdot\text{min}\cdot\text{mL}^{-1}\pm\text{SD}$ ) for the *in vitro* dispersion of formulations in the presence of active enzyme preparation and the presence of inactivated enzyme preparation. Significance tested at  $p = 0.05$ .

Formulation	Active enzyme preparation	Inactivated enzyme preparation	$\Delta(\text{AUC}_{\text{inactivated enzyme}} - \text{AUC}_{\text{active enzyme}})$
P-20	$(1.05\pm 0.09)\times 10^4$ (0-60 min)	$(1.08\pm 0.02)\times 10^4$ (0-60 min)	Not significant
P-20	$(2.45\pm 0.16)\times 10^5$ (0-24 h)	$(2.50\pm 0.02)\times 10^5$ (0-24 h)	Not significant
P-31	$(9.69\pm 0.15)\times 10^3$ (0-60 min)	$(1.01\pm 0.06)\times 10^4$ (0-60 min)	Not significant
P-31	$(2.17\pm 0.05)\times 10^5$ (0-24 h)	$(2.24\pm 0.17)\times 10^5$ (0-24 h)	Not significant
N-35	$(2.50\pm 0.10)\times 10^4$ (0-180 min)	$(4.78\pm 0.09)\times 10^4$ (0-180 min)	$(2.28\pm 0.13)\times 10^4$
N-35	$(1.09\pm 0.02)\times 10^5$ (0-24 h)	$(2.88\pm 0.08)\times 10^5$ (0-24 h)	$(1.79\pm 0.08)\times 10^5$

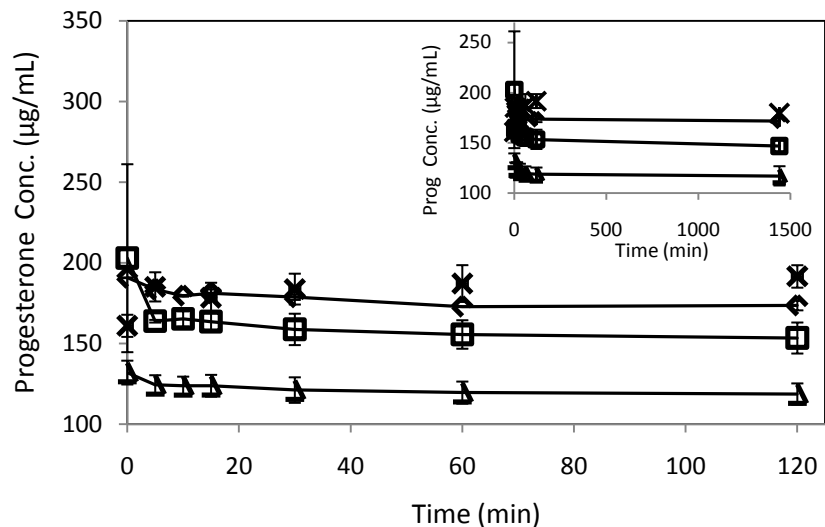


Figure 4.21 The progesterone concentration during the *in vitro* lipolysis of P-12 (triangle), P-20 (diamond), and P-31 (square). Five millimolar  $\text{Ca}^{2+}$  was not included in the SIF buffer. The cross represents the equilibrium solubility in the digested blank formulation.

A series of lipolysis experiments were carried out in the presence of 5 mM  $\text{Ca}^{2+}$ . In all cases, the medium was observed to be cloudy within 15 min of the addition of the enzyme preparation. As characterized in Section 3.4.3.3.2 of Chapter 3, a significant fraction of fatty acid released from PS80 was precipitated as  $\text{Ca}^{2+}$  salt. It is likely that the precipitate observed within 15 min was the calcium–fatty acid salt, although progesterone precipitate can not be excluded. During lipolysis, the progesterone concentration decreased for P-20 and P-31 formulations. Lipolysis conditions did not influence the progesterone concentration from P-12 formulation.

The reason for the loss of progesterone from solution during lipolysis in the presence of calcium ion may be related to a loss of micellar solubilization capacity. The results shown in Section 4.4.1 clearly demonstrate that in the presence of calcium ion about 50 to 60% of PS80 was hydrolyzed within the first 120 min. Further, due to the precipitation of calcium salt of fatty acid, the concentration of fatty acid in solution available for micellization was reduced. Thus, during lipolysis in the presence of calcium ion, both PS80 and fatty acid are lost from solution. The characterization of micelles of PS80 in Chapter 6 indicated that the size was independent of the total surfactant concentration within the employed range. It is reasonable to assume the aggregation number of micelles

of PS80 remains constant though the lipolysis. Therefore, we concluded that the decrease of the total concentration of surface-active species resulted in the decrease in the number of micelles to solubilize progesterone. The observation that equilibrium solubility of progesterone in the lipolytic products formed during the lipolysis of the blank formulation decreased (Figure 4.22) supports the conclusion that the loss of progesterone from solution is related to the loss of micellar solubilization capacity.

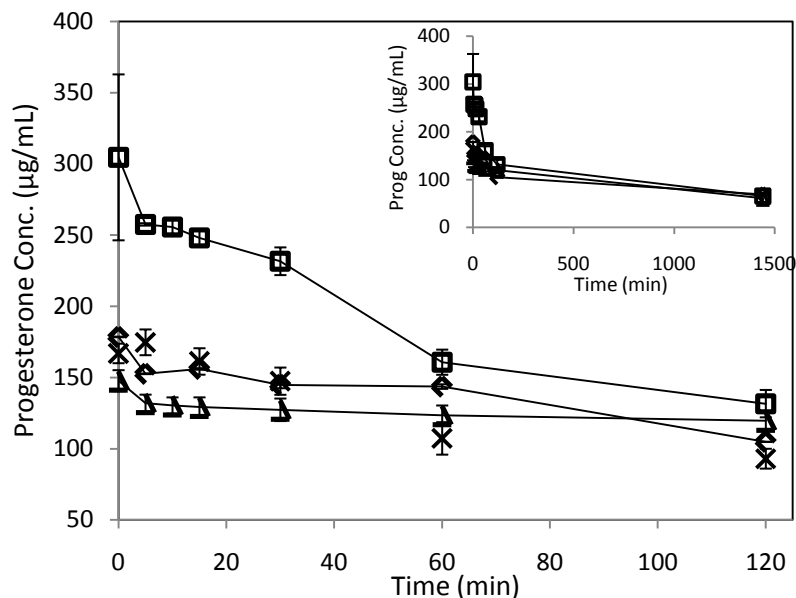


Figure 4.22 The progesterone concentration during the *in vitro* lipolysis of P-12 (triangle), P-20 (diamond), and P-31 (square).  $\text{Ca}^{2+}$  was included in the SIF buffer. The cross represents the equilibrium solubility of progesterone in the digested blank formulation.

#### 4.4.4.3. 17 $\beta$ -Estradiol in PS80 formulations exposed to lipolytic conditions

The effect of lipolysis on 17 $\beta$ -estradiol-containing formulations of PS80 was studied. All studies were carried out in the absence of calcium. The initial concentration of PS80 upon dispersion of the formulation was 1% w/v. The E-5 formulation created an initial drug concentration in the SIF buffer of  $57 \pm 2$   $\mu\text{g/mL}$ , a value lower than equilibrium solubility ( $73$   $\mu\text{g/mL}$  in 1% PS80 solution at  $37^\circ\text{C}$ ). Dispersion of E-7 resulted in an initial concentration of  $78 \pm 2$   $\mu\text{g/mL}$ , a value close to the equilibrium solubility. Dispersion E-14 resulted in an initial concentration of  $161 \pm 1$   $\mu\text{g/mL}$ , giving a value of the supersaturation ratio close to 2.0. Compared to the equilibrium solubility of 17 $\beta$ -

estradiol in lipolytic products during the lipolysis of the blank formulation, an obvious effect of lipolysis on the creation and maintenance of supersaturated 17 $\beta$ -estradiol is presented in Figure 4.23. During lipolysis of E-5, the concentration of 17 $\beta$ -estradiol decreased by only 24% by 24 h. Similarly, only 10% of the drug precipitated by 6 h from the lipolysis of E-7 and concentration decreased by only about 30% by 24 h. For E-14, 90% of 17 $\beta$ -estradiol remained in the solution after 120 minutes. By 240 minutes the concentration dropped to 60%. The AUC<sub>0-240 min</sub> values (Table 4.6) in the presence of lipolysis conditions and in the presence of inactive enzyme were  $(3.23\pm 0.12)\times 10^5 \text{ug}\cdot\text{min}\cdot\text{mL}^{-1}$  and  $(3.12\pm 0.09)\times 10^5 \text{ug}\cdot\text{min}\cdot\text{mL}^{-1}$  respectively. Student t-test results indicate that the treatments had no effect on area under the concentration-time curve. On the other hand a significant effect of lipolysis on the solubilization of 17 $\beta$ -estradiol was observed at long exposure. At 24 hours, only 28% of the drug remained in the solution during the lipolysis of E-14 whereas 61% of the drug remained in the solution when exposed to the inactive enzyme.

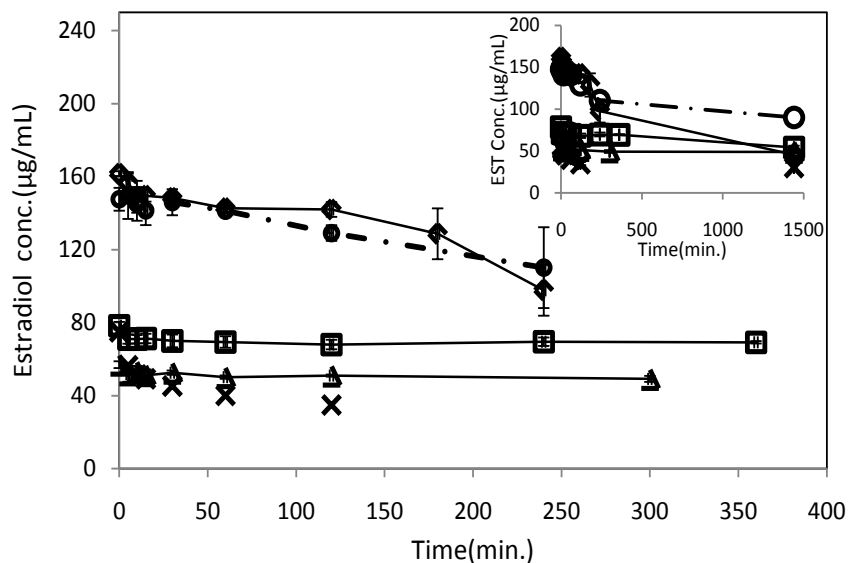


Figure 4.23 The 17 $\beta$ -estradiol concentration during the *in vitro* lipolysis of E-5 (triangle), E-7 (square), and E-14 (diamond). The cross represents the equilibrium solubility of estradiol in the digested blank formulation. The circle with the dashed line is the drug concentration during the *in vitro* dispersion of E-14.

#### 4.4.4.4. Nifedipine in PS80 formulations exposed to lipolytic conditions

Three formulations of nifedipine were examined. N-11 created an initial concentration of  $113 \pm 2$   $\mu\text{g/mL}$  in SIF buffer which was lower than the equilibrium solubility ( $156 \pm 3$   $\mu\text{g/mL}$  in 1% w/v PS80 solution at  $37^\circ\text{C}$ ). N-20 and N-35 gave concentrations at supersaturation ratios of 1.3 and 2.0, respectively. The experimental results suggested a rather complex relationship of lipolysis and nifedipine concentration (Figure 4.24). The equilibrium solubility of nifedipine in the lipolytic product formed during the lipolysis of the blank formulation decreased by over 60%. Despite this large drop in equilibrium solubility, during lipolysis of N-11, the concentration of nifedipine remained close to the initial concentration for up to 5 h. This is the first observation in this work that a system initially presenting drug in a subsaturated condition became supersaturated due to the action of lipase enzyme. The lipolysis of N-20 resulted in only 10% of drug loss in first 120 min followed by a decrease of the drug concentration to 34% of the initial concentration by 300 min. Figure 4.24 shows the N-20 system was supersaturated for at least 300 minutes. By 24 h, only 28% of the drug remained in solution. Taken together, drug concentration in N-11 and N-20 systems appeared to resist the effects of lipase for at least 300 minutes. In contrast, the concentration of nifedipine dropped markedly during the lipolysis of N-35. The drug concentration was decreased by 24% in the first 30 min. By 120 min, the drug concentration reached equilibrium solubility and the system was no longer supersaturated.

As stated previously, the particles acting as nuclei in the enzyme preparation likely have a significant effect on the precipitation of the drug from high supersaturation. The effect of lipolysis on the nifedipine solubilization was evident by the comparison of the concentration  $\text{AUC}_{0-180 \text{ min}}$  of N-35 in Figure 4.20 and Figure 4.24 (Table 4.6). The values of  $\text{AUC}-C_{0-180 \text{ min}}$  during the dispersion with no enzyme, with inactivated enzyme, and with active enzyme are  $(5.44 \pm 0.19) \times 10^5$ ,  $(4.78 \pm 0.09) \times 10^5$  and  $(2.50 \pm 0.10) \times 10^5$   $\mu\text{g} \cdot \text{min} \cdot \text{mL}^{-1}$ , respectively. The difference between the  $\text{AUC}_{\text{inactivated enzyme}}$  and  $\text{AUC}_{\text{active enzyme}}$  is statistically significant (Table 4.6). These values suggested that the precipitation of nifedipine in N-35 was dominated by the lipolysis of formulation.

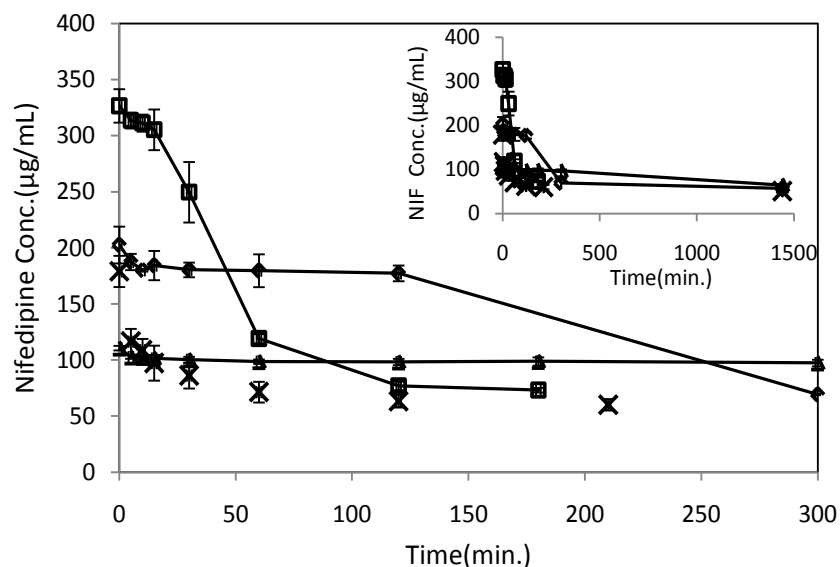


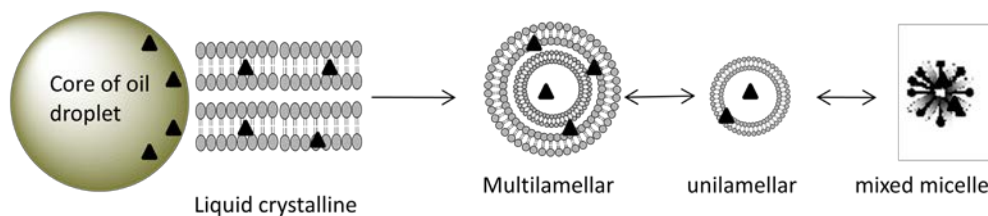
Figure 4.24 The nifedipine concentration during the *in vitro* lipolysis of N-11 (triangle), N-20 (diamond), and N-35 (square) formulations. The cross represents the equilibrium solubility of nifedipine in the digested blank formulation.

The role played by lipid assemblies (in the present study, mixed micelles of PS80 and oleic acid) in the maintenance of supersaturation is not clear. In a complex LBDDS containing oil and surfactant, the existence of a continuum pathway from the digesting oil droplets to the newly-formed lipid aggregates has been suggested (Patton and Carey 1979; Patton, Vetter et al., 1985; Hernell, Staggers et al., 1990; Staggers, Hernell et al., 1990; MacGregor, Embleton et al., 1997). A schematic presentation of this pathway is given in Scheme 4.2. The concentration of lipolytic products such as mono- and di-glycerides and fatty acids increases at the surface of oil droplets as lipolysis proceeds. These products transiently form a liquid crystalline phase at the surface. Drug may also be incorporated in this surface phase. Spontaneously, this phase erodes to form multilamellar vesicles which are transformed to unilamellar vesicles in the presence of bile salts. Eventually, these unilamellar vesicles form mixed micelle with bile salts. This series of lipid aggregates provide a continuous hydrophobic environment for poorly-water soluble drugs. Kaukonen et al. (Kaukonen, Boyd et al., 2004) has suggested that a hydrophobic drug is prevented from partitioning into the aqueous phase due to rather large lipid/water

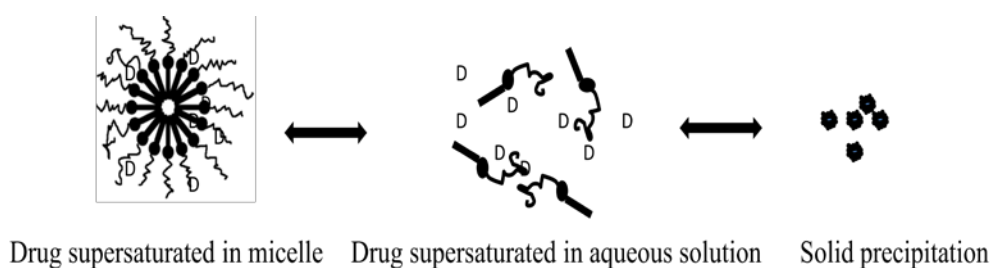


partition coefficient. If hydrophobic drug is “sequestered” in the variety of lipid assemblies present during lipolysis of LBDDS, the aqueous phase concentration may remain below the solubility limit.

In the current investigated system, micelles were the only lipid assembly present before and after lipolysis of PS80 and the continuum pathway outlined in Scheme 4.2 does not exist. It has been suggested that residence time of a drug molecule in a micelle will be similar to that of a surfactant monomer, somewhere on the order of a few milliseconds (Muller, 1978; Kahlweit, 1982). The relaxation time for the formation and dissolution of a PS80 micelle has been determined to be 8-10 seconds (Patist, Oh et al., 2001). Although no data exist in the literature, the kinetics of drug transferring between the digesting PS80 micelles and the mixed micelle of lipolytic products with BS/PC is likely to be rapid. From a classical point of view, it might be expected that as PS80 is progressively hydrolyzed and the fraction of oleic acid in the micelle increases, the solubilization potential of these mixed micelles would decrease. Since the micelles have a short life-time, the drug would rapidly be released into the media; precipitation would result. This scenario of decreased equilibrium solubilization in products of lipolysis was indeed observed for  $17\beta$ -estradiol (Figure 4.23) and nifedipine (Figure 4.24). The classical view of micelle solubilization does not help in explaining why  $17\beta$ -estradiol and nifedipine solutions could remain supersaturated for such a long time. Instead of the classical view, suppose the micelles could become supersaturated with drug. If the aqueous phase is supersaturated with drug, and the micelle-water partition coefficient remains unchanged (a significant assumption in this speculation), then the micelles also must be supersaturated. Under this scenario, the intermicelle concentration of drug would be reduced compared to that of the more classical view of solubilization. As a direct result of the micelles being supersaturated, the intermicelle concentration of drug would be in the metastable Zone 2 (Figure 4.10), rather than in the precipitation Zone 3. Of course, the concept of a supersaturated micelle is speculative and no data currently exists supporting this hypothesis.



Scheme 4.2 Schematic representation of the hydrophobic continuum pathway for drug during the digestion of a lipid.



Scheme 4.3 Partitioning of a drug between a supersaturated micelle and a supersaturated aqueous solution.

#### 4.4.5. Extent of supersaturation during *in vitro* lipolysis

The bioavailability of a poorly-water soluble drug is dependent on several factors, not the least of which is the concentration in solution at the site of absorption in the GI tract. Provided that other factors, such as first pass metabolism, have no effect on the bioavailability, the ability of a formulation to create and maintain the drug in a supersaturated state for an extended period of time has been hypothesized to improve the bioavailability. Although a number of studies have demonstrated improved oral bioavailability of a poorly-water soluble drug by a supersaturation approach (Gao, Guyton et al., 2004; Guzmán, Tawa et al., 2007; Overhoff, McConville et al., 2008), there are limited data to allow one to correlate supersaturation profile *in vitro* with pharmacokinetics profile *in vivo*.

The degree of supersaturation is quantified by the supersaturation ratio (SS) which is the ratio of drug concentration to the equilibrium solubility value. Eq. 4.2 can be applied by combining, at each time point, apparent solubility during *in vitro* lipolysis (Figures 4.21

and 4.23-4.24) with the equilibrium solubility in lipolytic products (Figure 4.16). As shown in Figures 4.25a-4.25c, the supersaturation ratios of progesterone, 17 $\beta$ -estradiol and nifedipine were shown to be sensitive to the extent of lipolysis. The P-20 and P-31 created maximum degree of supersaturation at time zero and performed poorly in maintaining the supersaturated state. Except for the values at time zero, the SS values were less than or equal to 1. As a result, the concentration of progesterone in solution remained constant up to 24 h. On the other hand 17 $\beta$ -estradiol showed a totally different supersaturation profile during the *in vitro* lipolysis (Figure 4.25b). In general, the supersaturation ratio increased steadily over 120 min for the three 17 $\beta$ -estradiol-loaded formulations. The degree of supersaturation was increased two-fold for E-7 and E-14 in the first two-hour period of the experiment. In the case of E-5, 17 $\beta$ -estradiol was initially subsaturated. However, after 30 min, 17 $\beta$ -estradiol became supersaturated due to decreased equilibrium solubility in the lipolytic products. In the case of nifedipine, the maximum degree of supersaturation occurred at 15 min in the lipolysis of N-35 giving the supersaturation ratio of 3.2. Over this value, the drug started to precipitate (Figure 4.25c). Other than that, the changes in supersaturation ratio during the lipolysis of N-11 and N-20 were similar to those in the E-5 and E-7 of 17 $\beta$ -estradiol formulations. Initially, nifedipine was subsaturated during the lipolysis of N-11 but later increased to 1.5 by 120 min. Lipolysis of N-20 increased the supersaturation ratio 2.5-fold by 120 min.

It has been suggested that solubilization in lipid aggregates may promote mass transfer of digested lipids and a poorly-water soluble drug through the unstirred water layer at the surface of enterocytes in the GI tract (Westergaard and Dietschy, 1976; Land, Li et al., 2006). The passive transport of drug through intestinal membranes into blood circulation is driven by free solute concentration. Enhancement of oral absorption would be expected to result from supersaturation.

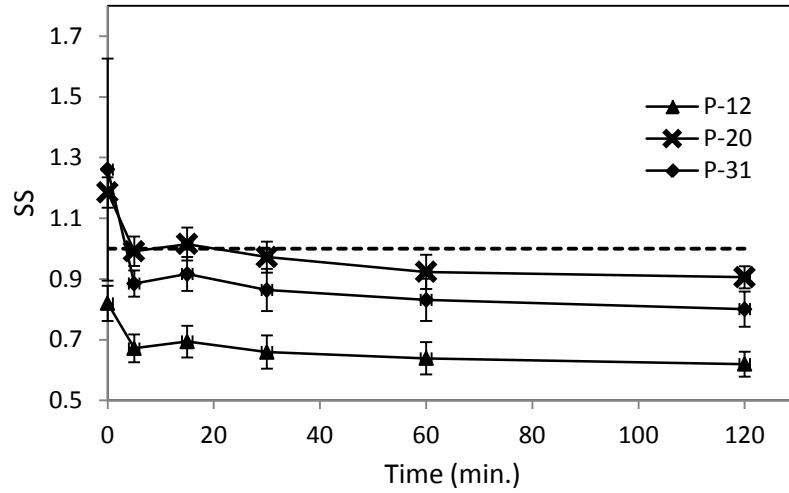


Figure 4.25a The supersaturation ratio during the *in vitro* lipolysis of progesterone formulation P-12 (triangle), P-20 (cross) and P-31 (diamond). The dashed line is supersaturation ratio equal to 1.

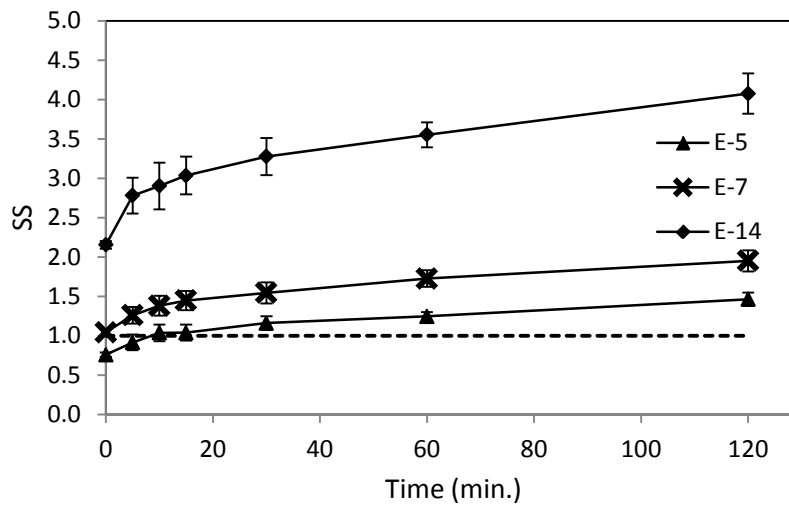


Figure 4.25b The supersaturation ratio during the *in vitro* lipolysis of 17 $\beta$ -estradiol formulations E-5 (triangle), E-7 (cross) and E-14 (diamond). The dashed line is supersaturation ratio equal to 1.

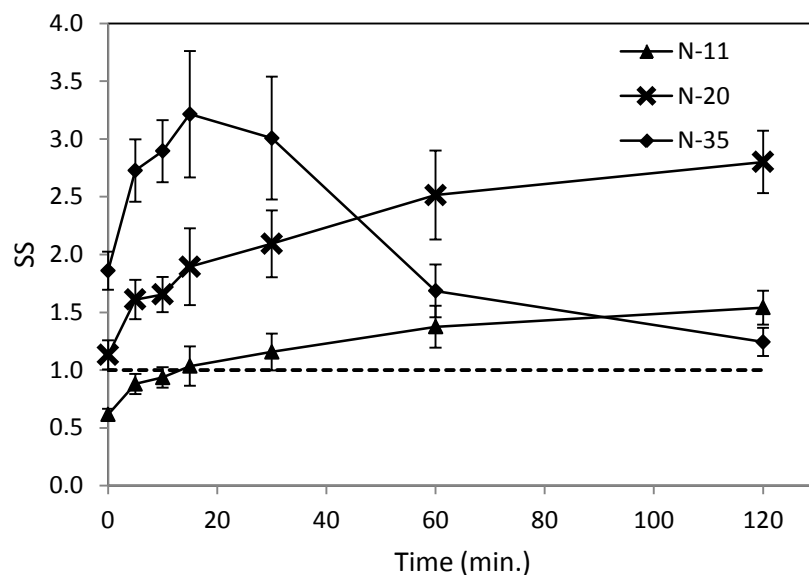


Figure 4.25c The supersaturation ratio during the *in vitro* lipolysis of nifedipine formulations N-11 (triangle), N-20 (cross) and N-35 (diamond). The dashed line is supersaturation ratio equal to 1.

Referring back to Figure 4.10, at fixed concentration of surfactant, the driving force for precipitation would increase as the initial drug concentration increases from Zone 1 to Zone 3. Figures 4.25a-4.25c show the extent of the supersaturation ratio was dependent upon the initial drug concentration prior to lipolysis. The calculated supersaturation ratios during *in vitro* lipolysis reflect the drug concentration in the solution for a given drug in a surfactant solution at fixed concentration (Figures 4.25a-4.25c). As seen in the production of fatty acid from the lipolysis of PS80 (see Section 4.4.1), the composition of lipolytic products at predetermined time were comparable in the presence of progesterone,  $17\beta$ -estradiol and nifedipine and in the absence of the drug. In other words, the lipid compositions were the same for all formulations at each time of sampling. Therefore, all supersaturation ratios in the three formulations of each drug it may be possible to estimate a stability index for each drug during the lipolysis of PS80. Referring back to the supersaturation profiles during *in vitro* lipolysis (Figures 4.25b and 4.25c), the supersaturation ratio of 4.08 appears to be the upper limit for  $17\beta$ -estradiol inducing rapid precipitation in a 2 h period of time. A supersaturation ratio of 3.21 appears to be the upper limit for nifedipine. Whenever the extent of supersaturation is over these limits,

17 $\beta$ -estradiol and nifedipine will precipitate rapidly. Compared to 17 $\beta$ -estradiol and nifedipine, the upper limit of rapid precipitation is far lower for progesterone (1.26). The maximum supersaturation ratio among the three formulations for each drug is plotted versus time (Figure 4.26). Since the solution concentration of PS80 was altered as function of time, the plot is actually a supersaturation ratio versus the concentration of PS80. As shown in Figure 4.29, the stability index of progesterone was the narrowest and 17 $\beta$ -estradiol the widest. Guided by this stability index, the lipolysis of N-35 will exhibit poor relative stability of the supersaturated state because the supersaturation ratio is over the upper limit.

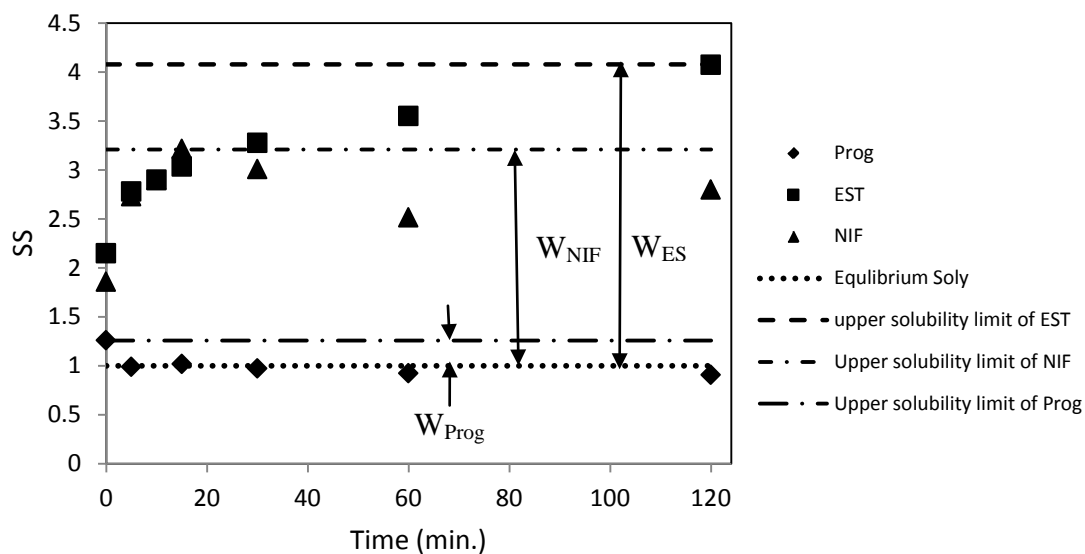


Figure 4.26 The approximate stability index of progesterone, 17 $\beta$ -estradiol and nifedipine in supersaturated state during the lipolysis of formulations.  $W_{EST}$ ,  $W_{NIF}$  and  $W_{Prog}$  are ranges of stability index for 17 $\beta$ -estradiol, nifedipine and progesterone, respectively.

In an attempt to further quantify the supersaturation behavior of these formulations, the areas under the supersaturation-time curves in Figures 4.25a-4.25c (AUC-SS) for the first 2 h were determined. SS equal to 1.0 was established as the baseline for the area determinations. The peak supersaturation ratio ( $SS_{max}$ ), the area under the supersaturation ratio-versus-time curve, and the time of the maximum degree of supersaturation during the *in vitro* lipolysis of each formulation ( $t_{max}$ ) are presented in Table 4.7. In addition, the area under the concentration-time curve (AUC-C) in Figures 4.21 and 4.23-4.24 was also

calculated and shown in the Table. The AUC-SS will be a descriptor that includes both the extent of supersaturation and the time which a drug stays in the supersaturated state. It will give a quantitative view of the capability of formulation to maintain a state of supersaturation during the lipolysis. As shown in Table 4.5, the E-14 performed best to maintain the supersaturation followed by the N-20 during the *in vitro* lipolysis of formulation.

A very good linear relationship between the AUC-SS and the AUC-C is demonstrated in Figure 4.27. The greater the extent of supersaturation, the higher drug concentration is over 2 h. Ignoring other possible factors, such as first pass metabolism, it may be hypothesized that increasing the AUC-SS would result in an increase in bioavailability. Currently, there are no data in the literature to test the hypothesis that the AUC-SS is a predictor of the bioavailability of a poorly-water soluble drug when administered *in vivo* by LBDDS. However, the substantial improvement in absorption of a poorly-water soluble drug has been related to the extent and stabilization of supersaturation (Raghavan, Kieper et al., 2001; Gao, Guyton et al., 2004; Vaughn, McConville et al., 2006; Miller, DiNunzio et al., 2008). The ultimate purpose of usage of supersaturation is to increase the free drug concentration at the site of absorption.

Table 4.7 The summary of maximum supersaturation ratio ( $SS_{max}$ ), time at  $SS_{max}$  ( $t_{max}$ ), area under the supersaturation curve and maximum concentration ( $C_{max}$ ), time at  $C_{max}$  and area under the concentration curve

Formulations	SS			Concentration		
	<i>in vitro</i>					
	$SS_{max}$	$AUC_{0-120}$ (min)	$t_{max}$ (min.)	$C_{max}$ ( $\mu\text{g.mL}^{-1}$ )	<i>in vitro</i> $AUC_{0-120}$ ( $\mu\text{g.min.mL}^{-1}$ )	$t_{max}$ (min.)
P-12		0	0	131 $\pm$ 14	(1.4 $\pm$ 0.1) $\times 10^4$	0
P-20	1.2	0.6	0	202 $\pm$ 15	(2.1 $\pm$ 0.2) $\times 10^4$	0
P-31	1.0	0.4	0	210 $\pm$ 51	(1.9 $\pm$ 0.04) $\times 10^4$	0
E-5	1.5	29.2	120	57 $\pm$ 2	(6.1 $\pm$ 0.1) $\times 10^3$	0
E-7	2.0	81.5	120	78 $\pm$ 3	(8.4 $\pm$ 0.3) $\times 10^3$	0
E-14	4.1	300.1	120	162 $\pm$ 1	(1.7 $\pm$ 0.03) $\times 10^4$	0
N-11	1.5	37.2	120	111 $\pm$ 2	(1.2 $\pm$ 0.03) $\times 10^4$	0
N-20	2.8	162.0	120	203 $\pm$ 16	(2.2 $\pm$ 0.1) $\times 10^4$	0
N-35	3.2	125.8	15	327 $\pm$ 15	(2.0 $\pm$ 0.1) $\times 10^4$	0

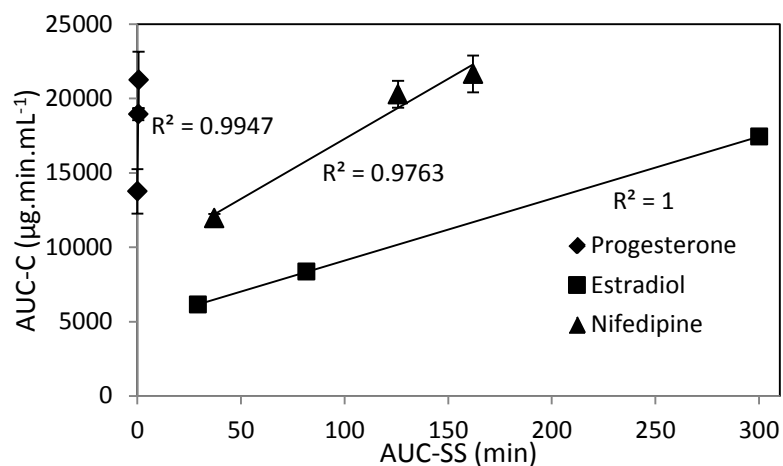


Figure 4.27 The linear relationship of AUC-SS and AUC-C



#### 4.5. Conclusion

Supersaturated solutions for the three model drugs could be formed in PS80 dispersed in fasted-state buffer. The ability to maintain a supersaturated state upon dispersion was drug-dependent. At a supersaturation ratio of 2, progesterone precipitated rapidly within 5 min while 17 $\beta$ -estradiol and nifedipine were protected from precipitating for a longer period of time. When the supersaturation ratio is close to 1, precipitation was prevented by PS80.

Comparison of AUC-C values in the absence of the enzyme and in the presence of the inactivated enzyme indicated that the particles in the enzyme preparation promoted progesterone and nifedipine precipitation at a supersaturation ratio of 2.

Results from the digested blank PS80 showed that the equilibrium solubility of 17 $\beta$ -estradiol and nifedipine was decreased with greater concentration of lipolytic products, while the equilibrium solubility of progesterone increased slightly. As a direct result of the change in equilibrium solubility during lipolysis, supersaturated solutions were created and maintained. The values of AUC-C in the presence of the inactivate enzyme and the active enzyme indicated that the lipolysis of PS80 had no effect on the solubilization of progesterone. The extent of supersaturation of 17 $\beta$ -estradiol steadily increased for all three formulations over 120 min. The greatest supersaturation ratio was 4.1. For N-11 and N-20, the extent of supersaturation steadily increased over 120 min. On the other hand, for N-35, nifedipine supersaturation ratio showed a local maximum at 3.2. AUC-SS demonstrated that PS-80 formulaitons of 17 $\beta$ -estradiol were most successful in remaining at supersaturated state and formulations of progesterone the least successful. The results showed that lipolysis of the surfactant excipient in PS80 resulted in a supersaturated state for model poorly-water soluble compounds progesterone, 17 $\beta$ -estradiol and nifedipine. The extent of the supersaturation was dependent upon the extent of hydrolysis of surfactant and was drug-dependent.

## Chapter 5

### Solubilization of Poorly-water Soluble Drugs in Model Mixed Micellar Systems

#### Composed of Selected Lipolytic Products of Polysorbate 80

##### 5.1. Summary

The first aim of this chapter is to quantify the solubilization of progesterone, 17 $\beta$ -estradiol and nifedipine in a series model mixed micelle systems composed of PS80 and OA. The model systems are chosen to simulate the solution composition during the *in vitro* lipolysis of PS80. The second aim of this chapter is to employ the molar solubilization capability and the micelle-water partition coefficient ( $K_{m/w}$ ) of model mixed micelles to predict the total drug solubility during the *in vitro* lipolysis. The negative deviation of from ideal mixing indicated that the addition of OA to the PS80 micelles led to decreased solubilization capacity for 17 $\beta$ -estradiol and nifedipine. The micelle-water partition coefficients of the drug in model systems were used to calculate the total drug solubility as a function of the composition of PS80 and oleic acid. It appears that the calculated equilibrium solubility of nifedipine in the model mixed micellar solutions composed of lipolytic products is closer to the equilibrium solubility of nifedipine in the dispersed LBDDS under simulated intestinal conditions than in the case of 17 $\beta$ -estradiol.

##### 5.2. Introduction

The ability of PS80 to create and maintain a drug in a supersaturated state as a function of time under simulated GI tract conditions was evaluated in Chapter 4. In order to assess the degree of supersaturation, the equilibrium solubility in the digested blank formulation was determined. The results indicated that the equilibrium solubility of progesterone in lipolytic products remained constant whereas the equilibrium solubility of 17 $\beta$ -estradiol and nifedipine decreased as a function of lipolysis. In this chapter, the ability of these aggregates to solubilize the drug is probed. The digestion of sophisticated LBDDSs containing triglycerides and surfactants will generate various aggregates such as liquid crystal phase(s), lamellar phase(s), unilamellar vesicles and mixed micelles (Kossena,

Boyd et al., 2003; Kossena, Charman et al., 2004; Kossena, Charman et al., 2005; Fatouros, Deen et al., 2007; Fatouros, Bergenstahl et al., 2007). Kossena et al. studied the relative contribution of each phase to the overall solubilization in the sample by using model systems containing the lipolytic products of triglycerides in a BS/PC solution. A similar approach was also used to investigate the effect of dilution on the size distribution of aggregates and the solubilization capacity (Ibardia-Arana, Kristensen et al., 2006). However, these studies were limited to apparent solubilization in the whole system, but no information was available on the molecular details of solubilization in terms of individual assemblies and interactions of drug-aggregates.

The effect on the solubilization of the alteration of lipid composition in solution due to lipolysis is not fully understood. This chapter represents a simplified approach to the question of effect of lipolysis on solubilization by focusing attention on mixed micelles of PS80 and oleic acid. Upon subjecting PS80 to lipolytic conditions, the only lipid byproduct is oleic acid. Presumably, the polyoxyethylene head group does not participate in the formation of lipid aggregates of lipolytic products. By isolating attention to mixed micelles of PS80 and oleic acid, it will be easier to examine the temporal effects of solubilization of drug. We can then build upon this knowledge with more sophisticated formulations.

We described here a series of model mixed micelles containing PS80 and oleic acid at different molar ratios so as to mimic the various lipid aggregates that form from lipolysis. Model mixed micellar system of known components allows us to study the solubilization mechanism under well-defined conditions. We hypothesize that the equilibrium solubilization of drug under simulated intestinal conditions may be correlated with the equilibrium solubility of drug in these series model mixed micellar solutions. In order to test the hypothesis, the solubilities of hydrophobic drugs in model mixed micellar systems were determined. The solubilization efficiencies of model systems were quantified by molar solubilization capacity and water-micelle partition coefficient. Solubilization of the drug in mixed micelle was then related to the solubilization in the individual surfactants, PS80 and OA, by the regular solution approximation employing the model of Treinor. Eventually, the fitted micelle-water partitioning coefficient of drugs in mixed micelles of PS80 and OA could be used to calculate the total drug

solubility as a function of time of lipolysis. Such an approach will potentially help a formulator to understand and manipulate those formulation factors that affect the solubilization of the drug in the GI tract, especially in the creation and maintenance of the supersaturated state.

### 5. 3. Materials and methods

#### 5.3.1. Materials

Progesterone (Prog, purity  $\geq 99\%$ ), Nifedipine (NIF, purity  $\geq 98\%$ ),  $17\beta$ -estradiol (EST, purity  $\geq 98\%$ ), 1,2-diacyl-sn-glycero-3-phosphocholine (type XVI-E) from egg yolk (PC), Trisma® maleate, and sodium cholate hydrate (NaC) (purity  $\geq 99\%$ ) were purchased from Sigma-Aldrich (St. Louis, MO, USA). High purity Polysorbate 80 (PS80) was a generous gift from Croda Inc. (Edison, NJ, USA). Oleic acid (OA) (purity  $\geq 97\%$ ) was purchased from Fisher Scientific (Pittsburgh, PA, USA). All chemicals were used as received. Water for the buffer solution was from a Milli-Q water purification system. Hydrophilic PTFE filters with  $0.2\ \mu\text{m}$  pore size (13mm) were purchased from Advantec MFS Inc. (Japan).

#### 5.3.2. Calculation of the molar ratio of PS80 to oleic acid

The *in vitro* lipolysis of PS80 with and without drug was carried out as described in Chapters 3 and 4. The PS80 in solution at the time of sampling was calculated as the difference between the initial amount of PS80 added and the amount of OA generated from PS80. Since the PC in simulated intestinal fasted-state digestion buffer (SIFs buffer) was hydrolyzed to FA as well, the amount of OA from PS80 was calculated the difference between the total amount of FA found by titration and the amount of FA from PC determined separately (control). FA generated from PS80 was calculated by Eq. (5.1)

$$\text{Moles of OA generated from PS80} = \text{Total FA titrated} - \text{FA from control} \quad (5.1)$$

The molar ratio of PS80 to OA at time of sampling was calculated by Eq. (5.2).

$$\text{Molar ratio} = \frac{\text{Mole of PS80}}{\text{OA generated from PS 80}} \quad (5.2)$$

In the case of lipolysis of drug-loaded formulations, the molar ratio was calculated for each formulation separately. After calculation of the molar ratio of PS80 to OA, the molar fraction of PS80 in the mixture of PS80 and OA is calculated by Eq. (5.3)

$$\text{Molar fraction of PS80} = \frac{\text{Mole of PS80}}{\text{Mole of PS80} + \text{Mole of OA}} \quad (5.3)$$

### 5.3.3. Preparation of model mixed micellar systems

Molar ratios of 9/1, 8/2, 7/3, 6/4 and 5/5 were chosen to represent the PS80/OA during various periods of the *in vitro* lipolysis of formulation. The limit of 5/5 was chosen for two reasons: (1) about 50% of PS was hydrolyzed in the *in vitro* lipolysis under optimum conditions and 5/5 will represent the upper limit in the lipolytic products; (2) judged by cloudy appearance, the systems of OA > PS80 are no longer composed of simple micelles.

Two series of solutions were prepared. To simplify the model system, tris maleate buffer (50 mM, ionic strength at 0.15, pH 7.5 at 37°C) was used in which bile salt/phospholipids were not included (T-series). To mimic the simulated intestinal conditions, 5 mM sodium cholate(NaC)/1.25 mM phospholipids was used to prepare the model mixed micellar systems as well (S-series). The two series of model systems are summarized in Table 5.1.

Table 5.1 The molar fraction of PS80 and molar ratio of PS80 to OA in the mixture of PS80 and OA prepared in tris maleate buffer (T-series) and SIFs buffer (5 mM NaC/1.25 mM PC) (S-series)

Tris maleate buffer or (SIFs buffer)	Molar fraction of PS80	Molar ratio of PS80 to oleic acid
T-1(S-1)	1	1/0
T-2(S-2)	0.9	9/1
T-3(S-3)	0.8	8/2
T-4(S-4)	0.7	7/3
T-5(S-5)	0.6	6/4
T-6(S-6)	0.5	5/5

Stock solutions of each ratio of PS80 to OA were prepared. The exact amount of PS80 and OA were weighed into a 20 mL scintillation borosilicate glass vial and then a specific volume of either tris maleate buffer or SIFs buffer was added to make up a total concentration of 30 mM surfactant. Prior to stirring overnight, the pH was adjusted to  $7.5 \pm 0.05$  at  $37^\circ\text{C}$ . After overnight equilibration, the pH was checked to ensure a value at  $7.5 \pm 0.05$ . Solutions a range of total concentration were prepared by diluting the above thoroughly-mixed stock solution. All solutions were equilibrated for one to two days, and the pH was checked before and after equilibration.

#### 5.3.4. Determination of molar solubilization capacity of mixed micellar systems

To evaluate the solubilization capacity, the equilibrium solubility of progesterone,  $17\beta$ -estradiol and nifedipine were determined in solutions prepared as in Section 5.3.3 at  $37 \pm 0.5^\circ\text{C}$ . Total surfactant concentrations of 0.5, 1, 2.5, 5, 15 and 30 mM at each molar ratio in T-series and S-series buffers were employed. The equilibrium solubility of model drugs in solutions of NaC/PC (fixed ratio of 4:1) with NaC concentrations of 0, 1, 2.5, 5, 10, 20 mM in tris maleate buffer (pH  $7.5 \pm 0.02$ ) were measured separately. In all solubility studies, an excess amount of drug was added to a 4 mL vial containing the

above media. The sample vials were purged by nitrogen gas, sealed and then rotated in a  $37\pm 0.5^\circ\text{C}$  oven. Aqueous samples were filtered through  $0.2\ \mu\text{m}$  PTFE membranes and diluted by isopropanol/water (1/1) to the appropriate concentration. All samples were analyzed by HPLC. Successive concentrations within  $\pm 5\%$  indicated equilibrium solubility was achieved.

Assuming that solubility in the bulk aqueous phase is independent of the presence of micelles, the total solubility of drug in a micellar solution has the following relationship (Alvarez-Núñez and Yalkowsky, 2000):

$$S_{\text{total}} = S_w + (C_{\text{total surfactant}} - \text{CMC}) * \kappa \quad (5.4)$$

where  $S_{\text{total}}$  is the total solubility of drug in the micellar solution;  $S_w$  is the solubility of drug in the bulk aqueous phase;  $C_{\text{total surfactant}}$  is the total surfactant concentration; CMC is the critical micelle concentration;  $\kappa$  is defined as the solubilization capacity. When both the solubility of drug and the concentration of surfactant are in mole units,  $\kappa$  is in units of mole of drug solubilized per mole of micellar surfactant.

When  $C_{\text{Total surfactant}} \gg \text{CMC}$ , Eq. (5.4) becomes:

$$S_{\text{total}} = S_w + C_{\text{total surfactant}} * \kappa \quad (5.5)$$

Solubilization capacity is obtained from the slope of the curve when  $S_{\text{total}}$  is plotted against  $C_{\text{total surfactant}}$ . Experiment data were fitted to Eq. 5.5 by Prism® software.

### **5.3.5. Determination of the micelle-water partition coefficient ( $K_{m/w}$ ) in a mixed micellar system**

If the micelle is considered to be a pseudo phase, the efficiency of solubilization can be measured by the partition coefficient ( $K_{m/w}$ ) of drug between the micelle phase and the aqueous phase.  $K_{m/w}$  is defined as the ratio of the molar fraction of drug in the micelle phase ( $X_m$ ) to that in the aqueous phase ( $X_a$ ). In terms of molar solubilization capacity,

$$X_m = \frac{\kappa}{1+\kappa} \quad (5.6)$$

where  $X_a = S_w * V_m$ .  $V_m$  is the molar volume of water, 0.01817L/mole at 37°C. Thus,

$$K_{m/w} = \frac{55.04\kappa}{(1+\kappa) * S_w} \quad (5.7)$$

Once the molar solubilization capacity is determined, the micelle-water partition coefficient can be calculated by Eq. (5.7) (Alvarez-Núñez and Yalkowsky, 2000).

### **5.3.6. Determination of the molar solubilization capacity and the micelle-water partition coefficient in sodium oleate**

The solubilization capacity and the micelle-water partition coefficient were estimated in sodium oleate solutions in a range of concentrations at ambient temperature. Normally, the solubilization capacity and the micelle-water partition coefficient in an individual surfactant can be determined as described in Sections 5.3.4 and 5.3.5. However, determining the solubilization of drug in sodium oleate micelles presents with a challenge. At pH 7.5 OA is not completely ionized (pKa of ~5). Nonionized OA is poorly-water soluble while ionized OA acts as an anionic surfactant and can form micelles. In OA micelles, the pKa of the carboxylic group has been reported to be 10 (Kanicky and Shah, 2003). In our hands, the apparent pKa of OA in the PS80 micelle solution was determined to be 7 in simulated intestinal conditions (pH 7.5, 37°C) (See Section 6.3.2). Under these conditions about 80% of the OA in the mixed micelle is ionized. So as to form OA micelles of equivalent percent ionized, a pH of 10.5 was employed in the solubilization experiments. Control experiments were carried out to validate that the drugs employed were not degraded in the high pH solution.

The exact amount of sodium oleate was weighed into a 20 mL scintillation borosilicate glass vial and then a calculated volume of deionized water was added to make a total concentration of 30 mM. Solutions were rotated at ambient temperature for three days. A series of micellar solutions at 30, 15, 5, 2.5, 1 and 0.5 mM were prepared by diluting the



above thoroughly-mixed stock solution. The pH of all solutions was adjusted to  $10.5 \pm 0.1$ . The solutions were then purged by nitrogen gas and sealed and rotated at room temperature. The pH was checked every three or four days due to the slow equilibrium between OA and sodium oleate and adjusted as necessary (Small, 1986). The equilibrium was achieved as indicated by a constant pH of  $10.5 \pm 0.1$  from two consecutive measurements. An excess amount of drug was added to a 4 mL vial containing the above media. The sample vials were purged by nitrogen gas, sealed and then rotated in ambient temperature for a week. Aqueous samples were filtered through  $0.2 \mu\text{m}$  PTFE membranes and diluted by 0.01M HCl in isopropanol to appropriate concentrations. All samples were analyzed by HPLC.

The molar solubilization capacity and micelle-water partition coefficient were obtained as described in Sections 5.3.4 and 5.3.5.

### 5.3.7. Calculation of total drug solubility in a model micellar system

The total solubility of drug in the mixed micellar system is presented in Eq. (5.4) and Eq. (5.5). Mathematical manipulation of Eq. (5.7) gives

$$\kappa = \frac{S_w * K_{m/w}}{(55.04 - S_w * K_{m/w})} \quad (5.8)$$

Then, Eq. (5.4) becomes

$$S_{\text{total}} = S_w + \frac{S_w * K_{m/w} * (C_{\text{total surfactant}} - \text{CMC})}{(55.04 - S_w * K_{m/w})} \quad (5.9)$$

When  $C_{\text{Total surfactant}} \gg \text{CMC}$ , Eq. (5.9) becomes:

$$S_{\text{total}} = S_w + \frac{S_w * K_{m/w} * C_{\text{total surfactant}}}{(55.04 - S_w * K_{m/w})} \quad (5.10)$$

Where  $S_w$ ,  $C_{\text{total surfactant}}$ ,  $\text{CMC}$ ,  $K_{m/w}$  and  $\kappa$  have the same meanings as previously defined.

Eq. (5.9) can be used to predict the total solubility of drug at the time of sampling during the *in vitro* lipolysis. Eq. (5.10) was used to predict the total drug solubility in all mixed micelle systems.

## **5.4. Results and Discussion**

### **5.4.1. Solubilization capacity ( $\kappa$ ) as a function of the molar fraction of PS80 in mixed micellar systems**

In the lipolysis experiments the composition of PS80 and OA in the formulation is altered as a function of time. The effect of alteration of PS80/OA composition on the solubilization of progesterone,  $17\beta$ -estradiol and nifedipine was evaluated by the molar solubilization capacity.

#### **5.4.1.1. $\kappa$ for progesterone**

The solubilization of progesterone in T-1 to T-6 is shown in Figure 5.1. As expected, at each molar ratio the solubility of progesterone increased linearly over the range of total surfactant concentration (PS80 plus OA) above the CMC. Generally, the solubilization behavior is attributed to the partition of the drug within micelles. The linearity suggested that the properties of micelles did not change markedly in the concentration range employed. The molar solubilization capacities of mixed micelles were obtained from the data fitted by linear regression. The results are given in Table 5.2. As the molar fraction of PS80 decreased from 1 (T-1) to 0.5(T-6), the molar solubilization capacities were relatively constant.

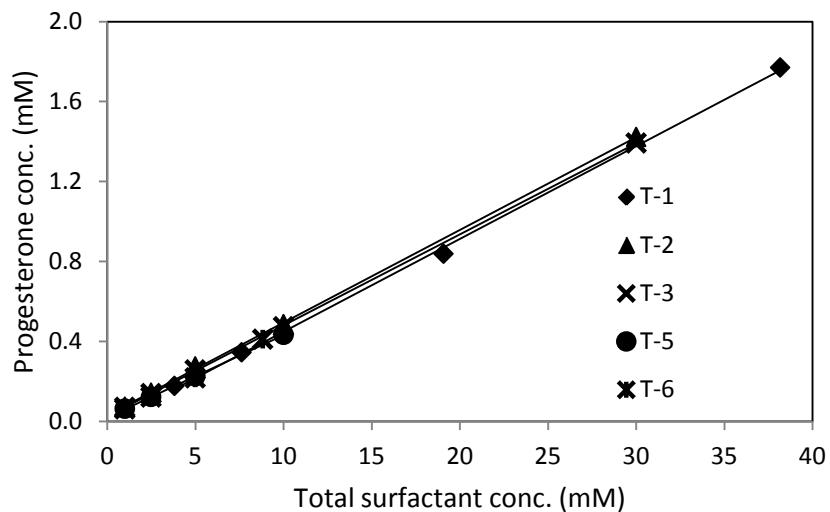


Figure 5.1 The solubilization of progesterone in PS80/OA mixed micelles with the molar fraction of PS80 at 1(diamond), 0.9 (triangle), 0.8 (cross), 0.6 (circle) and 0.5 (star) at  $37\pm 0.5^\circ\text{C}$ . Micellar solutions were prepared in tris maleate buffer (T-series).

Table 5.2 The fitted molar solubilization capacity ( $\kappa$ , mole of drug/mole of micellar surfactant) of mixed micellar systems for progesterone prepared in tris maleate buffer and SIF buffer

Molar fraction of PS80	Tris maleate buffer (T-series)		SIFs buffer (S-series)	
	fitted $\kappa$	95% CI	fitted $\kappa$	95% CI
1	0.048	0.001	0.050	0.002
0.9	0.045	0.001	0.054	0.001
0.8	0.045	0.000		
0.7			0.049	0.001
0.6	0.041	0.001		
0.5	0.044	0.002	0.052	0.002

A second series of model micellar systems were prepared in SIFs buffer (S-1 to S-6) to mimic the composition presented during the *in vitro* lipolysis closely. As shown in Figure 5.2, the solubilization of progesterone increased linearly as the total surfactant concentration (PS80 plus OA) in all compositions. Similar trends were observed where the molar solubilization capacities were kept constant in all composition solutions studied (Table 5.2). Compared to values obtained in systems prepared in a tris maleate buffer, the impact of the presence of NaC/PC on solubilization was all positive. The difference may be attributed to the presence of mixed micelles associated with NaC/PC.

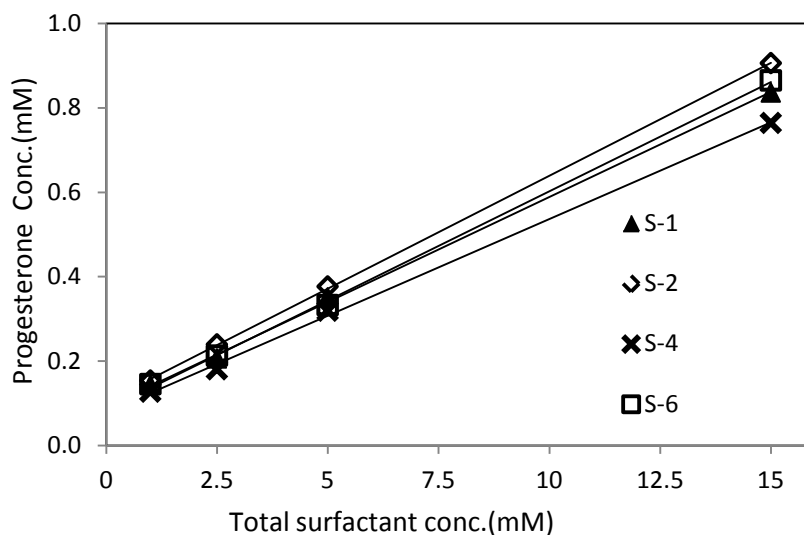


Figure 5.2 The solubilization of progesterone in PS80/OA mixed micelles with a molar fraction of PS80 at 1(triangle), 0.9 (diamond), 0.7 (cross), and 0.5 (square) at  $37\pm 0.5^\circ\text{C}$ . Micellar solutions were prepared in SIFs buffer (S-series).

To probe the effect of NaC/PC, the molar solubilization capacities of mixtures of these two surfactants were determined separately. Surprisingly, a nonlinear solubilization of progesterone was observed over the range of concentration (Figure 5.3). The break point was in the mixture of NaC/PC containing 5 mM NaC, the same concentration employed in the preparation of S-series solution and *in vitro* lipolysis. The slope was 0.01 when the concentration was below 5 mM whereas the slope increased to 0.017 when the NaC concentration was over 5 mM. The nonlinearity suggested that the structure and properties of aggregates of NaC and PC may have changed over the range of

concentration. It has been well accepted that the state of aggregation of bile salt/PC is a function of both the total lipid concentration and the molar ratio of bile salt to PC (Schurtenberger, Mazer et al., 1985; Almog, Kushnir et al., 1986; Vinson, 1989; Almog, Litman et al., 1990; Walter, Vinson et al., 1991; Coello, Meijide et al., 1996). Generally, two structure models of mixed micelle of bile salt/PC have been proposed in the literature, namely, the Small model and the mixed disk model (Small, 1967; Mazer, Benedek et al., 1980). The common property of these two models is that the micelles are oblate ellipsoids such that PC forms a bilayer core and bile salt is located around the perimeter. In addition, the mixed micelles are in equilibrium with the bile salt monomer, bile salt simple micelles, and PC vesicles (Scheme 5.1). Typically, the aggregates are micelles when the effective molar ratio of bile salt/PC is greater than the critical value of 0.4. At high concentration, such as 20 mM NaC/PC (molar ratio of 4/1), mixed micelles of low hydrodynamic radii are the only type of aggregates present. Upon dilution of NaC/PC with a buffer, bile salt monomers migrate from mixed micelles to the intermicelle region resulting in a decrease of effective molar ratio NaC/PC in the mixed micelles. Consequently, with dilution the mixed micelles grow to larger hydrodynamic radii and elongate. With further dilution, vesicles coexisting with the mixed micelles are formed (Mazer, Benedek et al., 1980; Egelhaaf and Schurtenberger, 2002; Pedersen, Egelhaaf et al., 2002).

Within each series the molar solubilization capacity of progesterone in mixed micelle of PS80 and OA was independent on the composition (Table 5.2). This observation is in a good agreement with results obtained in the digested blank formulation where the equilibrium solubility of progesterone remained constant during the *in vitro* lipolysis of PS80 (Section 4.4.4). The difference in solubilization behavior of progesterone between the S-series and T-series may be ascribed to the presence of NaC/PC in the S-series. The molar solubilization capacity of a mixture of NaC/PC was found to be 0.01 mole of drug/mole of micellar surfactant (slope of Figure 5.3 at 5 mM bile salt). The difference in solubilization capacity between the S-series and T-series was also 0.01 moles progesterone/mole surfactant. It is concluded that the difference between the S-series and T-series was due to the presence of the NaC/PS micelles in the S-series.

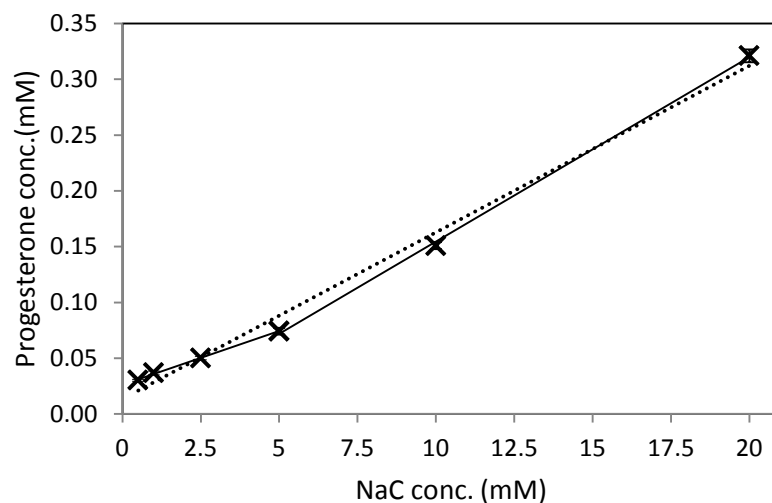
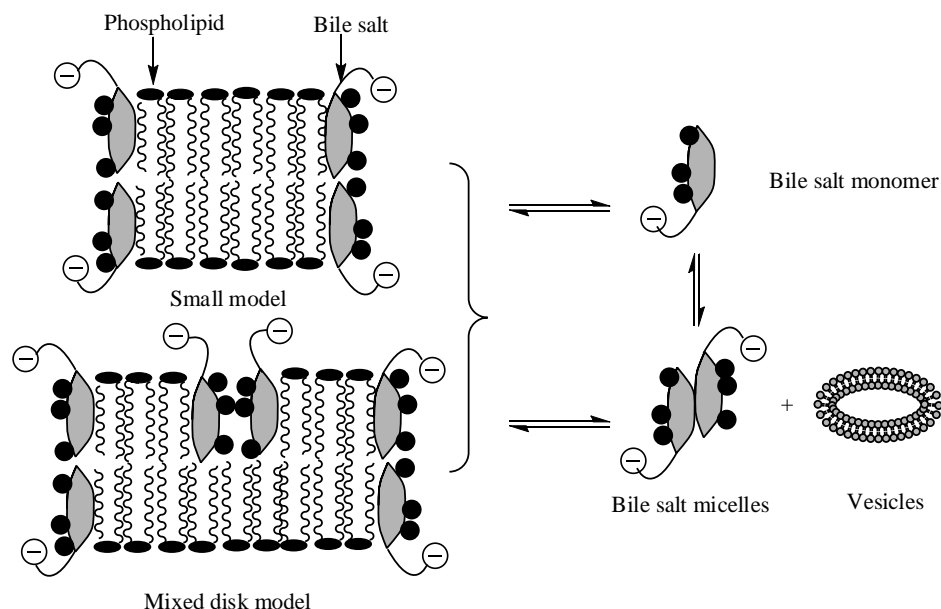


Figure 5.3 The solubilization of progesterone in a mixture of NaC and phospholipids (fixed ratio at 4:1) at 37 °C (error bars are within the symbol). The dashed line is the linear-regression fitting of all data from three replicates (slope =  $(1.44 \pm 0.06) \times 10^{-2}$ ,  $R^2=0.98$ ). The solid lines represent the linear-regression of data at concentrations less than and greater than 5 mM (slope below 5 mM =  $(0.84 \pm 0.05) \times 10^{-2}$ ,  $R^2=0.99$ ; slope above 5 mM =  $(1.67 \pm 0.02) \times 10^{-2}$ ,  $R^2=0.97$ ). The slopes of the two segments were significantly different as indicated by the F-test ( $P < 0.001$ ).



Scheme 5.1 A schematic presentation of the equilibrium between the mixed micelles of bile salt/phospholipids and bile salt monomer, simple micelles of bile salt and vesicles

#### 5.4.1.2. $\kappa$ for 17 $\beta$ -estradiol

The solubilization behavior of 17 $\beta$ -estradiol was determined in mixed micelles in T-series and S-series buffers. Figures 5.4 and 5.5 show that the solubility of 17 $\beta$ -estradiol increases with increasing total surfactant concentration in all compositions and in both T-series and S-series. The molar solubilization capacities, obtained from the slope of the curve fitted by linear regression, are listed in Table 5.3. Within 95% confidence, the molar solubilization capacities determined in T-1 and S-1 were identical, suggesting that the contribution of 5 mM NaC/PC to the total solubilization of drug in the model mixed micellar system was not significant. The molar solubilization capacity for 17 $\beta$ -estradiol decreased by 34% when the molar fraction of PS80 dropped to 50% in T-6 (S-6) mixture. This is consistent with the results obtained in the digested blank formulation where the equilibrium solubility in the formed lipolytic products decreased during *in vitro* lipolysis (Section 4.4.4).

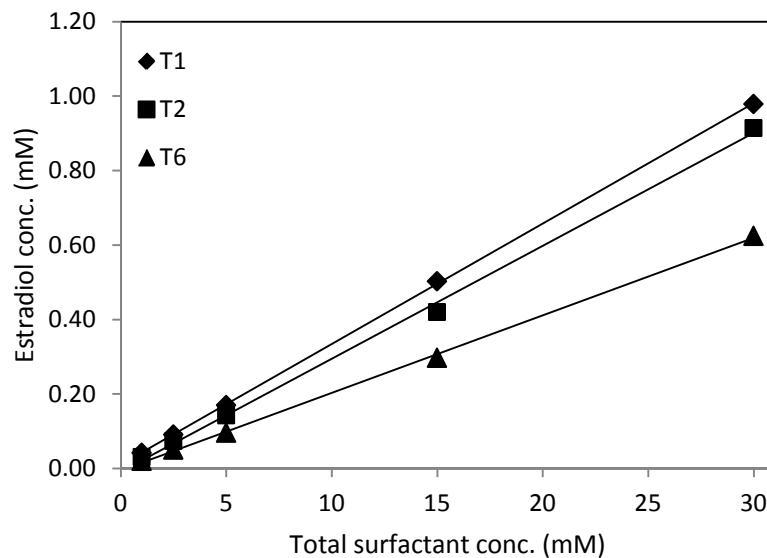


Figure 5.4 The solubilization of 17 $\beta$ -estradiol in PS80/OA mixed micelles with molar fraction of PS80 at 1 (diamond), 0.9 (square) and 0.5 (triangle) at 37 $\pm$ 0.5 $^{\circ}$ C. Micellar solutions were prepared in tris maleate buffer (T-series).

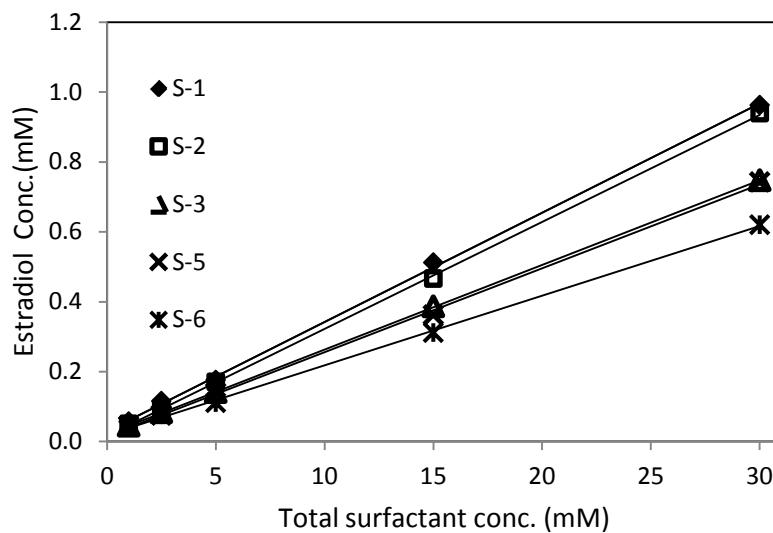


Figure 5.5 The solubilization of 17 $\beta$ -estradiol in PS80/OA mixed micelles with molar fraction of PS80 at 1 (diamond), 0.9 (square), 0.8 (triangle), 0.7 (cross) and 0.5 (star) at 37 $\pm$ 0.5 $^{\circ}$ C. The micellar solutions were prepared in SIFs buffer (S-series).



Table 5.3 The fitted molar solubilization capacities ( $\kappa$ , mole of drug /mole of micellar surfactant) of mixed micellar systems for 17 $\beta$ -estradiol prepared in tris maleate buffer and SIFs buffer

Molar fraction of PS80	Tris maleate buffer (T-series)		SIFs buffer (S-series)	
	fitted $\kappa$	95% CI	fitted $\kappa$	95% CI
1	0.032	0.002	0.031	0.002
0.9	0.030	0.0001	0.031	0.001
0.8			0.024	0.001
0.7			0.024	0.001
0.5	0.021	0.0001	0.020	0.001

A separate experiment was conducted to determine the solubilization capacity of NaC/PC (fixed ratio at 4:1) in order to evaluate the contribution of NaC/PC in the SIF buffer to the total solubilization of 17 $\beta$ -estradiol. An obvious nonlinearity was again evident, as shown in Figure 5.6. A break point in the figure was observed between 2.5 mM and 5 mM of NaC. The slope was 0.005 in the concentration region below 5 mM of NaC and 0.003 in the region above 10 mM of NaC. Iardia-Arana et al., reported a nonlinear solubilization of 17 $\beta$ -estradiol in sodium glycocholate in the concentration range from 2 mM to 30 mM (Iardia-Arana, Kristensen et al., 2006). Authors attributed the nonlinearity to the formation of bile salt micelles with increasing concentration. However, these authors concluded that solubilization of 17 $\beta$ -estradiol was linearly related to the concentration of sodium glycocholate/phospholipid. Despite the nonlinear dependence of solubilization on NaC/PC in the present work, the solubilization of 17 $\beta$ -estradiol was linearly related to PS80/oleic acid concentration in the SIFs buffer at all molar ratios tested. Moreover, the presence of NaC/PC in the S-series has little effect on the molar solubilization capacity giving identical values at each molar ratio of PS80 to oleic acid as that in T-series. It is concluded that NaC/PC mixed micelles had little effect on the solubilization in the S-series results.

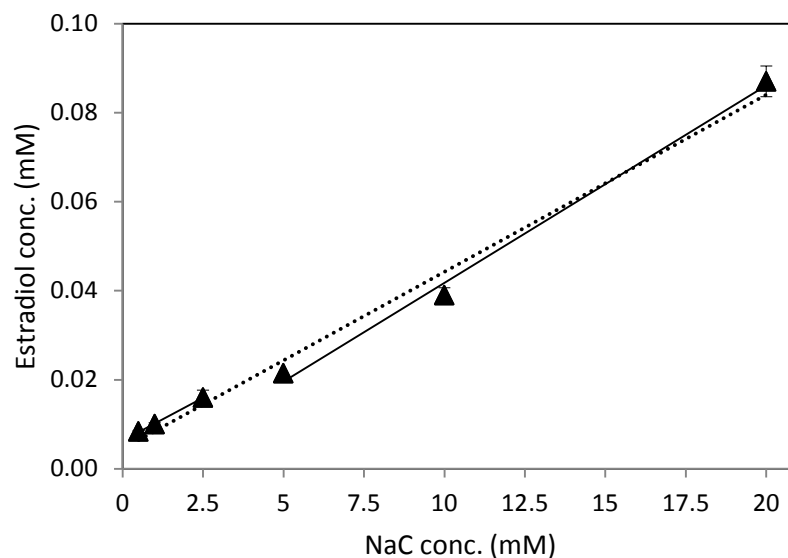


Figure 5.6 The solubility of  $17\beta$ -estradiol in mixture of NaCl and phospholipids (fixed ratio at 4:1) at  $37^{\circ}\text{C}$  (the error bars are smaller than the symbols). The dashed line is the linear-regression fitting of all data from three replicates (slope =  $(4.11\pm 0.15)\times 10^{-3}$ ,  $R^2=0.98$ ). The solid lines are linear-regressions of data at concentrations below 2.5 mM (slope1=  $(4.71\pm 0.15)\times 10^{-3}$ ,  $R^2=0.99$ ) and at concentrations above 5 mM (slope2 =  $(3.23\pm 0.33)\times 10^{-3}$ ,  $R^2=0.93$ ). Slopes of the two lines were significantly different as indicated by the F-test ( $P<0.02$ ).

#### 5.4.1.3. $\kappa$ for nifedipine

The results of solubility studies of nifedipine are shown in Figure 5.7 and Figure 5.8. As expected, the solubility of nifedipine increased within the range of total surfactant concentration above the CMC. In both series of buffers, the molar solubilization capacity for nifedipine decreased by approximately one half as the molar fraction of PS80 reduced from 1 to 0.5 (Table 5.4). This behavior was in stark contrast to that of progesterone, but somewhat similar to that of estradiol (Table 5.2). In comparing the results of the T-series and S-series in Table 5.4, it is evident that the presence of NaCl/PC depressed the solubilization of nifedipine in the mixture of PS80/OA. The extent of depression on the molar solubilization capacity reduced with increasing the molar fraction of oleic acid in the mixture. Further, the difference of molar solubilization capacity between T-series and S-series was 0.006 mole of drug/mole of micellar surfactant at a molar ratio of 9/1 and

0.003 at a molar ratio of 1/1. The exact reason for these differences is not clear. The dramatic decrease of the molar solubilization capacity in model systems composed of increasing amounts of fatty acid was in agreement with the results obtained in the digested blank formulation.

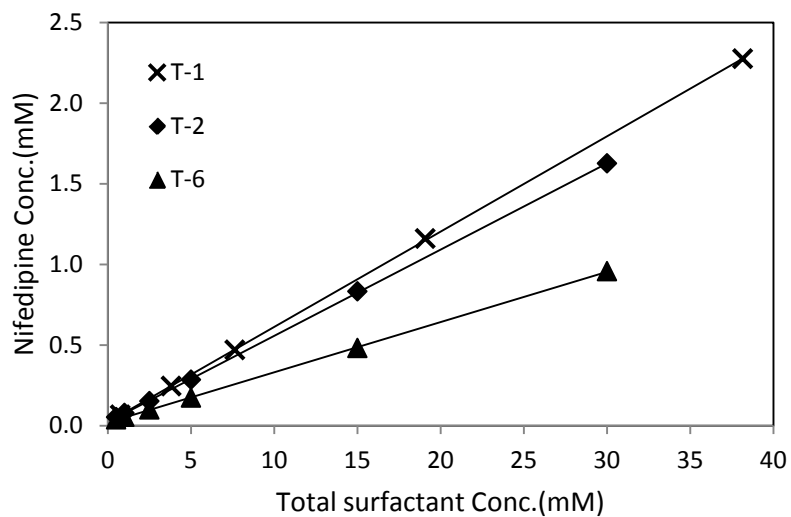


Figure 5.7 The solubilization of nifedipine in PS80/OA mixed micelles with molar fraction of PS80 at 1 (cross), 0.9 (diamond), and 0.5 (triangle) at  $37 \pm 0.5^\circ\text{C}$ . Micellar solutions were prepared in tris maleate buffer (T-series).

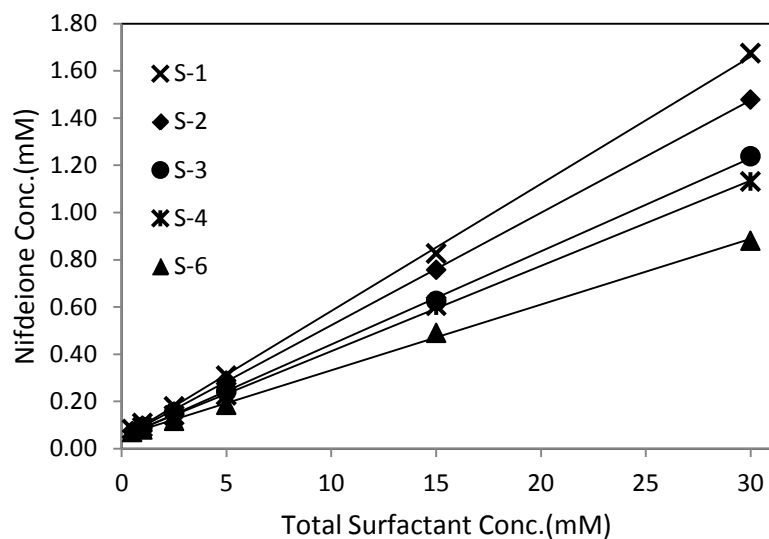


Figure 5.8 The solubilization of nifedipine in PS80/OA mixed micelles with molar fraction of PS80 at 1(cross), 0.9 (diamond), 0.8 (circle), 0.7 (star) and 0.5 (triangle) at  $37\pm 0.5^\circ\text{C}$ . The micellar solutions were prepared in SIFs buffer (S-series).

Table 5.4 The fitted molar solubilization capacity ( $\kappa$ , mole of drug / mole of micellar surfactant) of mixed micellar systems for nifedipine prepared in tris maleate buffer and SIF buffer

Molar fraction of PS80	Tris maleate buffer (T-series)		SIF buffer (S-series)	
	fitted $\kappa$	95% CI	fitted $\kappa$	95% CI
1	0.060	0.001	0.054	0.001
0.9	0.054	0.002	0.048	0.0001
0.8			0.039	0.0004
0.7			0.036	0.0004
0.5	0.031	0.000	0.028	0.001

The molar solubilization capacity of NaC/PC was determined in order to evaluate the contribution of NaC/PC to the total solubilization in the presence of PS80 and OA. Unlike the results of progesterone and 17 $\beta$ -estradiol, no obvious nonlinearities were observed in the solubilization of nifedipine in NaC/PC solution (Figure 5.9). The molar solubilization capacity of the mixture of NaC/PC (4/1) for nifedipine (0.008 mole of drug/mole of micellar surfactant) was smaller than progesterone (0.01 mole of drug/mole of micellar surfactant), but greater than 17 $\beta$ -estradiol (0.003 mole of drug/mole of micellar surfactant).

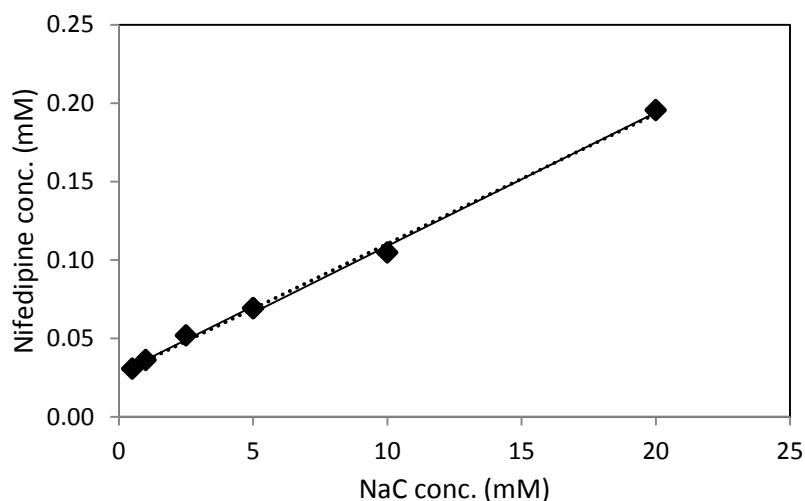


Figure 5. 9 The solubilization of nifedipine in mixture of NaC/PC (fixed ratio at 4:1) at 37°C (error bars are smaller than the symbols). The dashed line is the linear-regression fitting of all data from three replicates (slope =  $(8.41 \pm 0.20) \times 10^{-3}$ ,  $R^2=0.99$ ). The solid lines are linear regressions of data with a presumed breakpoint at 5 mM. For concentrations than 5 mM slope =  $(8.86 \pm 0.39) \times 10^{-3}$ ,  $R^2=0.99$ ; for concentrations greater than 5 mM slope =  $(8.37 \pm 0.40) \times 10^{-3}$ ,  $R^2=0.98$ . Slopes of the two segments were not significantly different as indicated by the results of the F-test ( $P=0.43$ ).

#### 5.4.1.4 Comparison of solubilization results for the three model drugs

In this section, the solubilization results for the model solutes will be discussed. The focus of this section will first be on the effect of PS80/OA content on nifedipine

solubilization, followed by discussion of the solubilization differences observed in S-series versus T-series buffers.

The data in Table 5.4 shows that the solubilities of nifedipine in both SIF and Tris-maleate buffers decrease markedly as the PS80/OA ratio drops. A few possible mechanisms may be responsible for such dramatic changes in solubility. The first possible mechanism would arise from preferential solubilization of the drug in the corona formed by polyoxyethylene chains in a PS80 micelle. If nifedipine were to be located to a significant extent in the POE-corona, all other factors being equal, then solubilization would be expected to diminish in mixed micelles with a reduced molar fraction of PS80. In order to estimate the influence of the POE chain on the solubilization, solubilities of nifedipine were determined in 1% and 10% of PEG-1000 which has approximately the same molecular weight as POE chains on PS80. The values of nifedipine solubility in 10% and 1% (w/v) PEG-1000 were  $(1.08 \pm 0.01) \times 10^{-1}$  mM and  $(2.29 \pm 0.03) \times 10^{-2}$  mM, respectively. The solubility of nifedipine in 1% of PEG-1000 was identical to the aqueous solubility under the same conditions. The solubility in 10% PEG-1000 was enhanced approximately 5-fold compared to that in 1% for nifedipine. The results with PEG-1000 support that the conclusion that nifedipine might be located in the corona and that the decreased number of PEO chains in a PS80/OA micelle would result in diminished solubilization. The chemistry of the putative interaction of nifedipine with PS80-containing micelles will be covered in Chapter 6.

A second possible mechanism to explain reduced solubilization would be a change in size of the micelle with the reduced molar fraction of PS80. For example, an increase of the micellar aggregation number and size was found in the mixing of nonionic surfactant and anionic surfactant such as Triton X-100 and  $C_{11}COONa$  (Dubin, Principi et al., 1989). Furthermore, the Nagarajan thermodynamic theory for mixed micelle formation also predicts an increase of aggregation number in mixed micelles compared to simple micelles (Nagarajan, 1985). If nifedipine is solubilized at the interface between the hydrophobic tail and the hydrophilic POE chain, the total surface area of the mixed micelle will have significant impact on the solubilization capability. Characterization of mixed micelles indicated that the size remained constant in spite of the change of molar

fraction of PS80 in SIF buffer (Chapter 6). It can be concluded that changes in the size of mixed micelles do not account for changes in solubilization capacity with PS80 content.

A third possible mechanism to explain reduced solubilization with a reduced mole fraction of PS80 would involve electrostatic repulsion of the drug and ionized oleic acid. If the micelle-solubilized drug was of similar charge, then electrostatic repulsion with ionic surfactant such as sodium oleate would result in reduced solubilization (Borges, Borissevitch et al., 1995; Chakraborty, Shukla et al., 2009). Further, it would be expected that the effect of electrostatic repulsion on solubilization would be greater with high mole ratio of ionized oleic acid in the micelle. In the present case, electrostatic repulsion should not be a significant issue as nifedipine is nonionized at pH 7.5. In fact, the NH group on nifedipine may act as a hydrogen bonding donor. The increase in charge density on the micelle surface would be expected to favor the formation of hydrogen bonding between the ionized carboxylic acid group and the drug. Thus, the solubilization might be actively facilitated by hydrogen bonding, not the opposite.

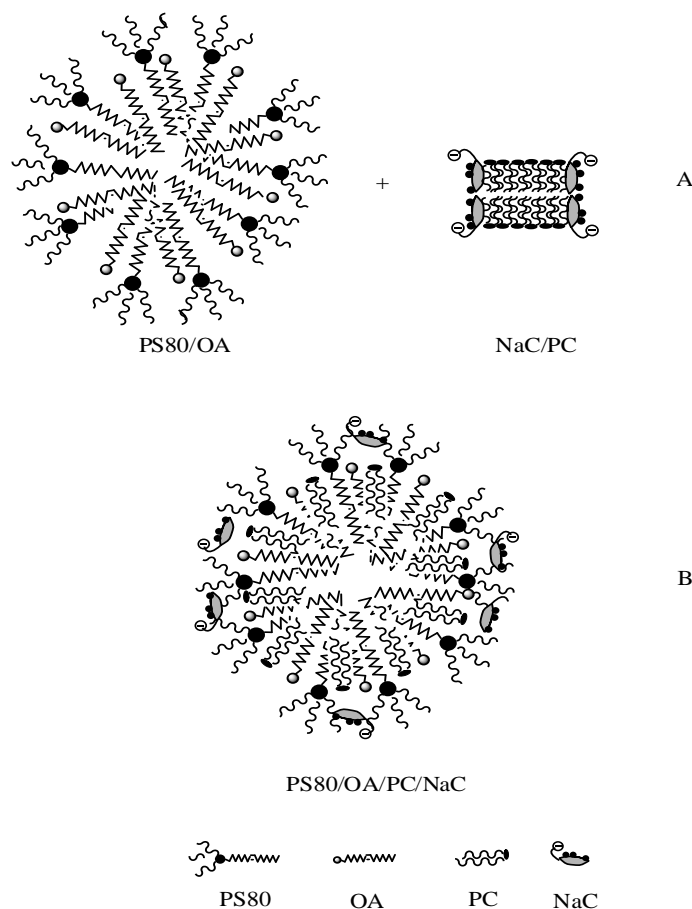
Overall, preferential localization in the PEO-containing micelle corona seems the most likely explanation for the solubilization behavior of nifedipine in mixed micelles of PS80/OA.

For all three model solutes, the solubilities in the S-series (SIF) were not equal to those observed in the T-series (maleate buffer). At present, the reasons for the observed differences in the solubilization capacities between the S-series and T-series are not clear, but must be related to the presence of NaC/PC. Several possible modes of aggregation would occur in a mixture of PS80 and OA in the presence of NaC/PC and could account for the observed effects. In the simplest of models, two independent populations of mixed micelles would co-exist, namely, PS80/OA mixed micelles and NaC/PC mixed micelles (Scheme 5.2A). Solubilization of drug would occur independently in both types of micelles. Applied to the current work, only PS80/OA micelles would be present in the T-series while in the S-series, both PS80/OA and NaC/PC micelles would be presumed to co-exist. In the independent population scenario, the solubilization capacities for all model drugs would be expected to be greater in S-series compared to T-series since in the S-series there are more lipid assemblies available to solubilize model drugs.

The solubilization results of 17 $\beta$ -estradiol and nifedipine are not in agreement with the independent population hypothesis. The results listed in Table 5.3 shows that there is no difference in the solubilization between T-series and S-series for 17 $\beta$ -estradiol. The results listed in Table 5.4 indicate that the solubilization capacity for nifedipine was depressed in the presence of NaC/PC. It is clear that two independent populations are not present when all four surfactants are present in the S-series.

It is possible to envision several mixed modes of assembly in the presence of PS80, OA, NaC and PC, where micelles might be composed of three or four of the surfactants in different ratios. Perhaps the simplest mixed mode of aggregation is formation of a single micelle type containing all surfactants PS80/OA/NaC/PC (Scheme 5.2B). The exact structure of such a complex assembly is not known, and Scheme 5.2B is simply intended to illustrate one possible example. In the GI tract, micelles containing fatty acid, monoglyceride, phospholipids and bile salt are arranged in a cylinder form with bile acid located between the polar heads of lipids such that the hydrophilic surface faces the aqueous phase (Hofmann, 1999). Replacing the monoglyceride with PS80 may result in the similar arrangement with the hydrophobic surface of NaC in contact with the POE chains and the hydrophilic surface of NaC exposed to aqueous phase. Certainly, it would be expected that the phase behavior of such a system would be at least as complex as that of the fatty acid, monoglyceride, phospholipids and bile salt system (Hofmann, 1999). Simple predictions about solubilization behavior of such a complex micelle are not yet possible.





Scheme 5.2 Possible lipid assemblies of PS80 and OA in the presence of NaC/PC. A. Two independent populations of mixed micelles, PS80/OA and NaC/PC. B. One population of mixed micelle containing all four surfactants PS80/OA/NaC/PC.

To further illustrate the relationship between the molar solubilization capacity and composition in SIF buffer, the normalized molar solubilization capacity ( $\kappa^*$ ) for each PS80/OA ratio was calculated by Eq. 5.11

$$\kappa^* = \frac{\kappa \text{ for PS80/OA}}{\kappa \text{ for PS80}} \quad (5.11)$$

As seen in Table 5.5, the normalized molar solubilization capacity of progesterone was independent of the molar fraction of PS80. In the cases of nifedipine and 17 $\beta$ -estradiol, the normalized molar solubilization capacities of mixed micelle decreased with the decreasing molar fraction of PS80 with the greatest effect being noted for 17 $\beta$ -estradiol.

Figure 5.10 is a plot of the molar solubilization capacity for the three model solutes as a function of mole fraction of PS80. The normalized molar solubilization capacities for nifedipine correlated very well with the molar fraction of PS80 in micelles. The correlation strongly suggested that solubilization of nifedipine is closely related to the proportion of PS80. On the other hand, the correlation between the normalized molar solubilization capacities and the PS80 concentration indicated that the solubilization of 17 $\beta$ -estradiol was less dependent upon the molar fraction of PS80. The solubilization of progesterone was independent of the composition of PS80 in the micelles.

Table 5.5 The normalized molar solubilization capacity ( $\kappa^*$ ) in SIF buffer for progesterone, 17 $\beta$ -estradiol and nifedipine in model micellar systems composed of PS80/OA at 37°C

Molar fraction of PS80	Progesterone		Nifedipine		17 $\beta$ -Estradiol	
	$\kappa$	$\kappa^*$	$\kappa$	$\kappa^*$	$\kappa$	$\kappa^*$
1	0.050	1.00	0.054	1.00	0.031	1.00
0.9	0.054	1.07	0.048	0.88	0.031	0.98
0.8			0.039	0.73	0.024	0.77
0.7	0.049	0.99	0.036	0.67	0.024	0.76
0.5	0.052	1.04	0.028	0.51	0.020	0.63

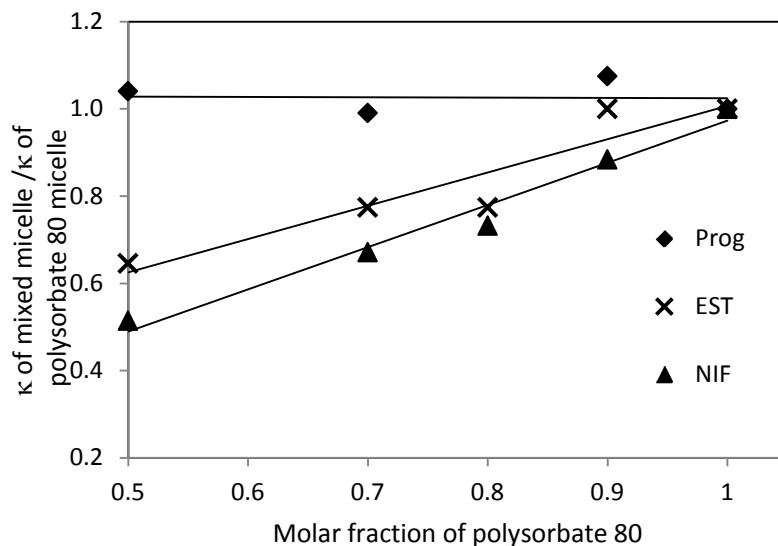


Figure 5.10 Correlation of the molar fraction of PS80 in micelles with the ratio of  $\kappa$  for progesterone (diamond,  $R^2 = 0.868$ ), 17 $\beta$ -estradiol (cross,  $R^2 = 0.8805$ ) and nifedipine (triangle,  $R^2 = 0.97$ ).

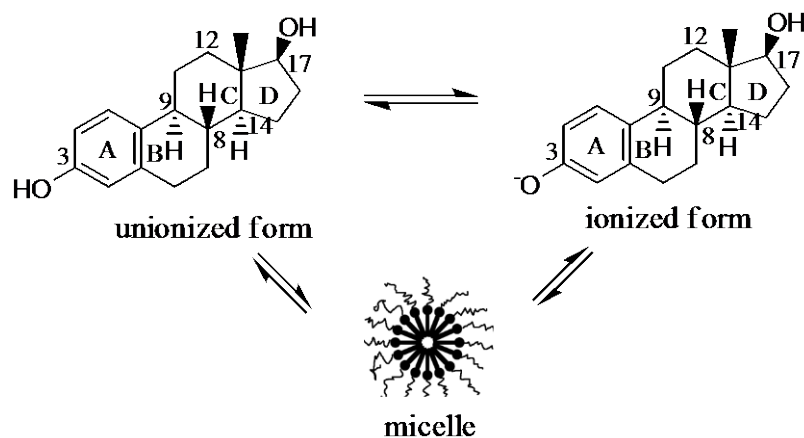
#### 5.4.1.5. Mixing effect of PS80 and OA on the ideal and real solubilization capacities

In mixed surfactants, the molar solubilization capacity can be estimated for the results of single surfactant solutions by Eq. (5.12) assuming the ideal mixing (Mohamed and Mahfoodh, 2006):

$$\kappa_{\text{ideal}} = X_1 \kappa_1 + X_2 \kappa_2 \quad (5.12)$$

where  $X_1$  and  $X_2$  are the molar fractions of PS80 and sodium oleate in mixture;  $\kappa_1$  and  $\kappa_2$  are the molar solubilization capacity for the drug in PS80 and sodium oleate solutions, respectively. The  $\kappa_1$  was determined at pH 7.5, 37°C to be 0.05 mole of drug/mole of PS80 for progesterone (Figure 5.1), 0.03 mole of drug/mole PS80 for 17 $\beta$ -estradiol (Figure 5.4) and 0.06 mole of drug/mole of PS80 for nifedipine (Figure 5.7). The values of  $\kappa_2$  (OA) were determined at pH 10.5, 25°C. OA forms a large vesicles coexisting with dispersed nonlamellar structures at pH 7.5 (Edwards, Silvander et al., 1995). Micelles are not formed at pH 7.5. To obtain sodium oleate micelles, the pH of 10.5 was employed. The pKa of carboxylic acid in the sodium oleate micelle was determined to be 10, giving the degree of ionization of OA in micelles to be 0.76 which was the same as that in the presence of PS80 at pH 7.5 where the pKa of OA in mixed micelle is 7. The

solubilization results are shown in Figures 5.11a, 5.11b and 5.11c. As can be seen, the solubility of all model drugs increased linearly over the range of sodium oleate concentration above the CMC. The apparent CMC of sodium oleate from the solubilization of progesterone and nifedipine was about 2.5 mM. The molar solubilization capacities of sodium oleate ( $\kappa_2$ ) were 0.21 and 0.03 for progesterone and nifedipine, respectively. On the other hand, the solubilization of 17 $\beta$ -estradiol increased the apparent CMC to about 5 mM. The increase of CMC may be attributed to the ionization of the drug. 17 $\beta$ -estradiol is un-ionized at pH 7.5, whereas the 3-phenolic group has a pK<sub>a</sub> of 10.71(Lewis, 1979) and will be partially ionized at pH 10.5. Electrostatic repulsion between the ionized drug and surfactant may be responsible for inhibiting micellization and thus increasing the CMC. Both the unionized and ionized drug can be solubilized in micelles with the equilibrium between the unionized and ionized form as shown in Scheme 5.3.



Scheme 5.3 The equilibrium between ionized and unionized 17 $\beta$ -estradiol in aqueous phase and micelle phase

Therefore, the apparent solubility of 17 $\beta$ -estradiol in sodium oleate at pH 10.5 would be a function of the solubility of free un-ionized and ionized drug in aqueous phase and un-ionized and ionized drug in micelle phase combined (Eq. 5.13);

$$S_{\text{total}} = S_i + S_u + S_{i-m} + S_{u-m} \quad (5.13a)$$

$$S_i = S_u \times 10^{\text{pH}-\text{pK}_a} \quad (5.13b)$$

where the  $S_i$  and  $S_u$  are solubilities of the free ionized and un-ionized drug in aqueous phase, respectively, and are related by Eq. 5.13b.  $S_{i-m}$  and  $S_{u-m}$  are solubilities of the micelle-bounded ionized and un-ionized drug, respectively. If  $S_{i-m}$  is considered to be small due to electrostatic repulsion between the anionic micelle and the anionic drug, Eq. (5.13a) becomes

$$S_{\text{total}} = S_u \times 10^{\text{pH}-\text{pK}_a} + S_u + S_{u-m} \quad (5.14)$$

The solubility of 17 $\beta$ -estradiol in the micelle will be

$$S_{u-m} = S_{\text{total}} - (S_u \times 10^{\text{pH}-\text{pK}_a} + S_u) \quad (5.15)$$

$S_u$  was determined to be  $6 \times 10^{-3}$  mM at  $25 \pm 0.5^\circ\text{C}$  which is close to the value of  $(8.9 \pm 0.6) \times 10^{-3}$  mM determined by others (Shareef, Angove et al., 2006). The molar solubilization capacity of sodium oleate for unionized 17 $\beta$ -estradiol was found to be was 0.04 mole/mole surfactant (slope in Figure 5.11b).

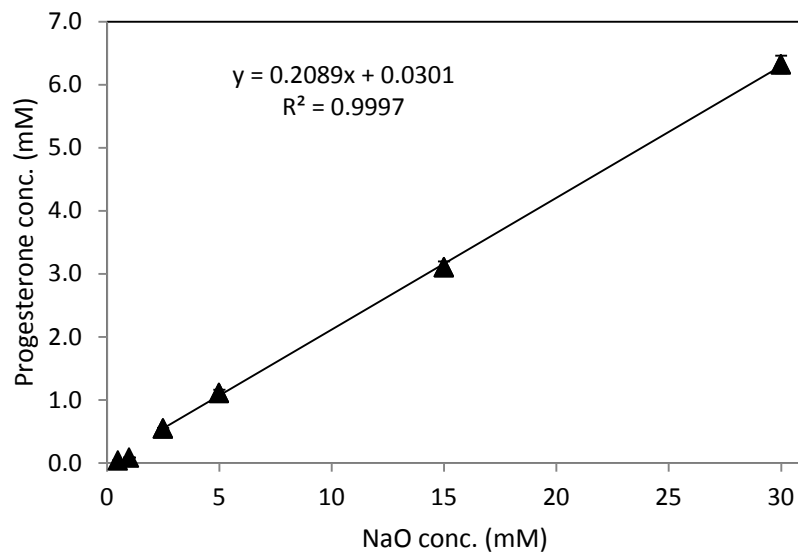


Figure 5.11a Solubilization of progesterone by sodium oleate at  $25\pm 2^\circ\text{C}$  at  $\text{pH } 10.5\pm 0.1$

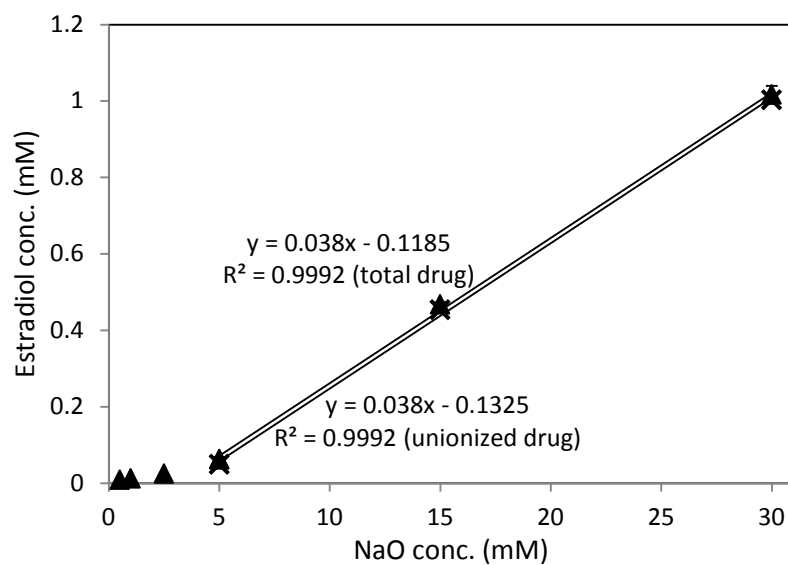


Figure 5.11b Solubilization of un-ionized and ionized  $17\beta$ -estradiol (triangle) and solubilization of un-ionized  $17\beta$ -estradiol (cross) by sodium oleate at  $25\pm 2^\circ\text{C}$  at  $\text{pH } 10.5\pm 0.1$

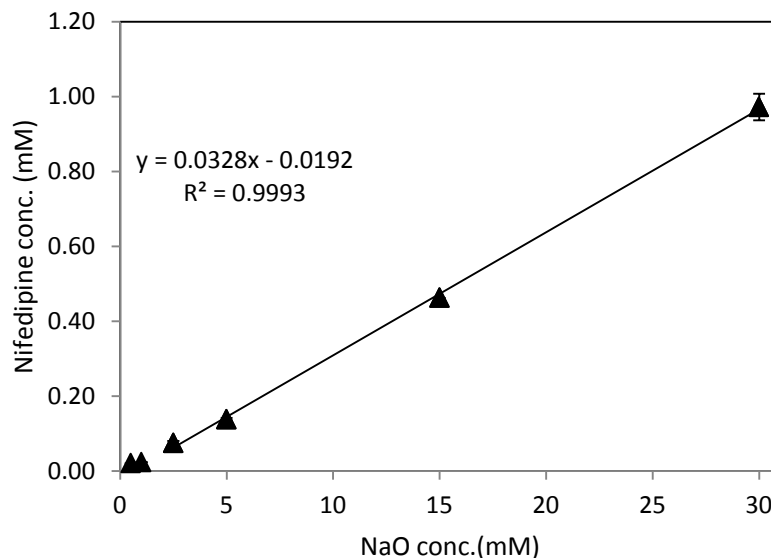


Figure 5.11c Solubilization of nifedipine by sodium oleate at  $25 \pm 2^\circ\text{C}$  at  $\text{pH } 10.5 \pm 0.1$

As indicated above,  $\text{pH}=10$  at  $25^\circ\text{C}$  conditions were employed in the determination of  $\kappa_2$  for sodium oleate while  $\text{pH}=7.5$  at  $37^\circ\text{C}$  was used for  $\kappa_1$  of PS80. The validity of employing widely different temperatures and  $\text{pH}$  values in Eq. 5.12 will be governed by a number of factors. The first factor is the temperature-dependence of CMC of the sodium oleate. An increase in temperature will enhance the molecular movement in the surfactant solution. As a result, a higher concentration of surfactant is required to maintain the aggregated state. The influence of temperature on the CMC of sodium oleate appears unresolved in the literature. CMC values ranging from 0.5 mM to 2.7 mM have been reported for sodium oleate in the temperature range of  $25^\circ\text{C}$  to  $30^\circ\text{C}$  (Tamamushi, Shirai et al., 1958; Drobosyuk, Borodulina et al., 1982; Akhter, 1997). Hildebrand et al. have suggested that sodium oleate exhibits two critical aggregation concentrations with a weak temperature dependence (Hildebrand, Garidel et al., 2003). These authors report that the first critical aggregation concentration is 0.9 mM at  $25^\circ\text{C}$  and 1.1 mM at  $35^\circ\text{C}$  whereas the second CMC is 2.4 mM at  $25^\circ\text{C}$  and 2.5 mM at  $35^\circ\text{C}$ .

The second factor to influence  $\kappa_2$  is size and shape of the sodium oleate micelle. Small-angle X-ray scattering studies indicated that the size and shape of sodium oleate micelles are independent of the concentration in the range of 0.05-0.2 g/g solution (approximately 0.16 to 0.65M) at  $27^\circ\text{C}$  (Reiss-Husson and Luzzati, 1964). Studies employing proton

longitudinal magnetic relaxation and self-diffusion measurements at 25°C also concluded the micelle shape is constant above 5 mM (Mahieu, Canet et al., 1991). On the other hand, the hydrodynamic radius of the sodium oleate micelle as been reporte to be 50 nm at 25°C and 40 nm at 37°C (Hildebrand, Garidel et al., 2003). All these studies seem to suggest that the size of sodium oleate micelles employed in the present study will not change significantly in the 25°C to 37°C temperature range. For this, it is concluded that the values of  $\kappa_2$  measured at 25°C are suitable to be used to estimate  $\kappa_{ideal}$  in Eq. (5.12) at 37°C.

The comparisons between ideal solubilization capacities ( $\kappa_{ideal}$ ) of the drug, as expressed by Eq. 5.12, and the experimental solubilization capacities ( $\kappa_{exp}$ ) of the drug are given in Figures 5.12a, 5.12b, and 5.12c. The results indicated that the  $\kappa_{exp}$  values were obviously less than those of  $\kappa_{ideal}$  at all the solution compositions. In order to more fully quantify the mixing effect of PS80 /OA mixed surfactants on the solubilization of progesterone, 17 $\beta$ -estradiol and nifedipine, the deviation ratio (R) between  $\kappa_{exp}$  and  $\kappa_{ideal}$  can be calculated as in Eq. (5.16) and plotted as function of molar fraction of PS80 in the model system (Figure 5.13).

$$R = \frac{\kappa_{exp}}{\kappa_{ideal}} \quad (5.16)$$

When R is greater than 1, the mixing effect on the solubilization is positive and the positive deviation of  $\kappa$  from ideal mixture will be observed. When R is less than 1, a negative deviation of  $\kappa$  from ideal mixture will be observed. As shown in Figure 5.13, the values of R were less than 1 at all mixing compositions for all model drugs, which suggested that the mixing of PS80 and OA had a negative effect on the solubilization of drugs. It is not possible to judge the global maximum negative deviation from ideality due to the lack of experimental data at PS80 molar fraction ranging from 0.1-0.4. Regardless of lack of data in the range 0.1-0.4, the rank-order of deviation ratios is progesterone > 17 $\beta$ -estradiol > nifedipine.



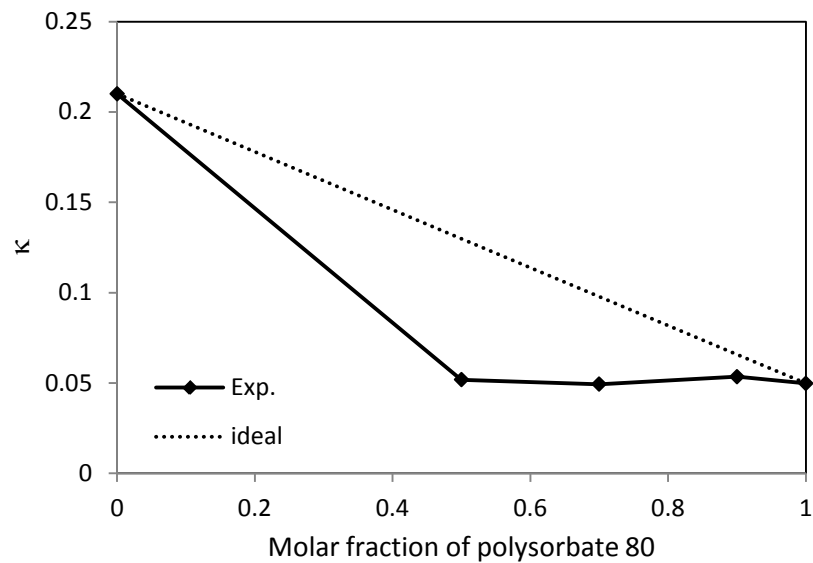


Figure 5.12a. Experimental and ideal molar solubilization capacities for progesterone in PS80/OA systems.

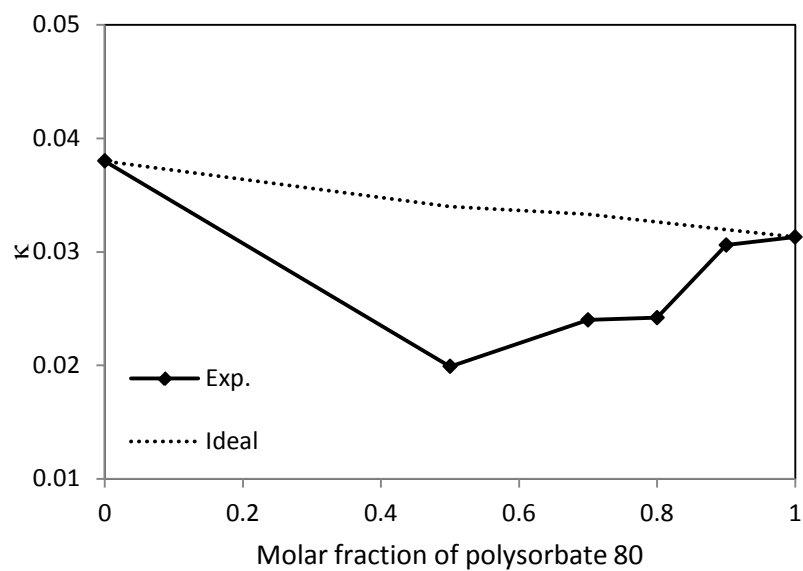


Figure 5.12b. Experimental and ideal molar solubilization capacities for 17β-estradiol in PS80/OA systems

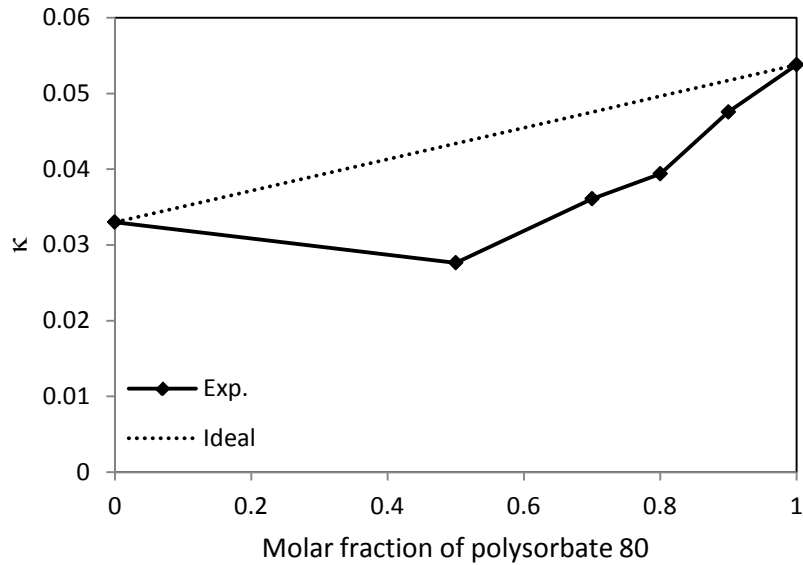


Figure 5.12c Experimental and ideal molar solubilization capacities for nifedipine in PS80/OA systems

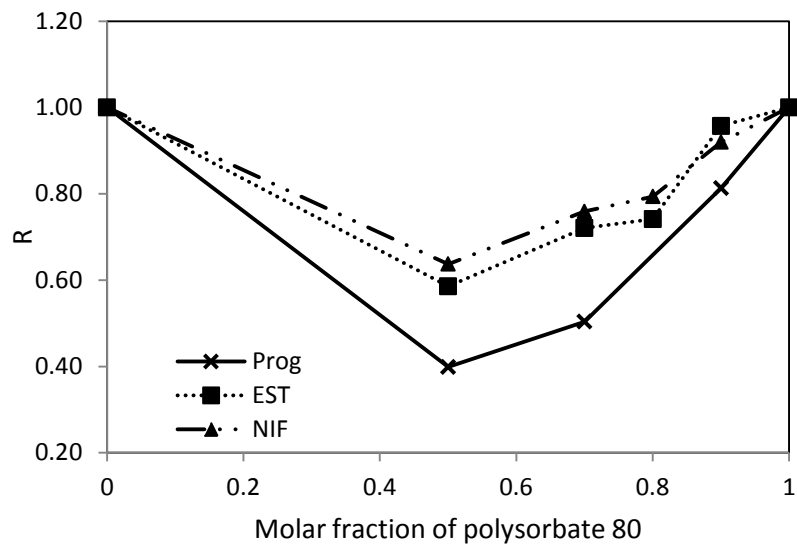


Figure 5.13 The deviation ratios for solubilization of progesterone (cross),  $17\beta$ -estradiol (square) and nifedipine (triangle) in PS80/OA systems

The molecular mechanism by which negative deviations from ideality resulted in Figures 5.12 and 5.13 are not known with any certainty, but several possibilities exist. The first factor is the compactness of the POE chains. In the absence of OA, the packing of the POE chains in the outer shell of PS80 are appreciably compressed to a smaller volume

than required for the undistorted coil (Schick, Eirich et al., 1962; Meguro, Akasu et al., 1976). Consequently, less water is trapped in the outer shell formed by the compact POE chains of PS80. Such compact POE chains, with less water, may provide a more receptive environment for solubilization of hydrophobic drug molecules. By increasing the molar fraction of OA in the mixed micelle, the packing of the POE chains in the outer shell becomes less compact due to the decrease in number of POE chains. Water content may increase in the formed mixed micelles due to a shallow domain in the POE chains and/or hydration at the ionized oleic acid head group. The higher water content forms a less favorable environment for solubilization of poorly-water soluble drug.

A second factor that may be responsible for negative deviation of ideality in PS80/OA mixed micelle solubilization is related to molecular packing. The increase in the molar fraction of anionic OA would be expected to increase the distance of separation of PS80 molecules and thereby reduce the steric self-repulsions of the PEO-containing headgroups. As a consequence, interactions between the OA and PS80 are expected to be less repulsive than PS80-PS80 the chains may be more densely packed.

It is likely that headgroup hydration and molecular packing exert significant effects, depending upon the expected loci of solubilization. According to logP and polar surface area values, progesterone is considered a non-polar compound, 17 $\beta$ -estradiol is semipolar and nifedipine is the most polar of the models. The strongly non-polar nature of progesterone suggests a locus of solubilization along the surfactant hydrocarbon chains, probably close to the headgroup. NMR investigation of drug locus in PS80 micelles suggests that 17 $\beta$ -estradiol and nifedipine are also solubilized at the interface with some greater fraction in the POE chains (Chapter 6). Therefore, the effect of compactness and hydration of PEO will modulate the solubilization of 17 $\beta$ -estradiol and nifedipine.

## 5.4.2. Micelle-water partition coefficient ( $K_{m/w}$ ) as a function of molar fraction of PS80 in the model systems

The molar solubilization capacity is a good tool to use to quantify the efficiency of surfactant to solubilize a solute, especially when comparing the capability of different surfactants to solubilize a single solute. However, solubilization capacity only reflects the solubility in micellar phase, but does not consider the solubility of solute in aqueous phase. An alternative approach to quantify the efficiency of solubilization is the micelle-water partition coefficient ( $K_m$ ) which represents the distribution of a solute between the micellar phase and aqueous phase. Therefore, the solubilization of different solutes can be compared based on thermodynamic grounds. The application of  $K_{m/w}$  requires that the micelle be considered a separate phase.

### 5.4.2.1. Experimental micelle-water partition coefficient

The micelle-water partition coefficients of drugs are calculated by Eq. (5.6) and listed in Table 5.7. In general, the tendency of a drug to partition into the micelle phase was greatest in PS80 micelles. The increase of the molar fraction of OA did not favor nifedipine or  $17\beta$ -estradiol partitioning into the micelle phase. The  $K_{m/w}$  for progesterone was insensitive to solution composition. In order to illustrate the relation between the partitioning behavior of a model drug and a molar fraction of PS80, the  $K_{m/w}$  is plotted versus molar fraction of PS80 (Figure 5.14).

Table 5.6 The micelle-water partition coefficients of progesterone,  $17\beta$ -estradiol and nifedipine in the model mixed micellar systems ( $\pm 95\%$  CI)

Molar fraction			
of PS80	Progesterone	Estradiol	Nifedipine
1	$(7.9 \pm 0.3) \times 10^4$	$(2.4 \pm 0.2) \times 10^5$	$(1.1 \pm 0.02) \times 10^5$
0.9	$(8.5 \pm 0.2) \times 10^4$	$(2.3 \pm 0.1) \times 10^5$	$(1.0 \pm 0.002) \times 10^5$
0.8		$(1.9 \pm 0.1) \times 10^5$	$(8.3 \pm 0.1) \times 10^4$
0.7	$(7.8 \pm 0.2) \times 10^4$	$(1.8 \pm 0.1) \times 10^5$	$(7.7 \pm 0.1) \times 10^4$
0.5	$(8.2 \pm 0.3) \times 10^4$	$(1.5 \pm 0.1) \times 10^5$	$(5.9 \pm 0.2) \times 10^4$

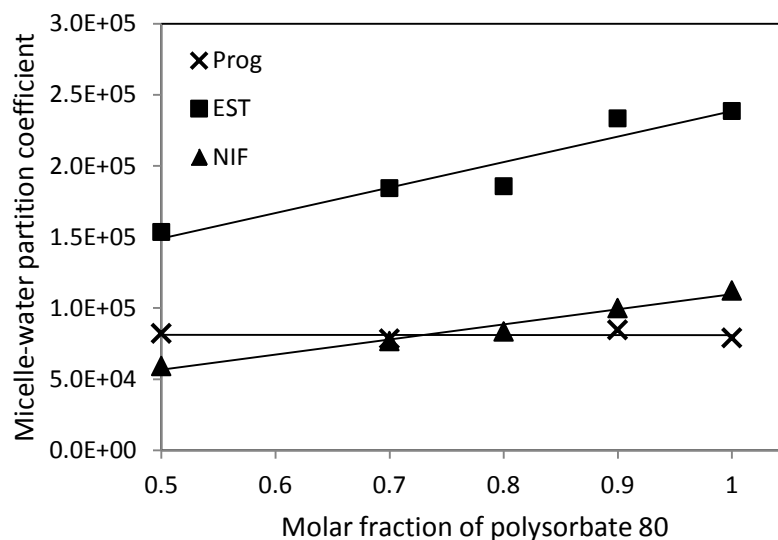


Figure 5.14 Micelle–water partition coefficients of progesterone (cross,  $R^2 = 0.0016$ ),  $17\beta$ -estradiol (square,  $R^2 = 0.9098$ ) and nifedipine (triangle,  $R^2 = 0.9757$ ) as a function of molar fraction of PS80 in the model systems at  $37^\circ\text{C}$

Generally, a large octanol-water partition coefficient ( $K_{o/w}$ ) of drug implies greater hydrophobic nature. Typically, increasing the hydrophobicity of a drug increases the driving force for micelle solubilization. A good linear relationship between  $\log K_{o/w}$  values of a series of drugs and  $\log K_{m/w}$  values in PS80 micelles has been observed (Alvarez-Núñez and Yalkowsky, 2000). The  $\log K_{m/w}$  values for each drug in mixed surfactant at PS80 molar fractions of 1, 0.9, 0.7 and 0.5 are plotted against  $\log K_{o/w}$  (Figure 5.15). Linearity was not observed. According to the rank order of  $\log K_{o/w}$ , the values of  $\log K_{w/m}$  of nifedipine at all the composition solutions were higher than expected. The higher than expected values of  $\log K_{m/w}$  might arise in situations in which solute is distributed between two different sites in the micelle, one hydrophobic (micelle core) and the other less so (micelle palisades or PEO corona). This subject of drug localization in a PS80 micelle will be explored in detail in Chapter 6.

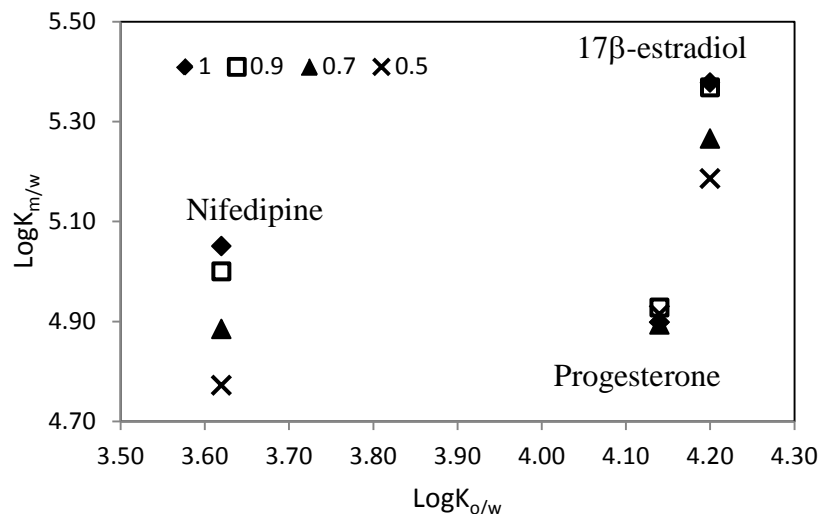


Figure 5.15 The correlation of  $\log K_{o/w}$  and  $\log K_{m/w}$  at molar fractions of PS80 of 1 (diamond), 0.9 (square), 0.7 (triangle) and 0.5 (cross)

#### 5.4.2.2. Fitting of the Treiner model of micelle-water partition coefficient to data for the model solutes

Treiner et al. suggested that the partition coefficient of a neutral organic molecule in a mixed binary micellar system is related to the component simple micellar solutions as described in Eq. (5.17) (Treiner, Vaution et al., 1985; Treiner, Khodja et al., 1987; Treiner, Nortz et al., 1988; Treiner, Nortz et al., 1990).

$$\ln K_{mic(1,2)} = X_1 \ln K_{mic1} + (1 - X_1) \ln K_{mic2} + BX_1(1 - X_1) \quad (5.17)$$

where  $K_{mic(1,2)}$ ,  $K_{mic1}$ , and  $K_{mic2}$  are micelle-water partition coefficients in mixed and simple micelles of 1 and 2, respectively;  $X_1$  is the molar fraction of surfactant 1 in mixed micelle;  $B$  is an empirical parameter incorporating surfactant-solute and surfactant-surfactant interactions. When  $B$  equals 0, partitioning of the drug upon mixing of two surfactants is ideal. When  $B$  is greater than 0, the mixing of two surfactants leads to greater solubilization efficiency due to favorable interactions. When  $B$  is less than 0, the mixing of two surfactants leads to decreased solubilization efficiency due to unfavorable interactions.

Eq (5.17) was fitted to the experimental values of  $K_{m/w}$  listed in Table 5.6. The results are presented in Figures 5.16a, 5.16b and 5.16c. The solid line in these figures represents the relationship of  $K_{m/w}$  values to the molar fraction of PS80 according to Eq. (5.17) with the fitted B parameters. The equation fits the experiment results reasonably well. In tune with the deviation ratios, the addition of OA to the PS80 micelle solution led to a negative effect on the solubilization of each drugs suggested by a negative deviation from ideal mixing. The fitted B coefficients were  $-2.08 \pm 1.01$  for progesterone,  $-1.76 \pm 0.65$  for  $17\beta$ -estradiol and  $-1.35 \pm 0.35$  for nifedipine, respectively. The negative values of B indicated that the formation of mixed micelle of PS80 and OA was not favorable to the micellar solubilization of all poorly-water soluble drugs tested. Other studies of mixtures of neutral and charged surfactants have also shown decreases in solubilization of neutral solutes. For example, the B parameter was found to be -2.1 in solubilization of heptabarbital in the mixture of  $C_{12}Na$  and  $C_{12}E_{23}$ . In mixture of  $C_{12}Na + C_{12}Cl$  where the interactions between surfactants are strong, the B was fitted to be -8.8 by Eq. (5.17) (Treiner, Nortz et al., 1990). As discussed in the variations of deviation ratios for poorly soluble drugs in model systems, the formation of mixed micelles is favorable when the interactions between surfactants are stronger than in simple micelles. Consequently, the partitioning of drug to the micellar phase is possibly impeded (negative value for B) due to the more compact packing of surfactants in mixed micelles. The extent of such depression on solubilization would then be determined by the locus of the solubilized drug in micelles.

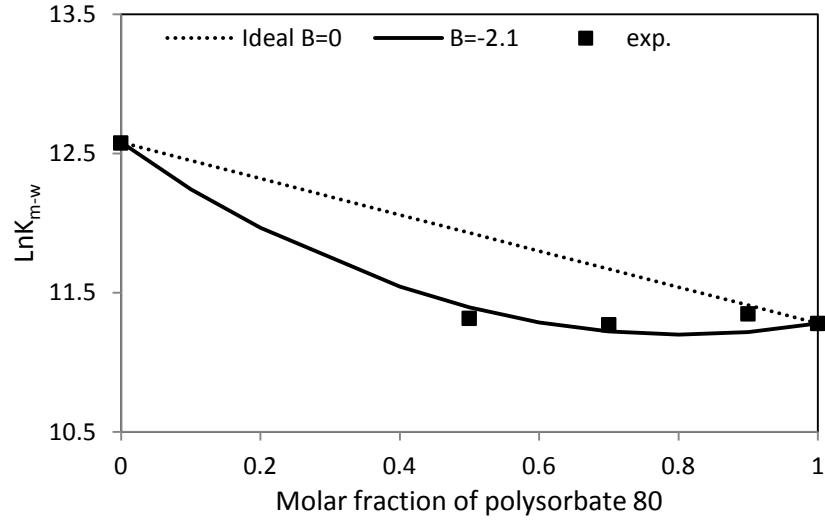


Figure 5.16a Micelle-water partition coefficients ( $K_{m/w}$ ) for progesterone in a mixed micelles of PS80 and OA in SIF buffer. The solid line represents the calculated  $K_{m/w}$  values fitted using Eq. (5.17).

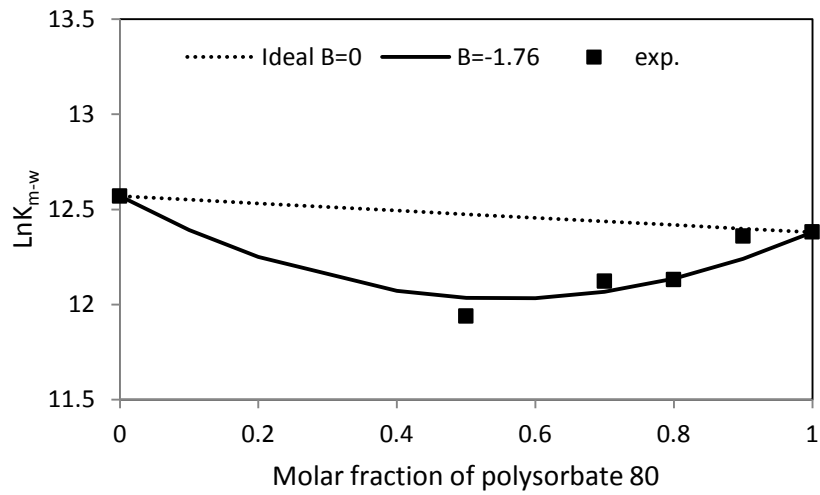


Figure 5.16b Micelle-water partition coefficients ( $K_{m/w}$ ) for  $17\beta$ -estradiol in a mixed micelles of PS80 and OA in SIF buffer. The solid line represents the calculated  $K_{m/w}$  values fitted using Eq. (5.17).



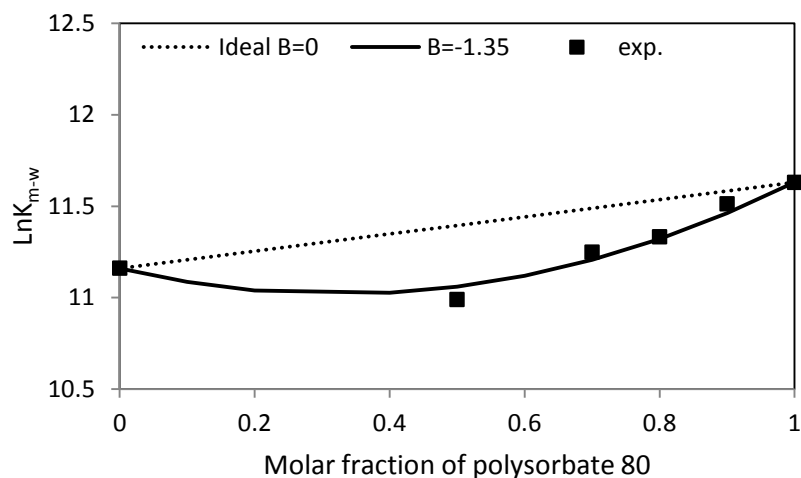


Figure 5.16c Micelle-water partition coefficients ( $K_{m/w}$ ) for nifedipine in a mixed micelle of PS80 and OA in SIF buffer. The solid line represents the calculated  $K_{m/w}$  values fitted using Eq. (5.17).

Table 5.7 Fitting parameters for progesterone,  $17\beta$ -estradiol and nifedipine

	Progesterone		$17\beta$ -estradiol		Nifedipine	
	$K_2$	B	$K_2$	B	$K_2$	B
Fitted value	12.56	-2.08	12.55	-1.76	11.15	-1.35
95% CI	0.31	1.01	0.23	0.65	0.13	0.35
$R^2$	0.99		0.99		0.99	

#### 5.4.3. Predicted total drug solubility in SIF solution as function a time

At several points in this study the importance of the extent of supersaturation on the mechanism of action of oral LBDDSs has been stressed. The extent of supersaturation has been defined in this work according to Eq. (4.2). In the current chapter, work has focused on the denominator of Eq. (4.2), namely, equilibrium solubility, as a function of micelle composition. In the current section, the application of  $K_{m/w}$  for the prediction of drug solubility in a blank digested formulation is explored. The predicted total equilibrium solubility of a drug in varying ratios of OA/PS80 in SIF was calculated by Eq. (5.9) and Eq. (5.17) and presented as a function of lipolysis of time in a blank digested

formulation. All calculated values are compared with the experimental equilibrium solubility in the digested formulation (listed in Section 4.4.3). The results are presented in Figures 5.17a, 5.17b and 5.17c. In statistics, the residual sum of squares (RSS) is a measure of the discrepancy between the experimental data and an estimation model. The smaller the RSS, the better the fit of the model to the data. The values of RSS between the calculated equilibrium solubility in model solutions and equilibrium solubility in actual lipolytic products are 0.27, 0.39 and 0.50 for nifedipine, 17 $\beta$ -estradiol and progesterone, respectively. The calculated total equilibrium solubility of nifedipine in the series of model mixed micellar solutions appears to be closest to the equilibrium solubility of nifedipine in the dispersed PS80 under simulated intestinal conditions. The largest discrepancy between the values in the digested blank formulation and calculated values was observed for progesterone.

The exact reason why the OA/PS80 model systems show limited success in predicting the equilibrium solubility of the three drugs in lipolytic products is not known. It should be noted here that the OA/PS80 systems include NaC/PC from the SIFs buffer. The concentration of NaC/PC remains constant in all the molar ratios of PS80 to OA. The lipolytic products of PC, lysoPC and fatty acid, (Section 3.4.2.1) are not included in the OA/PS80 model system. This means that the lipid aggregates in the model systems may not exactly reflect those appearing during *in vitro* lipolysis. The effect of NaC/PC on the solubilization was evident by comparing the calculated total drug concentration in a series of mixed micelles of PS80 and OA in trisma buffer (no NaC/PC) with the results obtained from a series of mixed micelles of PS80 and OA in SIF buffer. As shown in Figure 5.17c, the calculated total nifedipine concentration in a series of mixed micelles of PS80 and OA in trisma buffer (no NaC/PC) is higher than that calculated in a series of mixed micelles of PS80 and OA in SIF buffer solution (containing NaC/PC). On the other hand, the presence of NaC/PC has little effect on the solubilization of 17 $\beta$ -estradiol (Figure 5.17b). If the influence of NaC/PC and all lipolytic products on the solubilization is included in the OA/PC model systems, the accuracy of fitting of Eq. (5.17) might be improved.

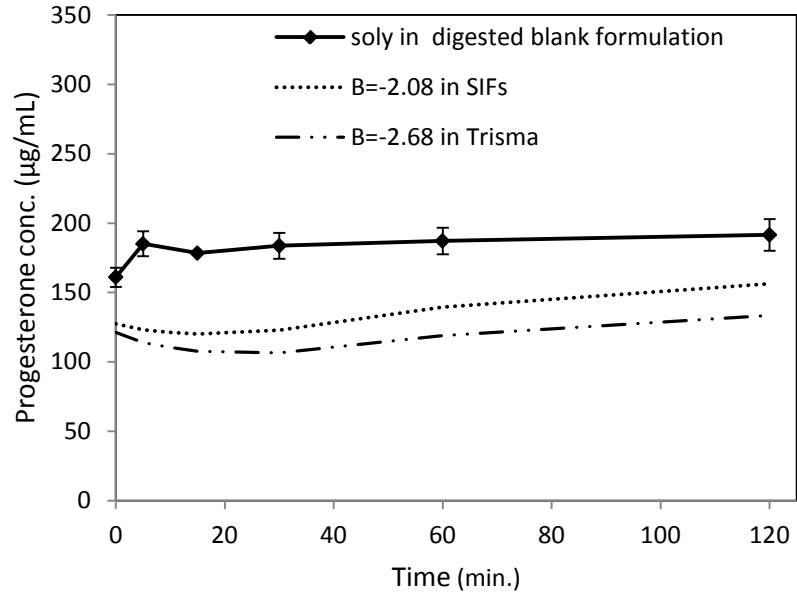


Figure 5.17a Comparison of the experimental equilibrium concentration of progesterone in a digested blank formulation (solid line), calculated progesterone concentration in model systems composed of PS80 and OA in SIF and  $B = -2.08$  (dotted line) and calculated progesterone concentration in model systems composed of PS80 and OA in trisma buffer and  $B = -2.68$  (dashed line)

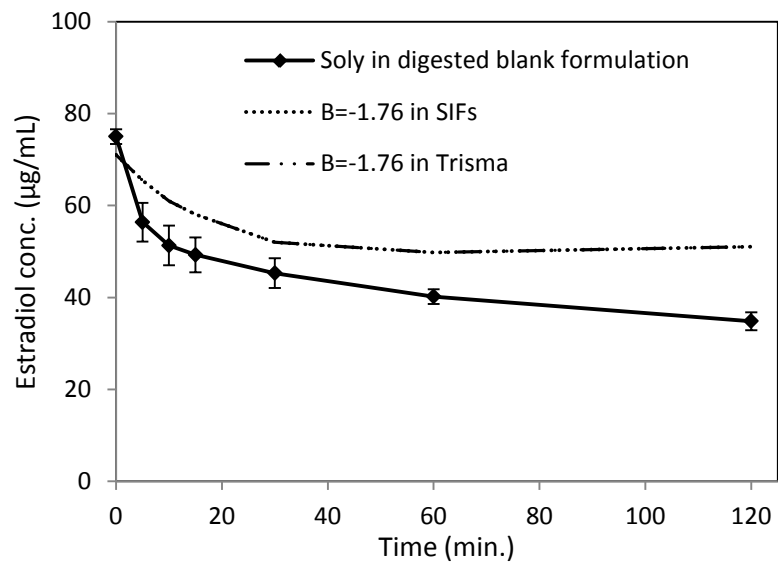


Figure 5.17b Comparison of the experimental equilibrium  $17\beta$ -estradiol concentration in a digested blank formulation (solid line), calculated  $17\beta$ -estradiol concentration in model system composed of PS80 and OA in SIF at a different molar ratios and  $B = -1.76$  (dotted line) and calculated  $17\beta$ -estradiol concentration in model systems composed of PS80 and OA in trisma buffer and  $B = -1.76$  (long dashed line)

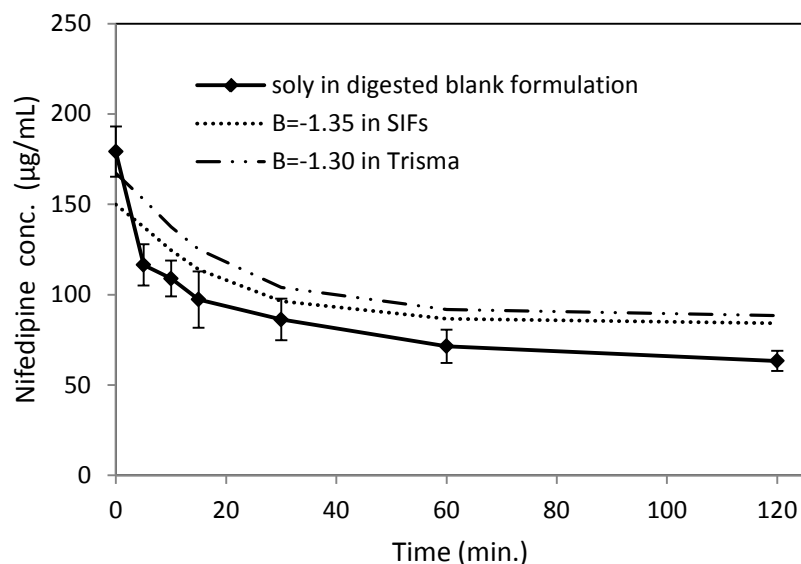


Figure 5.17c Comparison of the experimental equilibrium nifedipine concentration in a digested blank formulation (solid line), calculated nifedipine concentration in model system composed of PS80 and OA in SIF and B= -1.35 (dotted line) and calculated nifedipine concentration in model systems composed of PS80 and OA in trisma buffer and B=-1.30 (dashed line)

## 5.5. Conclusion

The solubilization of model drugs in a series of model mixed micelles of PS80 with OA is drug-dependent. The molar solubilization capacity of model mixed micelles composed of PS80 and OA from molar ratios of 9/1 to 1/1 decreased for  $17\beta$ -estradiol and nifedipine while remaining constant for progesterone. The negative deviation from ideal mixing indicated that the addition of OA to the PS80 micelles led to less solubilization of model poorly-water soluble drugs. The equilibrium solubilization of nifedipine in PS80 under simulated intestinal conditions was predicted most successfully by fitted micelle-water partition coefficients of the drug in the series of model mixed micelles. However, model mixed micellar solutions are far less successful in predicting the solubilization of estradiol and progesterone. The results demonstrated that it may be possible to correlate the equilibrium solubilization of nifedipine in PS80 under simulated intestinal conditions with the equilibrium solubility of drug in these series model mixed micellar solutions by accounting for the solubilization of some of the lipid aggregates generated during lipolysis.

## Chapter 6

### Characterization of Model Mixed Micellar Systems and Studies on Inter-molecular Interactions between Micelles and Drugs

#### 6.1. Summary

In this chapter, the model mixed micellar systems composed of selected lipolytic products were characterized in terms of the ionization state of OA in mixed micelles, the size of mixed micelles, and population of aggregates. The values of pKa of OA in mixed micelles were determined by potentiometric titration in a PS80 micelle solution. The size and population of model mixed micelles were determined by the pulsed-gradient spin-echo NMR (PGSE-NMR) and dynamic light scattering (DLS) methods. The results showed that the ionization of OA in mixed micelles and the size of mixed micelles were independent of composition. In the absence of bile salt/phospholipids, only one type of mixed micelle PS80/OA was found by both PGSE-NMR and DLS. In the presence of bile salt/phospholipids, model mixed micellar systems were characterized by DLS. Peak overlap prohibited the study of PS80/OA in the presence of bile salts/phospholipid by NMR. From the DLS results, it was concluded that one population of mixed micelles exists in mixtures of PS80/OA/bile salt/phospholipids.

NMR methods were applied to the study of solute localization in PS80 micelles. Proton chemical shifts of PS80 were monitored by <sup>1</sup>HNMR in the presence of model poorly-water soluble drug to infer the possible inter-molecular interactions between micelles and drugs. Prominent changes of chemical shifts on surfactant protons located at the interface of hydrocarbon core and hydrophilic corona formed by polyoxyethylene chain suggested that 17-β estradiol and nifedipine were solubilized in this region. Strong interactions between nifedipine and PS80 were further evident by Fourier transform infrared spectroscopy (FTIR). Finally, the loci of drug solubilized in the micelles were proposed.

## 6.2. Introduction

It has been established that various structures, such as liquid crystal, lamellar phase, unilamellar vesicles and mixed micelles, are formed during the *in vivo* digestion of LBDDSs (Kossena, Boyd et al., 2003; Kossena, Charman et al., 2004; Kossena, Charman et al., 2005; Fatouros, Bergenstahl et al., 2007). Formation of each type of aggregates is dependent upon the nature of the lipids used in the delivery system. The capability of aggregates to solubilizing poorly-water soluble drug is not only determined by the nature of the aggregates, but also by nature of the drug. Compared to numerous solubilization studies in simple bile salt micelles and bile salt/phospholipids mixed micelles (Wiedmann and Kamel, 2002), little information is available on the solubilization of drug in the formed various aggregates during the lipolysis of a LBDDS.

In Chapter 5, model mixed micellar systems containing selected lipolytic products that mimic the progress of formation of aggregates were developed. By following the production of fatty acid, the molar ratio of PS80 to OA can be calculated as a function of time (Appendix 2). A series of solutions with physical stable compositions were prepared to represent the compositions at the times of sampling during the *in vitro* lipolysis of a formulation. Subsequently, the solubilization capacity of model systems for progesterone, 17 $\beta$ -estradiol and nifedipine was studied. The rationale behind this approach is that the model mixed micellar system allows examination of the solubilization mechanism of a system with physical stable compositions. The nature of these aggregates will be evaluated by PGSE-NMR and DLS methods in this chapter. To further understand the solubilization behavior of drugs in model systems and eventually *in vitro* lipolysis of PS80, the locus of the drug solubilized in the micelles will be explored by <sup>1</sup>HNMR and FTIR.

## 6.3. Materials and methods

### 6.3.1. Materials

Progesterone (purity  $\geq 99\%$ ), nifedipine (purity  $\geq 98\%$ ), 17 $\beta$ -estradiol (purity  $\geq 98\%$ ), 1,2-diacyl-sn-glycero-3-phosphocholine (type XVI-E) from egg yolk (PC), Trisma® maleate, sodium cholate hydrate (NaC, purity  $\geq 99\%$ ), deuterium oxide (99.98 atom %  $\pm 0.01$  atom % D) and sodium deuterioxide (40wt. % in D<sub>2</sub>O, 99% atom% D) were purchased from Sigma-Aldrich (St. Louis, MO, USA). Polysorbate 80 (PS80) was a generous gift from

Croda Inc. (Edison, NJ, USA). Oleic acid (OA, purity  $\geq 97\%$ ) was purchased from Fisher Scientific (Pittsburgh, PA, USA). All chemicals were used as received. Water for buffer solutions was from a Milli-Q water purification system. Hydrophilic PTFE filters (13mm, 0.2  $\mu\text{m}$  pore size) were purchased from Advantec MFS Inc. (Japan).

### **6.3.2. Determination of the apparent pKa of micellar oleic acid**

#### **6.3.2.1. pH probe characterization**

Potentiometric titration has been used in the literature to determine the apparent pKa of weak acids in micellar solutions (Feinstein and Rosano, 1969; Tanaka, Nakashima et al., 1995; da Silva, Bogren et al., 2002; Kanicky and Shah, 2003). However, during the studies outlined below, it was observed that the glass electrode exhibited a sluggish response in micellar solution. Concerns were raised about the accuracy of the pH measured by this approach. In order to validate the accuracy and response, the pH electrode was characterized with respect to response curve, response time and drift. Figure 6.1 shows the response curves of a glass electrode in pure water, 0.15M NaCl solution, and aqueous solutions of PS80 as a function of surfactant concentration. The curves were obtained by measuring the electrode potential upon the addition of small amounts of 0.1N HCl to aqueous solutions. According to the Nernst equation, the ideal slope of electrical potential-proton concentration curve is 61.6mV at 37°C. Except in the case of 30 mM PS80, the linearity of the response curve in the presence of PS80 was excellent; slopes of the curve in the presence of PS80 are comparable with the values measured in the absence of surfactants and the theoretical values. The results indicated the glass electrode could follow the pH change accurately up to surfactant concentrations of 10 mM. The accuracy and precision of pH measurements in the micellar solution were further demonstrated by comparing potentials of a 10 mM phosphate buffer in the absence and presence of 10 mM PS80 at pH 4.6 and 7.5 at 37°C. The measured potentials of the phosphate buffer at pH4.6 in the absence and presence of PS80 are  $132.5 \pm 0.3$  mV and  $134.2 \pm 0.7$  mV, respectively. The measured potentials of the phosphate buffer at pH7.5 in the absence and presence of PS80 are  $-23.5 \pm 0.3$  mV and  $-23.1 \pm 0.1$  mV, respectively.



The glass electrode to pH change was further characterized by the response time and drift. Response time was the duration necessary for the electrode to detect a pH change upon rapidly adding 30  $\mu\text{L}$  of 0.9M HCl to 30 mL of a selected solution with an initial HCl concentration of 0.1 mM. The results are shown in Table 6.1. The response time in the PS80 micellar solution was comparable to the value reported by Gerakis et al., (Gerakis, Koupparis et al., 1993). The pH drift rate in the 10 mM tris maleate buffer in the absence and presence of 10 mM PS80 were measured. Compared to the buffer solution without surfactant, the drift rate of the glass electrode was higher in the micellar solution (Table 6.2).

In summary, the glass electrode was suitable for pH titration of PS80 in spite of a relatively sluggish response. Thus, in the titration of OA in a mixed micellar solution, longer equilibration time was employed. The pH electrode was calibrated by standard solutions at pH 2, 7 and 10 in order to cover the titration range used in the experiments.

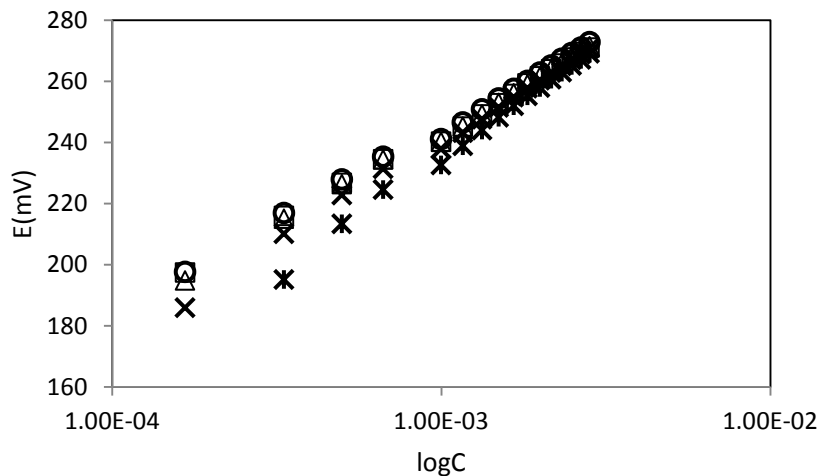


Figure 6.1 Response curve of an electrode in pure water (open circle,  $E= 425.18+60.19\log C$ ,  $R=0.996$ ), 0.15M NaCl solution (open square,  $E= 421.29+60.29\log C$ ,  $R=0.996$ ), 1 mM PS80 (open triangle,  $E= 426.15+61.03\log C$ ,  $R=0.996$ ), 10 mM PS80 (cross,  $E= 440.67+64.78\log C$ ,  $R=0.996$ ) and 30 mM PS80 (star,  $E= 466.15+77.16\log C$ ,  $R=0.996$ ) in 0.15M NaCl solution at 37°C

Table 6.1 Response time of a pH electrode and  $\Delta E$  at infinite time in pure water and an aqueous solution of PS80 at different concentrations at 37°C

Solutions	Time (s)	$\Delta E$ at infinite time (mV)
H <sub>2</sub> O w/NaCl	11±1	60.3±1.1
10 mM PS80 w/NaCl	10±1	62.1±0.5
30 mM PS80 w/NaCl	11±2	81.8±2.7

Table 6.2 The drift of glass electrode in 5 min. at 37°C

	Initial E(mV)	Final E(mV)	Drift(mV/5 min)
10 mM Tris buffer	-29.4	-28.5	-0.18
10 mM PS80 in 10 mM Tris buffer	-26.8	-24.7	-0.42

### 6.3.2.2. Titration of oleic acid in mixed micelles

A total 10 mM of PS80 and OA at a molar ratio 9-to-1 or 1-to-1 was prepared in 0.15M NaCl. The solution was stirred overnight to ensure the formation of mixed micelles. A 30 mL portion of this solution was titrated manually with 0.1N HCl or 0.25N NaOH at 37 ±1°C. At first, the pH of the solution was adjusted to about 10.3 by 1N NaOH and then titrated by 0.1N HCl down to ~3.2. In each ratio, the experiments were repeated three times. The apparent pKa of each solution was obtained by fitting the titration data with the Eq. (6.1)

$$[\text{H}^+] + \frac{B_0 V_b}{(V_0 + V_a + V_b)} = \frac{K_w}{[\text{H}^+]} + \frac{A_0 V_a}{(V_0 + V_a + V_b)} + \frac{K_a C_0 V_0}{([\text{H}^+] + K_a)(V_0 + V_a + V_b)} \quad (6.1)$$

where  $K_a$  is the apparent dissociation constant of OA in the micellar solution;  $B_0$  and  $A_0$  are molar concentrations of NaOH and HCl, respectively, in titrant solutions;  $V_0$ ,  $V_a$  and  $V_b$  are the initial sample volumes, volumes of HCl and NaOH titrant added,

respectively;  $K_w$  is the ion product of water ( $3.14 \times 10^{-14}$  at  $37^\circ\text{C}$ ) and  $[\text{H}^+]$  is the molar concentration of the proton which is calculated from the measured pH.

### 6.3.3. NMR sample preparation

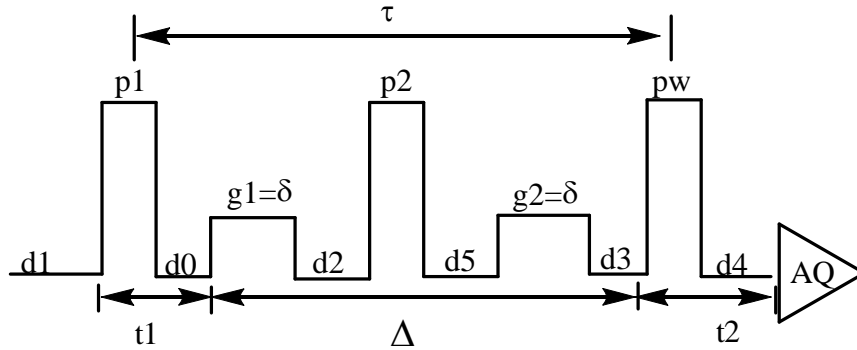
The micellar solutions composed of PS80 and OA at molar ratios 9/1, 8/2 and 6/4 were prepared as outlined in Section 5.3.3. Deuterium oxide and sodium deuterioxide were used in forming the solutions. Instead of a 50 mM tris maleate buffer, a 50 mM phosphate buffer in  $\text{D}_2\text{O}$  was prepared to avoid the interference of the characteristic chemical shift of polyoxylethyene (POE) protons at  $\sim 3.7$  ppm with tris maleate. In addition, bile salt and phospholipids were not included in the buffer solution as in simulated fasted-state digestion buffer (SIF buffer) because the chemical shifts of NaC and PC overlapped with the hydrocarbon chain of surfactant in the range of 0.9ppm to 4ppm.

Exact weighed portions of PS80 and OA at different molar ratio were dissolved in phosphate buffer. TSP- $\text{d}_4$  (3-(Trimethylsilyl) propionic - 2, 2, 3, 3- $\text{d}_4$  acid sodium salt) at a concentration of 0.1% (w/v) was chosen as the internal standard. All samples were rotated at room temperature overnight to ensure the formation of mixed micelles. The ionization constant in  $\text{H}_2\text{O}$  and  $\text{D}_2\text{O}$  has a relationship of  $\text{pD} = \text{pH} + 0.44$  (Krezel and Bal, 2004). The pH was adjusted to  $7.94 \pm 0.05$  at  $37^\circ\text{C}$  accordingly, before and after equilibration.

### 6.3.4. Pulsed-gradient spin-echo nuclear magnetic resonance (PGSE-NMR)

Diffusion coefficient measurements were performed on a Varian 400MHz spectrometer at  $37 \pm 0.1^\circ\text{C}$  with gradient amplifier unit and a Highland, Performa II probe equipped with a z-gradient coil, providing a z-gradient strength ( $g$ ). The self diffusion coefficients were determined using a pulsed-gradient stimulated-spin echo sequence (Scheme 6.1).  $\Delta$  is the self diffusion time between two gradients in the pulse sequence. The length of the gradient pulse ( $g_1$  and  $g_2$ ) is  $\delta$ . Typically, values of  $\Delta$  and  $\delta$  for all experiments were 100ms and 7ms, respectively. Experiments were carried out by varying  $g$  from 2 to 38  $\text{Gcm}^{-1}$  in 15 steps and keeping all other timing parameters constant. The self-diffusion coefficient ( $D$ ) was calculated by the diffusion software package incorporated in the instrument. Thin-walled (3mm) glass NMR tubes were used to reduce the possibility of

convection causing the peak distortion at high temperature. The sample volume was fixed at 0.2 mL for all samples.



Scheme 6.1 Pulse sequence for pulsed-gradient stimulated spin-echo NMR

In the stimulated-echo sequence, the variables  $\tau$ ,  $\Delta$ ,  $t_1$  and  $t_2$  are calculated from the pulse sequence variable as follows:

$$\tau = (p1)/2 + d0 + g1 + d2 + pw/2$$

$$\Delta = g1 + d2 + p2 + d5 + g2 + pw + d3$$

$$t1 = p1/2 + d0$$

$$t2 = d4$$

To obtain absolute values for the self-diffusion coefficient ( $D$ ), the field gradient strength was calibrated from measurements on pure water as a reference at  $37 \pm 0.1^\circ\text{C}$ . The diffusion coefficient measured on the reference  $\text{H}_2\text{O}$  sample is exclusively for  $\text{H}_2\text{O}$ , and multiple species in the deuterium oxide such as  $\text{H}_2\text{O}$ ,  $\text{D}_2\text{O}$  and  $\text{HDO}$  are avoided. Spin-lattice relaxation time ( $T_1$ ) is considered as a standard for the choice of  $d_1$  in the diffusion coefficient measurement. Generally, the  $d_1$  should be 5 times the value of  $T_1$  to insure the signal recovers 95% of its initial value after being flipped into the magnetic transverse plane. The measured self-diffusion coefficient of pure water during the NMR experiment was  $3.02 \times 10^{-5} \text{ cm}^2/\text{s}$  with an experimental error less than 1%. The results were consistent with the literature value of  $3.037 \times 10^{-5}$  at  $37^\circ\text{C}$  (Holz, Heil et al., 2000). The calibration was carried out before and after each experimental period.

All chemical shifts were referred to the 0.1% (w/v) internal standard TSP-d<sub>4</sub> (3-(Trimethylsilyl) propionic - 2, 2, 3, 3-d<sub>4</sub> acid sodium salt) at zero. The assignments of chemical shifts of PS80 and a mixture of PS80 and oleic acid (molar ratio = 1:1) in buffer are given in Figures 6.2 and 6.3. As shown in these figures, the highest intensity peak at 3.7ppm was identified as a characteristic chemical shift of ethylene oxide protons. It is important to note that this peak is intense and relatively broad due to overlapping of all branches of polyoxyethylene protons on PS80 and possible contamination by free polyoxyethylene. Similarly, the peaks at 1.296ppm and 1.327ppm, which represented ethylene proton on the hydrocarbon chain, exhibited poor resolution.

Theoretically, the diffusion coefficient of a molecule may be determined by a resolved peak with a defined chemical shift. As recommended, the signal of interest was attenuated by 90% within the selected gradient strength. Consequently, the signal-to-noise ratio is significantly increased by the high gradient strength, and accuracy of measured diffusion coefficient will be affected. Thus, the attenuation of peak from polyoxyethylene protons was chosen to fit the Stejskal-Tanner equation because of high intensity compared to all other peaks. The representative Stejskal-Tanner exponential plot and signal attenuation is shown in Figure 6.4. Selection of polyoxyethylene protons also alleviated difficulties in determination of diffusion coefficient of mixed micelles because of the identity of a hydrocarbon chain of PS80 and OA resulting in overlapping chemical shifts. The only exception is the  $\alpha$ -proton on the OA. Conjugation of fatty acid to the polysorbitan resulted in a downshift of an  $\alpha$ -proton from 2.2ppm to 2.3ppm. In a micellar solution, the observed chemical shift is the population-averaged value of a monomer and micelles due to the fast exchange. The very low CMC of PS80 results in over 99% of molecules in micelles. The chemical shift of a monomer is considered negligible.

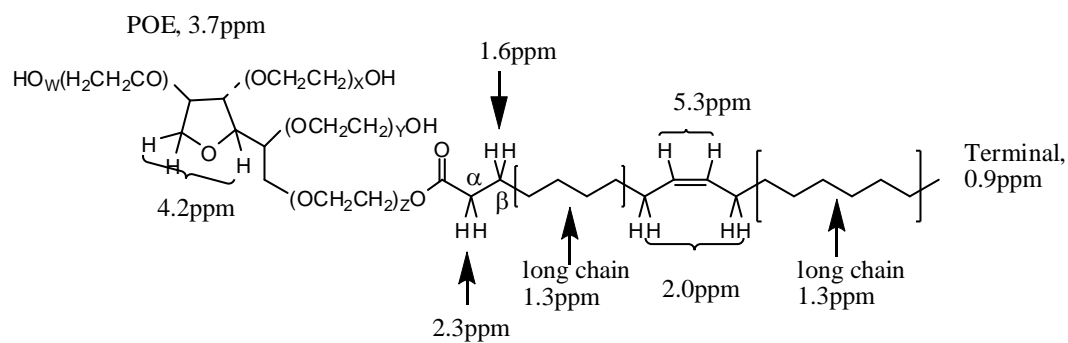
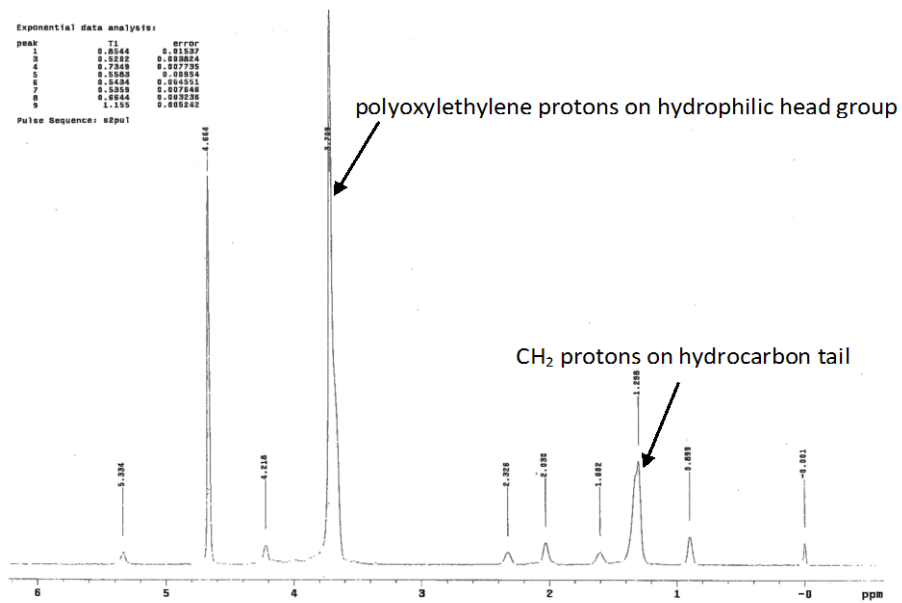


Figure 6.2 <sup>1</sup>H NMR spectrum of PS80 in D<sub>2</sub>O buffer solution

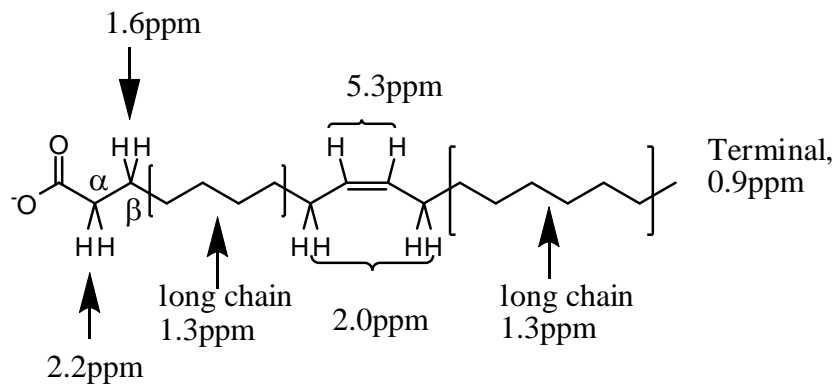
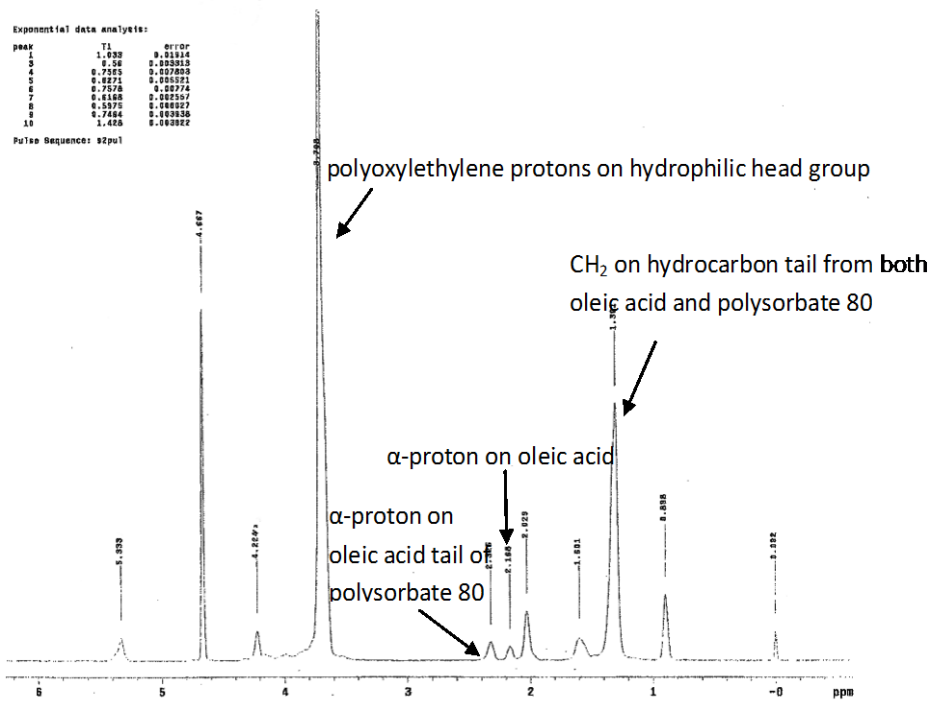


Figure 6.3  $^1\text{H}$ NMR spectrum of PS80/OA (1/1) in  $\text{D}_2\text{O}$  buffer solution

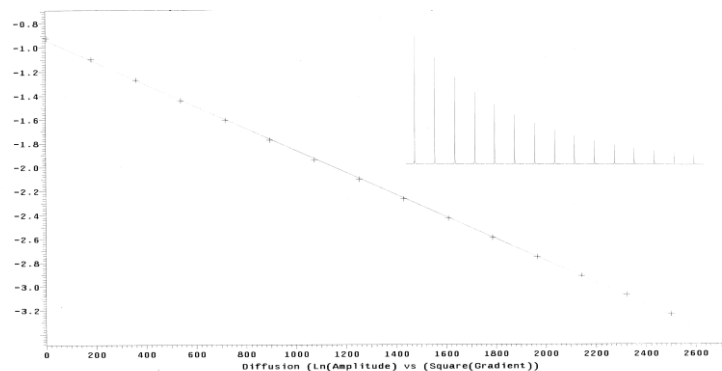
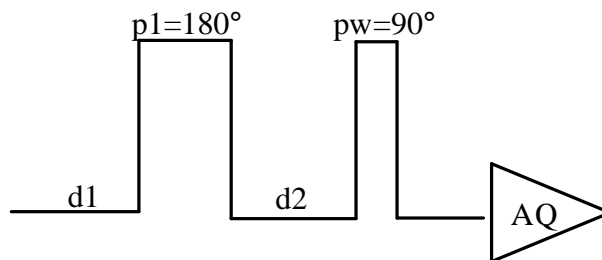


Figure 6.4 The Stejskal-Tanner exponential plot. (The insert is attenuated signals from polyoxyethylene protons)

### 6.3.5. Spin-lattice relaxation time (T1) measurement

T1 can be measured by various techniques such as inversion recovery, progressive saturation. In the present study T1 served as a means of estimating the require d1 in the pulse sequence for diffusivity determination. T1 was determined by the inversion recovery method at 400MHz on a Varian spectrometer. The pulse sequence of inversion recovery is shown in Scheme 6.2. This method is a non-selective experiment in which all peaks are inverted and measured simultaneously. The sequence is repeated for a series of arrayed d2. The intensity of peaks in a series of spectra is plotted against arrayed d2 to give the T1. Proton chemical shift was referred to the TSP-d<sub>4</sub> assigned as zero.





Scheme 6.2 Pulse sequence of inversion recovery for measurement of T1

A PS80 micelle solution and PS80/OA (1:1) mixed micelle solution at total concentration of 30 mM in deuterium phosphate buffer (pD  $7.9 \pm 0.05$ ) were prepared as in Section 6.3.3. To 1 mL of each solution was added an excess amount of progesterone and nifedipine. Nifedipine samples were protected from light. All samples were rotated in  $25^\circ\text{C}$  for a week. Before performing the NMR experiment, all samples were filtered through a  $0.2\ \mu\text{m}$  PTFE filter. The volume of 0.5 mL of the sample was loaded in a 5mm NMR tube. Experiments were carried out at  $37 \pm 0.1^\circ\text{C}$ .

### 6.3.6. Measurement of chemical shifts of PS80 in the presence of model drugs

The change of proton chemical shifts on PS80 in the presence of nifedipine and  $17\beta$ -estradiol was measured by  $^1\text{H}$ NMR on a Varian 400 MHz spectrometer at  $37 \pm 0.1^\circ\text{C}$ . All solutions were prepared as in Section 6.3.3. Spectra were recorded for 30 mM of PS80 solution and 30 mM of PS80 solubilized with the drug. The difference between chemical shifts in the sample without the drug and the sample saturated with the drug are attributed to the presence of the drug.

The drug-saturated sample was prepared by adding excess amounts of model drugs to 30 mM of PS80 and rotated four days at room temperature. After equilibrium, the sample was filtered through a  $0.2\ \mu\text{m}$  PTFE membrane, and 0.5 mL of the filtrated was transferred to a 5mm NMR tube. All chemical shifts are referred to TSP (3-(Trimethylsilyl) propionic-2,2,3,3-d<sub>4</sub> acid sodium salt) at 0 ppm. The concentration of TSP is 0.1 % w/v.

### 6.3.7. Dynamic light scattering (DLS)

The particle size was measured by the dynamic light scattering method (Delsa<sup>TM</sup>Nano C particle analyzer, Beckman Coulter®, Inc). Solutions composed of PS80 and OA at

different molar ratios in SIF buffer were prepared and equilibrated in  $37\pm 1$  °C water bath overnight. The pH of all solutions was adjusted to  $7.5\pm 0.02$  at  $37^\circ\text{C}$ . The temperature of scattering cells was controlled at  $37\pm 0.1^\circ\text{C}$ . The PMMA disposable cuvette (Plastibrand®, Germany) was rinsed with Milli-Q water filtered through a  $0.1\ \mu\text{m}$  membrane. Prior to measurement, the solution was filtered through a  $0.45\ \mu\text{m}$  PVDF membrane (Acrodisc®LC 13 mm syringe filter) to a cuvette. The sample was equilibrated in the cell for 20 mins before scanning.

The incident light through the scanning cell can be scattered by aggregates. Due to Brownian motion of aggregates, the intensity of scattered light will fluctuate around a mean value. The time dependence of this fluctuation is related to the translational diffusion of aggregates. Therefore, the size of aggregates can be calculated by the Stokes-Einstein equation Eq. (6.2)

$$D = \frac{kT}{6\pi\eta r} \quad (6.2)$$

where  $k$  is Boltzmann's constant,  $T$  is 310K and viscosity of the medium ( $\eta$ ) (taken as pure water) is  $6.918\times 10^{-4}\ \text{kg}/(\text{m}\cdot\text{s})$ .

A logarithm scale decay time (digital correlator) is used to determine the autocorrelation function of scattered light intensity with the time domain method. The autocorrelation function is given by Eq. (6.3):

$$g^{(1)}(\tau) = B \sum_i (A_i)\exp(-\Gamma_i\tau) \quad (6.3)$$

$B$  is a constant dependent upon instrumental parameters such as the aperture size. The  $100\ \mu\text{m}$  detection aperture was set in the experiments due to the low concentration of some samples.  $A_i$  is the relative intensity of light scattered by a particle with decay constant  $\Gamma$  and is related to relative amount of such particles by Eq. (6.4).

$$\Gamma = Dq^2 \quad (6.4)$$

$\Gamma$  is proportional to the diffusion coefficient and  $q$  is the magnitude of the scattering vector ( $=4\pi n\sin(\theta/2)/\lambda$ ) which is determined by the refractive index of medium, the scattering angle( $\theta$ ) and the wavelength of the light( $\lambda$ ). The refractive index employed was that of water, 1.3313. The scattering angle was  $165^\circ$  in all experiments. Data was analyzed by a non-negatively constrained least squares (NNLS) algorithm.

Since  $g(\tau)$  is proportional to the relative scattering from each species, it contains information on the statistical measurements of distribution of diffusion coefficient.

The fraction of total light intensity scattered by each species is given by Eq. (6.5)

$$f_i = \frac{C_i M_i P_i}{\sum C_i M_i P_i} \quad (6.5)$$

where  $C_i$  is the concentration of the species,  $M_i$  is the molecular weight of the species and  $P_i$  is the form factor for light scattering. The mean diffusion coefficient of all species is the sum of  $f_i$  weighted diffusion coefficients of each species.

$$\bar{D} = \sum f_i D_i \quad (6.6)$$

The variance ( $\mu^2$ ) of the distribution of the diffusion coefficient by cumulants analysis is given by

$$\mu^2 = (D^2 - \bar{D}^2) q^4 \quad (6.7)$$

and is a quantitative characterization of solution polydispersity (Koppel, 1972).

$$\text{Polydispersity} = \mu^2 / \Gamma^2 \quad (6.8)$$

$$\text{Polydispersity index} = (\Gamma - \bar{\Gamma})^2 / \bar{\Gamma}^2 \quad (6.9)$$

In general, the 0.05-0.08 of polydispersity index indicates a monodispersed solution and 0.08-0.7 is a mid-range of polydispersed solution.

### 6.3.8. Fourier transform infrared (FTIR)

FTIR was used to monitor the change of  $\nu_{C-O}$  on the polyoxylethylene chain and  $\nu_{C=O}$  on PS80 in the presence of model drugs. Infrared spectra were recorded on the BIO-RAD FTS3000MX spectrometer with Merlin version 2.3.7 software. The recording range was from  $700 \text{ cm}^{-1}$  to  $4000 \text{ cm}^{-1}$  with an effective resolution of  $4 \text{ cm}^{-1}$  and 128 scans. The attenuated total reflectance (ATR) method is used where the liquid sample has very good contact with the zinc selenide (ZnSe) crystal which has a high refractive index (2.403 @ 10.6 Mm).

Exact weighed portion of PS80 was dissolved in  $D_2O$  and the excess amount of drug was added to the micellar solution at ambient temperature. Samples were taken at 3, 24, 48, 72 h and filtered through a  $0.2 \text{ }\mu\text{m}$  PTFE membrane directly into the IR cell. Since

samples were taken on different days, the spectrum of PS80 in the absence of drug prepared at the same time was recorded at 3 h, 24 h, 48 h, and 72 h.

To perform spectral subtraction, spectra of solvent, surfactant in solvent and surfactant with drug in solvent were recorded. The bands from a solvent such as D<sub>2</sub>O were subtracted from the spectrum of the sample of PS80 and PS80 with the drug. The final spectra analysis was made between the subtracted spectra. Experiments were carried out at ambient temperature.

## **6.4. Results and discussion**

### **6.4.1. Characteristics of model systems critical for drug solubilization**

The extent of solubilization of surfactant aggregates is determined by numerous factors, such as nature of the surfactant, nature of the drug, temperature, pH, ionic strength, etc. In this section, the focus will be on characterizing the properties of PS80, OA and PS80/OA assemblies with respect to size, extent of ionization and locus of solubilization of model solute. The characteristics of self-assembled aggregates of OA are dependent on the ionization state. In general, non-ionized fatty acids often assemble into vesicles while ionized fatty acids tend to form micelles. Vesicles are bilayer aggregates, are larger than micelles, and offer loci for drug solubilization that are markedly different than those offered by micelles.

#### **6.4.1.1. Ionization of oleic acid in micellar solution**

The pK<sub>a</sub> of monomeric OA is approximately 5, a value similar to other carboxylic acids. Non-ionized OA is poorly-water soluble while ionized OA acts as an anionic surfactant and can form micelles. In oleate micelles, the pK<sub>a</sub> of the carboxylic group has been determined to be about 10 (Kanicky and Shah, 2003). Determination of the apparent pK<sub>a</sub> of OA in the mixed micelle will allow an estimation of the extent to which the acid is ionized at pH 7.5. Moreover, it might be possible to determine if different populations of PS80/OA mixed micelles co-exist in solution.

The apparent pK<sub>a</sub> was obtained by fitting Eq. (6.1) to the titration data. The results are shown in Figures 6.5 and 6.6. The model agreed well with experimental data for the 1:1 ratio of PS80/OA, but was less successful for the 9:1 ratio data. The fitted K<sub>a</sub>, fitting parameters and calculated apparent pK<sub>a</sub> values of oleic acid in micelle solutions are

summarized in Table 6.3. Two proton dissociations were observed in Figures 6.5 and 6.6. According to the mathematical model of titration, one is the proton dissociation of OA and another is the proton dissociation of water. The apparent pKa of OA in the micelle of PS80 is 7.1. Accordingly, at pH = 7.5, approximately 80% of OA would be ionized and act as an anionic surfactant in the presence of PS80. There is not significant difference between, the values of apparent pKa of OA in the micelle systems of PS80/OA 9/1 and 1/1 ( $p = 0.05$ ). The value of the apparent pKa of OA in PS80/OA mixed micelle is similar to that reported for other fatty acid/nonionic surfactant systems. da Silva et al. showed experimentally and theoretically that the pKa of lauric acid in an *n*-dodecyloxyethylene-glycomonoether(C<sub>12</sub>E<sub>8</sub>) micelle was approximately 6.6 (da Silva, Bogren et al., 2002). The pKa of tetradecanoic acid in a sugar-derived surfactant was found to be 6.3 (Whiddon, Bunton et al., 2002).

Regardless of the fatty acid chain length, an ionized fatty acid is located at the micellar interface (da Silva, Bogren et al., 2002). Shown in Scheme 6.3, are two possible arrangements of carboxylic acid head group at the interface of a mixed micelle. One arrangement has the carboxylic acid head group separated by the PS80 molecules (**A** for 9:1 ratio, **B** for 1:1 ratio). In another case, surfactants are clustered (**C** for 9:1 ratio, **D** for 1:1 ratio). In the cases of **C** and **D**, the ionized carboxylic acid head group will stabilize the proton of an adjacent unionized carboxylic acid. Consequently, it is more difficult to remove proton by the free hydroxide ions in the bulk solution. As a result, the measured pKa of the fatty acid will shift to a higher values (Kanicky and Shah 2003). The steric self-repulsion of the PS80 head group and the charge repulsion of the ionized OA may disfavor the arrangements of **C** and **D** compared with the arrangements of **A** and **B**.

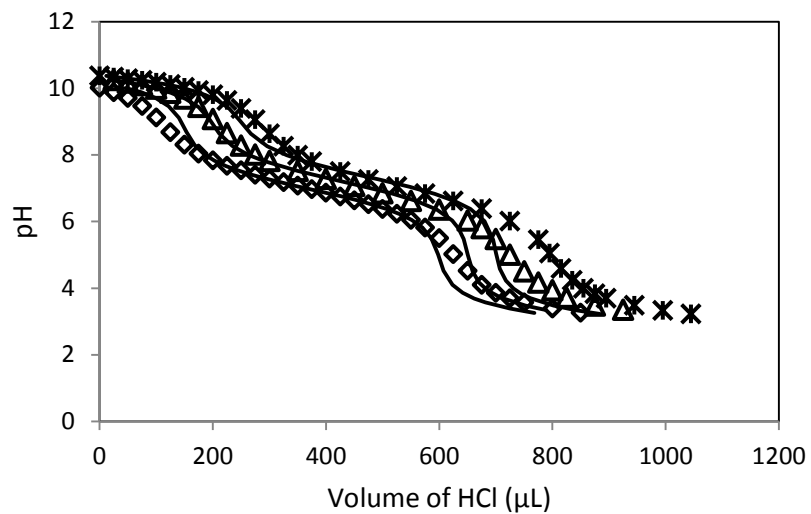


Figure 6.5 Titration curves of ionized form of OA in a mixed micelle of PS80/OA (9/1) at 37 °C (n=3). Symbols are experimental data and solid lines are the calculated values by fitting the data to Eq. (6.1).

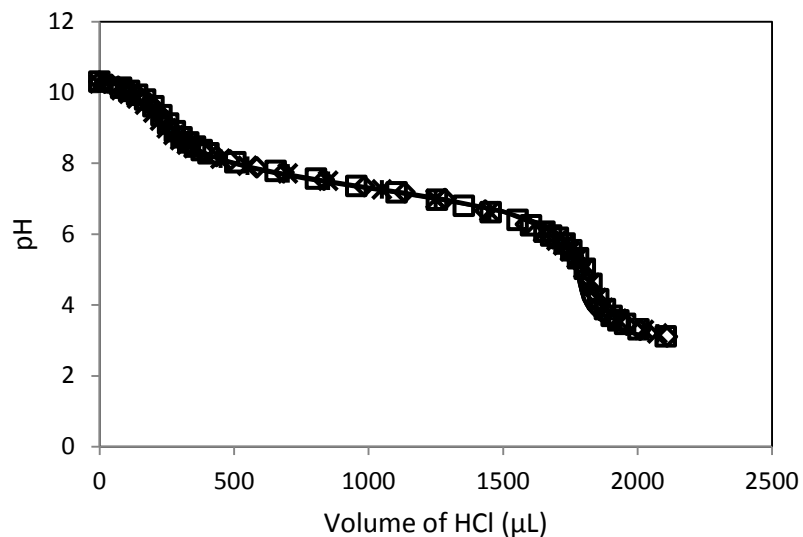
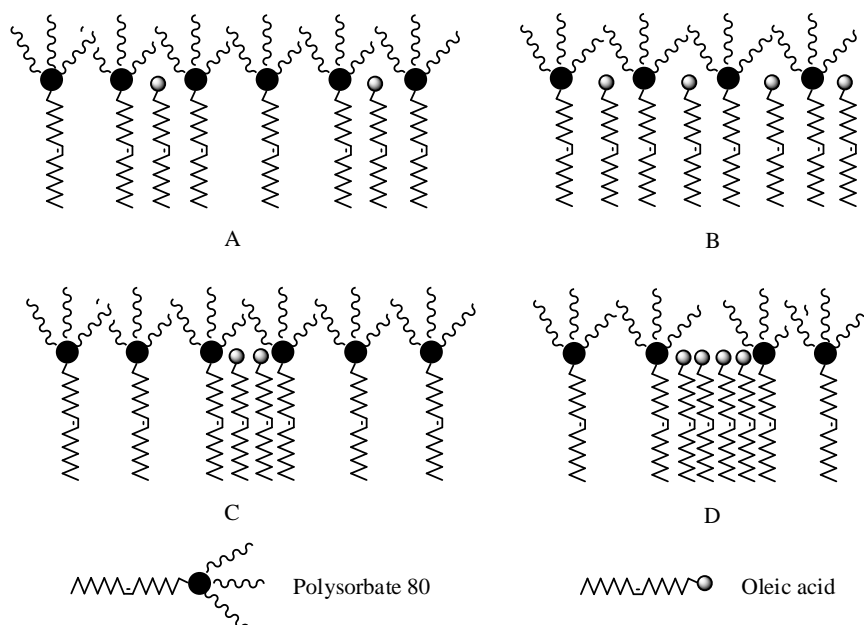


Figure 6.6 Titration curves of ionized form of OA in mixed micelle of PS80/OA (1/1) at 37 °C (n=3). Symbols are experimental data and solid lines are the calculated values by fitting the data to Eq. (6.1).

Table 6.3 The fitted  $K_a$ , fitting parameters and calculated apparent  $pK_a$  of OA in the mixed micelle solutions composed of PS80/OA at molar ratios of 9/1 and 1/1 (n=3).

PS80/OA	Fitted $K_a$	95% CI	$R^2$	$pK_a$	AVE	SD
9/1-1	8.7E-08	4.4E-08	0.99	7.06	7.06	0.01
9/1-2	8.9E-08	3.1E-08	0.99	7.05		
9/1-3	8.7E-08	3.6E-08	0.99	7.06		
1/1-1	7.1E-08	4.6E-09	0.99	7.15	7.11	0.04
1/1-2	7.5E-08	4.6E-09	0.99	7.12		
1/1-3	8.6E-08	4.6E-09	0.99	7.07		



Scheme 6.3 Possible arrangements of PS80 and OA in mixed micelles. A and C, PS80/OA (9/1); B and D, PS80/OA(1/1)

#### 6.4.1.2. Size and population of lipid aggregates in mixtures of PS80 and oleic acid

Small-angle neutron scattering, time-resolved fluorescence quenching, static or dynamic light scattering and nuclear magnetic resonance (NMR) have been employed to characterize the size of lipid aggregates directly or indirectly (Schurtenberger, Mazer et al., 1983; Brown, Pu et al., 1988; Söderman, Stilbs et al., 2004; Valentini, Vaccaro et al., 2004; Waters, Leharne et al., 2007; Kätzel, Vorbau et al., 2008). Among these, NMR self-diffusion coefficient measurement is a popular method due to high chemical selectivity, non-invasiveness, and broad range of accessible diffusion coefficients. Compared to other methods, NMR provides molecular information. However, the application of the Stejskal-Tanner equation requires signal intensity from a well-resolved peak. In the case of multiple component systems, where signals are overlapped, appreciation of NMR techniques becomes problematic. In the present work, overlapping peak signals precluded the inclusion of NaC/PC in NMR studies. As a complimentary method, the dynamic light scattering method was used to characterize complex systems, without regard to the presence of NaC/PC.



#### 6.4.1.2.1. Pulsed-gradient spin-echo nuclear magnetic resonance (PGSE-NMR) studies.

When a paired magnetic pulsed gradient is applied to a sample, self-diffusion of molecules results in signal attenuation. Assuming the chemical shifts are resolved, the diffusion coefficient of a molecule could be determined by the Stejskal-Tanner equation. (Stejskal and Tanner, 1965).

$$S(q) = S(0)e^{-Db(q)} \quad (6.10)$$

Here  $b = (\gamma G \delta)^2 (\Delta - \delta/3)$  and  $D$  is the diffusion coefficient.

The diffusion coefficients of PS80/OA assemblies in the absence of NaC/PC were determined. Since the surfactant monomer exchanges very rapidly with the micellar surfactant, on the time scale of 100 ms, the measured apparent diffusion coefficient is the population average of the specific diffusion coefficients of the monomer and micelle. In all cases, the apparent diffusion coefficient decreased with increasing total surfactant concentration (Figure 6.7). This trend had been noticed in the literature and in our laboratory (Amidon, Higuchi et al., 1982; Kossena, Boyd et al., 2003; Wiedmann, Liang et al., 2004; Apperley, Forster et al., 2005; Lafitte, Thuresson et al., 2007; Feng, 2009). The concentration of 0.1 mM was below the CMC of PS80 (0.22 mM) and sodium oleate (1.1 and 2.5 mM) (Hildebrand, Garidel et al., 2003). At such low concentrations, the diffusing species is assumed to be the monomer of PS80 or OA. At very low concentration, only the chemical shifts of polyoxyethylene (POE) and hydrocarbon chain of OA were detected and signal-to-noise ratio suffered. Consequently, the variation in the diffusion coefficient was greater at such low concentration in comparison with those at concentrations above the CMC.

The effect of surfactant concentration and compositions on the apparent diffusion coefficient of mixed micelles can be explained by the interactions between micelles. As the micelle concentration increases, each micelle must avoid an increasing number of micelles resulting in a decrease in the apparent diffusion coefficient. On the other hand, it has been proposed that high charge repulsion forces between the micelles increase the diffusion coefficient (Pisárcik, Devínský et al., 1996). The apparent diffusion coefficient of PS80/OA micelles would likely be the balance of these two interactions.

NMR studies of PS80 micelles in the presence of progesterone were conducted as a function of surfactant concentration to assess if solubilization of drug would influence the diffusion coefficient. The signal from polyoxyethylene group at 3.7 ppm was used to determine the diffusion coefficient of PS80 micelles saturated with progesterone. The use of polyoxyethylene chemical shift had been proved valid in our laboratory and in the literature (Spernath, Yaghmur et al., 2003; Balakrishnan, Rege et al., 2004; Apperley, Forster et al., 2005; Feng, 2009). As shown in Figure 6.7, the solubilization of progesterone did not change the self-diffusion coefficient of PS80 micelles significantly. Similar results have been reported by others (Apperley, Forster et al., 2005; Feng, 2009).

The hydrodynamic radii of aggregates can be calculated by the Stokes-Einstein equation Eq. (6.2) assuming that micelles are spherical. The validity of the assumption is challenged in the case of polymeric surfactant. Recently, the small angle x-ray scattering revealed that PS80 forms core-shell cylindrical micelles at a concentration of 38 mM (pH7.2, ionic strength 2.44 mM) (Aizawa, 2009). Concentrations of a prepared sample in the present study were equal or less than 30 mM (pH 7.5, ionic strength 150 mM).

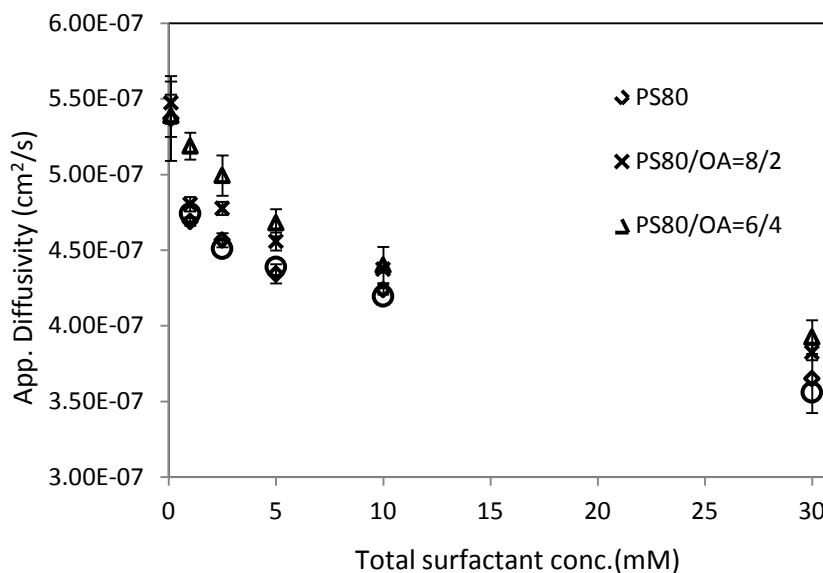


Figure 6.7 The apparent diffusion coefficients of PS80 micelles (diamond) and mixed micelles of PS80/OA at molar ratio 8/2 (cross), 6/4 (triangle) and progesterone-saturated micelle of PS80 (circle) at  $37 \pm 0.1$  °C.

When the molecule is either within one compartment or within two compartments exchanging very rapidly on the time scale of NMR method, the expected signal attenuation is linear with the increase of gradient strength. On the contrary, if a molecule resides in more than two compartments with significantly different diffusivities, a biexponential Stejskal-Tanner plot will be observed. In all studies, excellent fitting of a single-exponential Stejskal-Tanner equation was observed (Figure 6.4).

Several possible populations of mixed micelles are consistent with the observed fit of the Stejskal-Tanner equation to the NMR data. The most obvious possibility is that only one population of lipid aggregates exists in the mixture of PS80 and OA. In other words, the ratio of PS80/OA in the micelle is identical to the ratio of total concentrations in solution. A second possibility to explain the excellent fit of the Stejskal-Tanner equation would be two or more populations of mixed micelles of similar size co-exist in solution. For example, it could be envisioned that mixed micelles rich in PS80 could co-exist with mixed micelles rich in OA. A third possibility is that several aggregates of different sizes co-exist in solution, with one assembly dominating the population. Shick and Manning have reported that mixing ratio of anionic and non-ionic surfactants had no effect on the

compositions of mixed micelles as determined by electrophoresis and conductivity measurements (Schick and Manning, 1966).

An interaction parameter ( $\beta$ ) has been used to quantify the stability of mixed micelles (Treiner, Nortz et al., 1990). A value of  $\beta < 0$  indicates a synergistic interaction between the two surfactants that promotes the formation of the mixed micelle. A survey of literature indicated that  $\beta$  is always less than zero when mixing an ionic surfactant with a non-ionic surfactant (Table 6.4). While parameter  $\beta$  is distinct from the parameter  $B$  (Section 5.4.2.2), Treiner et al. showed a strong correlation between the two (Treiner, Nortz et al., 1990). Nishikido proposed that attractive ion-dipole interactions between the anionic carboxylic group and polyoxyethylene groups facilitate mixed micelle formation (Nishikido, 1977). Further, they proposed that the interactions are enhanced by the formation of hydrophobic interactions between the hydrocarbon chains. This effect would seem especially true in the mixture of PS80 and OA since both surfactants have the same long hydrocarbon chain.

In order to obtain the size of the micelle, the two-state distribution model was used to fit apparent diffusivity data (Wiedmann and Kamel, 2002). This model assumes that surfactant is located both in bulk solution and associated as micelles. If the exchange between two states is fast, the measured diffusion coefficient is the population average of specific diffusion coefficients of a monomer and a micelle Eq. (6.11).

$$D_{obs} = f_{mon}D_{mon} + f_{mic}D_{mic} \quad (6.11)$$

$D_{obs}$  is the observed diffusion coefficient of the micellar solution;  $f_{mon}$ ,  $f_{mic}$  are molar fractions of surfactant as monomer and as micelle, respectively;  $D_{mon}$ ,  $D_{mic}$  are diffusion coefficients of monomer and the micelle, respectively.

Table 6.4 Interaction parameter ( $\beta$ ) of mixing ionic surfactant and nonionic surfactant in the literature

Ionic surfactant	Nonionic surfactant	$\beta$	Ref
Sodium oleate	C <sub>12</sub> E <sub>6</sub>	-2.7	a
	C <sub>14</sub> E <sub>6</sub>	-3.0	
SDS	C <sub>8</sub> E <sub>6</sub>	-3.1	b
	C <sub>10</sub> E <sub>4</sub>		
	C <sub>12</sub> E <sub>8</sub>	-4	
	C <sub>12</sub> E <sub>23</sub>	-2.6	c
	C <sub>14</sub> E <sub>23</sub>		
	DM	-4- -3.25	d
	Brij 35	-4.82-1.95	e
	Brij 97	-5.54- - 7.40	
AOT	C <sub>12</sub> E <sub>6</sub>	-4.2	f

a. Theander and Pugh 2003

b. (Rosen 1989)

c. (Treiner, Vaution et al. 1985)

d. (Zhang, Zhang et al. 2004)

e. (Glenn, van Bommel et al. 2005)

f. (Moroi, Akisada et al. 1977)

The fractions of surfactant present as monomer and in the micelle can be expressed in terms of the CMC by the following equations:

$$f_{\text{mon}} = \text{CMC}/[\text{surf}]_{\text{total}} \quad (6.12)$$

$$f_{\text{mic}} = 1 - \text{CMC}/[\text{surf}]_{\text{total}}, \quad (6.13)$$

Substituting Eq. (6.12) and Eq. (6.13) into Eq. (6.11)

$$D_{\text{obs}} = \{\text{CMC}/[\text{surf}]_{\text{total}}\}D_{\text{mon}} + \{1 - \text{CMC}/[\text{surf}]_{\text{total}}\}D_{\text{mic}} \quad (6.14)$$

$$D_{\text{obs}} [\text{surf}]_{\text{total}} = [\text{surf}]_{\text{total}}D_{\text{mic}} + \text{CMC}(D_{\text{mon}} - D_{\text{mic}}) \quad (6.15)$$

Eq. (6.15) shows that a plot of  $D_{obs} [\text{surf}]_{total}$  as a function of  $[\text{surf}]_{total}$  should be linear with a slope of  $D_{mic}$  and intercept of  $\text{CMC}(D_{mon} - D_{mic})$ . Figures 6.8-6.10 show the results of plotting data for PS80, PS80/OA (8/2), and PS80/OA (6/4) according to Eq. (6.15). The model was in excellent agreement with the data. Table 6.5 summarizes the diffusion coefficients, calculated hydrodynamic radi and  $R^2$  values from 3 replicates in each case. Within the standard deviation, the diffusion coefficients of a PS80 micelle and mixed micelles of PS80/OA at molar ratios 8/2 and 6/4 were identical, suggesting that the size was independent of the composition. The diffusion coefficient of the PS80 micelle was close to the literature value of  $3.5 \times 10^{-7} \text{ cm}^2/\text{s}$  (Lafitte, Thuresson et al., 2007). The hydrodynamic radius calculated by the Stoke-Einstein equation was consistent with the value of  $9.1 \pm 2.2 \text{ nm}$  measured by fluorescence methods (Croy and Kwon, 2005).

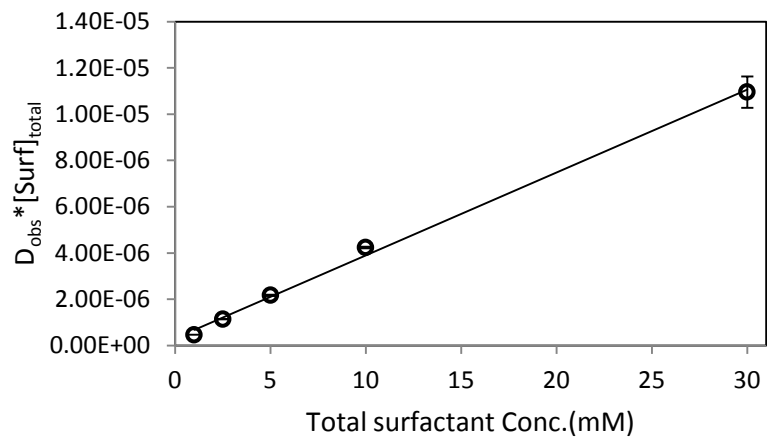


Figure 6.8 Plot of  $D_{obs} * [Surf]_{total}$  as a function of total concentration of PS80.

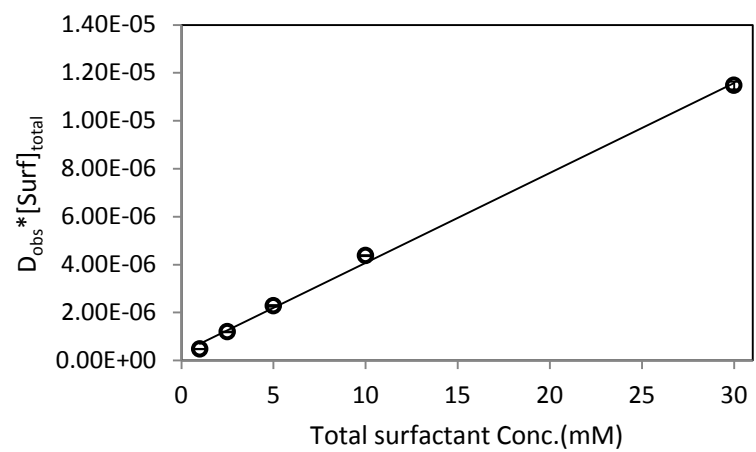


Figure 6.9 Plot of  $D_{obs} * [Surf]_{total}$  as a function of total surfactant concentration of PS80/OA (8/2).

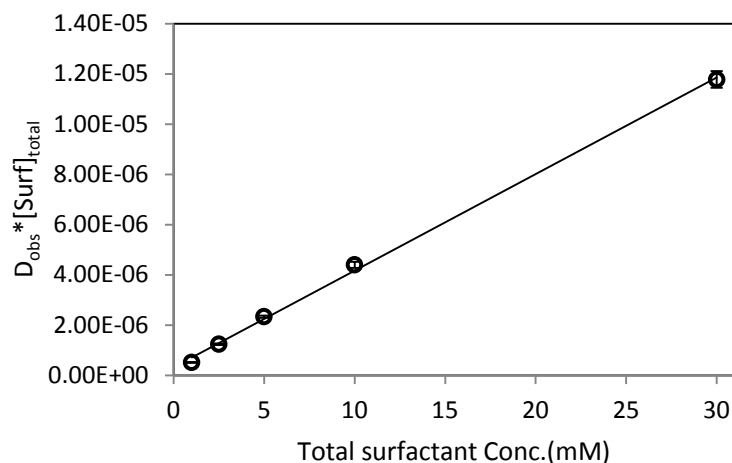


Figure 6.10 Plot of  $D_{obs} * [Surf]_{total}$  as a function of total surfactant concentration of PS80/OA (6/4).

Table 6.5 Diffusion coefficients and hydrodynamic radii of lipid aggregates in the PS80 solution and mixture of PS80 and OA at different molar ratios

Molar ratio of PS80 to oleic acid	Diffusion coefficient ( $m^2/s$ ) $\pm$ SD	hydrodynamic radius (nm) $\pm$ SD	$R^2$
1/0	3.6e-11 $\pm$ 2.2e-12	9.3 $\pm$ 0.6	0.998
8/2	3.8e-11 $\pm$ 5.3e-13	8.9 $\pm$ 0.1	0.998
6/4	3.9e-11 $\pm$ 1.4e-12	8.7 $\pm$ 0.3	0.999

#### 6.4.1.2.2. Dynamic light scattering (DLS) method

To corroborate the results obtained by NMR technique, the hydrodynamic radii of PS80 micelles at concentrations of 76 mM, 7.6 mM and 3.8 mM were measured by DLS. The hydrodynamic radii and polydispersity index are summarized in Table 6.6. Due to rather large variations in experimental results there was no statistical difference between the average sizes at each concentration. The hydrodynamic radius of simple PS80 micelle in tris maleate buffer was found to be 15.4 $\pm$ 2.3 nm, a value greater than that determined by PGSE-NMR (Table 6.5). A significant difference between values measured by DLS and



NMR was also evident in other micellar solutions composed of PS80 and OA at different molar ratios (Figure 6.11). The polydispersity index in DLS between 0.05 and 0.08 indicated that the micelle population was monodispersed. This is consistent with observations by the NMR method.

Table 6.6 Hydrodynamic radii of PS80 micelles in tris maleate buffer and polydispersity index at 37°C (Average  $\pm$  SD, n=3)

PS80 Conc. (mM)	hydrodynamic radius (nm)	Polydispersity Index
3.8	14.4 $\pm$ 1.4	0.09 $\pm$ 0.05
7.6	18.1 $\pm$ 3.5	0.07 $\pm$ 0.02
76	13.8 $\pm$ 4.2	0.07 $\pm$ 0.01

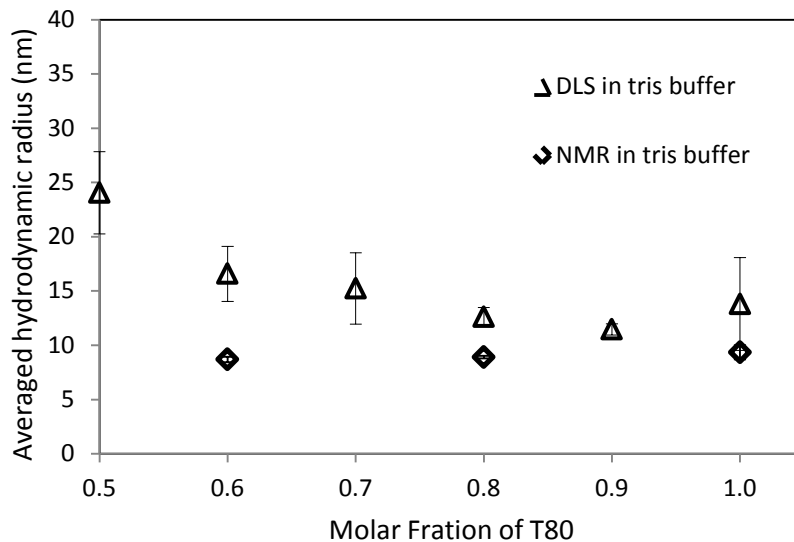


Figure 6.11 The hydrodynamic radii of micelles measured by DLS method (triangle) and PGSE-NMR method (diamond) at different molar fraction of PS80.

Additional DLS measurements of micelles of PS80 in the presence of 5 mM NaC/1.25 mM PC were conducted. Within the standard variation, the hydrodynamic radii of lipid aggregates were not significantly different, giving the average value of 11.3 $\pm$ 1.0 nm

(Table 6.7). Occasionally, minor populations with radii less than 3 nm or more than 300 nm appeared. A polydispersity index less than 0.08 and a high percentage of intensity (>70%) of a population an average radius of  $11.3 \pm 1.0$  nm in solutions at concentrations of 7.6 mM and 5.7 mM suggested only one major aggregate. However, the polydispersity of the radius increased at concentrations of 3.8 mM and 1.9 mM. Occasionally, a population of large aggregates was observed. The hydrodynamic radii of PS80/oleic acid at molar ratio of 9/1 and 1/1 in 5 mM NaC/PC solution are given in Table 6.8 and 6.9. Within the standard deviation, the PS80 micelle radii in solution concentrations ranging from 30 mM to 1.9 mM of PS80 were unchanged. The averaged values were  $10.5 \pm 1.6$  for 9/1 ratio solution and  $12.0 \pm 1.2$  for 1/1 ratio solution, respectively. This is in agreement with the results obtained by NMR, in which the size was independent of the composition.

Table 6.7 Hydrodynamic radii of PS80 micelle in SIF buffer and polydispersity index at 37°C as measured by DLS (Average  $\pm$  SD, n=3)

Conc. (mM)	Hydrodynamic Radius	Polydispersity Index
1.9	$12.07 \pm 2.63$	$0.08 \pm 0.06$
3.8	$11.82 \pm 3.66$	$0.06 \pm 0.04$
5.7	$11.52 \pm 3.35$	$0.04 \pm 0.03$
7.6	$9.81 \pm 2.38$	$0.03 \pm 0.02$

Table 6.8 Hydrodynamic radii of mixed micelles of PS80/OA at a molar ratio of 9/1 in SIFs buffer and polydispersity index at 37°C as measured by DLS(Average  $\pm$  SD, n=3)

Conc. (mM)	Hydrodynamic Radius	Polydispersity Index
1.9	13.90 $\pm$ 4.69	0.03 $\pm$ 0.02
3.8	11.28 $\pm$ 4.00	0.02 $\pm$ 0.01
5.7	11.99 $\pm$ 2.75	0.02 $\pm$ 0.02
7.6	12.29 $\pm$ 4.59	0.02 $\pm$ 0.01
30	10.59 $\pm$ 0.84	0.03 $\pm$ 0.02

Table 6.9 Hydrodynamic radii of mixed micelles of PS80/OA at a molar ratio of 1/1 in SIF buffer and polydispersity index at 37°C as measured by DLS (Average  $\pm$ SD, n=3)

Conc. (mM)	Hydrodynamic Radius	Polydispersity Index
1.9	13.31 $\pm$ 4.79	0.01 $\pm$ 0.01
3.8	10.37 $\pm$ 3.47	0.02 $\pm$ 0.01
5.7	10.30 $\pm$ 4.30	0.02 $\pm$ 0.01
7.6	9.70 $\pm$ 0.98	0.02 $\pm$ 0.01
30	9.06 $\pm$ 1.82	0.02 $\pm$ 0.01

Numerous studies have been done to characterize the size and structures of aggregates of bile salt and phospholipids. The hydrodynamic radii ranging from 2 nm to 20 nm were reported in the mixed micelles phase (Mazer, Benedek et al., 1980; Mueller 1981; Schurtenberger, Mazer et al., 1985). Structures characterized by small angle x-ray, QELS, DLS and cryo-TEM included small spheroidal mixed micelles at high concentrations of bile salt, mixed disk or disk shape mixed micelles and flexible cylindrical mixed micelles (Mazer, Benedek et al., 1980; Mueller, 1981; Walter, Vinson et al., 1991). Such diversity is determined by the molar ratio of bile salt to phospholipids and the type of bile salt. On

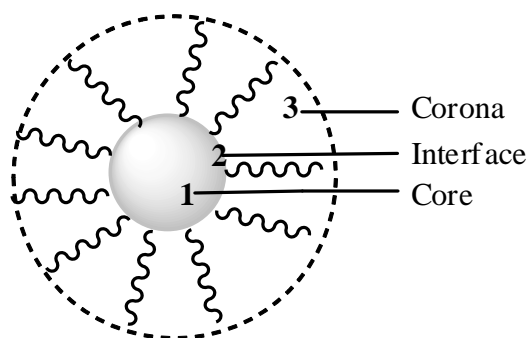
the other hand, very little information is available regarding the size and structure of mixed aggregates of lipolytic products with bile salt and phospholipids. Hjelm et al. characterized a mixture system composed of cholyglycine, phospholipids, oleate/oleic acid and monoolein by small angle neutron scattering (Hjelm, Schteingart et al., 1999). The study revealed that globular mixed micelles with repulsive electrostatic interactions were formed. In addition, the mixed micelles were similar in size and shape to those of bile salts with phospholipids, bile salts with oleate/oleic acid, or bile salts with monoolein. This is in agreement with the results assessed by the DLS method (Ilardia-Arana, Kristensen et al., 2006).

In summary, the assumption applied in Chapter 5 which only one major type of PS80/OA mixed micelle existed in the absence and presence of bile salt/phospholipids appears to be valid. The size of PS80/OA micelles was independent of the composition and close to that of the PS80 micelles.

#### **6.4.2 Inter-molecular interactions between model drugs and mixed micelles**

Solubilization studies reported in Chapter 5 indicated that the molar solubilization capacities of PS80/OA mixed micelles decreased for 17 $\beta$ -estradiol and nifedipine while remaining relatively constant for progesterone with increasing OA. It is anticipated that studies on the solubilization locus of drug in the micelles will improve the understanding of the mechanism of solubilization of poorly-water soluble drugs during the lipolysis of PS80, and provide a prediction tool for formulation design.

For non-polymer surfactant, drugs may be solubilized in the hydrocarbon core, at the interface between the core and the hydrophilic head group or adsorbed on the surface of micelles. For non-ionic surfactant having a polyoxyethylene chain, additional loci of solubilization may exist. Drugs can be solubilized in the non-polar hydrocarbon core region (zone 1 on Scheme 6.4), at the interface of a hydrophilic head group and hydrophobic core (zone 2 on Scheme 6.4), or in the polar corona region formed by a polymeric hydrophilic segment (zone 3 on Scheme 6.4). The locus of solubilization in the micelles is determined by the molecular properties of both the drug and the surfactant.



Scheme 6.4 Possible loci of poorly-water soluble drugs in the micelles of PS80 and mixed micelles of PS80/OA.

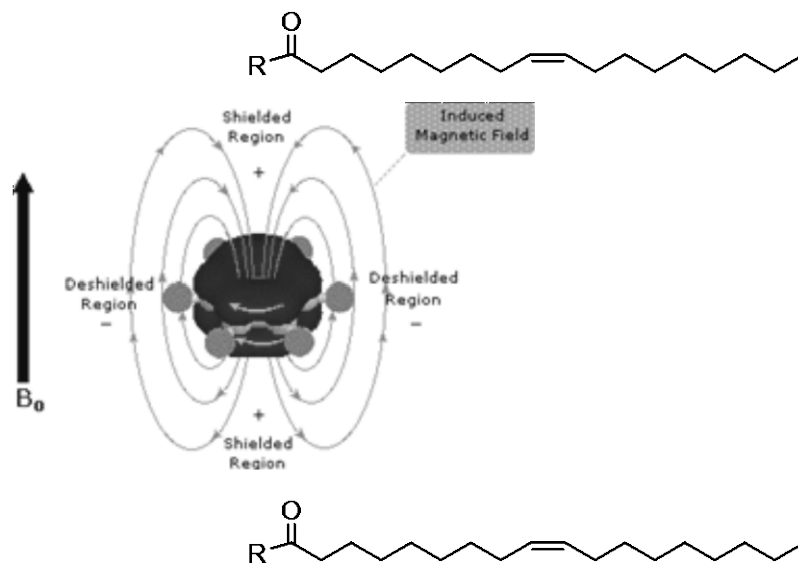
A variety of methods have been used to probe the interactions between solutes and micelles, such as fluorescence spectroscopy, UV spectroscopy, and NMR spectroscopy (Yoshida and Moroi, 2000). Among them, NMR spectroscopy is a reliable, direct, and highly differentiating method used to assess the interactions between solutes and micelles (Luan, Song et al., 2009). 2D-NMR such as ROSEY is a powerful tool to directly identify the interactions between a drug and a surfactant when located within 5 Å. In the case of weak chemical signals, interactions between solutes and micelles can also be inferred by other NMR techniques such as relaxation times (rotational and translational) and  $^1\text{H}$  and  $^{13}\text{C}$  chemical shifts.

In the following sections,  $^1\text{H}$ -NMR chemical shifts and Fourier-transform infrared spectroscopy (FTIR) will be employed to probe the characteristics of the solubilization loci of model drugs in PS80 micelles.  $^1\text{H}$ -NMR chemical shifts was chosen as this method was the only one capable of detecting putative interactions in the concentration range employed. FTIR was chosen to probe both the C-O stretch of the PEO chain and the C=O stretch of the ester in PS80 in the presence of model solutes.

#### 6.4.2.1 $^1\text{H}$ chemical shifts of PS80

An NMR signal is produced when the nuclei spin is immersed in an external magnetic field. A secondary magnetic field produced by electrons surrounding the nuclei spin in covalent compounds exists in response to the external magnetic field. It is opposed to the stronger external magnetic field and shields the nuclei from the applied field. Compared to the  $\delta$ -bond electrons, electrons in the aromatic  $\pi$  orbital, such as benzene, induce much stronger secondary fields resulting in shielding or deshielding of the NMR signal

dependent upon the location of nuclei in the induced magnetic field (Scheme 6.5). This phenomenon is reflected in the change of chemical shifts in the NMR spectrum. The largest change in chemical shift of protons of surfactant molecules corresponds to those in closest contact to solute molecules. By this feature, the relative changes in proton chemical shifts on PS80 were obtained by comparing the NMR spectra of PS80 in the absence and in the presence of drugs.



Scheme 6.5 Secondary magnetic field induced by  $\pi$ -electrons on the benzene ring.

#### 6.4.2.1.1. $^1\text{H}$ chemical shifts on PS80 in the presence of progesterone

Spectra of 30 mM PS80 solution and 30 mM of PS80 saturated with progesterone were recorded. The relative change of chemical shifts of PS80 in the presence of progesterone is shown in Figure 6.15. Typically, errors in the chemical shifts measured by NMR are on the order of 0.002 ppm (Bernardez, 2008). As expected, the presence of progesterone did not result in a change of chemical shifts on PS80 since there is no induced magnetic field. The location of solubilized progesterone can only be inferred from the results of solubilization so far. As suggested by the NMR, as the ratio of OA increased the aggregation number increased and the number of micelles decreased.

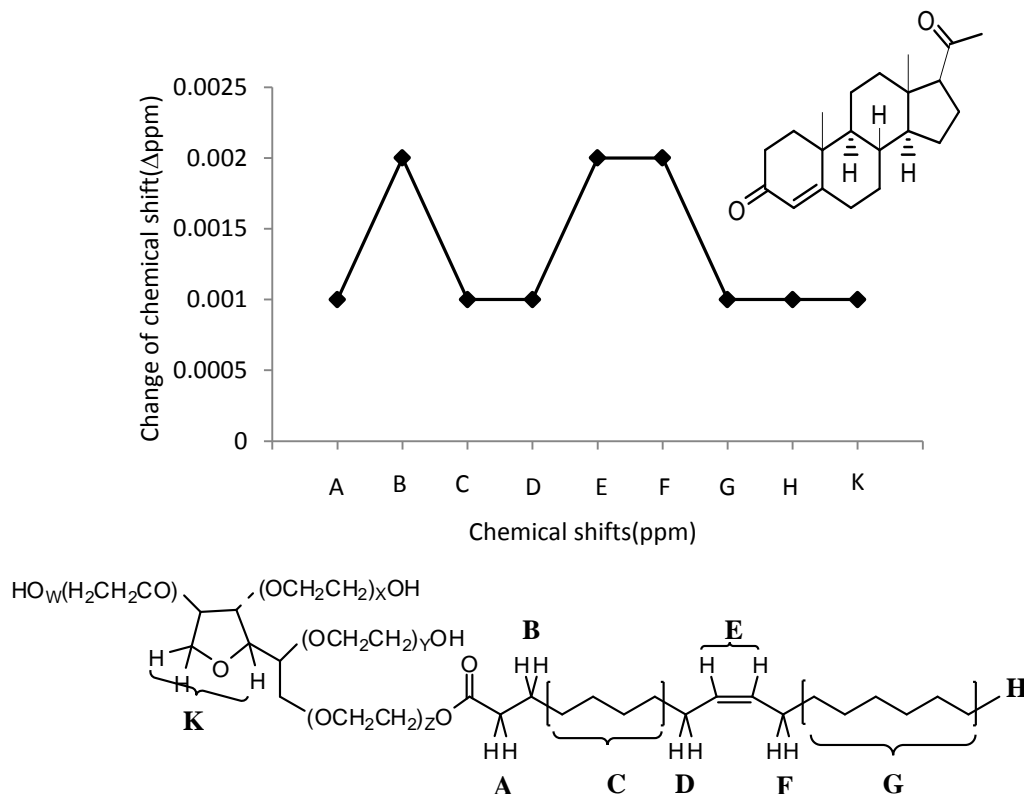


Figure 6.12  $^1\text{H}$  chemical shifts on PS80 in the presence of progesterone

#### 6.4.2.1.2. $^1\text{H}$ chemical shifts on PS80 in the presence of $17\beta$ -estradiol

An aromatic ring is present in the structure of  $17\beta$ -estradiol. The proton chemical shifts of PS80 around the aromatic ring could potentially be influenced by the induced magnetic field. As shown in Figure 6.13, the largest relative changes of 0.003 ppm and 0.005 ppm were observed for the  $\alpha$  and  $\beta$  protons on the fatty acid hydrocarbon tail of PS80. Upon formation of micelles, these two protons are located at the interface between the lipophilic hydrocarbon core and the hydrophilic POE corona. Unlike the solubilization of progesterone, the NMR results strongly suggest that  $17\beta$ -estradiol is solubilized at the interface. Since the solubilization is a dynamic process, the drug is not locked in one place. The characteristic time scale of the drug translocating within the micelle is faster than that of NMR. Therefore, the observed chemical shift of the surfactant is a population average of all possible locations of the drug.

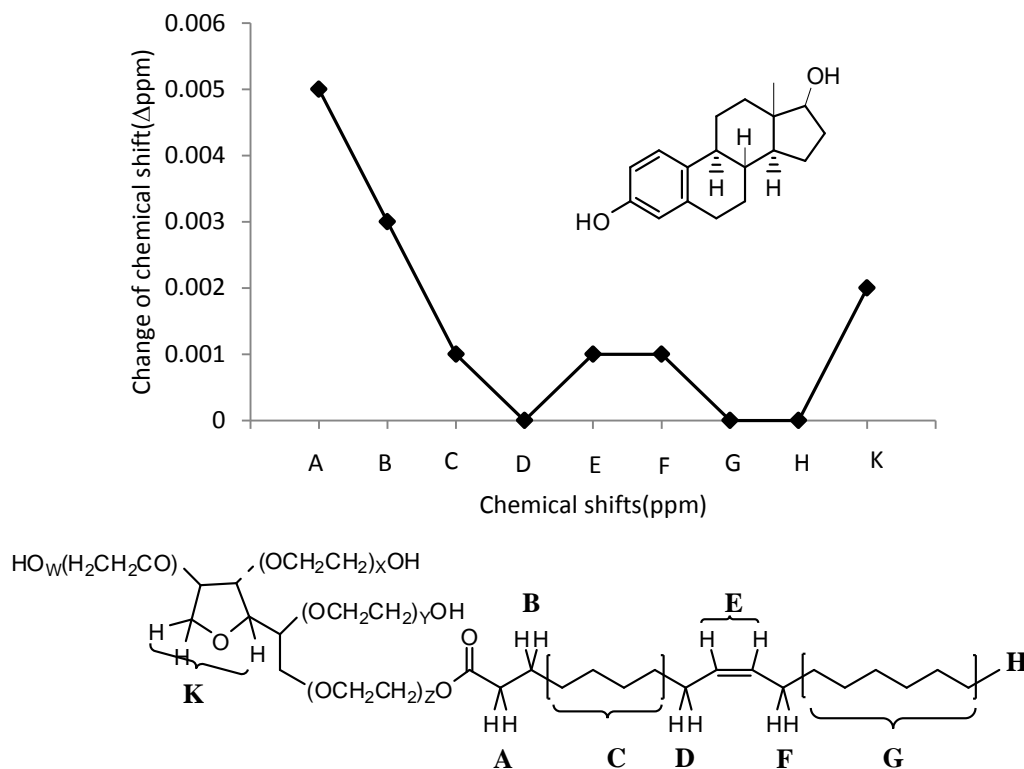


Figure 6.13  $^1\text{H}$  chemical shifts on PS80 in the presence of  $17\beta$ -estradiol

#### 6.4.2.1.3. $^1\text{H}$ chemical shifts on PS80 in the presence of nifedipine

As shown in Figure 6.14, upon solubilization of nifedipine, prominent changes of 0.006 ppm, 0.007 ppm and 0.006 ppm on PS80 were observed on the protons at the A, B and C positions, respectively. These protons are located at the interface region of the micelle as well as at the outer portion of the core. The results indicated that nifedipine may be solubilized both at the interface and hydrophobic regions.

The relative changes of proton chemical shifts on PS80 in the presence of nifedipine were greater than those of in the presence of  $17\beta$ -estradiol. Generally, the change of proton chemical shifts in the presence of an aromatic ring is dependent upon the amount of solubilized drug. The molar solubilization capacities of PS80 for nifedipine and  $17\beta$ -estradiol are 0.0538 and 0.0313, respectively. Thus, it is not surprising to see a greater effect by nifedipine.



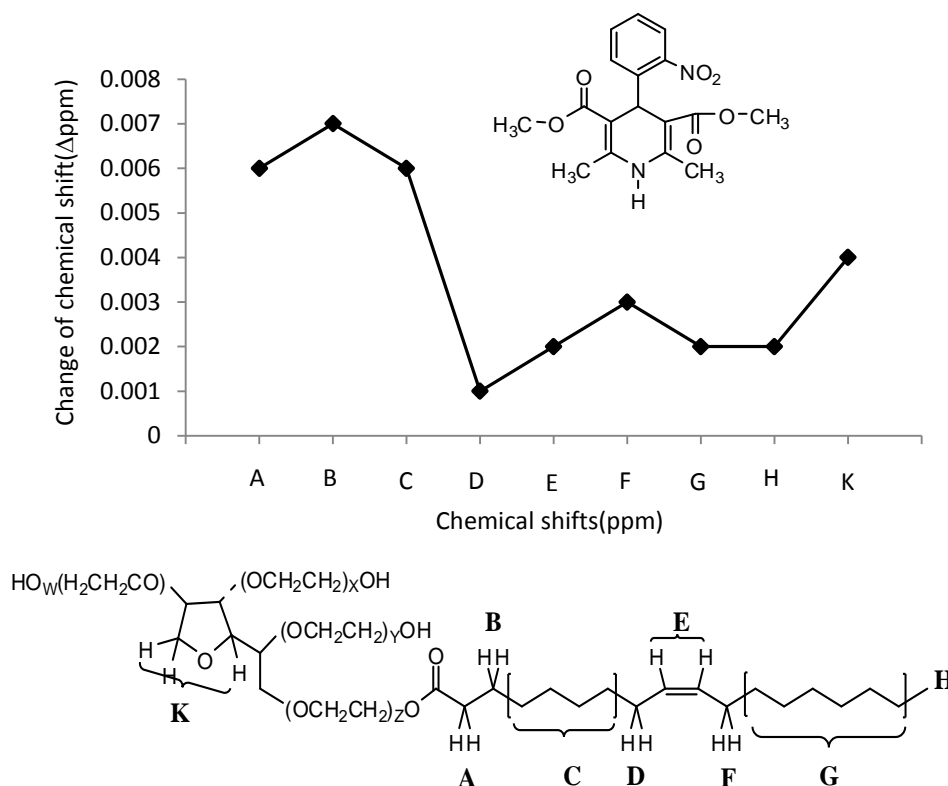


**Figure 6.14** <sup>1</sup>H chemical shifts on PS80 in the presence of nifedipine

#### 6.4.2.1.4. Conclusions of <sup>1</sup>H-NMR chemical shifts experiments

The interactions of drugs with micelles were probed in the molecular level by the NMR technique. The change of chemical shifts on surfactant in the presence of drugs inferred that major site of solubilization for 17β-estradiol was at the interface, while for nifedipine both the interface of the hydrocarbon core appear to be sites of solubilization. At this point, we may only speculate that the solubilization loci may remain the same in the mixed micelle of PS80/OA. Should this be the case, the decrease in solubilization capacities observed in PS80/OA (molar ratio 1/1) mixed micelles would be due to the reduced total interfacial area.

#### 6.4.2.2 Stretching vibration of C-O of POE chain and C=O of ester on PS80

The putative interactions of PS80 with either progesterone or nifedipine were explored by Fourier-transform infrared spectroscopy (FTIR). Potentially, the NH on the nifedipine is a hydrogen-bond donor and oxygen is a hydrogen-bond acceptor. As well, the terminal

OH on PS80 is a potential hydrogen-bond donor and oxygen on POE chains are potential hydrogen-bond acceptors. When forming a hydrogen-bond between the drug and PS80, the IR absorption of  $(C=O)_v$ ,  $(N-H)_v$ ,  $(O-H)_v$ , and  $(C-O)_v$  would shift to different frequencies compared to the drug and surfactant alone. Dyer et al. showed that the frequency shift of a carbonyl group provided information about the location of drug in the micelle (Dyer, Lei et al., 2008). Unfortunately, in our case the frequency of  $(C=O)_v$  stretching of the drug was not identifiable either in neat PS80 or in the aqueous solution. Under these conditions, the drug concentration was too low compared to PS80, and the absorption frequency was overwhelmed by that of  $(C=O)_v$  of the surfactant. Therefore, we focused our attention on the shifts of  $(C=O)_v$  and  $(C-O)_v$  frequencies associated with the surfactant. The spectrum of neat PS80 is given in Figure 6.15. The  $(C-O)_v$  frequency shift of the polyoxyethylene (POE) group induced by the solubilization of progesterone and nifedipine in neat PS80 is shown in Table 6.10. Solubilization of nifedipine caused a significant shift in  $(C-O)_v$  frequency. On the contrary, a shift in  $(C-O)_v$  frequency was not observed in the solubilization of progesterone. These results indicate that nifedipine has a strong interaction with the polyoxyethylene while the progesterone does not show such strong interaction.

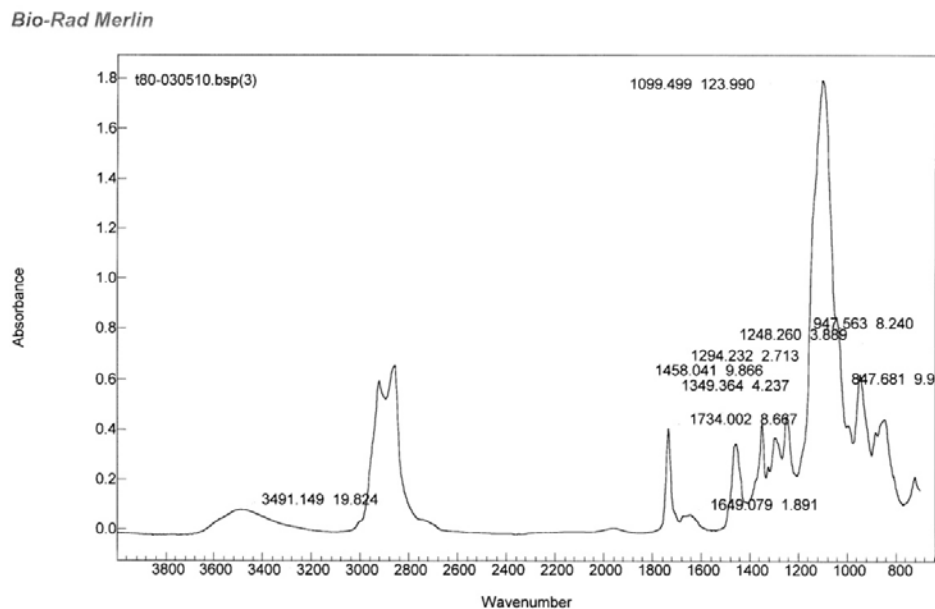


Figure 6.15 FTIR spectrum of neat PS80

Table 6.10 Absorption frequencies of (C-O)<sub>v</sub> on a polyoxyethylene (POE) group in the absence and presence of progesterone and nifedipine

Sample	C-O <sub>v</sub> POE (cm <sup>-1</sup> )
Neat PS80	1099.499
PS80+ Progesterone	1099.423
Neat PS80	1099.541
PS80+Nifedipine	1095.813

To further investigate the possible location of drugs in the micelles, the changes of (C=O)<sub>v</sub> and (C-O)<sub>v</sub> in 30 mM of PS80 prepared in D<sub>2</sub>O with saturated progesterone and nifedipine were monitored at 3, 24, 48 and 72 h. The D<sub>2</sub>O vibration and stretching band appeared at 2469.6cm<sup>-1</sup> and 1204.7cm<sup>-1</sup>. The latter is close to the (C-O)<sub>v</sub> at ~1091cm<sup>-1</sup> on the POE. The possible effect on this band needs to be considered when the spectral subtraction method is employed. The relative frequency changes of (C-O)<sub>v</sub> and (C=O)<sub>v</sub> between the control and the sample were plotted as a function of time (Figure 6.16). Clearly, the blue shift of (C-O)<sub>v</sub> and red shift of (C=O)<sub>v</sub> exhibited a maxima at 24 h. The blue shift of (C-O)<sub>v</sub> can be attributed to the increased electron density at the C-O bond as a result of a formation of an hydrogen-bond. Generally, the hydrogen bonding is weaker for deuterium than for hydrogen atoms (McDougall and Long, 1962). Consequently, with the replacement of hydrogen by deuterium as a function of time, the interactions between nifedipine with a POE chain become weaker at 72 h as shown in Figure 6.16.

A shift in (C=O)<sub>v</sub> frequency due to hydrogen bonding is independent of whether the bonding is inter- or intramolecular. In general, (C=O)<sub>v</sub> frequency will shift to a lower frequency with the formation of the hydrogen-bond and the extent to which the shift takes place will depend upon the degree of hydrogen bonding. As seen in Figure 6.16, the

extent of the shift was small in the aqueous solution. Thus, it is not clear that any observed shift is attributed to the formation of the hydrogen-bond involving any C=O group. We can only hypothesize that there are a variety of possibilities to form the hydrogen bonding between the nifedipine and surfactant. Such change was not observed in the sample of progesterone.

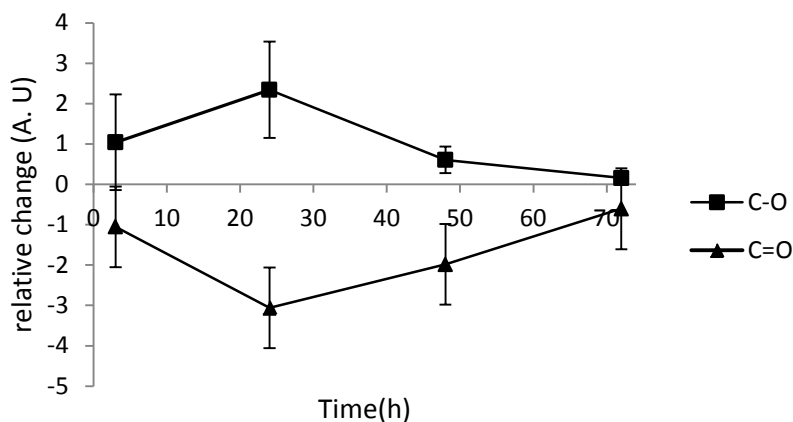


Figure 6.16 Relative change of absorption of C-O on a POE chain and C=O on PS80 in a PS80 solution prepared in the D<sub>2</sub>O saturated with nifedipine at 3 h, 24 h, 48 h and 72 h

#### 6.4.3. Summary of solubilization of model drugs in the micelles and the proposed location

The locus of drug solubilized in micelles determined by many factors, including the polarity and structure of the solute. The physical properties of model drugs and molar solubilization capacity of PS80 micelles and PS80/OA (1/1) mixed micelles are given in Table 6.11.

Table 6.11 The physical properties and molar solubilization capacity of PS80 and PS80/oleic acid (1/1) for progesterone, 17 $\beta$ -estradiol and nifedipine

Compound	logP(exp.)	Molar Volume <sup>a</sup>	Polar surface area <sup>b</sup>	Molar solubilization capacity in PS80	Molar solubilization capacity in PS80/OA(1/1)
Progesterone	4.14	441	34.1	0.05	0.05
17 $\beta$ -estradiol	4.20	385	40.5	0.03	0.02
Nifedipine	3.63	418	110	0.05	0.03

<sup>a</sup> Calculated from the crystal data obtained from the Cambridge Structure Database

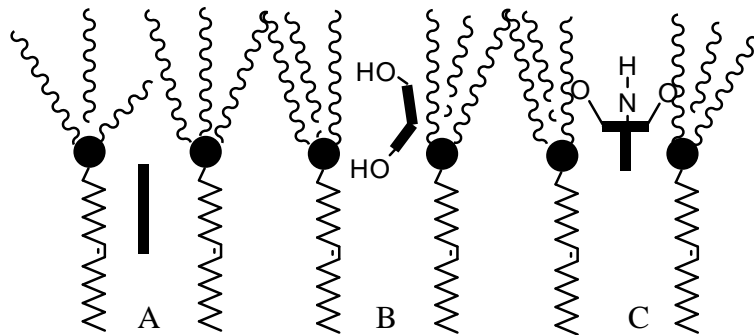
<sup>b</sup> From Scifinder®. Calculated using Advanced Chemistry Development (ACD/Labs) Software V11.02.

With respect to the polarity, the rank order of logP and polar surface area is nifedipine > 17 $\beta$ -estradiol > progesterone. Progesterone is considered to be a non-polar compound, 17 $\beta$ -estradiol is semipolar and nifedipine is most polar. El Eini and Barry have shown that the polyoxyethylene surfactants formed heavily-hydrated micelles (El Eini, Barry et al., 1973; El Eini, Barry et al., 1976). The number of water molecules varied from 5.2 per ethylene oxide unit for C<sub>16</sub>OE<sub>17</sub> to 10.5 for C<sub>16</sub>OE<sub>63</sub> (El Eini, Barry et al., 1976). Most of this water is associated the outer part of polyoxyethylene chain, with very little closer to the hydrocarbon core due to the crowding of polyoxyethylene chain. Therefore, micelles formed by a polyoxyethylene surfactant like PS80 offer a wide range of polarity for solubilization of various drugs with different polarity. A likely site for non-polar progesterone would be close to the hydrocarbon core. This was supported by the solubilization of progesterone in mixed micelles of PS80/OA where the molar solubilization capacity was insensitive to the molar fraction of OA. Of course, this assumes that the size of micelles was not changed with increasing the OA content. Additional support for the localization of progesterone close to the hydrocarbon core was provided studies of the solubilization of hydrocortisone, dexamethasone, testosterone and progesterone by the long-chain polyoxyethylene ether nonionic surfactants (El Eini,

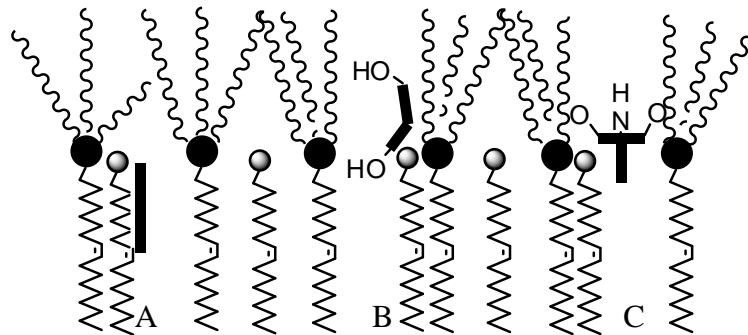
Barry et al., 1976). These authors observed that the molar solubilization capacities increased as the polyoxyethylene chain length increased. By calculating thermodynamic parameters for solubilization, less polar steroids, testosterone and progesterone, were thought to be solubilized in the region close to hydrocarbon core.

In the present study, the locus of the semipolar drug, 17 $\beta$ -estradiol, and the most polar drug, nifedipine, is likely at the interface. This was evident by the change of NMR chemical shifts on PS80 protons which are located at the interface. In addition, the molar solubilization capacity decreased with increasing molar ratio of OA in the mixed micelles (Table 6.11) suggesting that the solubilization of 17 $\beta$ -estradiol and nifedipine is less controlled by the hydrocarbon core but more dependent upon the chemical environment of the surface of the micelles.

The proposed loci of solubilization are shown in Schemes 6.6a and 6.6b. With the flat conformation and the non-polar function group, progesterone is most easily solubilized in the region close to the hydrocarbon core. The observed molar solubilization capacities for progesterone possibly reflected the constant core volume in spite of changing the molar ratio of PS80 to OA. The solubilization of nifedipine and 17 $\beta$ -estradiol at the interface close to the corona is favored due to the more polar property and the possible formation of hydrogen bonding between the polyoxyethylene chain and the drug. As a result, the insertion of molecules between the head groups is less favored in the mixed micelles with a high content of OA. The linear relationship between the molar solubilization capacity of the PS80/OA mixed micelle with the molar fraction of PS80 (Figure 5.10) indicated the solubilization of nifedipine is strongly related to the content of PS80 and suggested considerable amount of nifedipine is solubilized in the corona. Such a linear relationship was not observed on 17 $\beta$ -estradiol indicating that a less significant amount of drug solubilized in the corona area compared to that solubilized at interface.



Scheme 6.6a Possible loci of drugs in the PS80 micelles



Scheme 6.6b Possible loci of drugs in the PS80/OA (1/1) mixed micelles

## 6.5. Conclusions

The apparent  $pK_a$  of OA in the micellar solution of PS80 was determined to be 7.1 and independent of the composition. Ionized OA acted as an anionic surfactant and formed mixed micelles with PS80. The size of mixed micelles was independent of the composition giving a similar value to PS80 micelles. One type of mixed micelles was confirmed by PGSE-NMR and DLS methods in the absence of bile salt/phospholipid. However, the presence of bile salt/phospholipids rendered the identification of a single micelle structure difficult. Together with solubilization determination, it is suggested that only one type of PS80/OA micelle exists. Other aggregates may exist at such low content that the contribution to the total solubilization was negligible. Prominent changes of NMR chemical shifts on protons which are located on the interface of the hydrocarbon tail and the hydrophilic corona formed by the polyoxyethylene chain suggested that 17- $\beta$

estradiol and nifedipine were solubilized on the interface of micelles. Strong interactions between nifedipine and PS80 were further evident by Fourier transform infrared spectroscopy (FTIR) indicating that considerable amount of nifedipine is also solubilized in the corona area. The different solubilization behavior of three model drugs may result from the different loci in micelles.



## Chapter 7

### Conclusions and Future Studies

In summary, the following experimental results have been observed:

- 1) The dynamic *in vitro* lipolysis model was sensitive to different ester-containing substrates under the optimal conditions. The variation of the extent of lipolysis as a measured production of fatty acid was within the acceptable range in-a-day and day-to-day. The dynamic *in vitro* lipolysis model is a suitable method to study the mechanism of the drug solubilization during the lipolysis of model LBDDSs.
- 2) We hypothesized that the lipolysis of PS80 in the model LBDDS results in a supersaturated state for model poorly-water soluble compounds. A supersaturated state for model poorly-water soluble drugs resulted from the lipolysis of PS80. Progesterone showed the least stability in a supersaturated state while 17 $\beta$ -estradiol showed the most stability in a supersaturated state.
- 3) As hypothesized, the extent of the supersaturation decreased for progesterone and increased for 17 $\beta$ -estradiol while reaching a maximum for nifedipine within 2 hrs as the lipolysis of PS80 progressed. The extent of the supersaturation of model drugs was dependent upon the initial drug concentration and the extent of the hydrolysis of formulation.
- 4) The equilibrium solubilization capacity decreased for 17 $\beta$ -estradiol and nifedipine while it remained constant for progesterone as a molar fraction of PS80 reduced in the model mixed micellar solutions composed of selected lipolytic products. This was in tune with the experimental results obtained in the lipolytic products produced during the *in vitro* lipolysis of a blank formulation.
- 5) Our second hypothesis was that it is possible to correlate the equilibrium solubilization of model drugs formulated in PS80 under simulated intestinal conditions by accounting for the solubilization behavior in lipid aggregates generated during lipolysis. The equilibrium solubilization of nifedipine in the dispersed model

LBDDS under simulated intestinal conditions was predicted successfully by the model mixed micellar solutions composed of lipolytic products. However, model mixed micellar solutions were only moderately successful in predicting the extent of solubilization of  $17\beta$ -estradiol and least successful in predicting the extent solubilization of progesterone.

- 6) The characterization of model mixed micelles composed of selected lipolytic products by NMR, DLS and acid-base titration showed that the size of mixed micelles and ionization of micellar oleic acid are independent of the composition of PS80 and OA. Independence of size and ionization of anionic surfactant indicated that the different solubilization behavior of drugs resulted from the different loci of solubilization in the micelles which were further supported by change of surfactant chemical shifts in the presence of drugs, nefedipine and  $17\beta$ -estradiol.

The overall goal of the current dissertation is to provide a better understanding of the capability of lipoidal components in a model LBDDS formulation to create and maintain a drug in a supersaturated state in simulated GI conditions as well as those factors that affect drugs in a supersaturated state. Possible future studies are as follows:

- I. The capability to create and maintain drugs in a supersaturated state in simulated GI tract conditions could be further evaluated on other ester-containing surfactants such as Cremophor RH40, Cremophor EL and TPGS. The ultimate goal is to quantify the relationship between the properties of lipoidal components and capability to create and maintain drugs in a supersaturated state in the GI tract conditions and provide guidance for excipients selection.
- II. With the selected lipoidal excipients, the relationship between the properties of drugs and capability to be maintained in a supersaturated state in simulated GI tract conditions could be further quantified by the methodologies used in this dissertation. This may facilitate the formulation development for a new API.
- III. We could build upon this knowledge with more sophisticated formulations including lipoidal excipients other than surfactants. Eventually, *in vivo* performance of LBDDSs could be predicted reliably by the *in vitro* performance in simulated GI tract conditions.

By probing the physicochemical mechanism of solubilization of poorly-water soluble drugs in the GI tract when administered by LBDDSs, a better understanding of interactions between poorly-water soluble drugs and digestible excipients under conditions in the GI tract will emerge.

## APPENDIX

### **Appendix 1. Studies with nifedipine**

#### **A1.1. Solid characterization of nifedipine collected in determination of equilibrium solubility**

Nifedipine was used as received in all solubility studies. An excess amount of nifedipine was added to the tris maleate buffer (pH 7.5) and rotated for two weeks in a  $37\pm 0.5^\circ\text{C}$  incubator. The remaining solid was collected, dried by nitrogen and then dried in a vacuum chamber at ambient temperature overnight. Samples were characterized by differential scanning calorimetry (DSC). Two commercial standards (NIF-std1 and NIF-std2) and two independent collected samples (NIF-sample 1 and sample 2) were weighed into individual aluminum DSC pans and encapsulated. Nitrogen at a flow rate of 60 mL/min was used as the purge gas. The temperature of each sample was decreased to  $-15^\circ\text{C}$  at  $20^\circ\text{C}/\text{min}$  and equilibrated at this temperature for 15 min. The temperature was then increased to  $350^\circ\text{C}$  at  $5^\circ\text{C}/\text{min}$ .

#### **A1.2. Stability assay for nifedipine**

##### **A1.2.1. Stability when exposed to natural light**

Three groups of samples, four samples in each of group, were prepared. A nifedipine solution was prepared by adding 100  $\mu\text{L}$  of stock solution in acetonitrile to a 9.9 mL tri maleate buffer (pH 7.88 at room temperature and pH 7.50 at  $37^\circ\text{C}$ ). The solution was divided into 12 individual HPLC vials, eight of which were amber glass vials and four were clear glass vials. The amber glass vials were also wrapped in aluminum foil. Four vials were stored at room temperature and four vials at  $37^\circ\text{C}$ . Four samples in clear glass vials were exposed to natural light at room temperature. Samples from each group were taken at times 0 h, 2 h, 19 h, and 24 h and kept at  $-20^\circ\text{C}$ . All samples were analyzed by the validated method. The stability was assessed by the area of the 7.8 min peak.

### **A1.2.2. Stability in the presence of enzyme**

To test if the ester functional groups of nifedipine can be hydrolyzed by components of the enzyme preparation, the following experiments were conducted. The enzyme solution was prepared according to the standard protocol (Section 3.3.4). The pH of tris-maleate buffer was adjusted to 7.5 at  $37\pm 0.5$  °C. To 14.85 mL of buffer was added 150  $\mu$ L of stock solution in acetonitrile to make a total volume of 15 mL. The final acetonitrile was 1% v/v. The solution was incubated about 3 min at 37 °C and distributed into six individual amber vials, 2 mL each. These six vials were categorized into three groups. One vial in the 1<sup>st</sup> group (G1) was taken as time zero and contained no enzyme preparation. One vial in the 2<sup>nd</sup> group (G2) was taken as the control by adding inactivated enzyme (see Section 4.3.4). The third group included four vials (G3-1, -2, -3, -4) to which were added active enzyme preparation at the concentration of 0.08 mL enzyme solution/total solution. All samples were incubated in a  $37\pm 1$ °C water bath. Samples were taken at 1 h, 2 h, 4 h and 24 h. To achieve the same initial concentration in each vial, 160  $\mu$ L of buffer was added to G1, 160  $\mu$ L of inactivated enzyme solution was added to G2 and 160  $\mu$ L of active enzyme solution was added to the G3 vials. At the appropriate time each sample was filtered and diluted with an equal volume of acetonitrile. All samples were analyzed by HPLC. The stability was assessed by the area of the peak eluting at 7.8 min.

### **A1.3. Results and Discussion**

#### **A1.3.1. Stability of drug**

The photosensitivity of nifedipine has been reported in detail (Schmid, Perry et al., 1988; Logan and Patrick, 1990; Grundy, Kherani et al., 1994). Under our laboratory conditions, the photosensitivity of nifedipine was re-examined, especially under exposure to natural light. Nifedipine has two ester functional groups as shown in Figure 4.1. Since esters are the primary target of pancreatic lipase, one stability concern might be that the nifedipine could be hydrolyzed by this or other enzymes in the preparation. Moreover, the ester bond is often more susceptible to hydrolysis under base conditions. Thus, the chemical stability of nifedipine in the absence and presence of an enzyme preparation and upon exposure to natural light were evaluated in the tris maleate buffer (pH7.5) at ambient temperature and at  $37\pm 0.5$ °C.

#### A1.3.1.1. Stability as exposed to natural light

In the chromatogram, a peak eluting at 6.68 min increased while the peak of nifedipine eluting at 7.67 min decreased (Figure A1.1) indicating that nifedipine was degraded by exposure to natural light. Due to the photosensitivity, all further experiments with nifedipine were carried out under low light conditions. The area under the peak eluting at 7.8 min is plotted as a function of time (Figure A1.2). When sample solutions were protected from natural light, the 7.8 min peak remained relatively constant up to 24 h at ambient temperature and at  $37\pm 0.5^\circ\text{C}$ . However, a dramatic decrease of peak area was observed as the sample solutions were exposed to natural light. After 19 h of exposure to natural light, only 7% of nifedipine was detected in the solution.

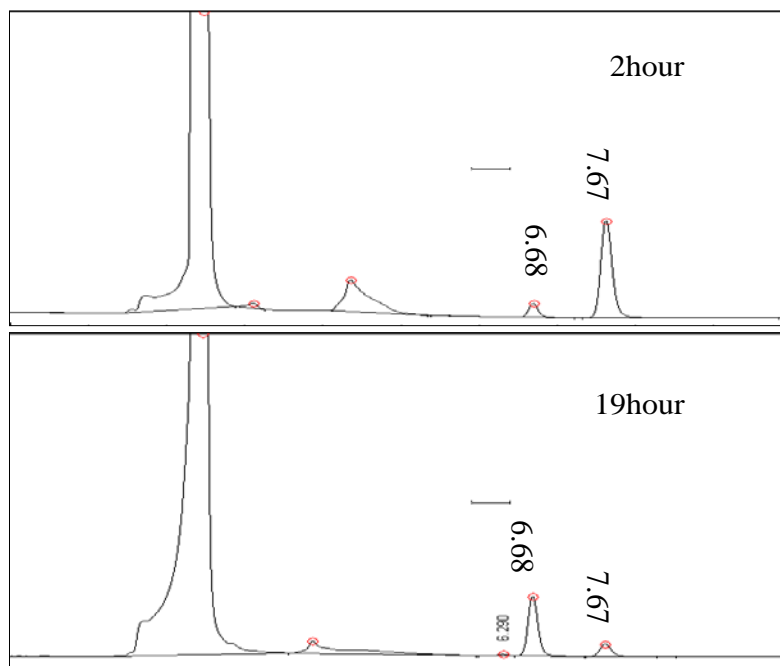


Figure A1.1 HPLC chromatograms of nifedipine exposed to natural light at 2 h and 19 h at ambient temperature

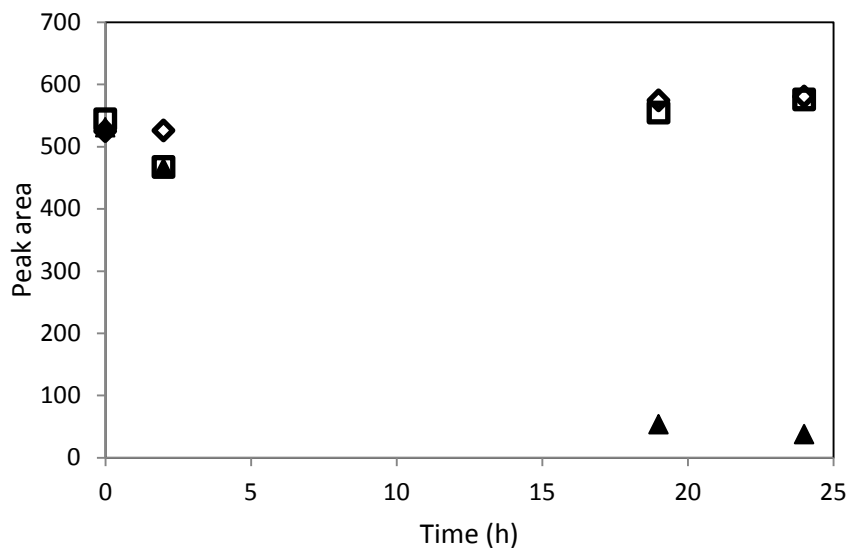


Figure A1.2 The area of the nifedipine peak under ambient temperature (diamond) and  $37\pm 0.5^{\circ}\text{C}$  (square) protected from exposure to natural light, and upon exposure to natural light at ambient temperature (triangle)

#### **A1.3.1.2. Stability in the presence of enzyme**

For comparison purposes, two control samples (G1 and G2) were prepared and chromatogram peak areas were determined. Sample G1 included nifedipine in a tris maleate buffer and sample G2 was prepared in the presence of an inactivated enzyme. As shown in Table A1.1, within an RSD of 1%, peak areas in all groups were identical indicating that there was no degradation of nifedipine in the presence of an enzyme preparation and in solution at pH 7.5 at  $37^{\circ}\text{C}$ . In addition, measurement of the peak area in the presence of an inactivated enzyme indicated nifedipine did not bind to the enzyme protein.

Table A1.1 The stability of nifedipine in the presence or absence of pancreatic enzyme

Time(h)	Sample	Retention time(min.)	Peak Area
with no enzyme preparation			
	G1	7.63	545.34
with inactive enzyme preparation			
	G2	7.64	551.19
with active enzyme			
1	G3-1	7.67	549.14
2	G3-2	7.65	546.69
4	G3-3	7.66	559.14
24	G3-4	7.65	558.00

#### A1.3.1.3. Polymorphic form of nifedipine

The excess solid material collected from the solubility samples prepared in tris maleate buffer (pH7.5) was characterized by DSC. The DSC trace of collected samples was identical to that of the original commercial material used for solubility analysis (Sigma-Aldrich, St. Louis, MO, USA). The DSC plots are shown in Figures A1.3a and A1.3b. The melting point of collected samples (~173°C) was the same as that of the starting material (commercial) and consistent with the reported melting point of the most stable polymorph (Grooff, De Villiers et al., 2007).

Three polymorphic forms (I, II and III) had been reported for nifedipine (Burger and Koller, 1996). The DSC results confirm that the commercial nifedipine is form I (most stable). Tiggle, et al. have reported the crystal structure of form I (Triggle, Shefter et al., 1980). Four 1,4-dioxane solvates and a dihydrate form have also been reported. The melting point dihydrate form is 165°C and its solubility (3.01±0.56 µg/ mL) in water is lower than that of the form I at 30°C (Caira, Robbertse et al., 2003). The hydrate form arises from a 1,4-dioxane solvate in water. It is not formed in the mixture of organic



solvent with water such as dioxane: water, methanol: water and ethanol: water. Caira, et al. found that the hydrated form is not stable and converted to the stable form I very rapidly. Conclusively, there was no new polymorph appearing during the incubation for equilibrium solubility.

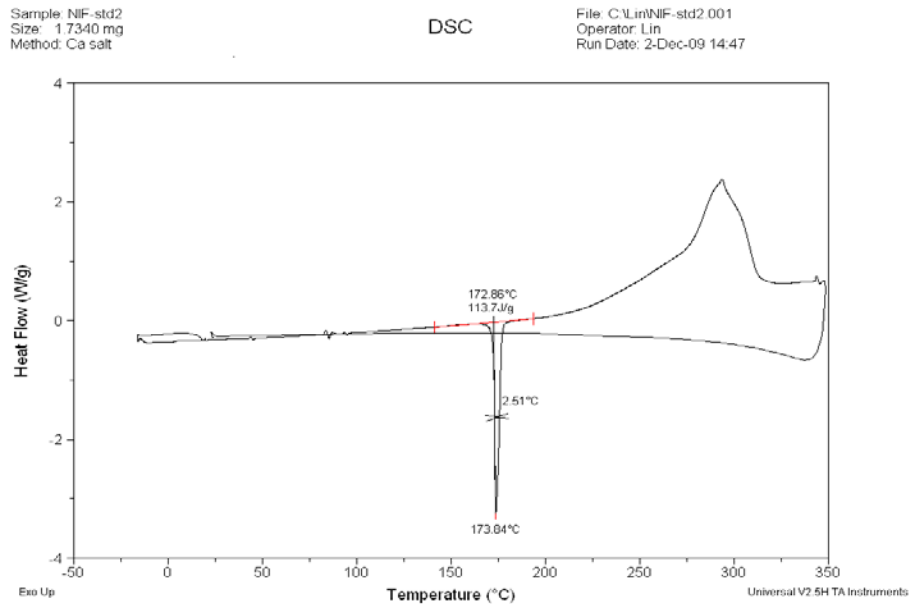


Figure A1.3a DSC plot of commercial nifedipine

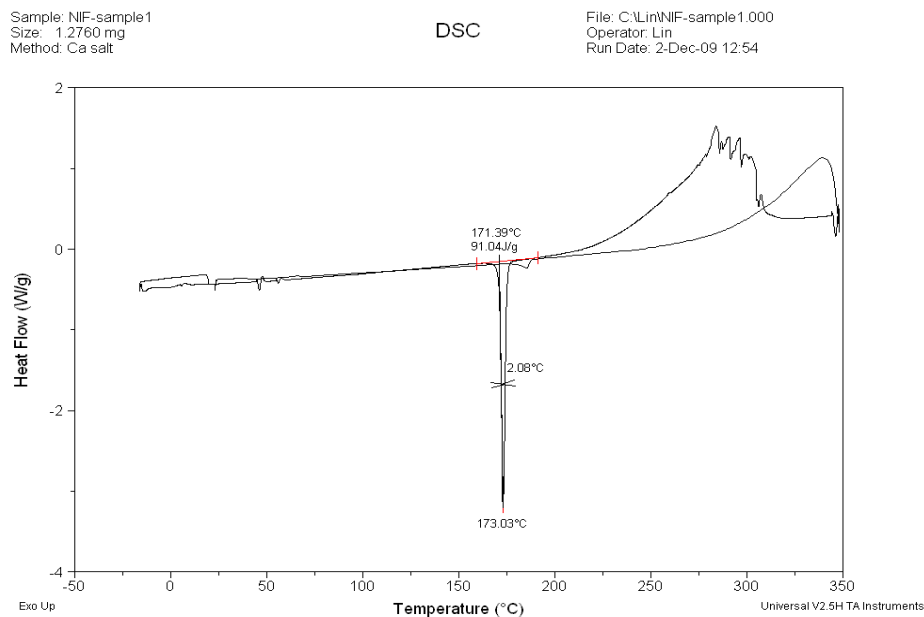


Figure A1.3b DSC plot of collected solid material from the determination of aqueous solubility of nifedipine in tris maleate buffer at 37°C (pH7.5)

## Appendix 2. Surfactant composition during the lipolysis of formulations

The lipolytic products of PS80 are PEG (20) sorbitan and oleate (Scheme 4.1). The PEG (20) sorbitan is water soluble and is assumed not to be a component of any lipid aggregates. Fatty acid and PS80 are amphiphilic species able to form aggregates when the concentration exceeds that of the critical micellar concentration. During lipolysis, a mole of PS80 will release 1 mole of fatty acid and thus the total molar concentration of PS80 plus fatty acid was maintained constant. The calculated fatty acid released from PS80 and molar ratios of PS80 to fatty acid in the period of 120 min are listed in Tables A2.1- A2.4. Due to the viscosity of the formulation, the amount of formulation added was calculated by subtracting the weight of the transfer pipette before and after addition of the formulation to SIFs buffer from the total weighed formulation. Therefore, it is impossible to give the exact same initial concentration of PS80 for each repetition. The protocol was strictly followed to reduce the variation of the initial concentration to a minimum. The variation of weight of formulation was 5% within progesterone-loaded formulations, 4% within nifedipine-loaded formulation and 2% within 17 $\beta$ -estradiol-loaded formulation, respectively. To truly reflect the alteration of composition, the molar ratio of PS80 to

fatty acid was calculated. The molar ratio of PS80 to fatty acid is related not only to the released fatty acid but also to the initial concentration of PS80. During the lipolysis of the blank PS80, the molar ratio changed from  $11.42 \pm 0.30$  at 5 min to  $0.73 \pm 0.09$  at 120 min (Table 5.2). Generally, the greater variations on the molar ratio were observed in the first 10 min across all the formulations tested. The values from the lipolysis of drug-loaded formulations were higher than those in the lipolysis of the blank formulation at 5 min and 10 min. Within drug-loaded formulations, the molar ratios in the lipolysis of E-14 mg/g were  $23.13 \pm 2.41$   $\mu\text{mol}$  and  $9.37 \pm 0.74$  at 5 min and 10 min, respectively. The values were significantly higher than those in the lipolysis of E-5 mg/g and E-7 mg/g. Also, a relatively high value was seen in the lipolysis of N-11 mg/g at 5 min. The molar ratios at 15 min, 30 min, 60 min and 120 min were unchanged in all cases.

Table A2.1 Fatty acid (FA) released from PS80 and molar ratio of PS80 to fatty acid released from PS80 during the lipolysis of blank formulation

Time(min.)	FA from PS80 ( $\mu\text{mol} \pm \text{SD}$ )	Molar ratio of PS80/FA from PS80
5	$14.93 \pm 0.36$	$11.42 \pm 0.30$
10	$28.57 \pm 1.28$	$5.50 \pm 0.29$
15	$40.30 \pm 1.53$	$3.60 \pm 0.18$
30	$68.50 \pm 2.73$	$1.71 \pm 0.11$
60	$95.02 \pm 3.96$	$0.95 \pm 0.08$
120	$107.58 \pm 5.25$	$0.73 \pm 0.09$

Table A2.2 Fatty acid (FA) released from PS80 and molar ratios of PS80 to fatty acid released from PS80 during the lipolysis of progesterone-loaded formulations

FA from PS80 ( $\mu\text{mol}\pm\text{SD}$ )			
Time (min)	P-12	P-20	P-31
5	14.93 $\pm$ 0.59	12.57 $\pm$ 2.31	12.94 $\pm$ 2.12
10	25.07 $\pm$ 1.65	23.94 $\pm$ 1.55	22.79 $\pm$ 1.95
15	35.27 $\pm$ 2.65	34.70 $\pm$ 2.60	31.26 $\pm$ 3.19
30	61.10 $\pm$ 6.10	60.57 $\pm$ 4.13	55.3 $\pm$ 3.35
60	92.33 $\pm$ 6.62	90.65 $\pm$ 5.36	88.65 $\pm$ 3.24
120	108.08 $\pm$ 2.01	107.68 $\pm$ 6.80	106.12 $\pm$ 7.06
Molar ratio of PS80/FA from PS80			
5	11.61 $\pm$ 0.64	14.72 $\pm$ 2.06	14.59 $\pm$ 2.99
10	6.53 $\pm$ 0.66	7.13 $\pm$ 0.17	7.72 $\pm$ 0.94
15	4.36 $\pm$ 0.57	4.61 $\pm$ 0.26	5.37 $\pm$ 0.77
30	2.11 $\pm$ 0.40	2.21 $\pm$ 0.16	2.58 $\pm$ 0.24
60	1.05 $\pm$ 0.9	1.15 $\pm$ 0.05	1.23 $\pm$ 0.03
120	0.74 $\pm$ 0.07	0.81 $\pm$ 0.02	0.86 $\pm$ 0.12

Table A2.3 Fatty acid (FA) released from PS80 and molar ratios of PS80 to fatty acid released from PS80 during the lipolysis of 17 $\beta$ -estradiol-loaded formulations

FA from PS80 ( $\mu\text{mol}\pm\text{SD}$ )			
Time (min)	E-5	E-7	E-14
5	12.58 $\pm$ 1.34	12.44 $\pm$ 1.99	8.40 $\pm$ 0.89
10	23.63 $\pm$ 3.54	23.56 $\pm$ 1.67	19.48 $\pm$ 1.37
15	29.75 $\pm$ 0.92	34.32 $\pm$ 0.96	29.84 $\pm$ 1.71
30	61.10 $\pm$ 10.61	61.61 $\pm$ 1.31	55.40 $\pm$ 3.69
60	99.60 $\pm$ 12.09	97.62 $\pm$ 2.43	90.95 $\pm$ 6.09
120	121.60 $\pm$ 11.67	117.02 $\pm$ 3.96	112.45 $\pm$ 5.78
Molar ratio of PS80/FA from PS80			
5	15.29 $\pm$ 1.65	15.81 $\pm$ 2.32	23.13 $\pm$ 2.41
10	7.72 $\pm$ 1.26	7.78 $\pm$ 0.57	9.37 $\pm$ 0.74
15	5.85 $\pm$ 0.25	5.01 $\pm$ 0.11	5.76 $\pm$ 0.34
30	2.39 $\pm$ 0.57	2.35 $\pm$ 0.08	2.64 $\pm$ 0.22
60	1.06 $\pm$ 0.24	1.11 $\pm$ 0.03	1.22 $\pm$ 0.13
120	0.68 $\pm$ 0.15	0.76 $\pm$ 0.03	0.79 $\pm$ 0.08

Table A2.4 Fatty acid (FA) released from PS80 and molar ratio of PS80 to fatty acid released from PS80 during the lipolysis of nifedipine-loaded formulations

FA from PS80 ( $\mu\text{mol}\pm\text{SD}$ )			
Time (min)	N-11	N-20	N-35
5	6.11 $\pm$ 1.80	10.80 $\pm$ 2.29	13.31 $\pm$ 1.65
10	20.22 $\pm$ 3.20	26.17 $\pm$ 4.52	20.96 $\pm$ 4.31
15	33.74 $\pm$ 2.90	40.44 $\pm$ 6.20	30.26 $\pm$ 3.85
30	65.18 $\pm$ 3.50	71.04 $\pm$ 7.50	59.49 $\pm$ 2.70
60	97.10 $\pm$ 3.68	96.15 $\pm$ 4.26	96.43 $\pm$ 1.79
120	111.63 $\pm$ 2.30	108.13 $\pm$ 1.35	115.93 $\pm$ 1.15
Molar ratio of PS80/FA from PS80			
5	31.83 $\pm$ 8.92	16.98 $\pm$ 4.24	14.36 $\pm$ 1.54
10	8.57 $\pm$ 1.60	6.32 $\pm$ 1.25	8.93 $\pm$ 1.87
15	4.67 $\pm$ 0.60	3.72 $\pm$ 0.77	5.76 $\pm$ 0.68
30	1.92 $\pm$ 0.22	1.66 $\pm$ 0.29	2.42 $\pm$ 0.26
60	0.96 $\pm$ 0.11	0.96 $\pm$ 0.08	1.10 $\pm$ 0.11
120	0.70 $\pm$ 0.07	0.74 $\pm$ 0.03	0.75 $\pm$ 0.08

Based on the data in Tables A2.1 to A2.4 is feasible to prepare series of model systems to represent the composition of lipolytic products in the time course of lipolysis. The major fatty acid released from the PS80 is oleic acid. Therefore, the molar PS80/OA were chosen as 9/1, 8/2, 7/3, 6/4, 5/5 where the molar fractions of PS80 in the mixture were 0.9, 0.8, 0.7, 0.6 and 0.5. The range of molar ratios covered the composition from about 5 min to 120 min of *in vitro* lipolysis. The mixtures with known composition were prepared for future solubilization studies.

### Appendix 3. Calculation of aggregation number, total micelle surface area and total micelle core volume

Theoretically, the volume of a spherical micelle ( $V$ ) can be calculated by Eq. (A3.1)

$$V = f_1V_1 + f_2V_2 \quad (\text{A3.1})$$

Where the  $f_1$  and  $f_2$  are molar fractions of PS80 and OA in the mixture;  $V_1$  and  $V_2$  are molecular volumes of PS80 and OA, which are taken as 2004 and 514  $\text{\AA}^3$ , respectively (Croy and Kwon, 2005). The aggregation number is calculated by Eq. (A3.2)

$$N_{\text{agg}} = \frac{4\pi r^3}{3V} \quad (\text{A3.2})$$

Where  $r$  is the radius of micelles measured by PGSE-NMR (Figure A3.1).

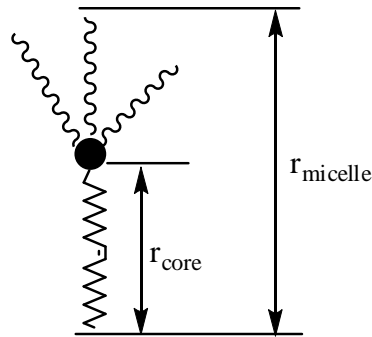


Figure A3.1 The schematic presentation of radius of hydrophobic core ( $r_{\text{core}}$ ) and radius of micelle ( $r_{\text{micelle}}$ )

One mole of surfactant solution contains of  $6.02 \times 10^{23}$  surfactant molecules. Thus, the micelle number is

$$N_{\text{micelle}} = \frac{6.02 \times 10^{23}}{N_{\text{agg}}} \quad (\text{A3.3})$$

By knowing the micelle number of 1 mole of surfactant solution, the total interface surface area ( $A_{\text{total}}$ ) and total core volume of micelle ( $V_{\text{total}}$ ) will be calculated by Eq. (A3.4) and Eq. (A3.5).

$$A_{\text{total}} = A_{\text{core}} \times N_{\text{micelle}} \quad (\text{A3.4})$$

$$V_{\text{total}} = V_{\text{core}} \times N_{\text{micelle}} \quad (\text{A3.5})$$

Where  $A_{\text{core}}$  is the interface surface area/micelle and  $V_{\text{core}}$  is the core volume of hydrophobic tail/micelle, calculated by Eq. (A3.6) and Eq. (A3.7) (Stokes and Fennell Evans, 1997)

$$V_{\text{core}} = (27.4 + 26.9n) \times N_{\text{agg}} \quad (\text{A3.6})$$

$$A_{\text{core}} = 4\pi (1.5 + 1.265n)^2 \times N_{\text{agg}} \quad (\text{A3.7})$$

where  $n$  is the carbon number of hydrophobic tail.



## Reference

- Abdel-Mottaleb, M. M. A. and A. Lamprecht (2011). "Standardized in vitro drug release test for colloidal drug carriers using modified USP dissolution apparatus I." Drug Development and Industrial Pharmacy **37**(2): 178-184.
- Aizawa, H. (2009). "Morphology of Polysorbate 80 (Tween 80) micelles in aqueous 1,4-dioxane solutions." Journal of Applied Crystallography **42**(4): 592-596.
- Akhter, M. S. (1997). "Effect of acetamide on the critical micelle concentration of aqueous solutions of some surfactants." Colloids and Surfaces A: Physicochemical and Engineering Aspects **121**(2-3): 103-109.
- Almog, S., T. Kushnir, et al. (1986). "Kinetics and structural aspects of reconstitution of phosphatidylcholine vesicles by dilution of phosphatidylcholine-sodium cholate mixed micelles." Biochemistry **25**(9): 2597-2605.
- Almog, S., B. J. Litman, et al. (1990). "States of aggregation and phase transformations in mixtures of phosphatidylcholine and octyl glucoside." Biochemistry **29**(19): 4582-4592.
- Aloulou, A., J. A. Rodriguez, et al. (2006). "Exploring the specific features of interfacial enzymology based on lipase studies." Biochimica et Biophysica Acta (BBA) - Molecular and Cell Biology of Lipids **1761**(9): 995-1013.
- Alvarez-Núñez, F. A. and S. H. Yalkowsky (2000). "Relationship between Polysorbate 80 solubilization descriptors and octanol-water partition coefficients of drugs." International Journal of Pharmaceutics **200**(2): 217-222.
- Alvarez, F. J. and V. J. Stella (1989). "The role of calcium ions and bile salts on the pancreatic lipase-catalyzed hydrolysis of triglyceride emulsions stabilized with lecithin." Pharmaceutical Research **6**(6): 449-457.
- Amidon, G. E., W. I. Higuchi, et al. (1982). "Theoretical and experimental studies of transport of micelle-solubilized solutes." Journal of Pharmaceutical Sciences **71**: 77-84.
- Amidon, G. E., W. I. Higuchi, et al. (1982). "Theoretical and experimental studies of transport of micelle-solubilized solutes." Journal of Pharmaceutical Sciences **71**(1): 77-84.
- Amidon, G. L., H. Lennernäs, et al. (1995). "A theoretical basis for a biopharmaceutic drug classification: the correlation of in vitro drug product dissolution and in vivo bioavailability." Pharmaceutical Research **12**(3): 413-420.
- Andersson, L., B. Sternby, et al. (1994). "Hydrolysis of Phosphatidylethanolamine by Human Pancreatic Phospholipase A2: Effect of Bile Salts." Scandinavian Journal of Gastroenterology **29**(2): 182-187.
- Apperley, D. C., A. H. Forster, et al. (2005). "Characterisation of indomethacin and nifedipine using variable-temperature solid-state NMR." Magnetic Resonance in Chemistry **43**(11): 881-892.
- Atef, E. and A. A. Belmonte (2008). "Formulation and in vitro and in vivo characterization of a phenytoin self-emulsifying drug delivery system (SEDDS)." European Journal of Pharmaceutical Sciences **35**(4): 257-263.
- Aungst, B. J. (2000). "Intestinal permeation enhancers." Journal of Pharmaceutical Sciences **89**(4): 429-442.

- Balakrishnan, A., B. D. Rege, et al. (2004). "Surfactant-mediated dissolution: Contributions of solubility enhancement and relatively low micelle diffusivity." Journal of Pharmaceutical Sciences **93**(8): 2064-2075.
- Balakrishnan, P., B-J. Lee, et al. (2009). "Enhanced oral bioavailability of Coenzyme Q10 by self-emulsifying drug delivery systems." International Journal of Pharmaceutics **374**(1-2): 66-72.
- Bernardez, L. A. (2008). "Investigation on the locus of solubilization of polycyclic aromatic hydrocarbons in non-ionic surfactant micelles with <sup>1</sup>H NMR spectroscopy." Colloids and Surfaces A: Physicochemical and Engineering Aspects **324**(1-3): 71-78.
- Bhat, P. A., A. A. Dar, et al. (2008). "Solubilization capabilities of some cationic, anionic, and nonionic surfactants toward the poorly water-soluble antibiotic drug erythromycin." Journal of Chemical and Engineering Data **53**(6): 1271-1277.
- Borges, C. P. F., I. E. Borissevitch, et al. (1995). "Charge- and pH-dependent binding sites of dipyridamole in ionic micelles: A fluorescence study." Journal of Luminescence **65**(2): 105-112.
- Borgstrom, B., C. Erlanson-Albertsson, et al. (1979). "Pancreatic colipase: chemistry and physiology." Journal of Lipid Research **20**(Copyright (C) 2011 U.S. National Library of Medicine.): 805-816.
- Borné, J., T. Nylander, et al. (2002). "Effect of lipase on monoolein-based cubic phase dispersion (cubosomes) and vesicles." The Journal of Physical Chemistry B **106**(40): 10492-10500.
- Borst, P. and R. O. Elferink (2002). "Mammalian ABC transporters in health and disease." Annual Review of Biochemistry **71**(1): 537.
- Boucrot, P. (1972). "Is there an entero-hepatic circulation of the bile phospholipids?" Lipids **7**(5): 282-288.
- Brewster, M. E., R. Vandecruys, et al. (2008). "Comparative interaction of 2-hydroxypropyl-[beta]-cyclodextrin and sulfobutylether-[beta]-cyclodextrin with itraconazole: Phase-solubility behavior and stabilization of supersaturated drug solutions." European Journal of Pharmaceutical Sciences **34**(2-3): 94-103.
- Brown, W., Z. Pu, et al. (1988). "Size and shape of nonionic amphiphile micelles: NMR self-diffusion and static and quasi-elastic light-scattering measurements on C12E5, C12E7, and C12E8 in aqueous solution." The Journal of Physical Chemistry **92**(21): 6086-6094.
- Burger, A. and K. Koller (1996). "Polymorphis and pseudopolymorphism on nifedipine." Scientia Pharmaceutica **64**: 293-301.
- Caira, M. R., Y. Robbertse, et al. (2003). "Structural characterization, physicochemical properties, and thermal stability of three crystal forms of nifedipine." Journal of Pharmaceutical Sciences **92**(12): 2519-2533.
- Chakrabarti, S. B., F. M (1978). "Bioavailability of phenytoin in lipid-containing dosage forms in rats. ." J. Pharm. Pharmacol **30**: 330-331.
- Chakraborty, S., D. Shukla, et al. (2009). "Assessment of solubilization characteristics of different surfactants for carvedilol phosphate as a function of pH." Journal of Colloid and Interface Science **335**(2): 242-249.

- Charman, S. A., W. N. Charman, et al. (1992). "Self-emulsifying drug delivery systems: Formulation and biopharmaceutic evaluation of an investigational lipophilic compound." Pharmaceutical Research **9**(1): 87-93.
- Charman, W. N., C. J. H. Porter, et al. (1997). "Physicochemical and physiological mechanisms for the effects of food on drug absorption: The role of lipids and pH." Journal of Pharmaceutical Sciences **86**(3): 269-282.
- Chiu, Y.-Y., K. Higaki, et al. (2003). "Human jejunal permeability of cyclosporin A: Influence of surfactants on P-glycoprotein efflux in caco-2 cells." Pharmaceutical Research **20**(5): 749-756.
- Christensen, J. Ø., K. Schultz, et al. (2004). "Solubilisation of poorly water-soluble drugs during in vitro lipolysis of medium- and long-chain triacylglycerols." European Journal of Pharmaceutical Sciences **23**(3): 287-296.
- Clark, M. L., H. C. Lanz, et al. (1969). "Bile salt regulation of fatty acid absorption and esterification in rat everted jejunal sacs in vitro and into thoracic duct lymph in vivo." The Journal of Clinical Investigation **48**(9): 1587-1599.
- Coello, A., F. Meijide, et al. (1996). "Aggregation behavior of bile salts in aqueous solution." Journal of Pharmaceutical Sciences **85**(1): 9-15.
- Constantinides, P. P. and K. M. Wasan (2007). "Lipid formulation strategies for enhancing intestinal transport and absorption of P-glycoprotein (P-gp) substrate drugs: *In vitro-In vivo* case studies." Journal of Pharmaceutical Sciences **96**(2): 235-248.
- Cornaire, G., J. Woodley, et al. (2004). "Impact of excipients on the absorption of P-glycoprotein substrates in vitro and in vivo." International Journal of Pharmaceutics **278**(1): 119-131.
- Crommelin, D. and H. Schreier (1994). Liposomes. Colloidal drug delivery systems. J. Kreuter. New York, Basel, and Hong Kong, Marcel Dekker: 73-190.
- Crommelin, D., H. Talsma, et al. (1993). Physical stability on long term storage. Phospholipids handbook. G. Cevc. New York, Basel and Hong Kong, Marcel Dekker: 335-348.
- Crouse, R. G. (1961). "Human pharmacology of griseofulvin: The effect of fat intake on gastrointestinal absorption1." The Journal of Investigative Dermatology **37**(6): 529-533.
- Croy, S. R. and G. S. Kwon (2005). "Polysorbate 80 and cremophor EL micelles deaggregate and solubilize nystatin at the core-corona interface." Journal of Pharmaceutical Sciences **94**(11): 2345-2354.
- Cuiné, J., W. Charman, et al. (2007). "Increasing the proportional content of surfactant (Cremophor EL) relative to lipid in self-emulsifying lipid-based formulations of danazol reduces oral bioavailability in beagle dogs." Pharmaceutical Research **24**(4): 748-757.
- Cuiné, J. F., C. L. McEvoy, et al. (2008). "Evaluation of the impact of surfactant digestion on the bioavailability of danazol after oral administration of lipidic self-emulsifying formulations to dogs." Journal of Pharmaceutical Sciences **97**(2): 995-1012.
- Cunningham, K. M., R. J. Baker, et al. (1991). "Use of technetium-99m(V)thiocyanate to measure gastric emptying of fat." J Nucl Med **32**(5): 878-881.

- da Silva, F. L. B., D. Bogren, et al. (2002). "Titration of fatty acids solubilized in cationic, nonionic, and anionic micelles. Theory and Experiment." The Journal of Physical Chemistry B **106**(13): 3515-3522.
- Dahan, A. and A. Hoffman (2006). "Use of a dynamic in vitro lipolysis model to rationalize oral formulation development for poor water soluble drugs: Correlation with in vivo data and the relationship to intra-enterocyte processes in rats." Pharmaceutical Research **23**(9): 2165-2174.
- Dahan, A. and A. Hoffman (2007). "The effect of different lipid based formulations on the oral absorption of lipophilic drugs: the ability of in vitro lipolysis and consecutive ex vivo intestinal permeability data to predict in vivo bioavailability in rats. ." European Journal of Pharmaceutics and Biopharmaceutics **67**(1): 96.
- Dahan, A. and A. Hoffman (2008). "Rationalizing the selection of oral lipid based drug delivery systems by an in vitro dynamic lipolysis model for improved oral bioavailability of poorly water soluble drugs." Journal of Controlled Release **129**(1): 1-10.
- Dahan, A., A. Mendelman, et al. (2007). "The effect of general anesthesia on the intestinal lymphatic transport of lipophilic drugs: Comparison between anesthetized and freely moving conscious rat models." European Journal of Pharmaceutical Sciences **32**(4-5): 367-374.
- Dahan, A. H., A., Ed. (2006). Enhanced gastrointestinal absorption of lipophilic drugs. Enhancement in drug delivery, CRC press.
- Dahim, M. and H. Brockman (1998). "How colipase-fatty acid interactions mediate adsorption of pancreatic lipase to interfaces." Biochemistry **37**(23): 8369-8377.
- Dai, W.-G. (2010). "In vitro methods to assess drug precipitation." International Journal of Pharmaceutics **393**(1-2): 1-16.
- Dai, W.-G., L. C. Dong, et al. (2007). "Parallel screening approach to identify solubility-enhancing formulations for improved bioavailability of a poorly water-soluble compound using milligram quantities of material." International Journal of Pharmaceutics **336**(1): 1-11.
- Davey, R. J., P. T. Cardew, et al. (1986). "Rate controlling processes in solvent-mediated phase transformations." Journal of Crystal Growth **79**(1-3, Part 2): 648-653.
- Davis, A. F. and J. Hadgraft (1991). "Effect of supersaturation on membrane transport: 1. Hydrocortisone acetate." International Journal of Pharmaceutics **76**(1-2): 1-8.
- Dintaman, J. M. and J. A. Silverman (1999). "Inhibition of P-glycoprotein by D- $\alpha$ -tocopheryl polyethylene glycol 1000 succinate (TPGS)." Pharmaceutical Research **16**(10): 1550-1556.
- Dressman, J. B., G. L. Amidon, et al. (1998). "Dissolution testing as a prognostic tool for oral drug absorption: Immediate release dosage forms." Pharmaceutical Research **15**(1): 11-22.
- Dressman, J. B. and C. Reppas (2000). "In vitro-in vivo correlations for lipophilic, poorly water-soluble drugs." European Journal of Pharmaceutical Sciences **11**(Supplement 2): S73-S80.
- Drobosyuk, V. M., M. R. Borodulina, et al. (1982). "Dispersing power of resin and fatty acids." Zh. Prikl. Khim. (Leningrad) **55**(Copyright (C) 2010 American Chemical Society (ACS). All Rights Reserved.): 2105-2107.

- Dubin, P. L., J. M. Principi, et al. (1989). "Influence of ionic strength and composition on the size of mixed micelles of sodium dodecyl sulfate and Triton X-100." Journal of Colloid and Interface Science **127**(2): 558-565.
- Dyer, J., X. Lei, et al. (2008). "FT-IR characterization of the distribution of 2-phenylcycloalkanones in micellar environments." The Journal of Physical Chemistry C **112**(21): 8046-8050.
- Edwards, K., M. Silvander, et al. (1995). "Aggregate structure in dilute aqueous dispersions of oleic acid/sodium oleate and oleic acid/sodium oleate/egg phosphatidylcholine." Langmuir **11**(7): 2429-2434.
- Egelhaaf, S. U. and P. Schurtenberger (2002). "Shape transformations in the lecithin-bile salt system: from cylinders to vesicles." The Journal of Physical Chemistry **98**(34): 8560-8573.
- Egloff, M.-P., F. Marguet, et al. (1995). "The 2.46 Å resolution structure of the pancreatic lipase-colipase complex inhibited by a C11 alkyl phosphonate." Biochemistry **34**(9): 2751-2762.
- El Eini, D. I. D., B. W. Barry, et al. (1973). "Micellar properties of aqueous solutions of n-alkylpolyoxyethylene surfactants." journal of pharmacy and pharmacology **25**: suppl. 166.
- El Eini, D. I. D., B. W. Barry, et al. (1976). "Micellar size, shape, and hydration of long-chain polyoxyethylene nonionic surfactants." Journal of Colloid and Interface Science **54**(3): 348-351.
- Fatouros, D., G. Deen, et al. (2007). "Structural development of self nano emulsifying drug delivery systems (SNEDDS) during in vitro lipid digestion monitored by small-angle X-ray scattering." Pharmaceutical Research **24**(10): 1844-1853.
- Fatouros, D. G., B. Bergenstahl, et al. (2007). "Morphological observations on a lipid-based drug delivery system during in vitro digestion." European Journal of Pharmaceutical Sciences **31**(2): 85-94.
- Feinle, C., T. Rades, et al. (2001). "Fat digestion modulates gastrointestinal sensations induced by gastric distention and duodenal lipid in humans." Gastroenterology **120**(5): 1100-1107.
- Feinstein, M. E. and H. L. Rosano (1969). "Influence of micelles on titrations of aqueous sodium and potassium soap solutions." The Journal of Physical Chemistry **73**(3): 601-607.
- Feng, S. (2009). Studies on drug solubilization mechanism in simple micelle systems. Pharmaceutical Sciences Lexington, University of Kentucky. **Ph. D.**
- Fernandez, S., S. Chevrier, et al. (2009). "In vitro gastrointestinal lipolysis of four formulations of piroxicam and cinnarizine with the self emulsifying excipients Labrasol® and Gelucire® 44/14." Pharmaceutical Research **26**(8): 1901-1910.
- Fernandez, S., V. Jannin, et al. (2007). "Comparative study on digestive lipase activities on the self emulsifying excipient Labrasol®, medium chain glycerides and PEG esters." Biochimica et Biophysica Acta (BBA) - Molecular and Cell Biology of Lipids **1771**(5): 633-640.
- Fernandez, S., J.-D. Rodier, et al. (2008). "Lipolysis of the semi-solid self-emulsifying excipient Gelucire® 44/14 by digestive lipases." Biochimica et Biophysica Acta (BBA) - Molecular and Cell Biology of Lipids **1781**(8): 367-375.

- Fleisher, D., C. Li, et al. (1999). "Drug, meal and formulation interactions influencing drug absorption after oral administration: Clinical implications." Clinical Pharmacokinetics **36**(3): 233-254.
- Freie, A. B., F. Ferrato, et al. (2006). "Val-407 and Ile-408 in the  $\beta$ 5'-Loop of Pancreatic Lipase Mediate Lipase-Colipase Interactions in the Presence of Bile Salt Micelles." Journal of Biological Chemistry **281**(12): 7793-7800.
- Frijters, C. M., R. Ottenhoff, et al. (1997). "Regulation of mdr2 P-glycoprotein expression by bile salts." Biochem. J. **321**(2): 389-395.
- Gao, P., A. Akrami, et al. (2009). "Characterization and optimization of AMG 517 supersaturatable self-emulsifying drug delivery system (S-SEDDS) for improved oral absorption." Journal of Pharmaceutical Sciences **98**(2): 516-528.
- Gao, P., M. E. Guyton, et al. (2004). "Enhanced oral bioavailability of a poorly water soluble drug PNU-91325 by supersaturatable formulations." Drug Development & Industrial Pharmacy **30**(2): 221-229.
- Gao, P. and W. Morozowich (2006). "Development of supersaturatable self-emulsifying drug delivery system formulations for improving the oral absorption of poorly soluble drugs." Expert Opinion on Drug Delivery **3**(1): 97-110.
- Gao, P., B. D. Rush, et al. (2003). "Development of a supersaturatable SEDDS (S-SEDDS) formulation of paclitaxel with improved oral bioavailability." Journal of Pharmaceutical Sciences **92**(12): 2386-2398.
- Garrigues, T. M., M. J. Segura-Bono, et al. (1994). "Compared effects of synthetic and natural bile acid surfactant on xenobiotic absorption. II. Studies with sodium glycocholate to confirm a hypothesis." International Journal of Pharmaceutics **101**(3): 209-217.
- Gerakis, A. M., M. A. Koupparis, et al. (1993). "Micellar acid--base potentiometric titrations of weak acidic and/or insoluble drugs." Journal of Pharmaceutical and Biomedical Analysis **11**(1): 33-41.
- Gershkovich, P. and A. Hoffman (2007). "Effect of a high-fat meal on absorption and disposition of lipophilic compounds: The importance of degree of association with triglyceride-rich lipoproteins." European Journal of Pharmaceutical Sciences **32**(1): 24-32.
- Gershkovich, P., B. Qadri, et al. (2007). "Different impacts of intestinal lymphatic transport on the oral bioavailability of structurally similar synthetic lipophilic cannabinoids: Dexamabinol and PRS-211,220." European Journal of Pharmaceutical Sciences **31**(5): 298-305.
- Goddeeris, C., J. Coacci, et al. (2007). "Correlation between digestion of the lipid phase of smedds and release of the anti-HIV drug UC 781 and the anti-mycotic drug enilconazole from smedds." European Journal of Pharmaceutics and Biopharmaceutics **66**(2): 173-181.
- Gomez-Orellana, I. (2005). "Strategies to improve oral drug bioavailability." Expert Opinion on Drug Delivery **2**(3): 419-433.
- Griffin, B. T. and C. M. O'Driscoll (2006). "A comparison of intestinal lymphatic transport and systemic bioavailability of saquinavir from three lipid-based formulations in the anaesthetised rat model." Journal of Pharmacy and Pharmacology **58**(7): 917-925.

- Grooff, D., M. M. De Villiers, et al. (2007). "Thermal methods for evaluating polymorphic transitions in nifedipine." Thermochimica Acta **454**(1): 33-42.
- Grooff, D., W. Liebenberg, et al. (2011). "Preparation and transformation of true nifedipine polymorphs: Investigated with differential scanning calorimetry and X-Ray diffraction pattern fitting methods." Journal of Pharmaceutical Sciences **100**(5): 1944-1957.
- Grove, M., J. Nielsen, et al. (2006). "Bioavailability of seocalcitol IV: Evaluation of lymphatic transport in conscious rats." Pharmaceutical Research **23**(11): 2681-2688.
- Grove, M., G. P. Pedersen, et al. (2005). "Bioavailability of seocalcitol I: Relating solubility in biorelevant media with oral bioavailability in rats - effect of medium and long chain triglycerides." Journal of Pharmaceutical Sciences **94**(8): 1830-1838.
- Grundy, J. S., R. Kherani, et al. (1994). "Photostability determination of commercially available nifedipine oral dosage formulations." Journal of Pharmaceutical and Biomedical Analysis **12**(12): 1529-1535.
- Guzmán, H. R., M. Tawa, et al. (2007). "Combined use of crystalline salt forms and precipitation inhibitors to improve oral absorption of celecoxib from solid oral formulations." Journal of Pharmaceutical Sciences **96**(10): 2686-2702.
- Hauss, D. J., Ed. (2007). Oral lipid-based formulations : enhancing the bioavailability of poorly water-soluble drugs. Drugs and the pharmaceutical sciences, New York : Informa Healthcare.
- Hauss, D. J., S. E. Fogal, et al. (1998). "Lipid-based delivery systems for improving the bioavailability and lymphatic transport of a poorly water-soluble LTB<sub>4</sub> inhibitor." Journal of Pharmaceutical Sciences **87**(2): 164-169.
- Hermoso, J., D. Pignol, et al. (1996). "Lipase activation by nonionic detergents." Journal of Biological Chemistry **271**(30): 18007-18016.
- Hermoso, J., D. Pignol, et al. (1997). "Neutron crystallographic evidence of lipase-colipase complex activation by a micelle." EMBO J **16**(18): 5531-5536.
- Hernell, O., J. E. Staggars, et al. (1990). "Physical-chemical behavior of dietary and biliary lipids during intestinal digestion and absorption. 2. Phase analysis and aggregation states of luminal lipids during duodenal fat digestion in healthy adult human beings." Biochemistry **29**(8): 2041-2056.
- Higuchi, T. (1960). "Physical chemical analysis of the percutaneous absorption process." Journal of the Society of Cosmetic Chemists **11**: 85-97.
- Hildebrand, A., P. Garidel, et al. (2003). "Thermodynamics of demicellization of mixed micelles composed of sodium oleate and bile salts." Langmuir **20**(2): 320-328.
- Hjelm, R. P., C. D. Scheingart, et al. (1999). "Structure of conjugated bile salt-fatty acid-monoglyceride mixed colloids: studies by small-angle neutron scattering." The Journal of Physical Chemistry B **104**(2): 197-211.
- Hofmann, A. F. (1999). "The continuing importance of bile acids in liver and intestinal disease." Arch Intern Med **159**(22): 2647-2658.
- Hofmann, A. F. and B. Borgström (1962). "Physico-chemical state of lipids in intestinal content during their digestion and absorption." Federation Proceedings **21**: 43-50.
- Hofmann, A. F. and B. Borgström (1964). "The intraluminal phase of fat digestion in man: The lipid content of the micellar and oil phases of intestinal content obtained

- during fat digestion and absorption." The Journal of Clinical Investigation **43**(2): 247-257.
- Holm, R., C. J. H. Porter, et al. (2003). "Examination of oral absorption and lymphatic transport of halofantrine in a triple-cannulated canine model after administration in self-microemulsifying drug delivery systems (SMEDDS) containing structured triglycerides." European Journal of Pharmaceutical Sciences **20**(1): 91-97.
- Holz, M., S. R. Heil, et al. (2000). "Temperature-dependent self-diffusion coefficients of water and six selected molecular liquids for calibration in accurate <sup>1</sup>H NMR PFG measurements." Physical Chemistry Chemical Physics **2**(20): 4740-4742.
- Hörter, D. and J. B. Dressman (2001). "Influence of physicochemical properties on dissolution of drugs in the gastrointestinal tract." Advanced Drug Delivery Reviews **46**(1-3): 75-87.
- Hunt, J. N. and M. T. Knox (1968). "A relation between the chain length of fatty acids and the slowing of gastric emptying." The Journal of Physiology **194**(2): 327-336.
- Hunter, J., B. H. Hirst, et al. (1993). "Drug absorption limited by P-glycoprotein-mediated secretory drug transport in human intestinal epithelial caco-2 cell layers." Pharmaceutical Research **10**(5): 743-749.
- Hwang, J., L. K. Tamm, et al. (1995). "Nanoscale complexity of phospholipid monolayers investigated by Near-Field Scanning Optical Microscopy." Science **270**(5236): 610-614.
- Iervolino, M., S. L. Raghavan, et al. (2000). "Membrane penetration enhancement of ibuprofen using supersaturation." International Journal of Pharmaceutics **198**(2): 229-238.
- Ilardia-Arana, D., H. G. Kristensen, et al. (2006). "Biorelevant dissolution media: Aggregation of amphiphiles and solubility of estradiol." Journal of Pharmaceutical Sciences **95**(2): 248-255.
- Kahlweit, M. (1982). "Kinetics of formation of association colloids." Journal of Colloid and Interface Science **90**(1): 92-99.
- Kalantzi, L., K. Goumas, et al. (2006). "Characterization of the Human Upper Gastrointestinal Contents Under Conditions Simulating Bioavailability/Bioequivalence Studies." Pharmaceutical Research **23**(1): 165-176.
- Kanicky, J. R. and D. O. Shah (2003). "Effect of premicellar aggregation on the pKa of fatty acid soap solutions." Langmuir **19**(6): 2034-2038.
- Karpf, D. M., R. Holm, et al. (2004). "Influence of the Type of Surfactant and the Degree of Dispersion on the Lymphatic Transport of Halofantrine in Conscious Rats." Pharmaceutical Research **21**(8): 1413-1418.
- Kätzel, U., M. Vorbau, et al. (2008). "Dynamic light scattering for the characterization of polydisperse fractal systems: II. Relation between structure and DLS results." Particle & Particle Systems Characterization **25**(1): 19-30.
- Kaukonen, A., B. Boyd, et al. (2004). "Drug solubilization behavior during in vitro digestion of simple triglyceride lipid solution formulations." Pharmaceutical Research **21**(2): 245-253.
- Khamkar, G. S. (2011). "Self Micro Emulsifying Drug Delivery System (SMEED) o/w microemulsion for BCS class II drugs: An approach to enhance an oral bioavailability." International Journal of Pharmacy and Pharmaceutical Sciences **3**(SUPPL. 3): 1-3.



- Khoo, S.-M., G. A. Edwards, et al. (2001). "A conscious dog model for assessing the absorption, enterocyte-based metabolism, and intestinal lymphatic transport of halofantrine." Journal of Pharmaceutical Sciences **90**(10): 1599-1607.
- Khossravi, M., Y. H. Kao, et al. (2002). "Analysis methods of Polysorbate 20: A new method to assess the stability of Polysorbate 20 and established methods that may overlook degraded Polysorbate 20." Pharm Res **19**(5): 634-639.
- Kim, R. B., M. F. Fromm, et al. (1998). "The drug transporter P-glycoprotein limits oral absorption and brain entry of HIV-1 protease inhibitors." The Journal of Clinical Investigation **101**(2): 289-294.
- Kohli, K., S. Chopra, et al. (2010). "Self-emulsifying drug delivery systems: an approach to enhance oral bioavailability." Drug Discovery Today **15**(21-22): 958-965.
- Koppel, D. E. (1972). "Analysis of macromolecular polydispersity in intensity correlation spectroscopy: The method of cumulants." The Journal of Chemical Physics **57**(11): 4814-4820.
- Kossena, G. A., B. J. Boyd, et al. (2003). "Separation and characterization of the colloidal phases produced on digestion of common formulation lipids and assessment of their impact on the apparent solubility of selected poorly water-soluble drugs." Journal of Pharmaceutical Sciences **92**(3): 634-648.
- Kossena, G. A., W. N. Charman, et al. (2004). "Probing drug solubilization patterns in the gastrointestinal tract after administration of lipid-based delivery systems: A phase diagram approach." Journal of Pharmaceutical Sciences **93**(2): 332-348.
- Kossena, G. A., W. N. Charman, et al. (2005). "Influence of the intermediate digestion phases of common formulation lipids on the absorption of a poorly water-soluble drug." Journal of Pharmaceutical Sciences **94**(3): 481-492.
- Krezel, A. and W. Bal (2004). "A formula for correlating pKa values determined in D2O and H2O." Journal of Inorganic Biochemistry **98**(1): 161-166.
- Kuksis, A. (1987). Fat absorption. A. Kuksis. Boca Raton, CRC press. **2**: 65-86.
- Ladas, S. D., P. E. Isaacs, et al. (1984). "Comparison of the effects of medium and long chain triglyceride containing liquid meals on gall bladder and small intestinal function in normal man." Gut **25**(4): 405-411.
- Lafitte, G., K. Thuresson, et al. (2007). "Transport properties and aggregation phenomena of polyoxyethylene sorbitane monooleate (Polysorbate 80) in pig gastrointestinal mucin and mucus." Langmuir **23**(22): 10933-10939.
- Land, L. M. (2005). An investigation of the physicochemical mechanisms underlying enhanced oral bioavailability following administration of hydrophobic drugs via lipid-based delivery systems. Pharmaceutical Sciences. Lexington, University of Kentucky. **Ph. D.**
- Land, L. M., P. Li, et al. (2006). "Mass transport properties of progesterone and estradiol in model microemulsion formulations." Pharm. Res. **23**(Copyright (C) 2010 American Chemical Society (ACS). All Rights Reserved.): 2482-2490.
- Larsson, A. and C. Erlanson-Albertsson (1986). "Effect of phosphatidylcholine and free fatty acids on the activity of pancreatic lipase-colipase." Biochimica et Biophysica Acta (BBA) - Lipids and Lipid Metabolism **876**(3): 543-550.
- Lewis, K. M. A., R. D. (1979). "pKa values of estrone, 17 beta-estradiol and 2-methoxyestrone." Steroids **34**(5): 485-499.

- Li, C., D. Fleisher, et al. (2001). "Regional-dependent intestinal absorption and meal composition effects on systemic availability of LY303366, a lipopeptide antifungal agent, in dogs." Journal of Pharmaceutical Sciences **90**(1): 47-57.
- Lindfors, L., S. Forssén, et al. (2008). "Nucleation and crystal growth in supersaturated solutions of a model drug." Journal of Colloid and Interface Science **325**(2): 404-413.
- Lipinski, C. A., F. Lombardo, et al. (2001). "Experimental and computational approaches to estimate solubility and permeability in drug discovery and development settings." Advanced Drug Delivery Reviews **46**(1-3): 3-26.
- Lipp, M. M., K. Y. C. Lee, et al. (1996). "Phase and morphology changes in lipid monolayers induced by SP-B protein and its amino-terminal peptide." Science **273**(5279): 1196-1199.
- Ljusberg-Wahren, H., F. Seier Nielsen, et al. (2005). "Enzymatic characterization of lipid-based drug delivery systems." International Journal of Pharmaceutics **298**(2): 328-332.
- Logan, B. K. and K. S. Patrick (1990). "Photodegradation of nifedipine relative to nitrendipine evaluated by liquid and gas chromatography." Journal of Chromatography B: Biomedical Sciences and Applications **529**: 175-181.
- Luan, Y., A. Song, et al. (2009). "Location of probe molecule in double-chain surfactant aggregates in absence and presence of water-soluble polymer by NMR." Soft Matter **5**(13): 2587-2595.
- MacGregor, K. J., J. K. Embleton, et al. (1997). "Influence of lipolysis on drug absorption from the gastro-intestinal tract." Advanced Drug Delivery Reviews **25**(1): 33-46.
- Mahieu, N., D. Canet, et al. (1991). "Micellization of sodium oleate in water-d<sub>2</sub> as probed by proton longitudinal magnetic relaxation and self-diffusion measurements." The Journal of Physical Chemistry **95**(4): 1844-1846.
- Marsac, P. J., H. Konno, et al. (2006). "A comparison of the physical stability of amorphous felodipine and nifedipine systems." Pharmaceutical Research **23**(10): 2306-2316.
- Martinez, M., G. Amidon, et al. (2002). "Applying the biopharmaceutics classification system to veterinary pharmaceutical products: Part II. Physiological considerations." Advanced Drug Delivery Reviews **54**(6): 825-850.
- Mattson, F. H. and L. W. Beck (1955). "The digestion in vitro of triglycerides by pancreatic lipase." J. Biol. Chem. **214**(Copyright (C) 2011 American Chemical Society (ACS). All Rights Reserved.): 115-125.
- Mazer, N. A., G. B. Benedek, et al. (1980). "Quasielastic light-scattering studies of aqueous biliary lipid systems. Mixed micelle formation in bile salt-lecithin solutions." Biochemistry **19**(4): 601-615.
- Mazer, N. A. and M. C. Carey (1983). "Quasi-elastic light-scattering studies of aqueous biliary lipid systems. Cholesterol solubilization and precipitation in model bile solutions." Biochemistry **22**(2): 426-442.
- McDougall, A. O. and F. A. Long (1962). "Relative hydrogen bonding of deuterium. II. Acid ionization constants in H<sub>2</sub>O and D<sub>2</sub>O." The Journal of Physical Chemistry **66**(3): 429-433.

- Meguro, K., H. Akasu, et al. (1976). "Packing of polyethylene oxide chains in a mixed micelle." Journal of the American Oil Chemists' Society **53**(4): 145-148.
- Mellaerts, R., R. Mols, et al. (2008). "Ordered mesoporous silica induces pH-independent supersaturation of the basic low solubility compound itraconazole resulting in enhanced transepithelial transport." International Journal of Pharmaceutics **357**(1-2): 169-179.
- Miller, D., J. DiNunzio, et al. (2008). "Targeted intestinal delivery of supersaturated itraconazole for improved oral absorption." Pharmaceutical Research **25**(6): 1450-1459.
- Mohamed, A. and A.-S. M. Mahfoodh (2006). "Solubilization of naphthalene and pyrene by sodium dodecyl sulfate (SDS) and polyoxyethylenesorbitan monooleate (Tween 80) mixed micelles." Colloids and Surfaces A: Physicochemical and Engineering Aspects **287**(1-3): 44-50.
- Mohsin, K., M. A. Long, et al. (2009). "Design of lipid-based formulations for oral administration of poorly water-soluble drugs: Precipitation of drug after dispersion of formulations in aqueous solution." Journal of Pharmaceutical Sciences **98**(10): 3582-3595.
- Momsen, M. M., M. Dahim, et al. (1997). "Lateral packing of the pancreatic lipase cofactor, colipase, with phosphatidylcholine and substrates." Biochemistry **36**(33): 10073-10081.
- Mu, H. and T. Porsgaard (2005). "The metabolism of structured triacylglycerols." Progress in Lipid Research **44**(6): 430-448.
- Mueller, E. A., J. M. Kovarik, et al. (1994). "Influence of a fat-rich meal on the pharmacokinetics of a new oral formulation of cyclosporine in a crossover comparison with the market formulation." Pharmaceutical Research **11**(1): 151-155.
- Mueller, K. (1981). "Structural dimorphism of bile salt/lecithin mixed micelles. A possible regulatory mechanism for cholesterol solubility in bile? X-ray structural analysis." Biochemistry **20**(2): 404-414.
- Muller, N. (1972). "Kinetics of micelle dissociation by temperature-jump techniques. Reinterpretation." The Journal of Physical Chemistry **76**(21): 3017-3020.
- Muller, N. (1978). "Attempt at a unified interpretation of the self-association of 1-1 ionic surfactants in solvents of low dielectric constant." Journal of Colloid and Interface Science **63**(2): 383-393.
- Mullin, J. W. (1961). Crystallization, London, Butterworths.
- Nagarajan, R. (1985). "Molecular theory for mixed micelles." Langmuir **1**(3): 331-341.
- Nerurkar, M. M., P. S. Burton, et al. (1996). "The Use of surfactants to enhance the permeability of peptides through caco-2 cells by inhibition of an apically polarized efflux system." Pharmaceutical Research **13**(4): 528-534.
- Neslihan Gursoy, R. and S. Benita (2004). "Self-emulsifying drug delivery systems (SEDDS) for improved oral delivery of lipophilic drugs." Biomedicine & Pharmacotherapy **58**(3): 173-182.
- Nielsen, A. E. and O. Söhnel (1971). "Interfacial tensions electrolyte crystal-aqueous solution, from nucleation data." Journal of Crystal Growth **11**(3): 233-242.

- Nishikido, N. (1977). "Mixed micelles of polyoxyethylene-type nonionic and anionic surfactants in aqueous solutions." Journal of Colloid and Interface Science **60**(2): 242-251.
- O'Driscoll, C. M. (2002). "Lipid-based formulations for intestinal lymphatic delivery." European Journal of Pharmaceutical Sciences **15**(5): 405-415.
- O'Máille, E. R. and T. G. Richards (1977). "Possible explanations for the differences in secretory characteristics between conjugated and free bile acids." The Journal of Physiology **265**(3): 855-866.
- Overhoff, K., J. McConville, et al. (2008). "Effect of stabilizer on the maximum degree and extent of supersaturation and oral absorption of tacrolimus made by ultra-rapid freezing." Pharmaceutical Research **25**(1): 167-175.
- Patist, A., S. G. Oh, et al. (2001). "Kinetics of micellization: its significance to technological processes." Colloids and Surfaces A: Physicochemical and Engineering Aspects **176**(1): 3-16.
- Patton, J., R. Vetter, et al. (1985). "The light microscopy of lipid digestion." Food Microstructure: 29-41.
- Patton, J. S., P. A. Albertsson, et al. (1978). "Binding of porcine pancreatic lipase and colipase in the absence of substrate studies by two-phase partition and affinity chromatography." Journal of Biological Chemistry **253**(12): 4195-4202.
- Patton, J. S. and M. C. Carey (1979). "Watching fat digestion." Science **204**(4389): 145-148.
- Patton, J. S. and M. C. Carey (1981). "Inhibition of human pancreatic lipase-colipase activity by mixed bile salt-phospholipid micelles." American Journal of Physiology - Gastrointestinal and Liver Physiology **241**(4): G328-336.
- Pedersen, B. L., H. Brøndsted, et al. (2000). "Dissolution of hydrocortisone in human and simulated intestinal fluids." Pharmaceutical Research **17**(2): 183-189.
- Pedersen, J. S., S. U. Egelhaaf, et al. (2002). "Formation of polymerlike mixed micelles and vesicles in lecithin-bile salt solutions: a small-angle neutron-scattering study." The Journal of Physical Chemistry **99**(4): 1299-1305.
- Pellett, M. A., S. Castellano, et al. (1997). "The penetration of supersaturated solutions of piroxicam across silicone membranes and human skin in vitro." Journal of Controlled Release **46**(3): 205-214.
- Pellett, M. A., A. F. Davis, et al. (1994). "Effect of supersaturation on membrane transport: 2. Piroxicam." International Journal of Pharmaceutics **111**(1): 1-6.
- Perry, C. M. and S. Noble (1998). "Saquinavir soft-gel capsule formulation: A review of its use in patients with HIV infection." Drugs **55**(3): 461-486.
- Peters, G. H., S. Toxvaerd, et al. (1995). "Structure and dynamics of lipid monolayers: implications for enzyme catalysed lipolysis." Nature structural biology **2**: 395-401.
- Pisárcik, M., F. Devínsky, et al. (1996). "Spherical dodecyltrimethylammonium bromide micelles in the limit region of transition to rod-like micelles. A light scattering study." Colloids and Surfaces A: Physicochemical and Engineering Aspects **119**(2-3): 115-122.
- Poelma, F. G., B. R., et al. (1991). "Intestinal absorption of drugs. The influence of mixed micelles on the disappearance kinetics of drugs from the small intestine of the rat." J. Pharm. Pharmacol. **43**: 317-324.

- Porter, C. J., A. M. Kaukonen, et al. (2004). "Use of in vitro lipid digestion data to explain the in vivo performance of triglyceride-based oral lipid formulations of poorly water-soluble drugs: Studies with halofantrine." Journal of Pharmaceutical Sciences **93**(5): 1110-1121.
- Porter, C. J. H., A. M. Kaukonen, et al. (2004). "Susceptibility to lipase-mediated digestion reduces the oral bioavailability of danazol after administration as a medium-chain lipid-based microemulsion formulation." Pharmaceutical Research **21**(8): 1405-1412.
- Porter, C. J. H., C. W. Pouton, et al. (2008). "Enhancing intestinal drug solubilisation using lipid-based delivery systems." Advanced Drug Delivery Reviews **60**(6): 673-691.
- Porter, C. J. H., N. L. Trevaskis, et al. (2007). "Lipids and lipid-based formulations: optimizing the oral delivery of lipophilic drugs." Nature Reviews Drug Discovery **6**(3): 231-248.
- Pouton, C. W. (1997). "Formulation of self-emulsifying drug delivery systems." Advanced Drug Delivery Reviews **25**(1): 47-58.
- Pouton, C. W. (2000). "Lipid formulations for oral administration of drugs: non-emulsifying, self-emulsifying and 'self-microemulsifying' drug delivery systems." European Journal of Pharmaceutical Sciences **11**(Supplement 2): S93-S98.
- Pouton, C. W. (2006). "Formulation of poorly water-soluble drugs for oral administration: Physicochemical and physiological issues and the lipid formulation classification system." European Journal of Pharmaceutical Sciences **29**(3-4): 278-287.
- Prentis, R. A. L., Y; Walker, S R (1988). "Pharmaceutical innovation by the seven UK-owned pharmaceutical companies (1964-1985)." Br J Clin Pharmacol **25**(3): 387-396.
- Raghavan, S. L., B. Kiepfer, et al. (2001). "Membrane transport of hydrocortisone acetate from supersaturated solutions; the role of polymers." International Journal of Pharmaceutics **221**(1-2): 95-105.
- Raghavan, S. L., A. Trividic, et al. (2000). "Effect of cellulose polymers on supersaturation and in vitro membrane transport of hydrocortisone acetate." International Journal of Pharmaceutics **193**(2): 231-237.
- Raybould, H. E., J. H. Meyer, et al. (1998). "Inhibition of gastric emptying in response to intestinal lipid is dependent on chylomicron formation." Am J Physiol Regul Integr Comp Physiol **274**(6): R1834-1838.
- Reiss-Husson, F. and V. Luzzati (1964). "The structure of the micellar solutions of some amphiphilic compounds in pure water as determined by absolute small-angle X-ray scattering techniques." The Journal of Physical Chemistry **68**(12): 3504-3511.
- Reymond, J.-P. and H. Sucker (1988). "In vitro Model for Ciclosporin Intestinal Absorption in Lipid Vehicles." Pharmaceutical Research **5**(10): 673-676.
- Rigler, M. W., R. E. Honkanen, et al. (1986). "Visualization by freeze fracture, in vitro and in vivo, of the products of fat digestion." Journal of Lipid Research **27**(8): 836-857.
- Santos, P., A. C. Watkinson, et al. (2011). "Enhanced permeation of fentanyl from supersaturated solutions in a model membrane." International Journal of Pharmaceutics **407**(1-2): 72-77.

- Schersten, T. (1973). "Formation of lithogenic bile in man " Digestion **9**: 540-553.
- Schick, M. and D. Manning (1966). "Micelle formation in mixtures of nonionic and anionic detergents." Journal of the American Oil Chemists' Society **43**(3): 133-136.
- Schick, M. J., F. R. Eirich, et al. (1962). "Micellar structure of non-ionic detergents." Journal of Physical Chemistry **66**(7): 1326-&.
- Schmid, B. J., H. E. Perry, et al. (1988). "Determination of nifedipine and its three principal metabolites in plasma and urine by automated electron-capture capillary gas chromatography." Journal of Chromatography B: Biomedical Sciences and Applications **425**: 107-119.
- Schurtenberger, P., N. Mazer, et al. (1983). "Static and dynamic light scattering studies of micellar growth and interactions in bile salt solutions." The Journal of Physical Chemistry **87**(2): 308-315.
- Schurtenberger, P., N. Mazer, et al. (1985). "Micelle to vesicle transition in aqueous solutions of bile salt and lecithin." The Journal of Physical Chemistry **89**(6): 1042-1049.
- Schwarb, F. P., G. Imanidis, et al. (1999). "Effect of concentration and degree of saturation of topical fluocinonide formulations on in vitro membrane transport and in vivo availability on human skin." Pharmaceutical Research **16**(6): 909-915.
- Seeballuck, F., M. B. Ashford, et al. (2003). "The effects of pluronic® block copolymers and Cremophor® EL on intestinal lipoprotein processing and the potential link with P-glycoprotein in caco-2 cells." Pharmaceutical Research **20**(7): 1085-1092.
- Sek, L., B. J. Boyd, et al. (2006). "Examination of the impact of a range of Pluronic surfactants on the in-vitro solubilisation behaviour and oral bioavailability of lipidic formulations of atovaquone." Journal of pharmacy and pharmacology **58**: 809-820.
- Sek, L., C. J. H. Porter, et al. (2002). "Evaluation of the in-vitro digestion profiles of long and medium chain glycerides and the phase behaviour of their lipolytic products." Journal of Pharmacy and Pharmacology **54**(1): 29-41.
- Shah, N. H., M. T. Carvajal, et al. (1994). "Self-emulsifying drug delivery systems (SEDDS) with polyglycolized glycerides for improving in vitro dissolution and oral absorption of lipophilic drugs." International Journal of Pharmaceutics **106**(1): 15-23.
- Shareef, A., M. J. Angove, et al. (2006). "Aqueous solubilities of estrone, 17 $\beta$ -estradiol, 17 $\alpha$ -ethynylestradiol, and bisphenol A." Journal of Chemical & Engineering Data **51**(3): 879-881.
- Small, D. M. (1967). Gastroenterology **52**: 607.
- Small, D. M. (1986). The physical chemistry of lipids : from alkanes to phospholipids New York, NY, Plenum Press.
- Small, D. M., D. J. Cabral, et al. (1984). "The ionization behavior of fatty acids and bile acids in micelles and membranes." Hepatology **4**(S2): 77S-79S.
- Söderman, O., P. Stilbs, et al. (2004). "NMR studies of surfactants." Concepts in Magnetic Resonance Part A **23A**(2): 121-135.
- Spernath, A., A. Yagmur, et al. (2003). "Self-diffusion nuclear magnetic resonance, microstructure transitions, and solubilization capacity of phytosterols and

- cholesterol in Winsor IV food-grade microemulsions." Journal of Agricultural and Food Chemistry **51**(8): 2359-2364.
- Staggers, J. E., O. Hernell, et al. (1990). "Physical-chemical behavior of dietary and biliary lipids during intestinal digestion and absorption. 1. Phase behavior and aggregation states of model lipid systems patterned after aqueous duodenal contents of healthy adult human beings." Biochemistry **29**(8): 2028-2040.
- Stejskal, E. O. and J. E. Tanner (1965). "Spin diffusion measurements: spin echoes in the presence of a time-dependent field gradient." The Journal of Chemical Physics **42**(1): 288-292.
- Stokes, R. J. and D. Fennell Evans (1997). Fundamentals of interfacial engineering. New York, NY, Wiley-VCH, Inc. .
- Suzuki, H. and Y. Sugiyama (2000). "Role of metabolic enzymes and efflux transporters in the absorption of drugs from the small intestine." European Journal of Pharmaceutical Sciences **12**(1): 3-12.
- Svasti, J. and B. H. Bowman (1978). "Human group-specific component. Changes in electrophoretic mobility resulting from vitamin D binding and from neuraminidase digestion." Journal of Biological Chemistry **253**(12): 4188-4194.
- Tamamushi, B.-i., M. Shirai, et al. (1958). "A study on the micellar solutions of sodium oleate and elaidate." Bulletin of the Chemical Society of Japan **31**(4): 467-472.
- Tanaka, T., T. Nakashima, et al. (1995). "A potentiometric titration study on the dissociation of bile acids related to the mode of interaction between different head groups of nonionic surfactants with free bile salts upon mixed micelle formation in water." Colloid & Polymer Science **273**(4): 392-398.
- Tokumura, T., Y. Tsushima, et al. (1987). "Enhancement of the oral bioavailability of cinnarizine in oleic acid in beagle dogs." Journal of Pharmaceutical Sciences **76**: 286-288.
- Treiner, C., A. A. Khodja, et al. (1987). "Micellar solubilization of 1-pentanol in binary surfactant solutions: a regular solution approach." Langmuir **3**(5): 729-735.
- Treiner, C., M. Nortz, et al. (1990). "Micellar solubilization in strongly interacting binary surfactant systems." Langmuir **6**(7): 1211-1216.
- Treiner, C., M. Nortz, et al. (1988). "Micellar solubilization in aqueous binary surfactant systems: Barbituric acids in mixed anionic + nonionic or cationic + nonionic mixtures." Journal of Colloid and Interface Science **125**(1): 261-270.
- Treiner, C., C. Vaution, et al. (1985). "Influence of sodium dodecylsulphate and of inorganic electrolytes on the micellar solubilization of butobarbitone in aqueous polyoxyethylene lauryl ether solutions at 298.15 K." Colloids and Surfaces **14**(2): 285-292.
- Triggle, A. M., E. Shefter, et al. (1980). "Crystal structures of calcium channel antagonists: 2,6-dimethyl-3,5-dicarbomethoxy-4-[2-nitro-, 3-cyano-, 4-(dimethylamino)-, and 2,3,4,5,6-pentafluorophenyl]-1,4-dihydropyridine." Journal of Medicinal Chemistry **23**(12): 1442-1445.
- Valentini, M., A. Vaccaro, et al. (2004). "Diffusion NMR spectroscopy for the characterization of the size and interactions of colloidal matter: The case of vesicles and nanoparticles." Journal of the American Chemical Society **126**(7): 2142-2147.

- Van Citters, G. and H. Lin (1999). "The ileal brake: A fifteen-year progress report." Current Gastroenterology Reports **1**(5): 404-409.
- Vandecruys, R., J. Peeters, et al. (2007). "Use of a screening method to determine excipients which optimize the extent and stability of supersaturated drug solutions and application of this system to solid formulation design." International Journal of Pharmaceutics **342**(1-2): 168-175.
- Varma, M. V. S. and R. Panchagnula (2005). "Enhanced oral paclitaxel absorption with vitamin E-TPGS: Effect on solubility and permeability in vitro, in situ and in vivo." European Journal of Pharmaceutical Sciences **25**(4-5): 445-453.
- Vaughn, J. M., J. T. McConville, et al. (2006). "Supersaturation produces high bioavailability of amorphous danazol particles formed by evaporative precipitation into aqueous solution and spray freezing into liquid technologies." Drug Development & Industrial Pharmacy **32**(5): 559-567.
- Vinod, S. (2005). The Role of Dissolution Testing in the Regulation of Pharmaceuticals. Pharmaceutical Dissolution Testing, Informa Healthcare: 81-96.
- Vinson, P. K. K., A.; Talmon, Y.; Walter, A. (1989). "cylindrical shape of micelles of bile salt and lecithin." Biophysic J. **56**: 669.
- Walter, A., P. K. Vinson, et al. (1991). "Cylindrical shape of micelles of bile salt and lecithin." Biophysic J. **60**: 1315.
- Walter, A., P. K. Vinson, et al. (1991). "Cylindrical shape of micelles of bile salt and lecithin." Biophysic J. **60**: 1315.
- Washington, C. (1990). "Drug release from microdisperse systems: a critical review." International Journal of Pharmaceutics **58**(1): 1-12.
- Waters, L., S. Leharne, et al. (2007). "Determination of micelle/water partition coefficients and associated thermodynamic data for dialkyl phthalate esters." Journal of Thermal Analysis and Calorimetry **90**(1): 283-288.
- Westergaard, H. and J. M. Dietschy (1976). "The mechanism whereby bile acid micelles increase the rate of fatty acid and cholesterol uptake into the intestinal mucosal cell." The Journal of Clinical Investigation **58**(1): 97-108.
- Whiddon, C. R., C. A. Bunton, et al. (2002). "Titration of fatty acids in sugar-derived (APG) surfactants: A <sup>13</sup>C NMR study of the effect of headgroup size, chain length, and concentration on fatty acid pKa at a nonionic micellar Interface." The Journal of Physical Chemistry B **107**(4): 1001-1005.
- Wickham, M., M. Garrod, et al. (1998). "Modification of a phospholipid stabilized emulsion interface by bile salt: effect on pancreatic lipase activity." J. Lipid Res. **39**(3): 623-632.
- Wickham, M., P. Wilde, et al. (2002). "A physicochemical investigation of two phosphatidylcholine/bile salt interfaces: implications for lipase activation." Biochim Biophys Acta **1580**(2-3): 110-122.
- Wiedmann, T. S. and L. Kamel (2002). "Examination of the solubilization of drugs by bile salt micelles." Journal of Pharmaceutical Sciences **91**(8): 1743-1764.
- Wiedmann, T. S., W. Liang, et al. (2004). "Excluded volume effect of rat intestinal mucin on taurocholate/phosphatidylcholine mixed micelles." Journal of Colloid and Interface Science **270**(2): 321-328.
- Winkler, F. K., A. D'Arcy, et al. (1990). "Structure of human pancreatic lipase." Nature **343**(6260): 771-774.



- Winstanley, P. A. and M. L. E. Orme (1989). "The effect of food on drug bioavailability." British Journal of Clinical Pharmacology **28**: 621-628.
- Yamagata, T., H. Kusuhara, et al. (2007). "Effect of excipients on breast cancer resistance protein substrate uptake activity." Journal of Controlled Release **124**(1-2): 1-5.
- Yamamura, S. and J. A. Rogers (1996). "Characterization and dissolution behavior of nifedipine and phosphatidylcholine binary systems." International Journal of Pharmaceutics **130**(1): 65-73.
- Yoshida, N. and Y. Moroi (2000). "Solubilization of polycyclic aromatic compounds into n-decyltrimethylammonium perfluorocarboxylate micelles." Journal of Colloid and Interface Science **232**(1): 33-38.
- Zangenberg, N. H., A. Müllertz, et al. (2001). "A dynamic in vitro lipolysis model: II: Evaluation of the model." European Journal of Pharmaceutical Sciences **14**(3): 237-244.
- Zangenberg, N. H., A. Müllertz, et al. (2001). "A dynamic in vitro lipolysis model: I. Controlling the rate of lipolysis by continuous addition of calcium." European Journal of Pharmaceutical Sciences **14**(2): 115-122.

## Vita

Date of Birth: March 16<sup>th</sup>, 1971

Place of Birth: Xi' An, People's Republic of China

### EDUCATION:

2006- Present Ph.D. candidate in Pharmaceutical Sciences, College of Pharmacy,  
University of Kentucky  
Advisor: Assoc. Prof. Paul M. Bummer

1997-2000 Ph.D. in Organic Chemistry  
Shanghai Institute of Materia Medica, Chinese Academy of Sciences  
Advisor: Prof. Yuyuan Xie

### PROFESSIONAL EXPERIENCE:

2006-present	Graduate Research Assistant	Pharmaceutical Sciences College of Pharmacy, University of Kentucky Advisor: Assoc. Prof. Paul M. Bummer
2002-2006	Research Associate	Pharmaceutical Sciences College of Pharmacy, University of Kentucky Advisor: Prof. Bradley D. Anderson
2000-2002	Postdoctoral Scholar	Pharmaceutical Sciences College of Pharmacy, University of Kentucky Advisor: Late Prof. Thomas G. Burke

### PUBLICATIONS:

1. *Supersaturation of poorly water soluble drugs during the lipolysis of model lipid-based drug delivery system under simulated intestinal conditions*, Song, Lin and Bummer, Paul M. (in preparation).
2. *Mechanistic study of solubilization of poorly water solubility drugs in the model mixed micelles composed of selected lipolytic products*, Song, Lin and Bummer, Paul M. (in preparation).
3. *Kinetics and Mechanisms of Activation of  $\alpha$ -Amino Acid Ester Prodrugs of Camptothecins*. Song, Lin; Bevins, Robert; Anderson, Bradley D. *Journal of Medicinal Chemistry* (2006), 49(14), 4344-4355.

4. *Validation of an HPLC method for analysis of DB-67 and its water soluble prodrug in mouse plasma.* Horn, Jamie; Jordan, Sherri L.; Song, Lin; Roberts, Michael J.; Anderson, Bradley D.; Leggas, Markos. *Journal of Chromatography, B: Analytical Technologies in the Biomedical and Life Sciences* (2006), 844(1), 15-22.
5. *Molecular Dynamics Simulations and Experimental Studies of Binding and Mobility of 7-tert-Butyldimethylsilyl-10-hydroxycamptothecin and Its 20(S)-4-Aminobutyrate Ester in DMPC Membranes.* Xiang, Tian-Xiang; Jiang, Zhi-Qiang; Song, Lin; Anderson, Bradley D. *Molecular Pharmaceutics* (2006), 3(5), 589-600.
6. *Dependence of nelfinavir brain uptake on dose and tissue concentrations of the selective P-glycoprotein inhibitor zosuquidar in rats.* Anderson, Bradley D.; May, Melissa J.; Jordan, Sherri; Song, Lin; Roberts, Michael J.; Leggas, Markos. *Drug Metabolism and Disposition* (2006), 34(4), 653-659.
7. *Degradation of camptothecin-20(S)-glycinate ester prodrug under physiological conditions.* Liu, Xinli; Zhang, Junhong; Song, Lin; Lynn, Bert C.; Burke, Thomas G. *Journal of Pharmaceutical and Biomedical Analysis* (2004), 35(5), 1113-1125.
8. *A Versatile Prodrug Approach for Liposomal Core-Loading of Water-Insoluble Camptothecin Anticancer Drugs.* Liu, Xinli; Lynn, Bert C.; Zhang, Junhong; Song, Lin; Bom, David; Du, Wu; Curran, Dennis P.; Burke, Thomas G. *Journal of the American Chemical Society* (2002), 124(26), 7650-7651.
9. *Synthesis and antitumor activity of Antineoplaston A10 analogs.* Song, Lin; Xie, Yuli; Xie, Yuyuan. *Chinese Journal of Pharmaceutical Sciences* (2000), 9(2), 77-79.
10. *Studies on synthesis and antitumor activity of phenol substituted bisphosphonate Schiff base.* Xie, Yuli; Song, Lin; Zhu, Qin; Xie, Yuyuan. *Chinese Journal of Medicinal Chemistry* (2000), 10(2), 88-91, 99.
11. *Synthesis and antibacterial activity of benzimidazole Schiff bases.* Song, Lin; Xie, Yuyuan; Wang, Huizhen. *Chinese Journal of Medicinal Chemistry* (2000), 10(2), 92-94.
12. *Synthesis, structure and antitumor activities of a new macrocyclic ligand with four neutral pendent groups: 1,4,7,10-tetrakisbenzyl-1,4,7,10-tetraazacyclododecane (L) and its Co, Ni and Cu complexes.* Kong, Deyuan; Meng, Linhua; Song, Lin; Xie, Yuyuan. *Transition Metal Chemistry (Dordrecht, Netherlands)* (1999), 24(5), 553-557.

## ABSTRACTS AND PRESENTATIONS

1. Effect of lipolysis of a model lipid-based drug delivery system on solubilization of nifedipine under simulated intestinal conditions. Song, Lin; Jayanth, Jayanth; Bummer, Paul M. AAPS annual meeting (2010), 12(S2).
2. Supersaturation of progesterone during lipolysis of a model lipid-based drug delivery system under simulated intestinal conditions. Song, Lin; Bummer, Paul M. AAPS PharmSci (2009), 11(S2).
3. Solubilization of a hydrophobic drug by lipid-based systems and under simulated intestinal conditions. Song, Lin; Bummer, Paul M. AAPS PharmSci (2008), 10(S2).
4. Demicellization of mixed micelles relevant to lipid-based drug delivery systems. Song, Lin; Bummer, Paul M. AAPS PharmSci (2007), 9(S2).
5. Kinetics and mechanism of a novel degradation pathway of 20(S)-glycinate and N-methylglycinate esters of camptothecins. Song, Lin; Anderson, Bradley D. AAPS PharmSci (2004), 6(S1).
6. Synthesis, stability, solubility and toxicity of prodrugs of 7-tert-butydimethylsilyl-camptothecin (DB-67). Song, Lin; Zhang, Junhong; Zimmer, Stefan G.; Bom, David; Burke, Thomas G; Anderson, Bradley D. AAPS PharmSci (2003), 5(S1).
7. A versatile pro-drug approach for the liposomal core loading of camptothecin anticancer drugs. Burke, Thomas G; Liu, Xinli; Zhang, Junhong; Song, Lin; Bom, David; Bevins, Robert; Zimmer, Stephen G. Proc. Am. Assoc. Cancer Res. (2002), 43: 5731.